ANALYSIS OF SPREAD FOOTING FOUNDATIONS AS A HIGHWAY BRIDGE ALTERNATIVE

A thesis presented to

the faculty of

the Russ College of Engineering and Technology of Ohio University

In partial fulfillment

of the requirement for the degree

Master of Science

Jill L. Meranda

November 2005

This thesis entitled

ANALYSIS OF SPREAD FOOTING FOUNDATIONS AS A

HIGHWAY BRIDGE ALTERNATIVE

by

JILL L. MERANDA

has been approved for

the Department of Civil Engineering

and the Russ College of Engineering and Technology by

Teruhisa Masada

Associate Professor of Civil Engineering

Dennis Irwin

Dean, Russ College of Engineering and Technology

MERANDA, JILL L. M.S. November 2005. Civil Engineering

Analysis of Spread Footing Foundations as a Highway Bridge Alternative (300pp.)

Director of Thesis: Teruhisa Masada

Spread footings have been utilized to support various types of civil engineering structures over the years. However, they have not seen much use in Ohio for highway bridge applications. Despite the success of previous spread footing studies, more research is needed to evaluate spread footings as a highway bridge foundation. Research is performed to determine a correlation between the contact pressure, settlement, and tilting of the footing. A correlation is found between settlement and tilting as they demonstrate global behaviors, unlike contact pressure, which reflects the stiffness of the underlying soil in localized areas. Methods from AASHTO LRFD Bridge Design Specifications (2004) and other researchers are evaluated and the Hough, Schmertmann, Burland-Burbidge, and Terzaghi-Peck methods are determined to be the most reliable. A cost analysis is performed to determine the effectiveness of using spread footings. Installing a typical spread footing may save nearly 63% as compared to pile foundations.

Approved:

Teruhisa Masada

Associate Professor of Civil Engineering

ACKNOWLEDGEMENTS

I would like to express my sincere gratitude to Dr. Teruhisa Masada for his help with my research and for providing direction for my thesis. I would also like to acknowledge Dr. Shad Sargand for providing me the opportunity to attend graduate school. Thank you to the thesis committee, which was comprised of Dr. Masada, Dr. Thomas Wolf, and Dr. Sargand. A special thanks to my friends and family for their continued support throughout my college career.

TABLE OF CONTENTS

TABLE OF CONTENTS (cont'd)

TABLE OF CONTENTS (cont'd)

TABLE OF CONTENTS (cont'd)

LIST OF TABLES

LIST OF TABLES (cont'd)

LIST OF TABLES (cont'd)

LIST OF FIGURES

LIST OF FIGURES (cont'd)

LIST OF FIGURES (cont'd)

LIST OF FIGURES (cont'd)

CHAPTER 1: INTRODUCTION

1.1 BACKGROUND

Shallow foundations have been utilized to support various types of civil engineering structures over the years. However, shallow foundations have not seen much use in Ohio and across the U.S. for highway bridges. Traditionally, a rather conservative approach is taken by specifying deep foundations such as H-piles and drilled piers to support the bridge superstructure and live loads. Shallow foundations are specified by bridge and foundation engineers only in rare site conditions such as shallow bedrock and overconsolidated subsoils. This is because their confidence level in shallow foundations is less than that in deep foundations when it comes to providing long-term foundations for highway bridges.

If subsurface conditions are reasonable for the use of spread footings, they can be a viable alternative to deep foundations. Data compiled by Moulton et al. (1982) and Hearn (1995) showed that deep foundations are actually as prone to settlement as shallow foundations. Cheney et al. (1982) and DiMillio (1982) showed that bridges can sustain substantially more tilting (of the order of 1/250 of the bridge span) and settlement (of the order of 2 to 3 inches or 50 to 76 mm) than what was previously thought. According to Amar et al. (1984), the cost associated with the spread footing is 17 to 67% less than the cost of deep foundations. About 50% of the bridge construction cost comes from the foundation (according to Briaud & Gibbens, 1997); therefore spread footings should seriously be considered for economical reasons at almost all bridge construction sites. To further encourage their use, comprehensive performance data must be compiled through successful case histories and made available to the practicing civil engineers.

A research team from Ohio Research Institute for Transportation and the Environment (ORITE) at Ohio University completed an initial study on field and laboratory performances of highway bridge spread footing foundations for the Ohio Department of Transportation (ODOT) and the Federal Highway Administration (FHWA) in 1997. Detailed information on the study can be found in the final report by Sargand et al. (1997). The team spent several years instrumenting and monitoring the field performance of over fifty spread footings at five highway bridge construction sites in Ohio. Three of these bridge sites rested on cohesionless soils, while the remaining two bridges rested on dominantly cohesive subsoils. None of the footings experienced an average settlement of more than 2 inches (50 mm) prior to the service load application. Differential settlement problems were not encountered, and the rotational movements experienced by any of the abutment/pier walls or columns were negligible. Overall, the field performance data compiled supported the view that spread footings can be cost-effective, and a sound alternative to conventional deep foundations at highway bridge construction sites. This outcome was not surprising, since the subsoil conditions at each site were relatively favorable (i.e., typical SPT-N value > 30) for implementation of shallow foundations.

Despite the success of this initial study conducted by ORITE, a further study is needed to continue evaluating spread footings as a highway bridge foundation. Some reasons for this need are listed below:

(1) It is a vital research topic from the nation's financial point of view. About 6,000 new bridges are constructed every year in the U.S., costing more than $300 billion (Briaud & Gibbens, 1997). The cost of constructing spread footings is on average about 50% of the cost of constructing deep foundations. However, the use of spread footings may require more comprehensive subsurface investigation work. The increased use of spread footings for highway bridge structures is still believed to translate into a substantial annual saving to the taxpayers.

(2) There is interest in this topic among practicing foundation engineers. This point is supported by the fact that a summary of the initial study by ORITE was quickly accepted for publication by the ASCE Journal of Geotechnical and Geoenvironmental Engineering (Sargand et al. 1999).

(3) There is a need to establish field performance of spread footings at highway bridge sites where subsoil conditions are not as ideal as those (i.e., SPT N-value > 30) encountered in the previous ORITE study. Successful demonstration of satisfactory performance of spread footings at such sites will give further encouragement to the state/local agencies and bridge/foundation engineers to specify spread footings more frequently in highway bridge construction.

(4) Additional data on the field performance of spread footings will contribute significantly to the national data base on spread footings, which FHWA has been developing.

(5) There is a need to further evaluate the reliability of settlement performance prediction methods for spread footings on cohesionless soils. Previous studies yielded somewhat mixed results on this issue.

1.2 OBJECTIVES

With the above providing backgrounds, objectives for the current thesis project were set forth as:

- Successfully instrument and monitor spread footing foundations at additional highway construction sites in Ohio.

- Evaluate the reliability of multiple geotechnical prediction methods applicable to spread footings, including the settlement prediction methods for footings outlined in Section 10, AASHTO LRFD Bridge Design Specifications (2004).

- Examine the economic aspects for using the spread footing for highway bridges, instead of deep foundations.

1.3 PROJECT TASKS

Task 1: Identify two bridge construction sites in Ohio that are using spread footings.

Task 2: Calculate the expected spread footing performance from subsurface exploration and other project data.

Task 3: Create a sensor installation plan to measure the anticipated spread footing performance variables.

Task 4: Collect field data as necessary during and after construction of the pier footing.

Task 5: Analyze the collected data to validate the methods presented in Section 10 of AASHTO LRFD Bridge Design Specifications (2004).

Task 6: Determine reliability of other geotechnical methods applicable to bridge spread footing foundations.

Task 7: Perform a relatively comprehensive economic analysis on a typical highway bridge spread footing and its equivalent pile foundation, using the recent cost figures available in Ohio and considering the cost of subsurface investigation and laboratory testing.

1.4 OUTLINE OF THESIS

Chapter 2 presents the results of an extensive literature review carried out as part of the current study. The contents of this chapter are arranged by topics such as field surveys and case histories, Standard Penetration Tests N values, experimental test results, settlement prediction methods, and cost effectiveness.

Chapter 3 summarizes the comprehensive design/analysis procedures presented in Section 10 of the AASHTO LRFD Bridge Design Specifications (2004). The first sections of this chapter deal with the AASHTO procedures to estimate engineering properties of soils and rock masses, including SPT tests. The next section summarizes the allowable bearing pressure on various types of soil and rock masses. Then, a section summarizes the bearing capacity determination methods proposed by AASHTO. The proposed AASHTO methods for estimating immediate settlements due to loading are presented. And, the last section describes the AASHTO proposed method for computing consolidation settlement. The contents are divided between the sections dealing with rock masses and the sections dealing with soils. Tables and figures included in the AASHTO Specifications are imported into the chapter to maintain accurate descriptions of the procedures.

Chapter 4 is used to present some important design/analysis considerations applicable to spread footings that are not included in the AASHTO LRFD Bridge Design Specifications (2004). The chapter first describes how the contact stress distribution can be different between the footing and its underlying soil, depending on the footing rigidity and characteristics of the bearing soil. A few methods for assessing the rigidity of the spread footing are depicted. A method to estimate the magnitude and distribution of the contact pressure at the soil-footing interface for a footing that is truly rigid is described. The settlement of a footing on cohesionless soils is explained by many methods. The last part of this chapter explains the rotational behavior of any spread footing using a formula based on the elastic theory.

Chapter 5 is dedicated to presenting all relevant information pertaining to the two highway bridge construction sites where spread footing foundations were instrumented and monitored during and after the construction. The background information for each site includes design characteristics of the bridge structure, subsurface conditions, field instrumentation plans, and construction history. Some photographs are provided to show how the bridge construction progressed and how each spread footing foundation was instrumented.

Chapter 6 presents field performance data collected at the two highway bridge construction sites described in Chapter 5. For each spread footing, the field performance data consists of pressure cell readings, footing settlement, and tilting of footing column/wall. Three-dimensional graphical plots are produced, whenever possible, to effectively present the field data for the entire footing and develop comprehensive discussions as to how the foundation behaved during each major construction stage. After presenting all the field performance data, a brief discussion to point out correlations that appear to exist among the field data follows.

Chapter 7 constitutes the analytical phase of the current study. The chapter presents a series of geotechnical analyses performed for the spread footings monitored at the two sites. The analytical methods evaluated in light of the latest field performance data for the FRA-670-0380 site, include not only those outlined in the AASHTO LRFD Bridge Design Specifications (2004) but also all the other methods described in Chapter 4. The MOT-70/75 site will be evaluated in Appendix A. The last section of Chapter 7 summarizes the economic aspect of using the spread footing foundations (including subsurface investigation and laboratory testing costs) for highway bridges, instead of deep foundations.

Chapter 8 first summarizes several tasks performed to meet the objectives of the current study and then draws important conclusions reached while performing these tasks. The field performance of the bridge shallow foundations monitored at the two sites in the current study are described in terms of not only each of the three performance parameters (contact pressure, settlement, tilting) but also in terms of the correlations that existed among the measured parameters. While summarizing the results of various geotechnical methods applicable to spread footing foundations, first the emphasis is placed on the methods outlined in the AASHTO LRFD Bridge Design Specifications (2004). Then, the summary expands to cover the geotechnical methods that are not addressed in the AASHTO Specifications.

Appendix A consists of an analysis of the footing rigidity, bearing capacity, and immediate settlement for the MOT-70/75 bridge site.

CHAPTER 2: LITERATURE REVIEW

2.1 GENERAL

A review of geotechnical literature can identify a large number of technical publications related to shallow foundations. Although emphasis is often placed on bearing capacity and tolerable movement issues, there are still a good number of book sections and papers focusing on other issues such as contact pressure distribution, settlement, rotational movement, and cost effectiveness.

In addition to the traditional approaches in analyzing the shallow foundations, new methods and techniques are becoming available as more sophisticated electronic and computational tools are being developed. These include centrifuge modeling (Sargand et al. 1997), nondestructive test methods such as the wave-activated stiffness (WAK) test (Briaud & Lepert, 1990), finite element methods (Paice et al. 1996), and neural networks (Shahin, at al. 2002). Each of these methods will be discussed later.

2.2 FIELD SURVEYS AND CASE HISTORIES

There have been many reported cases of field performance of spread footings for various building structures. However, when it comes to field case histories for highway bridges, only a relatively small number of cases can be found in literature.

Bozozuk (1978) examined the 1975 survey data obtained by Transportation Research Board (TRB) Committee A2K03. He noticed that in some cases large movements took place among the bridges supported by both spread footings and pile foundations. Horizontal movements were more critical that vertical movements based on his conclusions. Tolerable movements were defined as vertical movements less than 4 inches (102 mm) and horizontal movements less than 2 inches (51 mm).

Grover (1978) examined 79 bridges in Ohio and came to the conclusion that 1 inch (25 mm) or less is a tolerable amount of settlement for a bridge. A settlement between 2 and 3 inches (51 and 76 mm) is noticeable to drivers, however only minor damage will occur to the structure. An excess of 4 inches is objectionable to drivers and likely to cause damage to bridge.

Keene (1978) studied seven spread footing case histories in Connecticut and assessed factors that affect tolerable movement. Some cases had post-construction settlements of as much as 3 inches (76 mm) but no damage to the bridges occurred. He stressed the importance of staged construction practices to minimize post-construction settlement.

Walkinshaw (1978) reviewed the data for 35 bridges supported by spread footings in ten western states. He noted a poor riding quality resulted when vertical movement exceeded 2.5 inches (64 mm). However, larger vertical settlement could be tolerated by the structure.

The conditions of 148 bridges supported by spread footings on compacted fill in Washington were studied by DiMillio (1982). Each of the bridges was in good condition, posing no safety or functional problems. The bridges were found to easily tolerate differential settlements of 1 to 3 inches (25 to 76 mm).

Moulton et al. (1982) reviewed the data on 204 bridges in West Virginia which were placed on either pile foundations or spread footings. Each bridge experienced movements and in some cases damage. The average vertical and horizontal movements were at least 4 inches (102 mm) and 2.5 inches (64 mm) among the cases regardless of the foundation type. This finding dismisses the common belief that shallow foundations are more prone to settlement than deep foundations.

Meyerhof (1965) made some observations on the field performance of spread footings for both cohesionless and cohesive soils. The settlement of spread footings resting on cohesionless soil increases approximately in direct proportion to the square root of the base width, and is nearly complete at the end of the construction stages. However, if the footing rests on a cohesive soil then the settlement increases in direct proportion to the base width. The time rate of consolidation determined from the laboratory test results tends to be slower than the actual time rate exhibited by the footing in the field, because no allowance is made for lateral drainage or the pore water pressure resulting from shearing stresses. Spread footings may be considered perfectly rigid in most practices. This assumption leads to a nonuniform contact pressure between the footing base and bearing soil. The distribution pattern of the contact pressure at the footing base has no appreciable impact on the magnitude of the total settlement. However, it has an effect on the bending stresses in the footing.

Gifford et al. (1987) monitored field performance of spread footing foundations on cohesionless soils at twenty-one highway bridge sites. The overall settlement of the spread footings ranged from 0.23 to 0.94 inches (6 to 24 mm), with an average of 0.49

inches (12 mm). Typically about 2/3 of the total settlement took place prior to the deck construction.

Baus (1992) monitored twelve spread footings at three highway bridge construction sites in South Carolina. Each of the spread footings were on cohesionless soils. The maximum measured settlements ranged mostly between 0.3 and 0.7 inches (8 and 18 mm); however two outliers settled 1.6 in (41 mm) and 1.7 in (43 mm). An average of 0.66 inches (17 mm) was determined for eleven of the twelve foundations; the last one didn't measure settlement.

Sargand et al. (1997) instrumented and monitored over fifty spread footings at five highway bridge construction sites in Ohio. Bridges A through C were constructed over predominantly cohesionless (A-2, A-3, A-4) subsoils, while Bridges D and E were built at sites consisting mostly of cohesive (A-6, A-7-6) soils. At the Bridge A construction site, the SPT-N values varied from about 20 at the base of footing to 100+ at depths reaching 20 to 30 ft (6.1 to 9.1 m) below the footing. At the site of Bridge B, the SPT-N values stayed relatively constant (around 50) below the foundation depth on one end of the bridge, while at the other end the SPT-N values ranged from about 40 to 100+. Under the footings of Bridge C, the SPT-N values increased from approximately 10 to 25 within 30 ft (9.1 m). The five bore logs for Bridge D had SPT-N values that varied from as low as 30 at the base of the footing to 100+ at depths reaching 20 to 30 ft (6.1 to 9.1 m) below the footing. At the Bridge E site, ten bore logs were bored resulting in SPT-N values that start at 13 and gradually increased to 30 and higher. Seven of these bore logs had values of 100+ beneath the footing. The overall settlement of the spread footings among all the footings ranged from 0.08 to 1.43 inches (1 to 36 mm), with an average of 0.79 inches (20 mm). Typically about 70% of the total settlement took place prior to the deck construction. None of the footings experienced any significant differential movement problems. Limited data collected at the sites within 6 months after the bridge opening showed that the additional settlement induced by the live load application ranged between 0.05 and 0.5 inches (1 and 12 mm), with an average of 0.17 inches (4 mm).

2.3 SPT-N VALUE VERSUS SETTLEMENT

Meyerhof (1965) assembled his observations of settlement performance for buildings on sand. He stated that the SPT-N value depends mainly on the relative density of the soil, as well as the effective overburden pressure and groundwater conditions. The effect of the groundwater conditions is naturally reflected in the N value. However, he felt that for granular soils the effect of the soil grain properties on the compressibility characteristics is not fully accounted for in the N values. Table 2.1 (a) shows Meyerhof's data that was compiled for spread footings. Gifford et al. (1987) summarized several case histories for spread footings on sands based on the corrected SPT-N value. They are listed in Table 2.1 (b). They also summarized the results of their own investigation, which included twenty four spread footings – see Table 2.1 (c). Bowles (1987) compiled a small spread footing database for testing his settlement equation. Table 2.1 (d) shows a portion of his database that reported the SPT-N values.

Table 2.1: SPT-N Value Versus Settlement Data Found in Literature

(a) Data Compiled by Meyerhof

Structure	B (ft)	L/B	D_f/B	N	q_{max} (tsf)	S (inch)
T. Edison, Sao Paulo	60	NA	NA	15	2.4	0.60
Banco do Brasil, Sao Paulo	75	NA	NA	18	2.5	1.10
Iparanga, Sao Paulo	30	NA	NA	9	2.3	1.40
C.B.I. Esplanada, Sao Paulo	48	NA	NA	22	4.0	1.10
Riscala, Sao Paulo	13	NA	NA	20	2.4	0.50
Thyssen, Dusseldorf	74	NA	NA	25	2.5	0.95
Ministry, Dusseldorf	52	NA	NA	20	2.3	0.85
Chimney, Cologne	67	NA	NA	10	1.8	0.40

(b) Data Compiled from Literature by Gifford et al.

Source	B (ft)	L/B	D_f/B	N_c	q_{max} (tsf)	S (inch)
Bergdahl & Ottosson (1982)	16.4	1.7	0.5	24	1.9	0.47
Wennerstrand (1979)	10.9	4.4	0.6	7	1.0	1.46
DeBeer & Martens (1956)	9.8	3.4	1.0	50	2.4	0.83
DeBeer (1948)	19.0	4.2	0.4	17	0.8	0.47
DeBeer & Martens (1956)	8.5	8.1	0.8	9	2.1	1.30
Levy & Morton (1974)	13.0	1.8	1.3	32	5.3	0.47
DeBeer (1948)	19.7	2.7	0.5	42	1.6	0.31
DeBeer (1948)	19.7	2.7	0.6	42	2.2	0.16
DeBeer (1948)	23.0	5.1	0.3	42	1.4	0.47
DeBeer (1948)	17.0	5.4	0.4	42	1.0	0.39

(c) Data Compiled by Gifford et al.

Structure	B (ft)	L/B	D_f/B	N_c	q_{max} (tsf)	S (inch)
Bridge 1 – Abutment 1	17.00	3.75	NA	44	1.6	0.35
Bridge 1 – Abutment 2	17.00	3.75	NA	58	1.3	0.67
Bridge 2 – Abutment 1	15.25	3.44	NA	43	1.2	0.94
Bridge 2 – Abutment 2	16.75	3.13	0.24	19	1.2	0.76
Bridge 2 – Pier	12.50	3.28	0.40	12	0.9	0.61
Bridge 3 – W. Abutment	11.00	6.78	NA	34	0.9	0.42
Bridge 3 – E. Abutment	18.50	4.27	0.27	22	1.2	0.61
Bridge 3 – Pier 1 North	21.00	1.00	0.24	18	1.0	0.28
Bridge 3 – Pier 1 South	21.00	1.45	0.24	18	0.8	0.26
Bridge 3 – Pier 2 North	16.00	1.68	0.31	20	1.2	0.29
Bridge 3 – Pier 2 South	16.00	1.16	0.31	22	1.2	0.25
Bridge 4 – S. Abutment	8.10	5.30	NA	21	1.7	0.46
Bridge 4 – N. Abutment	8.10	5.30	NA	8	1.7	0.34
Bridge 5 – N. Abutment	16.75	4.59	0.36	42	1.2	0.23
Bridge 5 – S. Abutment	15.25	5.04	0.43	24	1.2	0.44
Bridge 6 – Abutment 2	15.25	4.41	0.59	39	0.9	0.83
Bridge 7 – Abutment 2	28.00	1.00	0.00	24	1.1	0.64

Table 2.1 (c) (cont'd):

Structure	B (ft)	L/B	D_f/B	N_c	q_{max} (tsf)	S (inch)
Bridge 8 – Abutment 1	20.00	5.04	1.10	23	1.5	0.46
Bridge 8 – Abutment 2	20.00	5.04	0.25	38	1.6	0.66
Bridge 9 – Abutment 1	21.75	2.04	NA	39	1.8	0.61
Bridge 9 – Abutment 2	16.00	2.79	0.0	49	1.7	0.28

(d) Data Compiled from Literature by Bowles

Source	B (ft)	L/B	Df/B	N	q_{max} (tsf)	S (inch)
D'Appolonia et al. (1968)	12.5	1.6	0.5	25	1.7	0.3-0.4
Davisson & Salley (1972)	124.0	1.0	0.0	12	1.6	5.3
Tschebotarioff (1951)	90.0	1.1	0.1	12	3.6	3.9

2.4 EXPERIMENTAL TEST RESULTS

Experimental methods are becoming more used to determine the behavior of shallow foundations. These methods can be powerful tools which gain further insights into the shallow foundation behaviors. However, they can also possess some shortcomings.

Sargand et al. (1997) applied the centrifuge modeling technique in an attempt to simulate the field performance of highway bridge spread footings in the laboratory. For this method, a full scale prototype is scaled down uniformly by a factor n. This model is placed in the centrifuge on soil samples conditioned properly to exhibit the field conditions. Then, the model is subjected to a gravity field that is n times the normal gravitational field and is created by the centrifuge. The settlement of the model is transformed to the prototype field settlement by multiplying the prototype settlement by 1/n. Other parameters can also be transformed to those of the prototype in the field, which can be obtained by dimensional analysis. The results of the experimental efforts were mixed. The load-settlement behaviors of the centrifuge spread footing models were reasonably close to that observed for three of the five bridge construction sites, while the behaviors were approximately twice as large for the other two project sites. The inconsistent outcome was attributed to the difficulty in accurately replicating the in-situ subsoil conditions inside the centrifuge. The centrifuge modeling technique is best suited for conducting parametric studies and examining failure modes.

Briaud and Lepert (1990) applied the surface wave theory to the soil-footing system and developed a nondestructive test method called the Wave Activated stiffness (K) test or simply WAK test. The WAK test is a dynamic load test executed by striking the center of the footing with a rubber-tipped sledgehammer. This sends a surface wave, which is recorded by two geophones on opposite sides of the footing. The test data is analyzed by a model, consisting of a mass supported on a spring and a dash-pot, to determine the stiffness of the bearing soil and estimate the load-settlement characteristics of the footing.

In the WAK test, the force-time signal (the input) and the velocity-time signal (the response) are recorded. Fast Fourier transforms of the force and velocity give an estimated stiffness (K) of the model. Comparing results from the WAK test and an actual static load test shows that the WAK test predicted the settlement accurately up to a settlement of 0.4 inches (10 mm). However, this test does not accurately predict the footing behavior under large load-displacement levels.

Paice et al. (1996) studied the effect of correlated soil stiffness on the settlement of a footing with uniform loading. Field theory and the finite element method are combined to analyze settlement under footings on spatially random soil. Poisson's ratio was kept constant while the value for Young's modulus was randomly assigned.

There was little effect on the expected settlement based on spatial correlation when the Young's modulus variances were within the limit. The expected settlement was seen to be approximately 12% higher than the determined value. However when the variance became higher, which was unlikely, the settlement was much higher than expected. An analysis by this method requires a large number of input parameter values, which may not be easily available.

Shahin et al. (2002) proposed the use of artificial neural networks (ANNs), a form of artificial intelligence that simulates the thought process of a human brain. ANNs require a large database of actual measured settlements to predict the settlement performance of future foundations. The steps outlined by Maier and Dandy (2000) were used to develop the ANN models by a PC software NEUFRAME Version 4.0. An advantage of ANNs is that once the model is trained, it can be used for a quick and accurate settlement without using charts or tables. However, a drawback of ANNs is that there is no theory or physical reasoning used in their development. Also, no physical models are produced

Briaud and Gibbens (1999) conducted load tests at the National Geotechnical Experimentation Site in College Station, Texas. The load test took place on five square spread footings with dimensions ranging from 3.3 to 10 ft (1 to 3 m). Each footing was embedded 30 in (0.75 m) into the sand and was loaded to settle 5.9 in (150 mm). The soil at the site was a silty, medium dense, fine sand that was fairly uniform. The soil possessed the following properties: D_{50} of 0.2 mm, SPT-N value of 18, CPT tip resistance q_c of 870 psi (6 MPa), friction angle ϕ of 32°, unit weight γ of 99 pcf (15.5 kN/m^3). Each footing and the bearing sandy soil underneath received several devices/sensors (such as load cells, settlement beams, telltales, LVDTs, and inclinometers) to monitor the footing performance and gain insight into the soil-footing interaction. The load test data indicated that:

- Footing size effect on the load vs. settlement (S) behavior became a non-issue when the bearing pressure q was plotted against S/B ratio.
- The depth of influence is essentially two times the footing width (2B), as 78% of the settlement takes place within depth 1B and 97% within depth 2B.
- The bearing soil experienced the maximum lateral displacement equivalent to 15% of the surface settlement under the edge of the footing.

2.5 SETTLEMENT PREDICTION METHODS

2.5.1 Footings on Cohesionless Soils

There have been a number of efforts made to develop a reliable method for predicting settlement of a footing resting on cohesionless soils. This is largely because it is very difficult to obtain relatively undisturbed samples of cohesionless soils.

Gifford et al. (1987) used field settlement data for spread footings and compared it to settlement predictions made by five methods on sands. The methods chosen were Burland-Burbidge (1984), D'Applonia et al. (1967), Hough (1959), Peck-Bazaraa (1969), and Schmertmann (1970). From the calculations, they concluded that the methods proposed by D'Appolonia et al. (1967) and by Burland-Burbidge (1984) were more accurate than the other methods. The Peck-Bazaraa (1969) method had a tendency to underpredict the field settlement, while the methods by Hough (1959) and Schmertmann (1970; CPT) often overpredicted the field settlement.

Baus (1992) evaluated six settlement prediction methods, Alpan (1964), Hough (1959), DeBeer (1965), Meyerhof (1965), Peck-Bazaraa (1969), and Schmertmann (1970; CPT), in light of his field data. The methods by Peck-Bazaraa (1969) and by Schmertmann (1970; CPT) provided better settlement predictions than the other four methods. Alpan (1964) underpredicted the settlement, while Hough (1959), DeBeer (1965), and Meyerhof (1965) overpredicted.

Briaud and Gibbens (1997) conducted a survey among bridge and foundation engineers for research work for FHWA. Ten prediction methods were used for this survey, which were Briaud (1992), Burland-Burbidge (1984), DeBeer (1965), Menard-Rousseau (1962), Meyerhof (1965; CPT & SPT), Peck-Bazaraa (1969), Peck-Hanson-Thornburn (1974), Schmertmann (1970; CPT & 1986; DMT), Shultze-Sherif (1973), and Terzaghi-Peck (1967). The best predictions resulted from the methods by Briaud (1992), Burland-Burbidge (1984), Peck-Bazaraa (1969), and Schmertmann (1986; DMT). Briaud (1992) and Burland-Burbidge (1984) were somewhat conservative for their methods, while the other two were slightly unconservative.

Sargand et al. (1997) examined six settlement prediction methods for the footings on cohesionless soil, Bridges A, B, and C. The methods used to predict settlement in their spread footing bridge research project in Ohio were Burland-Burbidge (1984), D'Applonia et al. (1967), Hough (1959), Peck-Bazaraa (1969), Schmertmann (1970;

CPT) and Terzaghi-Peck (1967). They concluded that the Hough (1959) method might be more accurate than the other methods, although it slightly underpredicted the actual field settlements. Two other methods, Schmertmann (1970; CPT) and D'Appolonia et al. (1967), estimated the settlement relatively close to the actual settlement. The Schmertmann (1970; CPT) method somewhat overestimated the field settlements, while the method by D'Appolonia et al. (1967) underestimated the field settlements.

Table 2.2 recaps the evaluations of the various geotechnical settlement prediction methods for footings resting on cohesionless soils that were used in the independent studies mentioned above. According to the table, the methods proposed by Burland-Burbidge, Hough, and Peck-Bazaraa were judged to be more reliable than the others.

Table 2.2: Summary of Settlement Prediction Method Assessments for Footings on Cohesionless Soils

Methods by:	Study by Gifford et al. (1987)	Study by Baus (1992)	Study by Briaud & Gibbens (1997)	Study by Sargand et al. (1997)
Alpan	---	Unconservative	---	---
Briaud	---	---	Reliable (C)	---
Burland-Burbidge	Reliable	---	Reliable (C)	Unconservative
D'Appolonia	Reliable	---	---	Unconservative
DeBeer	---	Conservative	Unconservative	---
Hough	Conservative	Conservative	---	Reliable
Menard-Rousseau	---	---	Unconservative	---
Meyerhof	---	Conservative	Unconservative	---
Peck-Bazaraa	Unconservative	Reliable	Reliable (UC)	Unconservative
Peck-Hanson-Thornburn	---	---	Unconservative	---
Schmertmann-CPT	Conservative	Reliable	Unconservative	Conservative
Schmertmann-DMT	---	---	Reliable (UC)	---
Schultz-Sherif	---	---	Conservative	---
Terzaghi-Peck	---	---	Unconservative	Unconservative

[Note] "C" = Conservative (Overprediction); UC = Unconservative (Underprediction).

Sargand et al. (2003) revisited the spread footing project from 1997, where four CPT-based settlement prediction methods were preformed and evaluated at two highway bridge construction sites. The four methods consisted of those proposed by Amar et al. (1989), DeBeer (1965), Meyerhof (1965), and Schmertmann (1970, 1978). The results of the study showed that the Schmertmann method is more reliable than the other methods in estimating the settlements of shallow foundations resting on cohesionless soils. This method took into account the varying deformations experienced by different layers within the influence zone. The DeBeer method is a little less accurate than the Schmertmann method, but still considers the soil to be in layers. The methods by Amar et al. and Meyerhof considered the soils in the influence zone as one homogenous elastic material and were not recommended by the researchers.

In a study by Shahin et al. (2002), ANN's were used in attempt to acquire more precise settlement predictions for cohesionless soils. Their study was fueled by the facts that most geotechnical methods for predicting the settlement of shallow foundations on cohesionless soils did not satisfy the desired level of accuracy and consistency. A sensitivity study revealed that soil compressibility (SPT-N value), footing width (B), and bearing pressure (q) were the most significant factors affecting settlement. The models performance was compared to the settlement predictions made by select geotechnical methods, Meyerhof (1965), Schultze-Sherif (1973), and Schmertmann et al. (1978). The results showed that the ANN models performed well more consistently, outperforming the traditional methods. The selected geotechnical methods worked well for small settlement cases. Both the Meyerhof (1965) and Schultze-Sherif (1973) methods generally underpredicted larger settlements, while the method by Schmertmann et al. (1978) overpredicted larger settlements.

Lee and Salgado (2003) examined the load-settlement response of vertically loaded footings, tested at the Texas A & M University campus. The finite element method based on nonlinear models and the conventional method proposed by Schmertmann were used. The results showed that the finite element analysis produced the load-settlement response of the actual footing better than the conventional model by Schmertmann. The outcome of their analysis reinforced their belief that the analytical method for spread footings resting on sand must be more realistic than simple elastic models because well-designed footings induce stress-strain states in the sand that are somewhere between the linear elastic range and the perfect plastic range.

2.5.2 Footings on Cohesive Granular Soils

The settlements of sandy soils are traditionally estimated on the basis of SPT-N values, while the settlements of clayey soils are estimated using consolidation test results. There are a large number of soil types, between these two opposite soils, that contains both granular and fine particles. The settlements of these "cohesive granular" soils may pose a unique problem, since they possess characteristics of both cohesive and cohesionless soils.

Picornell and del Monte (1988) investigated settlement of a steel mill factory at a site in Spain, containing a stratum of loose to medium dense silty sand. SPT, plate load, and laboratory consolidation tests were performed to characterize the stratum. Meyerhof

(1965) and Peck-Hanson-Thornburn (1974) made settlement predictions from SPT-N values. These values were within ± 20% of the actual settlement, provided that no allowance be made for the presence of the water table. Using the consolidation test results, the settlements calculated overpredict the actual settlement by approximately 10% to 20%. The consolidation test results therefore would be a viable alternative to estimate the settlement of cohesive granular soils provided that they contain sufficient amounts of fines for recovery of reasonably undisturbed samples.

2.5.3 Footings on Cohesive Soils

The methods used for estimating the settlement of a footing resting on cohesive soils have been fairly unified, although the mechanism involved in the cohesive soil case is more complicated. This is mainly due to the classical work by Terzaghi on his one-dimensional consolidation theory in 1942. Different empirical equations have been proposed to estimate the compression index or the recompression index resulting in some minor variations of the main theory.

Duncan (1993) discussed in his Terzaghi Lecture inherent limitations of conventional consolidation analysis. Two case histories, Bay Farm Island in San Francisco Bay and Kansai Airport near Osaka, Japan, were cited to show that consolidation can induce large settlements. He pointed out some fundamental limitations involved in the current application of the classic theory by revisiting Terzaghi's theory. Improved methods are needed to determine if embedded sand layers will provide drainage. These methods also can take into account variations in the coefficient of consolidation and nonlinear stress-strain relationship.

Oweis (2001) researched the use of spread footings on overconsolidated clays. The settlements for each of the piers were determined to be conservative. The estimated values were on average between 40% and 95% greater than the measured values. For the predictive methods, the total settlement for clay foundations includes both elastic and consolidation settlement. The methods were sufficient enough to predict total settlement but not satisfactory for differential settlements. Some of the settlements were significantly underpredicted and can be explained by the fact that the excess pore pressure was not dissipated before construction started.

2.6 COST EFFECTIVENESS

Few foundation types satisfy all the design considerations when planning highway bridge construction. The bridge design engineer should select the most economical option to be used. The spread footing is the most basic foundation type and usually costs less than the other types (deep foundations). Although detailed cost estimations are seldom published, some have researched the savings for using spread footings instead of deep foundations.

Briaud and Gibbens (1997) state that the best foundation is designed to the specified standards while also minimizing the cost and optimizing the safety. They estimated that spread footing foundations are approximately 20% less expensive than deep foundations. Also, they concluded in 1999 that 50% of the total bridge cost comes from the foundation costs. For this reason spread footings should always be considered when designing the bridge foundation.

Briaud and Gibbens (1997) outlined the cost savings the spread footing design may be able to provide on a national scale. According to them, there are approximately 600,000 bridge structures in the U.S. If each of them were replaced today, the cost would be $300 billion. To replace a typical bridge, the cost of using shallow foundations may be $90,000 less than the cost of using deep foundations. Approximately 6,000 bridges are built each year, so if one assumes that 50% of these bridges are supported by spread footings, the potential savings to the taxpayers will be $270 million.

Amar et al. (1984) determined that the cost of spread footings is approximately 17% to 67% the cost of deep foundations. Shields et al. (1980) designed two foundations of equal size for four different sites. Each site had designs for spread footing use and also deep foundations. The difference in cost for the foundations was limited to the foundation types. In each case, a saving was found when spread footings were used.

DiMillio (1982) presented three cases where a cost analysis is made between the two foundation options, shallow and deep, on WSDOT bridge construction projects. The design and construction of abutments for Ellingston Road Bridge was the first case. This site's subsurface consisted of approximately 24 ft (7.3 m) of embankment soil fill, underlain by a 45-ft (13.7-m) thick silty fine to coarse sand & gravel deposit, containing scattered compressible soil layers. An allowable bearing pressure of 3 tsf (290 kPa) was determined for this subsurface condition. The size of the spread footing corresponding to the allowable bearing pressure was 6 ft (1.8 m) wide by 46 ft (14.0 m) long. The cost of concrete for the spread footing abutments were $2,300 each and the cost of excavation for each abutment was $1,300. The alternate pile foundation cost was determined to be $21,900. The savings for this three span bridge was $14,700, or 67%.

The second case was the design and construction of abutments for Pilchuck River Bridge. The site's subsurface consisted of 29 ft (8.8 m) to 41 ft (12.5 m) of embankment soil fill. The spread footing and pile cap were designed to share the same size of 8 ft (2.4 m) in width by 74 ft (22.6 m) in length. Spread footings were determined to be 54% the cost of deep foundations.

The last case, the design of the North Fort Lewis Interchange, was designed with the two abutments on piles and the interior piers on spread footings. The piles however were only used for one of the abutments, and a spread footing foundation was used instead. The total savings of $6,975 was due to only the replacement of the pile foundation material for a spread footing foundation. This is a 65% savings from the total cost with piers.

Table 2.3 summarizes the cost comparisons between the pile foundation and spread footing options for each of the field cases. The average savings is around 60%, however the prices are slightly outdated.

Table 2.3: Summary of Cost Comparisons

Bridge Project	Price for Foundation Type		
	Spread Footings	Piles	Savings
Ellingston Road Crossing	$7,200	$21,900	$14,700
Pilchuck River Bridge	$31,348	$57,725	$26,377
North Ft. Lewis Interchange	$9,003	$25,382	$16,379

CHAPTER 3: AASHTO LRFD BRIDGE DESIGN SPECIFICATIONS

3.1 GENERAL

The American Association of State Highway & Transportation Officials (AASHTO) has been setting national standards for the design of bridges since 1931. In 1987, the AASHTO subcommittee reassessed U.S. bridge specifications and reviewed foreign design specifications and codes. A recommendation was made to adjust the conventional working stress design (WSD) so that the variability in the loadings and the material properties are reflected. With this new philosophy, the Load and Resistance Factor Design (LRFD) was implemented on the basis of recent developments in structural engineering and statistical methods. Sections 10.4, 10.5, and 10.6, contained in the AASHTO LRFD Bridge Design Specifications (2004), are relevant to the design and analysis of bridge spread footing foundations and are summarized in this chapter. Section 10.4 contains information on soil and rock properties, Section 10.5 explains limit states and resistance factors, and Section 10.6 details the design of spread footings.

Spread footings are designed based on bearing soil characteristics, the size of the foundation, and the construction materials used. An adequate soil bearing capacity, which will aid in determining whether there will be an excessive amount of settlement, must be provided for all spread footings designs. If a poor material is used beneath the foundation, problems will arise in both bearing capacity and settlement. A weak soil or rock should not be used if it will not be able to withstand the load applied without significant movements.

3.2 SOIL PROPERTIES

To begin the design of the spread footings, subsurface exploration must be performed over the bridge construction area. Insitu soil tests are performed to obtain information on the soil layers below the footings. The Standard Penetration Test (SPT) and Cone Penetration Test (CPT), along with other tests, can be administered to collect soil properties and achieve a better understanding of the soil conditions. Some tests can be used for all soil types; however others, such as the Vane Shear Test (VST) and Pressuremeter Test (PMT), apply only to a specific type and not others.

For the tests that require borings to be administered, the borings should be spread out and taken near the locations of the footings. At least one boring exploration should be taken for each substructure on the site. The exploration should penetrate through all unsuitable material and to a depth where the increase in stress from the applied load is less than ten percent of the overburden pressure at the same depth. If bedrock is encountered before the depth required is penetrated, then the exploration should go at least ten feet into the bedrock.

3.3 PROPERTIES OF ROCK MASS

Since rock material can be inconsistent in form, it is important for the rock to be tested. A few tests include an unconfined compression test, a point load test, and a splitting tensile test. Each test must have intact rock samples. Table 3.1 lists five different parameters and the ranges of values from which the rock is rated based on the Council of Scientific and Industrial Research (CSIR). Rock Quality Designation (RQD) is the

Table 3.1: Rock Classification Parameters and Ratings

<table>
<tr><th colspan="3">PARAMETERS</th><th colspan="7">RANGE OF VALUES</th></tr>
<tr><td rowspan="3">1</td><td rowspan="2">Strength of intact rock material</td><td>Point load strength index</td><td>>1200 psi</td><td>600 to 1200 psi</td><td>300 to 600 psi</td><td>150 to 300 psi</td><td colspan="3">For this low range - uniaxial compressive test is preferred</td></tr>
<tr><td>Uniaxial compressive strength</td><td>>30000 psi</td><td>15000 to 30000 psi</td><td>7500 to 15000 psi</td><td>3600 to 7500 psi</td><td>1500 to 3600 psi</td><td>500 to 1500 psi</td><td>150 to 500 psi</td></tr>
<tr><td colspan="2">Relative Rating</td><td>15</td><td>12</td><td>7</td><td>4</td><td>2</td><td>1</td><td>0</td></tr>
<tr><td rowspan="2">2</td><td colspan="2">Drill core quality RQD</td><td>90% to 100%</td><td>75% to 90%</td><td>50% to 75%</td><td>25% to 50%</td><td colspan="3"><25%</td></tr>
<tr><td colspan="2">Relative Rating</td><td>20</td><td>17</td><td>13</td><td>8</td><td colspan="3">3</td></tr>
<tr><td rowspan="2">3</td><td colspan="2">Spacing of joints</td><td>>10 ft</td><td>3 to 10 ft</td><td>1 to 3 ft</td><td>2 in to 1 ft</td><td colspan="3"><2 in</td></tr>
<tr><td colspan="2">Relative Rating</td><td>30</td><td>25</td><td>20</td><td>10</td><td colspan="3">5</td></tr>
<tr><td rowspan="2">4</td><td colspan="2">Conditions of joints</td><td>Very rough surfaces, Not continuous, No separation, Hard joint wall rock</td><td>Slightly rough surfaces, Separation <0.05 in, Hard joint wall rock</td><td>Slightly rough surfaces, Separation <0.05 in, Soft joint wall rock</td><td>Slicken-sided surfaces, OR Gouge <0.2 in thick, OR Joints open 0.05 to 0.2 in, continuous joints</td><td colspan="3">Soft gouge >0.2 in thick, OR Joints open >0.2 in, Continuous joints</td></tr>
<tr><td colspan="2">Relative Rating</td><td>25</td><td>20</td><td>12</td><td>6</td><td colspan="3">0</td></tr>
<tr><td rowspan="4">5</td><td rowspan="3">Ground water conditions (use one of the three evaluation criteria as appropriate to the method of exploration)</td><td>Inflow per 30 ft tunnel length</td><td>None</td><td><400 gal/hr</td><td>400 to 2000 gal/hr</td><td colspan="4">>2000 gal/hr</td></tr>
<tr><td>Ratio = joint water pressure/ major principal stress</td><td>0</td><td>0.0 to 0.2</td><td>0.2 to 0.5</td><td colspan="4">>0.5</td></tr>
<tr><td>General Condition</td><td>Completely Dry</td><td>Moist only (interstitial water)</td><td>Water under moderate pressure</td><td colspan="4">Severe water problems</td></tr>
<tr><td colspan="2">Relative Rating</td><td>10</td><td>7</td><td>4</td><td colspan="4">0</td></tr>
</table>

percentage of the core's total length that has pieces longer than 4 inches (100 mm) intact. The relative ratings for each parameter give a qualitative value. All of the relative ratings are then combined and a rock mass rating (RMR) is determined, where 100 is the highest rating. Table 3.2 gives descriptions for each rating based on CSIR rock mass classes.

Table 3.2: Rock Description Based on Ratings

RMR Rating	100 to 81	80 to 61	60 to 41	40 to 21	<20
Class No.	I	II	III	IV	V
Description	Very good rock	Good rock	Fair rock	Poor rock	Very poor rock

Hoek and Brown (1988) developed criteria to evaluate the shear strength of fractured rock. They used three parameters to define rock strength, the unconfined compression strength, q_u, and two dimensionless constants, m and s. Values for the two constants can be found in Table 3.3 and are based on rock type and quality. Equation 3-1 below shows the shear strength of the rock mass by Hoek and Brown's method.

$$\tau = \frac{1}{8}(\cot\phi - \cos\phi)m * q_u \tag{3-1}$$

where $\tau =$ shear strength of rock mass; $\phi =$ friction angle; and $q_u =$ average unconfined compressive strength.

As the friction angle is not a given value, it must be calculated. Equation 3-2 below will give its value.

$$\phi = \tan^{-1}\{4h\cos^2[30 + 0.33\sin^{-1}(h^{-1.5})] - 1\}^{-0.5} \quad (3\text{-}2)$$

where $h = 1 + \frac{16(m\sigma'_n + sq_u)}{3m^2 q_u}$; and σ'_n = effective normal stress.

Table 3.3: Material Constants for Different Rock Types and Qualities

Rock Quality	Constants	Rock Type: A= dolomite, limestone, marble; B= mudstone, siltstone, shale, slate; C= sandstone, quartzite; D= andesite, dolerite, diabase, rhyolite; E= amphibolite, gabbro gneiss, granite, norite, quartz-diorite				
		A	B	C	D	E
INTACT ROCK SAMPLES Laboratory size specimens free from discontinuities CSIR rating: RMR = 100	m s	7.00 1.00	10.00 1.00	15.00 1.00	17.00 1.00	25.00 1.00
VERY GOOD QUALITY ROCK MASS Tightly interlocking undisturbed rock with unweathered joints at 3 to 10 ft CSIR rating: RMR = 85	m s	2.40 0.082	3.43 0.082	5.14 0.082	5.82 0.082	8.567 0.082
GOOD QUALITY ROCK MASS Fresh to slightly weathered rock, slightly disturbed with joints at 3 to 10 ft CSIR rating: RMR = 65	m s	0.575 0.00293	0.821 0.00293	1.231 0.00293	1.395 0.00293	2.052 0.00293
FAIR QUALITY ROCK MASS Several sets of moderately weathered joints spaced at 1 to 3 ft CSIR rating: RMR = 44	m s	0.128 0.00009	0.183 0.00009	0.275 0.00009	0.311 0.00009	0.458 0.00009
POOR QUALITY ROCK MASS Numerous weathered joints at 2 to 12 in.; some gouge. Clean compacted waste rock. CSIR rating: RMR = 23	m s	0.029 3×10^{-6}	0.041 3×10^{-6}	0.061 3×10^{-6}	0.069 3×10^{-6}	0.102 3×10^{-6}
VERY POOR QUALITY ROCK MASS Numerous heavily weathered joints spaced < 2 in. with gouge. Waste rock with fines. CSIR rating: RMR = 3	m s	0.007 1×10^{-7}	0.010 1×10^{-7}	0.015 1×10^{-7}	0.017 1×10^{-7}	0.025 1×10^{-7}

For intact rock masses where the type of rock is known, Poisson's ratio and the elastic modulus can be estimated using Tables 3.4 and 3.5, respectively. These tables are modified after Kulhawy and Goodman (1987). Since these values are only estimates, insitu tests should be performed to determine actual values. Poisson's ratio should be determined from tests on intact rock cores whenever possible. The value of the elastic modulus obtained from the table is compared to the values determined by Equations 3-3 and 3-4, where the smallest of the three is used. The reduction factor (E_m/E_i) in Equation 3-4 is determined in Table 3.6, by Carter and Kulhawy (1988). The reduction factor is based on RQD.

Table 3.4: Values of Poisson's Ratio Depending on Rock Type

Rock Type	No. of Values	No. of Rock Types	Poisson's ratio, ν			Standard Deviation
			Minimum	Mean	Maximum	
Granite	22	22	0.09	0.2	0.39	3.55
Gabbro	3	3	0.16	0.18	0.2	0.97
Diabase	6	6	0.2	0.29	0.38	1.78
Basalt	11	11	0.16	0.23	0.32	2.6
Quartzite	6	6	0.08	0.14	0.22	2.32
Marble	5	5	0.17	0.28	0.4	2.49
Gneiss	11	11	0.09	0.22	0.4	2.31
Schist	12	11	0.02	0.12	0.31	3.18
Sandstone	12	9	0.08	0.2	0.46	1.19
Siltstone	3	3	0.09	0.18	0.23	1.65
Shale	3	3	0.03	0.09	0.18	1.45
Limestone	19	19	0.12	0.23	0.33	3.73
Dolostone	5	5	0.14	0.29	0.35	3.44

Table 3.5: Values of Elastic Modulus Depending on Rock Type

Rock Type	No. of Values	No. of Rock Types	Elastic Modulus, E_i (PSI x 10^6)			Standard Deviation (PSI x 10^6)
			Minimum	Mean	Maximum	
Granite	26	26	0.93	7.64	14.5	3.55
Diorite	3	3	2.48	7.45	16.2	6.19
Gabbro	3	3	9.8	11	12.2	0.97
Diabase	7	7	10	12.8	15.1	1.78
Basalt	12	12	4.2	8.14	12.2	2.6
Quartzite	7	7	5.29	9.59	12.8	2.32
Marble	14	13	0.58	6.18	10.7	2.49
Gneiss	13	13	4.13	8.86	11.9	2.31
Slate	11	2	0.35	1.39	3.79	0.96
Schist	13	12	0.86	4.97	10	3.18
Phyllite	3	3	1.25	1.71	2.51	0.57
Sandstone	27	19	0.09	2.13	5.68	1.19
Siltstone	5	5	0.38	2.39	4.76	1.65
Shale	30	14	0.001	1.42	5.6	1.45
Limestone	30	30	0.65	5.7	13	3.73
Dolostone	17	16	0.83	4.22	11.4	3.44

$$E_m = 145{,}000 * \left[10^{\left(\frac{RMR-10}{40}\right)} \right] \tag{3-3}$$

$$E_m = \left(E_m / E_i \right) * E_i \tag{3-4}$$

where E_m = elastic modulus of rock mass; E_i = elastic modulus of intact rock; RMR = rock mass rating ; and E_m/E_i = reduction factor.

Table 3.6: E_m/E_i Ratio Based on Rock Quality Designation

RQD (Percent)	E_m/E_i	
	Closed Joints	Open Joints
100	1.00	0.60
70	0.70	0.10
50	0.15	0.10
20	0.05	0.05

3.4 STANDARD PENETRATION TEST (SPT)

The Standard Penetration Test (SPT) is one of the most common insitu test methods for soils. When an SPT test has been conducted, the blow counts N (number of blows per 12 inches of penetration) are obtained and used to estimate soil properties. These properties include the internal friction angle and the relative density, along with a relative stratigraphy of the subsurface. To correct for the soil's overburden pressure, a correction factor, c_n, is applied to the blow counts and the corrected blow counts are denoted by N_1. Equations 3-5 and 3-6 show the relationship between the variables.

$$N_1 = c_n N \qquad (3\text{-}5)$$

$$c_n = 0.77 \log_{10}\left(\frac{20}{\sigma'_v}\right) \qquad (3\text{-}6)$$

where $c_n < 2.0$; and σ'_v = vertical effective stress (tsf).

The blow counts may need to be corrected a second time depending on the efficiency of the hammer. A conventional drop hammer has an efficiency of 60%, while an automatic trip hammer has an efficiency of 80%. If the conventional hammer is used, then the blow counts need not be corrected for, however the automatic hammer results in a need to correct the blow counts for hammer efficiency. To correct for this, Equation 3-7 should be used.

$$N_{1(60)} = \frac{ER}{60\%} * N_1 \qquad (3\text{-}7)$$

where ER = efficiency of the hammer used (%).

The drained friction angle for granular soils can be determined from the corrected blow counts and Table 3.7, modified after Bowles (1977). Since the SPT test is not dependable for rock and gravel materials, Table 3.8 and Figure 3.1 should be used to estimate the unconfined compressive strength and the friction angle from effective normal stress. Both the table and figure are based on findings by Terzaghi, Peck, and Mesri (1996).

Table 3.7: ϕ Values from Corrected Blow Counts

$N1_{60}$	ϕ (degrees)
< 4	25-30
4	27-32
10	30-35
30	35-40
50	38-43

Table 3.8: Compressive Strength Based on Rock Fill Type

Rock Fill Grade	Particle Unconfined Compressive Strength (psi)
A	>32000
B	24000 to 32000
C	18000 to 24000
D	12000 to 18000
E	≤12000

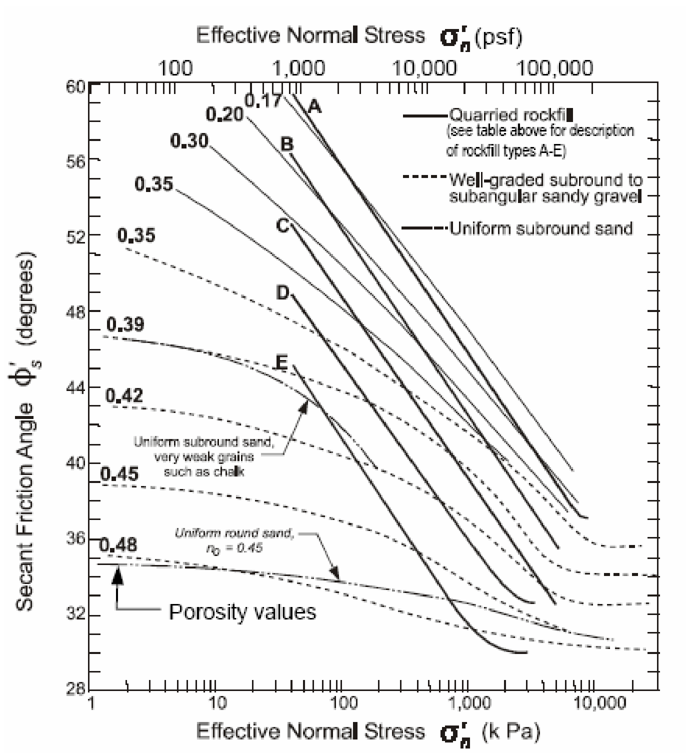

Figure 3.1: Drained Friction Angle for Gravels and Rock Fills

3.5 BEARING PRESSURE

The bearing stress of soil and rock material must be established in order to determine whether the material is suitable for foundations. From Table 3.9, modified after the Department of the Navy (1982), it can be seen that different compositions of soils and rocks will yield distinct values for the bearing stress under and around the footing. These bearing stresses listed limit the settlement to one inch. Rock material has a much higher allowable bearing stress than soil compositions do.

The distribution of bearing stress under the foundation depends on the material that supports the footing. For soils, cohesionless and cohesive, the stress on the effective area is assumed to be uniform. However, a foundation supported by rock material has a bearing stress distribution that is assumed to vary linearly.

Table 3.9: Bearing Stress for Types and Consistency of Soils

Type of Bearing Material	Consistency in Place	Bearing Stress (TSF)	
		Ordinar y Range	Recommended Value of Use
Massive crystalline igneous and metamorphic rock: graphite, diorite, basalt, gneiss, thoroughly cemented conglomerate (sound condition allows minor cracks)	Very hard, sound rock	60 to 100	80
Foliated metamorphic rock: slate, schist (sound condition allows minor cracks)	Hard sound rock	30 to 40	35
Sedimentary rock: hard cemented shales, siltstone, sandstone, limestone without cavities	Hard sound rock	15 to 25	20
Weathered or broken bedrock of any kind, except highly argillaceous rock (shale)	Medium hard rock	8 to 12	10
Compaction shale or other highly argillaceous rock in sound condition	Medium hard rock	8 to 12	10
Well-graded mixture of fine- and coarse-grained soil: glacial till, hardpan, boulder clay (GW-GC, GC, SC)	Very dense	8 to 12	10
Gravel, gravel-sand mixture, boulder-gravel mixtures (GW, GP, SW, SP)	Very dense Medium dense to dense Loose	6 to 10 4 to 7 2 to 6	7 5 3
Coarse to medium sand, and with little gravel (SW, SP)	Very dense Medium dense to dense Loose	4 to 6 2 to 4 1 to 3	4 3 1.5
Fine to medium sand, silty or clayey medium to coarse sand (SW, SM, SC)	Very dense Medium dense to dense Loose	3 to 5 2 to 4 1 to 2	3 2.5 1.5
Fine sand, silty or clayey medium to fine sand (SP, SM, SC)	Very dense Medium dense to dense Loose	3 to 5 2 to 4 1 to 2	3 2.5 1.5
Homogeneous inorganic clay, sandy or silty clay (CL, CH)	Very dense Medium dense to dense Loose	3 to 6 1 to 3 0.5 to 1	4 2 0.5
Inorganic silt, sandy or clayey silt, varied silt-clay-fine sand (ML, MH)	Very stiff to hard Medium stiff to stiff Soft	2 to 4 1 to 3 0.5 to 1	3 1.5 0.5

3.5.1 Cohesionless Soil

The drained strength of granular soils is evaluated by SPT tests as discussed previously. The drained friction angle is obtained directly from the corrected SPT-N blow count values. As stated in Section 3.4, Table 3.7 gives the relationship between the two. The friction angle should be selected carefully, keeping in mind that finer soils fall toward the low end and coarser grained soils toward the high end of the range. It can also be seen in the table that as the number of blow counts increases, so does the friction angle. In cohesionless soils, no excess pore water pressure will develop because the soil type has excellent drainability.

3.5.2 Cohesive Soils

In cohesive soils, when loading occurs rapidly and the pore pressure does not have a chance to dissipate, the undrained stress parameters should be used. The undrained shear strength is used for short-term effects of clays. However, if loading occurs more slowly or if the condition of the clay for long-term effects is needed, then drained stress parameters should be utilized.

3.5.3 Rock Mass

If the footing rests on rock material, the resulting bearing stress value from Table 3.9 may be larger than the unconfined compressive strength of the rock and/or the nominal resistance of concrete. The value to be used for the bearing stress should be the smaller of the unconfined compressive strength and the nominal resistance. The nominal resistance of concrete is 0.3*f'$_c$, where f'$_c$ = 28-day compressive strength.

3.6 BEARING CAPACITY

3.6.1 Cohesionless and Cohesive Soils

The nominal bearing capacity of a soil layer is determined using measured soil parameters that correspond to the soil conditions, applied loading, and the soil strength. The original concept was developed by Terzaghi & Peck. The drained strength parameters and the effective stress analysis discussed before are used to determine the nominal bearing resistance of a cohesionless soil. The bearing resistance of a cohesive soil is evaluated for undrained shear strength and total stress analysis. Munfakh, et al. (2001) described the bearing capacity with three terms, cohesion, surcharge, and unit weight, respectively, as seen in Equation 3-8.

$$q_n = cN_{cm} + \gamma D_f N_{qm} C_{wa} + 0.5\gamma B N_{\gamma m} C_{wb} \tag{3-8}$$

where $N_{cm} = N_c s_c i_c$; $N_{qm} = N_q s_q d_q i_q$; $N_{\gamma m} = N_\gamma s_\gamma i_\gamma$; c = undrained shear strength; N_c, N_q, N_γ = bearing capacity correction factors; γ = unit weight of soil; D_f = embedment depth of footing; B = footing width; C_{wa}, C_{wb} = groundwater correction factors; s_c, s_q, s_γ = shape correction factors; i_c, i_q, i_γ = inclination correction factors; and d_q = depth correction factor.

For purely cohesionless soils, the cohesion term (first term) in the bearing capacity equation (Equation 3-8) is dropped. The unit weight term (third term) of the equation will drop for soils that are completely cohesive, i.e. have a friction angle of zero. For all other soil materials, each of the three terms remains in the equation.

The bearing capacity correction factors, N factors, can be determined by using the internal friction angle of the soil beneath the footing. Table 3.10 gives a summary of values for each of the three N factors. N_c is from work by Prandtl (1921), while N_q is based on Reissner (1924) and N_γ from Vesic (1975). When the groundwater level is at a depth greater than one and a half times the width of the footing plus the depth of embedment, there is no effect on the bearing resistance. Above that depth, there is an effect on the resistance and the factors for groundwater depth should be used. These factors are presented in Table 3.11. The shape correction factors differ depending on whether the soil type is cohesionless ($\phi > 0°$) or cohesive ($\phi = 0°$) and should not be combined with the inclined load factor. Table 3.12 gives the equations that are used to determine the factors. The depth correction factor is based on the friction angle and the ratio of footing embedment depth to footing width. It should be taken as 1.0 if the soil above the footing bearing level is not as competent as those at the footing level. The values can be seen in Table 3.13 and should be interpolated in between the given values.

Table 3.10: N Factors Based on Friction Angle ϕ

ϕ	N_c	N_q	N_γ	ϕ	N_c	N_q	N_γ
0	5.14	1.0	0.0	23	18.1	8.7	8.2
1	5.4	1.1	0.1	24	19.3	9.6	9.4
2	5.6	1.2	0.2	25	20.7	10.7	10.9
3	5.9	1.3	0.2	26	22.3	11.9	12.5
4	6.2	1.4	0.3	27	23.9	13.2	14.5
5	6.5	1.6	0.5	28	25.8	14.7	16.7
6	6.8	1.7	0.6	29	27.9	16.4	19.3
7	7.2	1.9	0.7	30	30.1	18.4	22.4
8	7.5	2.1	0.9	31	32.7	20.6	26.0
9	7.9	2.3	1.0	32	35.5	23.2	30.2
10	8.4	2.5	1.2	33	38.6	26.1	35.2
11	8.8	2.7	1.4	34	42.2	29.4	41.1
12	9.3	3.0	1.7	35	46.1	33.3	48.0
13	9.8	3.3	2.0	36	50.6	37.8	56.3
14	10.4	3.6	2.3	37	55.6	42.9	66.2
15	11.0	3.9	2.7	38	61.4	48.9	78.0
16	11.6	4.3	3.1	39	67.9	56.0	92.3
17	12.3	4.8	3.5	40	75.3	64.2	109.4
18	13.1	5.3	4.1	41	83.9	73.9	130.2
19	13.9	5.8	4.7	42	93.7	85.4	155.6
20	14.8	6.4	5.4	43	105.1	99.0	186.5
21	15.8	7.1	6.2	44	118.4	115.3	224.6
22	16.9	7.8	7.1	45	133.9	134.9	271.8

Table 3.11: Groundwater Depth Correction Factors

D_w	C_{wa}	C_{wb}
0.0	0.5	0.5
D_f	1.0	0.5
$>1.5B+D_f$	1.0	1.0

Table 3.12: Shape Correction Factors

Factor	Friction Angle	Cohesion Term (s_c)	Unit Weight Term (s_γ)	Surcharge Term (s_q)
Shape Factors s_c, s_γ, s_q	$\phi = 0$	$1+\left(\dfrac{B}{5L}\right)$	1.0	1.0
	$\phi > 0$	$1+\left(\dfrac{B}{L}\right)\left(\dfrac{N_q}{N_c}\right)$	$1-0.4\left(\dfrac{B}{L}\right)$	$1+\left(\dfrac{B}{L}\tan\phi\right)$

Table 3.13: Embedment Depth Correction Factor

Friction Angle, ϕ (degrees)	D_f/B	d_q
32	1	1.20
	2	1.30
	4	1.35
	8	1.40
37	1	1.20
	2	1.25
	4	1.30
	8	1.35
42	1	1.15
	2	1.20
	4	1.25
	8	1.30

The following equations (Equations 3-9 to 3-12), from Vesic (1973), are used to determine the load inclination correction factors for cohesive and cohesionless soils:

$$i_\gamma = \left[1-\left(\frac{H}{(V+cBL\cot\phi)}\right)\right]^{(n+1)} \qquad \text{for all } \phi \qquad (3\text{-}9)$$

$$i_q = \left[1 - \frac{H}{\left(V + cBL\cot\phi\right)}\right]^n \qquad \text{for all } \phi \tag{3-10}$$

$$i_c = 1 - \left(\frac{nH}{cBLN_c}\right) \qquad \text{for } \phi = 0 \tag{3-11}$$

$$i_c = i_q - \left[\left(\frac{1 - i_q}{N_{q-1}}\right)\right] \qquad \text{for } \phi > 0 \tag{3-12}$$

where $n = \left[\frac{(2 + L/B)}{(1 + L/B)}\right]\cos^2\theta + \left[\frac{(2 + B/L)}{(1 + B/L)}\right]\sin^2\theta$; H = horizontal load (unfactored); B = footing width; L = footing length; V = vertical load (unfactored); and θ = projected direction of load in plane of footing.

Nominal bearing capacity can also be estimated using the results from the SPT tests. The average blow counts from the SPT test are corrected so they can be used in Equation 3-13.

$$q_n = \frac{N_{1(60)}B}{10}\left(C_{wa}\frac{D_f}{B} + C_{wb}\right) \tag{3-13}$$

The nominal capacity is factored using resistance factors that are based on the method used, the soil, and its condition at the strength limit state. Table 3.14 shows the values for the resistance factor. The factored resistance is determined by Equation 3-14 using the nominal bearing capacity and the resistance factors in Table 3.14.

$$q_r = \phi * q_n \tag{3-14}$$

where q_r = the factored bearing resistance; and ϕ = resistance factors.

Table 3.14: Resistance Factors for Shallow Foundations

METHOD/SOIL/CONDITION			RESISTANCE FACTOR
Bearing Resistance	ϕ	All Methods, soil and rock	0.45
		Plate Load Test	0.55
Sliding	ϕ_τ	Precast concrete placed on sand	0.90
		Cast-in-place concrete on sand	0.80
		Clay	0.85
		Soil on soil	0.90
	ϕ_{ep}	Passive earth pressure component of sliding resistance	0.50

3.6.2 Rock Mass

The RMR explained in Section 3.3 determines whether the rock mass is competent for supporting spread footings. More tests must be applied for weaker, incompetent rocks. The factored compressive resistance of the foundations should be smaller than the factored bearing stress. From the strength of the rock mass, the nominal resistance of the footings can be established.

3.7 SETTLEMENT

Settlement of spread footings is determined based on soil parameters that are established by testing the soil in the field and/or in the laboratory. The total settlement (S_t) includes elastic (S_e), primary consolidation (S_c), and secondary consolidation (S_s). Elastic settlement is the settlement that occurs immediately when loading is applied to the soil.

When the pore water is forced out of the soil voids, primary consolidation settlement begins. Secondary consolidation is usually a concern only for organic materials.

3.7.1 Cohesionless Soil

In cohesionless soils, deformation frequently begins as the loads are applied to the structure resulting in the occurrence of settlement during construction. Settlement from the direct load application, or elastic settlement, is the main movement in this type of soil. Consolidation settlement is often times indistinguishable from the elastic settlement, since pore water dissipates quickly in granular material.

The elastic half space method estimates the settlement of spread footings that are flexible and on infinitely deep homogenous soil. Spread footings for highway bridge applications are usually assumed rigid, but may actually function between completely rigid and completely flexible. Equation 3-15 is used to estimate the elastic settlement of the foundations.

$$S_e = \frac{q_o \sqrt{A}}{E_s \beta_z}\left(1 - \upsilon^2\right) \qquad (3\text{-}15)$$

where q_o = applied vertical stress; A = area of footing (L*B); E_s = Young's modulus of soil; β_z = rigidity factor; and υ = Poisson's ratio.

Rigidity factors can be determined by Table 3.15 and are based on the length to width (L/B) ratio and the rigidity of the footing. The accuracy of settlement relies heavily on the values estimated for Young's modulus and Poisson's ratio. Values for Young's modulus can be found in Table 3.16, as can values for Poisson's ratio. These values result from findings modified from the U.S. Department of the Navy (1982) as well as Bowles (1988).

Table 3.15: Rigidity Factor for Foundations (EPRI, 1983)

L/B	β_z	
	Flexible (average)	Rigid
Circular	1.04	1.13
1	1.06	1.08
2	1.09	1.10
3	1.13	1.15
5	1.22	1.24

The Hough method also computes immediate settlement estimation for cohesionless soils. For this method, an SPT test must be conducted and the blow counts corrected as explained in Section 3.4. This method is calculated by Equation 3-16.

$$S_e = \sum_{i=1}^{n} \Delta H_i = \sum_{i=1}^{n} H_c \frac{1}{C'} \log\left(\frac{\sigma'_o + \Delta\sigma_v}{\sigma'_o}\right) \tag{3-16}$$

where ΔH_i = elastic settlement of layer; n = number of soil layers within zone of influence; H_c = initial height of layer; C' = bearing capacity index; σ'_o = initial vertical effective stress; and $\Delta\sigma_v$ = increase in vertical stress.

Table 3.16: Values of Poisson's Ratio and Young's Modulus Based on Soil Type

Soil Type	Young's Modulus (tsf)	Poisson's Ratio
Clay: Soft sensitive	25-150	
Medium stiff to stiff	150-500	0.4-0.5 (undrained)
Very stiff	500-1000	
Loess	150-600	0.1-0.3
Silt	20-200	0.3-0.35
Fine Sand: Loose	80-120	
Medium dense	120-200	0.25
Dense	200-300	
Sand: Loose	100-300	0.20-0.36
Medium dense	300-500	
Dense	500-800	0.30-0.40
Gravel: Loose	300-800	0.20-0.35
Medium dense	800-1000	
Dense	1000-2000	0.30-0.40
Estimating E_s from SPT-N value		
Soil Type		Es (tsf)
Silts, sandy silts, slightly cohesive mixtures		$4N1_{60}$
Clean fine to medium sands and slightly silty sands		$7N1_{60}$
Coarse sands and sands with little gravel		$10N1_{60}$
Sandy gravel and gravels		$12N1_{60}$
Estimating E_s from q_c (static cone resistance)		
Sandy soils		$4q_c$

Each layer should be a maximum of 10 ft (3 m) thick, however typically the layers are about 5 ft (1.5 m) thick. The bearing capacity index depends on the type of soil the foundation rests on and therefore also on the corrected blow count value of the SPT test. Figure 3.2 correlates the blow counts and type of soil with the bearing capacity index and is based on original results by Hough (1959), modified by Cheney and Chassie (2000).

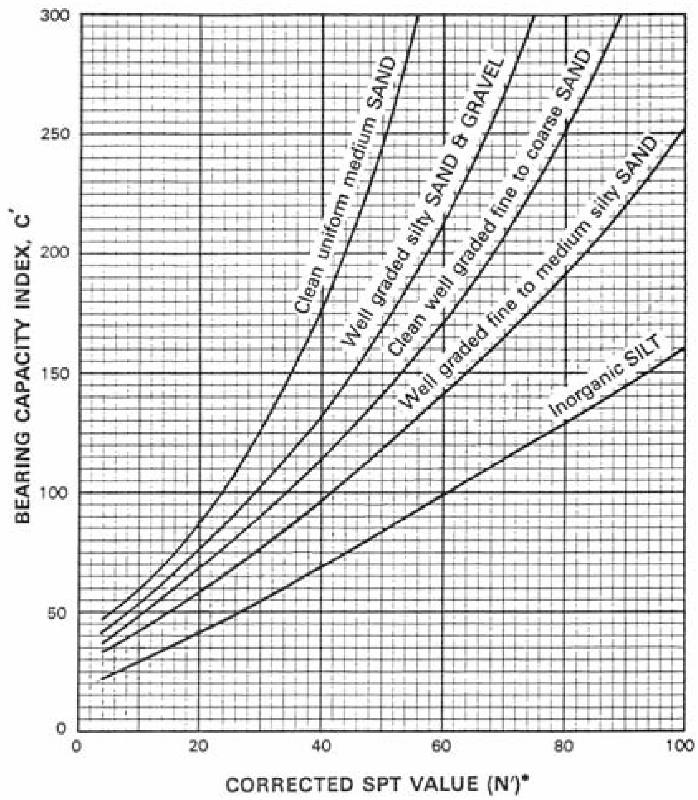

Figure 3.2: Bearing Capacity Index for Corrected SPT-N Values and Soil Types

3.7.2 Cohesive Soil

Cohesive soils undergo elastic, primary consolidation, and secondary settlement, however the elastic settlement is very small and sometimes neglected for design. Primary consolidation settlement usually takes quite a long time because the pore water pressure in the soil holds the applied load until the pore water dissipates. As a result of the pore water pressure within the soil, the consolidation is a time dependent settlement, and very important in cohesive soils.

Spread footings on cohesive soils should rest on overconsolidated clays, while normally and underconsolidated clays are not as suitable for the direct support of a footing. Overconsolidated clays have been stressed more in the past than the stress applied presently, which results in a settlement more like a granular soil's settlement. Underconsolidated clays have more stress currently than before and normally consolidated clays have the same stress now as in the past. The consolidation settlement is calculated differently for overconsolidated, normally consolidated, and underconsolidated clays, since the amount of settlement for each will differ. Equations 3-17, 3-18, and 3-19 show the calculation of this settlement.

For Overconsolidated ($\sigma'_p > \sigma'_o$):

$$S_c = \left[\frac{H_c}{1+e_o}\right]\left[C_{cr}\log\left(\frac{\sigma'_p}{\sigma'_o}\right) + C_c\log\left(\frac{\sigma'_f}{\sigma'_p}\right)\right] \tag{3-17}$$

For Normally Consolidated ($\sigma'_p = \sigma'_o$):

$$S_c = \left[\frac{H_c}{1+e_o}\right]\left[C_c\log\left(\frac{\sigma'_f}{\sigma'_p}\right)\right] \tag{3-18}$$

For Underconsolidated ($\sigma'_p < \sigma'_o$):

$$S_c = \left[\frac{H_c}{1+e_o}\right]\left[C_c\log\left(\frac{\sigma'_f}{\sigma'_{pc}}\right)\right] \tag{3-19}$$

where H_c = initial height of the soil layer; e_o = void ratio at initial vertical effective stress; C_r = recompression index; C_c = compression index; σ'_p = maximum past vertical effective stress; σ'_o = initial vertical effective stress; σ'_f = final vertical effective stress; and σ'_{pc} = current vertical effective stress.

The stresses are taken at the midpoint of each layer and the compression and recompression indices are determined from a consolidation compression curve for the soil. A standard compression curve can be seen in Figure 3.3. The values for C_r, C_c, and C_α can also be determined from Table 3.17, using soil parameters such as liquid limit (LL) and percent water content (w_n).

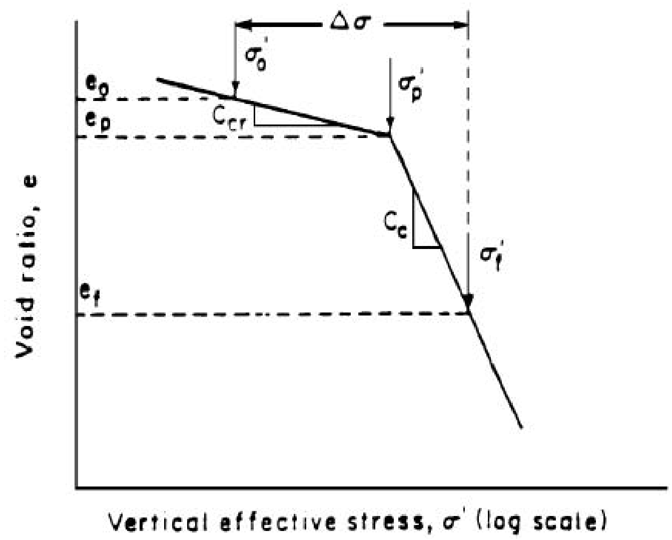

Figure 3.3: Consolidation Compression Curve (EPRI, 1983)

Table 3.17: Empirical Correlations for C_r, C_c, and C_α

Equation	Applicable Soils
$C_c = 0.009\ (LL - 10)$	Undisturbed clays of low to medium sensitivity
$C_c = 0.007\ (LL - 7)$	Remolded clays
$C_c = 0.01\ w_n$	Chicago clays
C_r = 10% to 20% of C_c	Most soils
$C_\alpha = 0.04\ C_c$	Inorganic clays and silts
$C_\alpha = 0.05\ C_c$	Organic clays and silts
$C_\alpha = 0.06\ C_c$	Peats

One dimensional (1-D) consolidation settlement can be determined for any time after the initial load is applied. The time, t, to get a certain percentage of the full consolidation settlement is found from Equation 3-20 below. Figure 3.4 compares the percent consolidation to the time factor. The length of the drainage path is the longest distance within the clay layer to a drainage boundary.

$$t = \frac{T(H_d)^2}{c_v} \tag{3-20}$$

where T = time factor; H_d = length of longest drainage path; and C_v = coefficient of consolidation.

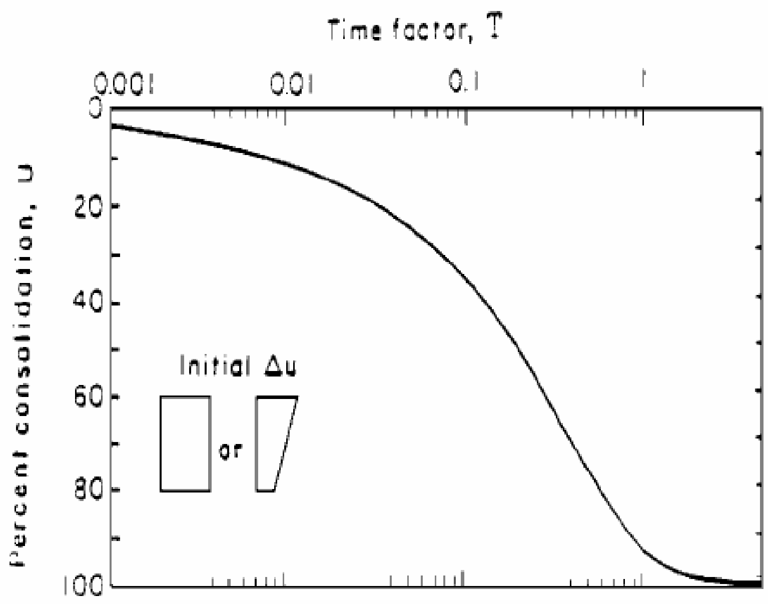

Figure 3.4: Time Factor Versus Percent Consolidation (EPRI, 1983)

When the width of a footing is small in comparison to the thickness, the loading is considered three dimensional (3-D) instead of one dimensional (1-D). The 3-D consolidation settlement is calculated by applying a reduction factor to the 1-D consolidation settlement. The ratio of the width to thickness of the footing and the overconsolidation ratio (σ'_p/σ'_o) are needed to determine the reduction factor from Figure 3.5.

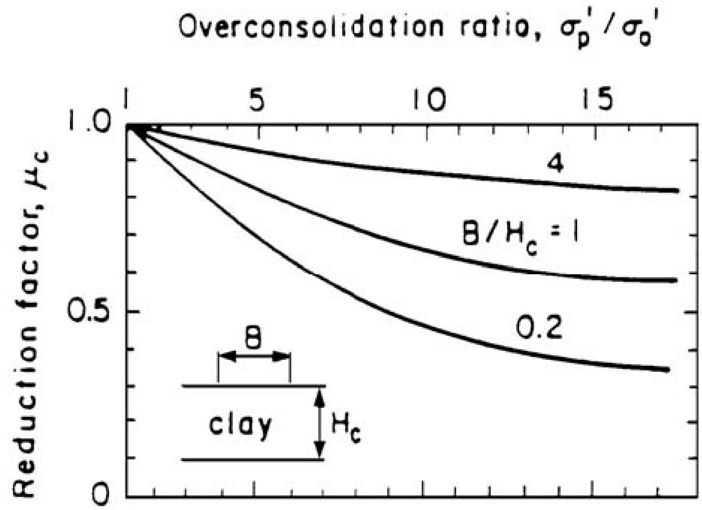

Figure 3.5: Reduction Factor for 3D Consolidation Settlement (EPRI, 1983)

Secondary settlement occurs in cohesive soils, however it is more prevalent in organic soils. Equation 3-21 gives values for secondary settlement, but should only be used as an estimate.

$$S_S = \frac{C_\alpha}{1+e_o} H_c \log\left(\frac{t_2}{t_1}\right) \tag{3-21}$$

where C_α = secondary compression index; t_1 = time when secondary settlement begins; and t_2 = time that corresponds to the service life of the structure.

3.7.3 Rock Mass

For foundations resting on rock, elastic settlement is the most important of the types of settlement. If the rock supporting the foundation is considered fair to good according to the cumulative rating found from Table 3.1 and the description in Table 3.2, then the elastic settlement is taken as 0.5 inches. However, if the rock is considered poor, then an analysis of the settlement must be done. The settlement for a poor rock, with RMR less than 10, is determined based on footing shape, by Equations 3-22 or 3-23.

Circular footings:

$$S_e = q_o(1-\upsilon^2)\frac{r(I_p)}{E_m} \tag{3-22}$$

where $I_p = \frac{\left(\sqrt{\pi}\right)}{\beta_z}$

Rectangular footings:

$$S_e = q_o(1-\upsilon^2)\frac{B(I_p)}{E_m} \tag{3-23}$$

where $I_p = \frac{\left(\sqrt{L/B}\right)}{\beta_z}$

The rigidity factor, β_z, is found in Table 3.15 for rigid footings. Poisson's ratio, υ, is determined as in Table 3.4 and the elastic modulus, E_m, as in Equation 3-3 or 3-4.

CHAPTER 4: ADDITIONAL GEOTECHNICAL METHODS

4.1 GENERAL

Chapter 3 described the methods that were recommended by AASHTO for estimating the settlement of spread footing foundations. These methods included elastic method for spread footings on rock mass, elastic method and Hough method for spread footings on cohesionless soil, and consolidation theory for spread footing on cohesive soils. There are several other geotechnical methods proposed for predicting spread footing performances. Most of these methods are for footings resting on cohesionless soils. Within this chapter the methods, not described in Chapter 3, the AASHTO LRFD Bridge Design Specifications (2004), will be outlined including assumptions, key formulas and tables and some comments provided by the proposer(s). Also mentioned in the chapter will be the determination of pressure magnitudes, footing's rigidity, and tilting of the footing and piers.

4.2 CONTACT PRESSURE

The contract pressure magnitude beneath a footing depends on applied loading, footing rigidity, and bearing soil type and stiffness. Theoretically, the contact pressure under a footing on sand is distributed in a concave upward fashion. However, the contact pressure under a footing on clay is believed to be distributed in a concave downward fashion. Contact pressure beneath the footing's edge is theoretically equal to zero if the footing is very flexible and will have a finite value if the footing is very rigid. Figure 4.1

gives a visual representation of the theoretical contact pressures beneath the footings for each of the different scenarios.

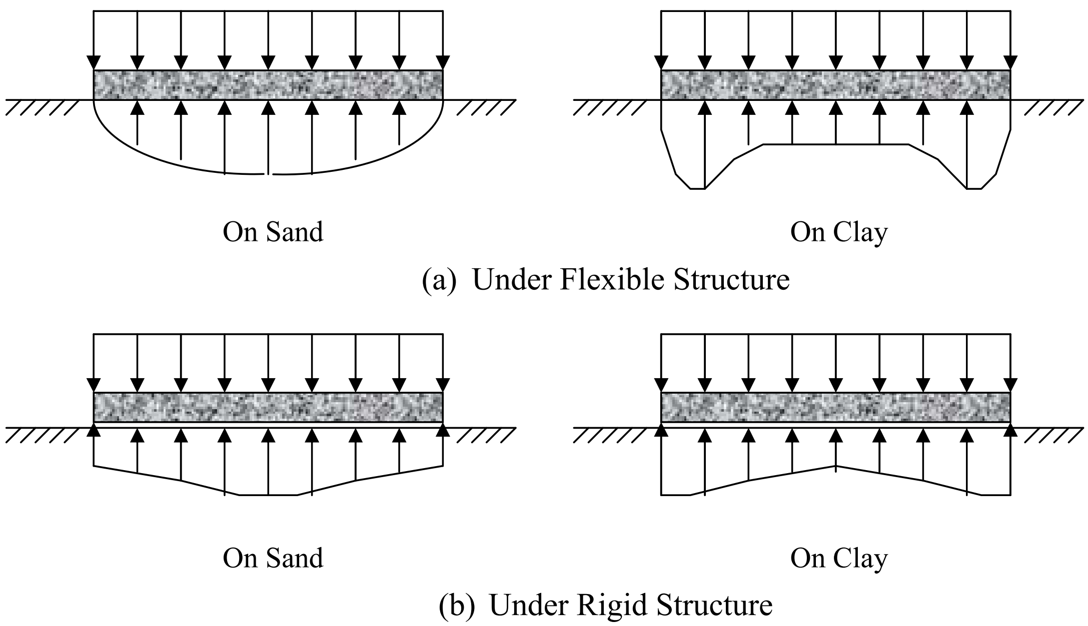

Figure 4.1: Theoretical Contact Pressure Distribution for Shallow Foundations
(after Johnson & Kavanagh, 1968)

The contact pressure distribution tends to be more linear when the footing is semi-rigid and confining stress acts over the contact area (due to the footing embedment depth), and may be estimated by the following concept given in Equation 4-1a.

$$q = \frac{P}{A} \pm \frac{M_L}{S_W} \pm \frac{M_W}{S_L} \qquad \text{(4-1 a)}$$

where q = contact pressure at any corner; P = applied pressure; A = footing area; M_W = bending moment about an axis taken along footing width; M_L = bending moment about an axis taken along footing length; S_W = section modulus of footing cross-section taken along footing width; and S_L = section modulus of footing cross-section taken along footing length.

The moment about the axis taken along the footing width (M_W) may be considered to be much less than that about the axis taken along the footing length (M_L), for spread footings supporting a bridge structure. Then, Equation 4-1a will simplify to result in Equation 4-1b.

$$q = \frac{P}{A} \pm \frac{M_L}{S_W} \qquad \text{(4-1 b)}$$

4.3 FOOTING RIGIDITY

In many design situations, the spread footings are automatically regarded as truly rigid structures. However, a footing should only be considered a rigid structure if it satisfies certain rigidity criteria. One rigidity criterion proposed by Gere and Timoshenko (1991) uses a parameter β, given in Equation 4-2, to classify the footings.

$$\beta = \left(\frac{k}{4EI}\right)^{0.25} \qquad \text{(4-2)}$$

where k = modulus of soil reaction; E = modulus of elasticity of the footing (or beam); and I = moment of inertia of the footing (or beam).

The footings are considered as short if $\beta L < 0.60$, medium-length if $0.6 < \beta L < 5$, and, long if $\beta L > 5$, where L = footing length. Short footings are regarded as rigid structures, since their deflections due to bending are negligible. Medium-length and long footings are not completely rigid structures.

Another rigidity criterion, proposed by Meyerhof (1953), determines if a footing acts as a rigid structure or a flexible structure. The relative stiffness factor is defined as shown in Equation 4-3.

$$K_r = \frac{EI}{E_s B^3} \tag{4-3}$$

where E_s = modulus of elasticity of bearing soil; and B = footing width.

The American Concrete Institute (ACI), which adopted the above criterion, states that a footing acts as a rigid structure if $K_r \geq 0.5$ and as a flexible structure if $K_r < 0.5$.

Tabsh and Al-Shawa (2005) realized that the Meyerhof approach did not address the effect of columns/walls attached to footings, so they revised the approach by incorporating the size of the columns/walls. Their method utilizes the modified relative stiffness factor, K_r', which is defined in Equation 4-4.

$$K_r' = \frac{Et^3}{k(1-\upsilon^2)(B-b)^2(L-\ell)^2} \tag{4-4}$$

where t = uniform footing thickness; υ = Poisson's ratio of bearing soil; B = overall footing width; b = wall/combined column dimension along the footing width; L = overall footing length; and ℓ = wall/combined column dimension along the footing length.

Based on some finite element modeling results, they concluded that the footing should be analyzed as a rigid footing if $K'_r > 1.0$.

For footings classified as rigid structures by these criteria, the soil pressure beneath the footing can be determined using simple strength of materials calculations given by Equation 4-1. This includes determination of soil pressures, vertical displacements, shear, and bending moments. By classifying the footing as non-rigid, it must be designed as a flexible member on elastic soil supports. An underestimation of the maximum bearing pressure and settlement occurs when a flexible footing is treated as a rigid one.

4.4 SETTLEMENT OF FOOTING ON COHESIONLESS SOILS

4.4.1 Alpan Method

Alpan (1964) proposed a formula which approximates the settlement using a correlation of SPT data and the settlement of a 1-ft square loading plate. Equation 4-5 gives the expression for the settlement of a footing by this method.

$$S_e = m'\left(\frac{2B}{1+B}\right)^2 \frac{\alpha_0}{12} q \tag{4-5}$$

where S_e = immediate settlement (ft); m′ = shape factor; B = footing width (ft); α_0 = parameter; and q = applied bearing pressure (tsf).

The shape factor, m′, is determined by Equation 4-6. As for the parameter, α_0, it is obtained using an average corrected SPT-N value. The SPT-N value is corrected for 60 percent of the input energy. This was described in Section 3.4. This corrected SPT-N value and the effective overburden pressure are used in Figure 4.2 to obtain an adjusted N' value by the Terzaghi and Peck curve. The N' value is then used in Figure 4.3 to determine α_0.

$$m' = (L/B)^{0.39} \tag{4-6}$$

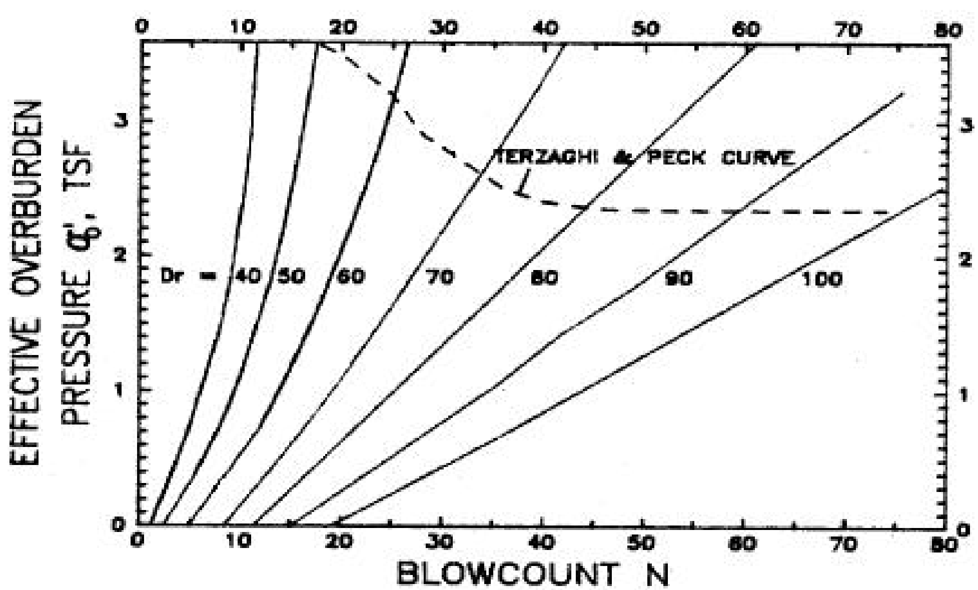

Figure 4.2: Determination of Adjusted N' Value for Alpan Method

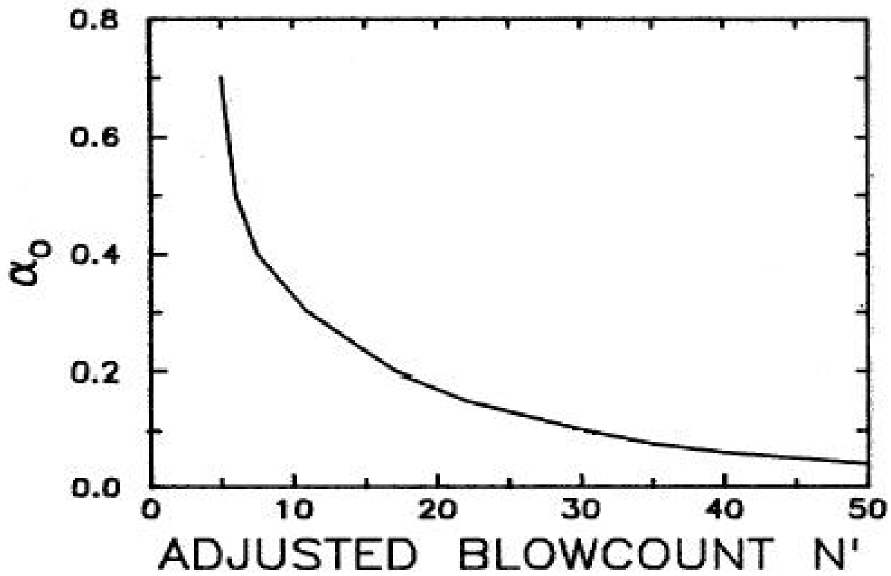

Figure 4.3: Determination of α_0 Value for Alpan Method

4.4.2 Anagnostropoulos Method

A simple formula was proposed by Anagnostropoulos et al. (1991), which was founded by their database of 150 shallow foundation cases. The determination of immediate settlement for this method is made by Equation 4-7.

$$S_e = \frac{2.37 q^{0.87} B^{0.7}}{N^{1.2}} \tag{4-7}$$

where S_e = immediate settlement (mm); q = applied bearing pressure (kPa); B = footing width (m); and N = average uncorrected SPT-N value within depth B of the footing base.

4.4.3 Bowles Method

Bowles (1987) proposed a method for computing the elastic settlement of a footing on a cohesionless soil. He developed the method by adjusting some of the influence factors involved in the conventional elastic settlement approach. His method has the following formula, Equation 4-8, as the general equation for static settlement.

$$S_e = \frac{(1-\upsilon^2)qB'}{E_s} I_s I_f \tag{4-8}$$

where S_e = immediate settlement (ft); υ = Poisson's ratio; q = applied bearing pressure (ksf); B' = B/2 for footing center and = B for footing corner (ft); E_s = modulus of elasticity of bearing soil (ksf); I_s = Steinbrenner influence factor; and I_f = Fox influence factor.

This empirical method uses an influence zone of depth 2B beneath the footing. The modulus of elasticity of the sand is estimated using Equation 4-9. The Steinbrenner influence factor, I_s, is determined by Equation 4-10. The F_2 part of this equation is left out when H is infinite and Poisson's ratio is 0.5 since it becomes negligible. However, if those values are not as stated above, then the F_2 portion of the equation is not negligible. Table 4.1 gives some values for F_1 and F_2 for ease, but interpolation must be used between the values. Values for the Fox influence factor are found in Table 4.2 for a Poisson's ratio of 0.3. Other values for this factor can be found in Bowles (1987).

$E_s = 10(N + 15)$ (4-9)

where N = average uncorrected SPT-N value.

$$I_s = F_1 + \frac{1-2\nu}{1-\nu} F_2 \quad (4\text{-}10)$$

where $F_1 = \frac{1}{\pi}(A_0 + A_1)$; $F_2 = \frac{n}{2\pi}\tan^{-1}(A_2)$; $A_0 = m \ln \frac{\left(1+\sqrt{m^2+1}\right)\sqrt{m^2+n^2}}{m\left(1+\sqrt{m^2+n^2+1}\right)}$;

$A_1 = \ln \frac{\left(m+\sqrt{m^2+1}\right)\sqrt{1+n^2}}{m+\sqrt{m^2+n^2+1}}$; $A_2 = \frac{m}{n\sqrt{m^2+n^2+1}}$; m = L′/B′;

n = H/B′; L′ = L/2 for footing center and = L for footing corner; H = thickness of elastic stratum (5B unless a hard stratum is encountered before reaching the depth of 5B).

Table 4.1: Values of F_1 and F_2 for Bowles Method

F_1 / F_2		L/B							
		1.0	2.0	2.5	3.0	3.5	4.0	4.5	5.0
H/B	0.5	0.049 0.074	0.040 0.084	0.038 0.085	0.038 0.086	0.037 0.087	0.037 0.087	0.036 0.087	0.036 0.087
	0.8	0.104 0.083	0.089 0.103	0.086 0.107	0.084 0.109	0.083 0.110	0.082 0.111	0.081 0.112	0.081 0.112
	1.0	0.142 0.083	0.125 0.109	0.121 0.114	0.118 0.117	0.116 0.119	0.115 0.120	0.114 0.121	0.113 0.122
	2.0	0.285 0.064	0.289 0.102	0.284 0.114	0.279 0.121	0.275 0.127	0.271 0.131	0.269 0.134	0.267 0.136
	4.0	0.408 0.037	0.476 0.069	0.484 0.082	0.487 0.093	0.486 0.102	0.484 0.110	0.482 0.116	0.479 0.121
	6.0	0.457 0.026	0.563 0.050	0.585 0.060	0.595 0.070	0.606 0.079	0.609 0.087	0.611 0.094	0.610 0.101
	8.0	0.482 0.020	0.611 0.038	0.643 0.047	0.664 0.055	0.678 0.063	0.688 0.071	0.694 0.077	0.697 0.084
	10.0	0.498 0.016	0.641 0.031	0.679 0.038	0.707 0.046	0.726 0.052	0.740 0.059	0.750 0.065	0.758 0.071

Table 4.2: Values of I_f at Poisson's Ratio of 0.3 for Bowles Method

D/B	L/B						
	1.0	1.2	1.4	1.6	1.8	2.0	5.0
0.05	0.979	0.981	0.982	0.983	0.984	0.985	0.990
0.10	0.954	0.958	0.962	0.964	0.966	0.968	0.977
0.20	0.902	0.911	0.917	0.923	0.927	0.930	0.951
0.40	0.808	0.823	0.834	0.843	0.851	0.857	0.899
0.60	0.738	0.754	0.767	0.778	0.788	0.796	0.852
0.80	0.687	0.703	0.716	0.728	0.738	0.747	0.813
1.00	0.650	0.665	0.678	0.689	0.700	0.709	0.780
2.00	0.562	0.571	0.580	0.588	0.596	0.603	0.675

Bowles made two suggestions for the determination of the immediate settlement using Equation 4-7. His first suggestion was to set the Fox depth influence factor (I_f) value to 1.0, because he believed that the uncorrected SPT-N value already included the depth effect. His second suggestion was to take 93% of the calculated settlement used for the rigid footing because the equation was actually for flexible footings.

4.4.4 Burland-Burbidge Method

Burland and Burbidge (1985) developed a procedure to estimate the footing settlement after examining over two hundred SPT case studies. From their method, immediate settlement of sand and gravel deposits is calculated by Equation 4-11.

$$S_e = \alpha_1 \alpha_2 \alpha_3 \left[\frac{1.25(L/B)}{0.25 + (L/B)} \right]^2 Bq' \tag{4-11}$$

where S_e = immediate settlement (ft); α_1 = a constant (0.14 for normally consolidated sands; 0.047 for overconsolidated sands); α_2 = compressibility index; and α_3 = correction for the depth of influence; q′ = applied stress at the level of foundation (tsf).

The average SPT-N value corrected for hammer efficiency only must be at least 15 and is adjusted by using Equation 4-12. For values of N that are less that 15, Equation 4-13 can be used to determine the adjusted value. Equation 4-14 is used to find the depth of stress influence (Z'). Once these values are calculated, they can be used in the equations for the compressibility index and the correction for the depth of influence.

$$N_{60a} = 15 + 0.5(N_{60} - 15) \tag{4-12}$$

$$N_{60a} = 1.25N_{60} \tag{4-13}$$

$$\frac{Z'}{B_R} = 1.4\left(\frac{B}{B_R}\right)^{0.75} \tag{4-14}$$

where B_R = 1 ft; and B = footing width (ft)

α_1 is a constant that equals 0.14 for normally consolidated sands and 0.047 for overconsolidated sands. Equations 4-15 and 4-16 define the compressibility index for normally and overconsolidated sands, respectively. Equation 4-17 gives a value for the correction for the depth of influence where H is equal to the smallest of 2B or Z'.

$$\alpha_2 = \frac{1.71}{(N_{60a})^{1.4}} \tag{4-15}$$

$$\alpha_2 = \frac{0.57}{(N_{60a})^{1.4}} \tag{4-16}$$

$$\alpha_3 = \frac{H}{Z'}\left(2 - \frac{H}{Z'}\right) \tag{4-17}$$

4.4.5 D′Appolonia Method

D′Appolonia et al. (1970) proposed a formula based on elastic theory for estimating settlements of footings on sands. Their formula incorporated influence factors due to embedment and compressive strata resulting in Equation 4-18.

$$S_e = \mu_0 \mu_1 \frac{qB}{M} \tag{4-18}$$

where S_e = immediate settlement (ft); μ_0 = embedment influence factor; μ_1 = compressible strata influence factor; q = average applied pressure (tsf); and M = modulus of compressibility (tsf).

The value of the embedment influence factor is a function of the D_f/B ratio, and Figure 4.4 gives the relationship. The value of the compressive strata influence factor depends on the length/width (L/B) ratio and the compressible layer thickness/width (H/B) ratio. Figure 4.5 is used to determine the values of μ_1 from the two ratios. Both of these charts are provided by Christian and Carrier (1978). The modulus of compressibility M is to be estimated through the average SPT-N value as seen in Figure 4.6.

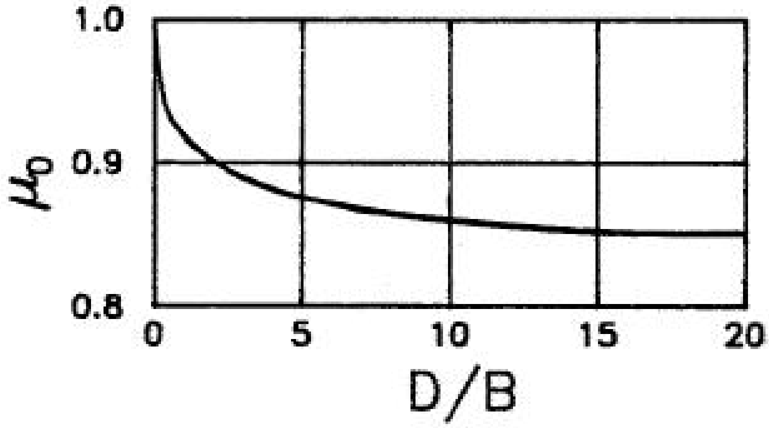

Figure 4.4: Values of μ_0 for D'Appolonia Method

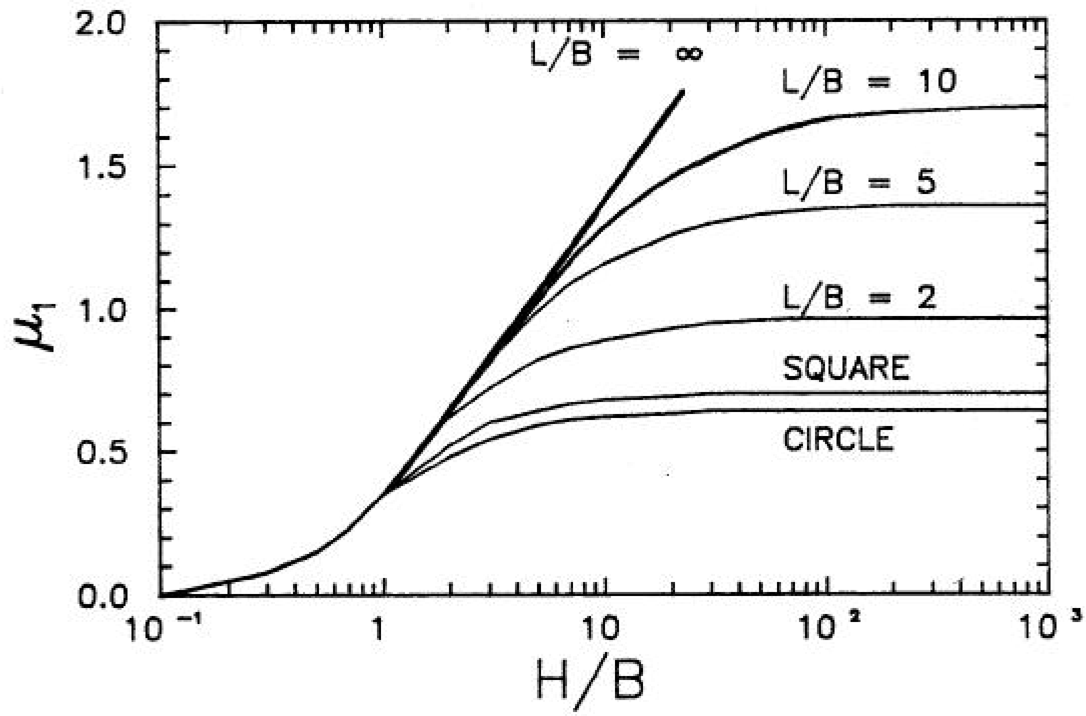

Figure 4.5: Determination of μ_1 for D'Appolonia Method

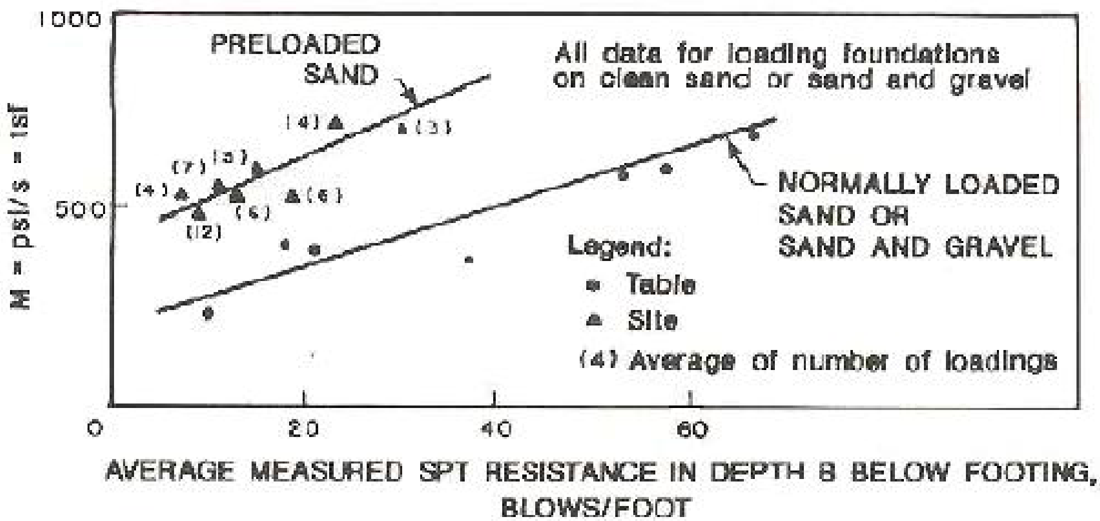

Figure 4.6: Determination of M for D'Appolonia Method

4.4.6 Department of the Navy Method

The Department of the Navy (1982) proposed a formula to predict immediate settlement of isolated footings on granular soils, and can be seen in Equation 4-19.

$$S_e = \frac{4q}{K_{v1}}\left(\frac{B}{B+1}\right)^2 \qquad \text{for } B \leq 20 \text{ ft} \qquad (4\text{-}19)$$

where S_e = immediate settlement (ft); q = applied bearing pressure (tsf); K_{V1} = modulus of subgrade reaction (tons/ft^3); and B = footing width (ft).

The Navy method is generally applicable to footings with width B less than 20 ft (6.1 m) and embedment depth less than B. For footings with widths exceeding 40 ft (12.2 m), the settlement given by the formula should be divided by 2. For footing widths between 20 and 40 ft (6.1 and 12.2 m), the settlement is to be interpolated between the two. The K_{V1} value is normally obtained from plate load test data. However, if the plate load data is not available, Figure 4.7 can be used to go from the SPT-N value to relative density. Then, Figure 4.8 provides a K_{V1} value for the cases where the water table is at least 1.5B below the base of footing. If the water table is at the base of footing, the chart K_{V1} value must be divided by 2.

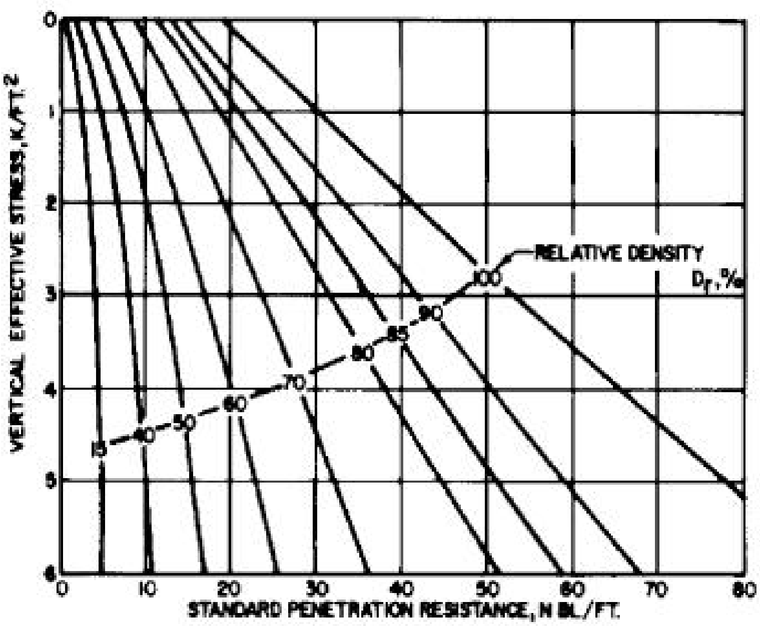

Figure 4.7: Correlation Determining D_r for Dept. of Navy Method

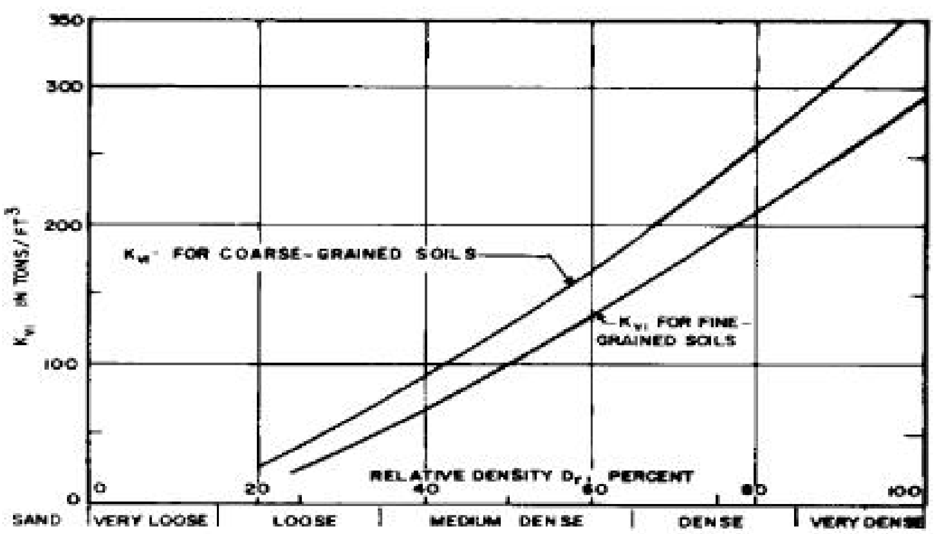

Figure 4.8: Determination of K_{v1} for Dept. of Navy Method

4.4.7 Meyerhof Method

One method by Meyerhof (1965) gives two immediate settlement equations which are based on the footing width and are shown in Equations 4-20 and 4-21.

$$S_e = \frac{8q}{N'} \quad \text{for } B \leq 4 \text{ ft} \tag{4-20}$$

$$S_e = \frac{12q}{N'}\left(\frac{B}{B+1}\right)^2 \quad \text{for } B > 4 \text{ ft} \tag{4-21}$$

The SPT-N value is corrected as long as the minimum average count is at least 15. Equation 4-22 is used for this correction where N is the original uncorrected SPT-N value.

$$N' = 15 + 0.5(N - 15) \qquad (4\text{-}22)$$

Meyerhof also proposed a variation of the Terzaghi & Peck settlement formula. In this method, Meyerhof believed that the uncorrected SPT-N value takes the groundwater level into effect so no correction factor is needed. The settlement for the Terzaghi & Peck method overestimated the field performance in Meyerhof's opinion so he reduced it to 2/3 the value. Equation 4-23 is the result of the changes for the immediate settlement calculations.

$$S_e = C_D \left[\frac{2q}{N} \right] \left(\frac{2B}{B+1} \right)^2 \qquad \text{for B > 4 ft} \qquad (4\text{-}23)$$

where S_e = immediate settlement (in); C_D = embedment correction factor; q = applied pressure (tsf); N = average uncorrected SPT-N value (blows/ft); and B = footing width (ft).

The embedment correction factor can be seen in Equation 4-24. The average SPT blow count is to be adjusted by Equation 4-22 if all of the following conditions are met: the soil is silty, the water table exists at or above the base of the footing, and the N-value is greater than 15.

$$C_D = 1 - \frac{D_f}{4B} \qquad (4\text{-}24)$$

The minimum factor of safety against bearing capacity failure should be 2.5 for the footing on cohesionless soil. Otherwise, additional settlement may be induced due to shear deformations in the granular soil.

4.4.8 Peck-Bazaraa Method

Peck and Bazaraa (1969) published a settlement prediction formula for spread footings on sand. Their formula was a modified version of the original developed by Terzaghi and Peck. The coefficient in front of the applied pressure q was reduced from 3 to 2 to decrease the original formula's tendency to overestimate the footing settlement. Unlike Meyerhof's modified version, this process requires a correction on the average SPT-N value and also involves a different way of determining the depth correction factor. The equation to calculate the immediate settlement is found in Equation 4-25.

$$S_e = C_D C_W \left[\frac{2q}{N_B}\right]\left(\frac{2B}{B+1}\right)^2 \qquad (4\text{-}25)$$

where S_e = immediate settlement (inches); C_D = embedment correction factor; C_w = water table correction factor; N_B = corrected SPT-N value; q = applied pressure (tsf); and B = footing width (ft).

The embedment correction factor is determined using Equation 4-26. The water table correction factor is calculated with Equation 4-27, where the total and total effective overburden pressures, σ_v and σ_v', are analyzed at a depth of 0.5B.

$$C_D = 1 - 0.4\sqrt{\frac{\gamma D_f}{q}} \tag{4-26}$$

$$C_w = \frac{\sigma_v}{\sigma_v'} \tag{4-27}$$

The SPT-N value used for Equations 4-28 and 4-29 is the average uncorrected value at a depth of B. However, the total effective overburden pressure is calculated at 0.5B below the base of the footing.

$$N_B = \frac{4N}{1 + 2\sigma_v'} \qquad \text{for } \sigma'_v < 1.5 \text{ ksf} \tag{4-28}$$

$$N_B = \frac{4N}{3.25 + 0.5\sigma_v'} \qquad \text{for } \sigma'_v \geq 1.5 \text{ ksf} \tag{4-29}$$

4.4.9 Peck-Hanson-Thornburn Method

Peck, Hanson, and Thornburn (1974) relied on their observations of settlement behavior of many spread footings. They proposed the following empirical formula, Equation 4-30.

$$S_e = \frac{q}{0.11 C_w N_1} \tag{4-30}$$

where S_e = immediate settlement (inches); q = applied bearing pressure (tsf); C_w = water table correction factor; and N_1 = average corrected SPT-N value within depth of 1B below the base of footing.

The water table correction factor depends on the depth to the water table, D_w, and the depth of footing embedment, D_f, and can be seen in Equation 4-31. For the corrected SPT-N values, one of the following equations must be used: Equations 4-32a, 4-32b, or 4-32c. The determining factor to establish which equation to use is the effective overburden stress at a depth of B. The SPT-N value is the average uncorrected between depths of 0 and 1B.

$$C_w = 0.5 + 0.5\left(\frac{D_w}{D_f + B}\right) \qquad (4\text{-}31)$$

$$N_1 = 0.77\log\left(\frac{20}{\sigma'_v}\right)N \qquad \text{for } 0 < \sigma'_v < 0.25 \text{ tsf} \qquad (4\text{-}32\text{ a})$$

$$N_1 = 2N \qquad \text{for } \sigma'_v = 0 \qquad (4\text{-}32\text{ b})$$

$$N_1 = 0.4N \qquad \text{for } \sigma'_v > 0.25 \text{ tsf} \qquad (4\text{-}32\text{ c})$$

The formula is believed to be valid as long as the bearing pressure is less than the allowable pressure resulting in a settlement less than 1 inch (25 mm) and the footing width is larger than 3 ft (0.91 m).

4.4.10 Schmertmann Method

Schmertmann (1970) studied the distribution of vertical strain within a linear elastic half-space under a uniform pressure. His settlement formula is given in Equation 4-33.

$$S_e = C_1 C_2 q \sum_{0}^{z_z} \left(\frac{I_z}{E_s} \right) \Delta z \tag{4-33}$$

where S_e = immediate settlement (in); C_1 = foundation depth correction factor; C_2 = soil creep factor; q = applied pressure; I_z = strain influence factor; and E_s = modulus of elasticity.

The foundation depth correction factor and the soil creep factor can be determined by Equation 4-34 and 4-35, respectively. For the creep factor the value for time elapsed, t, should be at least 0.1 years.

$$C_1 = 1 - 0.5 \left(\frac{\gamma D_f}{q} \right) \tag{4-34}$$

$$C_2 = 1 + 0.2 \log \left(\frac{t}{0.1} \right) \tag{4-35}$$

The granular soil strata to a depth of 2B below the footing is subdivided into several layers using the CPT plot of the tip resistance (q_c) vs. depth. Each layer should have approximately the same q_c value. The key strain influence factors were provided for two L/B ratios (1 and 10) and can be seen in Table 4.3. For a footing with its L/B ratio between 1 and 10, the two curves must be interpolated to produce a strain distribution profile curve suitable for the desired L/B value. Once the layers are set up and the profile drawn, the I_z value at the mid-point of each layer can be determined.

Table 4.3: Reference Values of Strain Influence Factor I_z for Schmertmann Method

(L/B) Ratio	I_z Value	Depth z
1	0.1	0
	0.5	0.5B
	0.0	2B
10	0.2	0
	0.5	B
	0.0	4B

When the CPT sounding data is not available, the SPT-N values can be converted to the CPT q_c values. One critical aspect in doing so is that the conversion factor depends on the mean soil grain size (see Robertson et al. 1983). According to Schmertmann (1970), the ratio of q_c/SPT-N is 2.0 for sandy silts & slightly cohesive silt-sand mixtures, 3.5 for clean fine to medium sands, 5.0 for coarse sands, and 6.0 for sandy gravels. For axisymmetric footings (L/B = 1.0), Equation 4-36 is used to determine E_s from q_c. However for footings with L/B > 10.0, or plane strain footings, E_s can be determined from Equation 4-37. Between these two types of footings, E_s can be assumed to vary linearly.

$$E_s = 2.5q_c \tag{4-36}$$
$$E_s = 3.5q_c \tag{4-37}$$

4.4.11 Schultze-Sherif Method

Schultze and Sherif (1973) developed a settlement equation for spread footings based on data from 48 field cases. Equation 4-38 gives the immediate settlement for their results.

$$S_e = \frac{fq\sqrt{B}}{N^{0.87}\left(1 + \frac{0.4D_f}{B}\right)} \tag{4-38}$$

where S_e = immediate settlement (ft); f = influence factor; q = applied bearing pressure (tsf); B = footing width (ft); N = average SPT-N value within 2B from the base of footing; and D_f = footing embedment depth (ft).

The value of the influence factor, f, depends on the compressible layer thickness to footing width (H/B) ratio and the footing length to width (L/B) ratio. Figure 4.9 is used to determine f, which is then applied in the settlement equation. The SPT-N value used for this method is the corrected value for a 60 percent energy ratio.

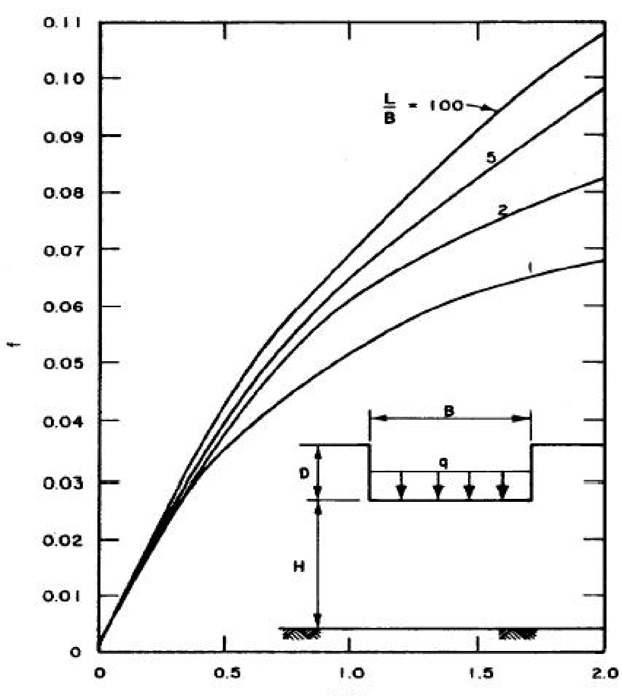

Figure 4.9: Determination of Influence Factor (f) for Schultz-Sherif Method

4.4.12 Terzaghi-Peck Method

Terzaghi and Peck (1967) proposed a simple, empirical method for estimating the settlement of a spread footing. Their equation gives an upper limit of immediate settlement for sands and can be seen in Equation 4-39.

$$S_e = C_D C_W \left[\frac{3q}{N}\right]\left(\frac{2B}{B+1}\right)^2 \tag{4-39}$$

where S_e = immediate settlement (inches); C_D = embedment correction factor; C_w = water table correction factor; N = average uncorrected SPT-N value for depth B below the base of footing; q = applied pressure (tsf); and B = footing width (ft).

The embedment correction factor is the same in form as was shown in Equation 4-24. This is because the Terzaghi-Peck method has many variations from other proposers. As for the water table correction factor, if the water table is at the ground surface, then C_w = 2.0. However, if the water table rests more than 2B below the footing then C_w = 1.0, while between these values C_w is interpolated.

4.5 SETTLEMENT OF FOOTING ON COHESIVE SOILS

Settlement analysis for a spread footing on cohesive soil is presented in great details in several books and reports including those by Duncan & Buchignani (1976) and American Society of Civil Engineers (ASCE), U.S. Army Corps of Engineers Manual No. 9 (1994).

It is also covered in the AASHTO LRFD Bridge Design Specifications, which was summarized in Section 3.7.2 of this report.

A loaded footing resting over a limited area on clay usually experiences both immediate and consolidation settlement. The immediate settlement occurs due to the almost instantaneous distortion of clay soil under the loaded area and in unsaturated clays, the immediate volume change. In saturated clays, the volume change takes place gradually over time, as explained by the well-known consolidation theory.

The first component (immediate settlement) is generally estimated by a formula based on the elastic theory, such as Equation 3-15. The ultimate settlement resulting from the second component (consolidation phenomenon) can be predicted by either Equations 3.17, 3.18, or 3.19, depending on the past stress history of the clay deposit. If one needs to find out the settlement after a specific amount of time under any constant loading, the time rate formula Equation 3-20 must be applied to back calculate the time factor T value. The overall degree of consolidation U corresponding to the T value is obtained from a chart such as Figure 3.4. Then, the settlement at the time is obtained by multiplying the ultimate settlement by the degree of consolidation.

The above procedure incorporating the time rate effect is for the cases involving normally consolidated clays. According to the AASHTO LRFD Bridge Design Specifications (2004), footings resting on overconsolidated clays experience settlements at much faster rates (about 10 times faster). The amount of settlement is computed either by the elastic theory formula Equation 3-15 or the consolidation theory formula Equation 3-17.

4.6 ROTATIONAL MOVEMENT OF FOOTING

According to Bowles (1988), the rotation of a footing can be estimated by a simple elastic theory formula, shown in Equation 4-41.

$$\tan\theta = \frac{1-\upsilon^2}{E_s}\left(\frac{M}{B^2 L}\right)I_\theta \qquad (4\text{-}41)$$

where θ = degree of rotation away from vertical axis (radians); υ = Poisson's ratio of bearing soil material; E_s = elastic modulus of bearing soil (tsf); M = overturning moment (ton-ft); B = footing width (ft); L = footing length (ft); and I_θ = influence factor.

The influence factor accounts for the effect of (L/B) ratio and footing rigidity. Its value can be obtained from Table 4.4, which was based on the information obtained from Tettinek and Matl (1953) and Taylor (1967). The overturning moment always exists for bridge abutments that retain soil fill only on one side (behind the wall). For pier footing foundations, an overturning moment can be created by two unequal spans meeting at the pier. Also, temporary uneven loading conditions created during construction can induce an overturning moment as well. Examples may include cases where girder beams are placed only on one side of the footing for a number of days or a backfilling operation using a bulldozer begin from one side.

Table 4.4: Influence Factor Value for Footing Rotation

(L/B) Ratio	Flexible Footing	Rigid Footing
0.10	1.045	1.59
0.20	1.60	2.42
0.50	2.51	3.54
0.75	2.91	3.94
1.00 (circular)	3.15 (3.00)	4.17 (5.53)
1.50	3.43	4.44
2.00	3.57	4.59
3.00	3.70	4.74
5.00	3.77	4.87
10.00	3.81	4.98
100.00	3.82	5.06

CHAPTER 5: PROJECT DESCRIPTIONS

5.1 GENERAL

Spread footings were instrumented at two bridge sites, FRA-670-0380 and MOT-70/75. Each bridge was monitored during the different phases of construction. Background information including design characteristics of the bridge structure, subsurface conditions, field instrumentation plans, and construction history data is presented for each site in this chapter.

5.2 FRA-670-0380 PROJECT

5.2.1 Bridge Structure

The bridge FRA-670-0380 is a two-span bridge that crosses over the I-670 highway, along High Street, between Goodale Street and Poplar Avenue, in the City of Columbus. The bridge construction project was identified by ODOT as “High Street Over I-670.” The superstructure is a composite type consisting of a concrete deck supported by steel girder beams. The deck has a total width of 78 ft (23.8 m), which not only supports traffic in two lanes but also pedestrians on walkways and shops on both sides. The city’s Convention Center and shopping district is located near this bridge. The north span is 102.9 ft (31.4 m) and the south span is 100.2 ft (30.5 m). Figure 5.1 presents a view of the bridge structure from below, on the I-670 level, shortly after the placement of the girder beams. Figure 5.2 shows a photograph of the bridge from High Street level, taken just after its completion.

Figure 5.1: Bridge Structure After Placement of Beams (FRA-670-0380)

Figure 5.2: General View of Bridge Deck at Completion (FRA-670-0380)

The bridge superstructure is supported by a massive concrete abutment wall at each end and a spread footing near the mid-span. Each abutment wall is supported by a 30-ft (9.1-m) deep pile group. The abutment walls were constructed more than several months prior to the commencement of the actual bridge construction and were supported on many drilled pier foundations. The ODOT Engineer assumed the abutment walls to be stationary structures and installed a permanent bench mark on the face of each abutment wall. The dimensions of the Central Pier footing consist of an 8.0 ft (2.43 m) width, a 40.25 ft (12.27 m) length, and a 3.0 ft (0.91 m) thickness. The footing is skewed from the transverse direction of the bridge by an angle of 21°18′50″ (21.31°). There are four load bearing columns with diameters of 3.0 ft (0.91 m) and heights of about 16.2 ft (4.94 m), spaced at 10.5 ft (3.2 m) center to center. The four columns are connected by a cap at the top. The cap has a length of 40.25 ft (12.27 m), width of 3.0 ft (0.91 m), and thickness of about 3.45 ft (1.05 m). Initial estimates of quantities for the bridge are listed in Table 5.1.

Table 5.1: Estimated Quantities for FRA-670-0380 Bridge

Item Description	Estimated Quantity
Class C Concrete (Footing)	75 yd^3 (57 m^3)
Class C Concrete (Abutment)	52 yd^3 (40 m^3)
Class C Concrete (Pier Columns + Cap)	67 yd^3 (51 m^3)
Class C Concrete (Superstructure)	464 yd^3 (355 m^3)
Structural Steel Beams & Members (Superstructure)	845,021 lb (384,100 kg)
Welded Stud Shear Connectors	4,428 each

5.2.2 Subsurface Conditions

According to the project documents provided by ODOT, two soil bore holes (RB-9 & 11) were placed in the vicinity of the Central Pier foundation. The boring log records are summarized for these holes in Table 5.2. In both of the bore holes, the groundwater table was not detected close to the bottom of the footing. Figure 5.3 was developed using the average SPT-N values recorded from both bore holes. Their averages are listed in Table 5.3.

Table 5.2: Soil Boring Logs (FRA-670-0380)

(a) Bore Hole RB-9

Depth Below BOF (ft)	SPT-N Value	Soil Description
0	32	Gray sandy silt, trace gravel, trace cobbles (A-4a)
5	65	(the same as above; A-4a)
10	73	Gray gravel, little sand, little silt, trace cobbles, trace shale (A-2-4)
15	83	(the same as above; A-2-4)
20	98	(the same as above; A-2-4)
25	61	(the same as above; A-2-4)

(b) Bore Hole RB-11

Depth Below BOF (ft)	SPT-N Value	Soil Description
0	69	Brown fine & coarse sand, some gravel, little silt (A-3a)
15	43	(the same as above; A-3a)
20	70	Gray fine & coarse sand, trace gravel (A-3a)
25	69	(the same as above; A-3a)

[Note] BOF = Bottom of Footing.

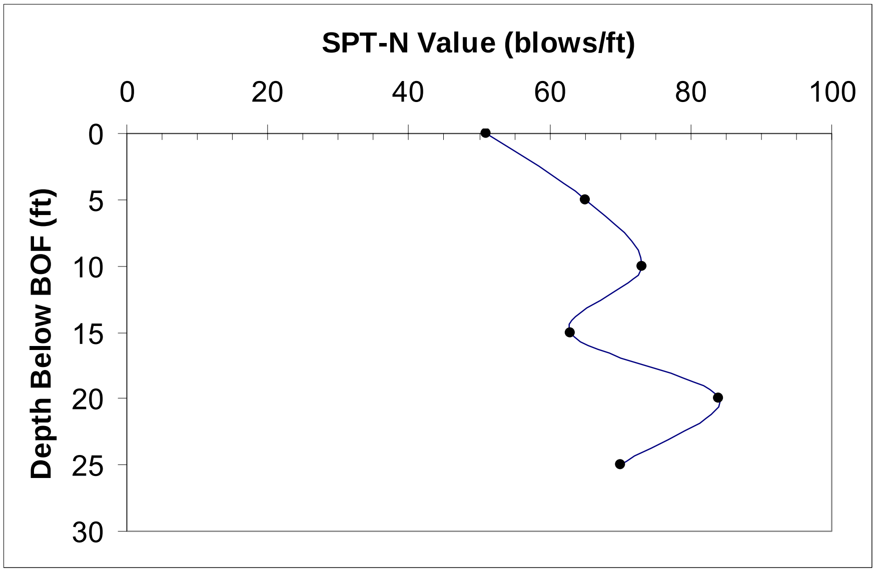

Figure 5.3: SPT-N Value Variations with Depth (FRA-670-0380)

Table 5.3: Average SPT-N Values (FRA-670-0380)

Depth Below BOF (ft)	SPT-N Value (blows/ft):		
	RB-9	RB-11	Average
0	32	69	51
5	65	---	65
10	73	---	73
15	83	43	63
20	98	70	84
25	61	79	70

5.2.3 Field Instrumentation Plans

Field instrumentation plans were developed to monitor the performance of the Central Pier foundation at the FRA-670-0380 site. Figure 5.4 illustrates the overall general field instrumentation schemes. The types of instrumentation used includes Geokon Model 4800E soil pressure cells, settlement monitoring points encased in riser pipes, and column tilt stations. Table 5.4 lists basic descriptions and specifications of the sensors/devices used at the FRA-670-0380 site.

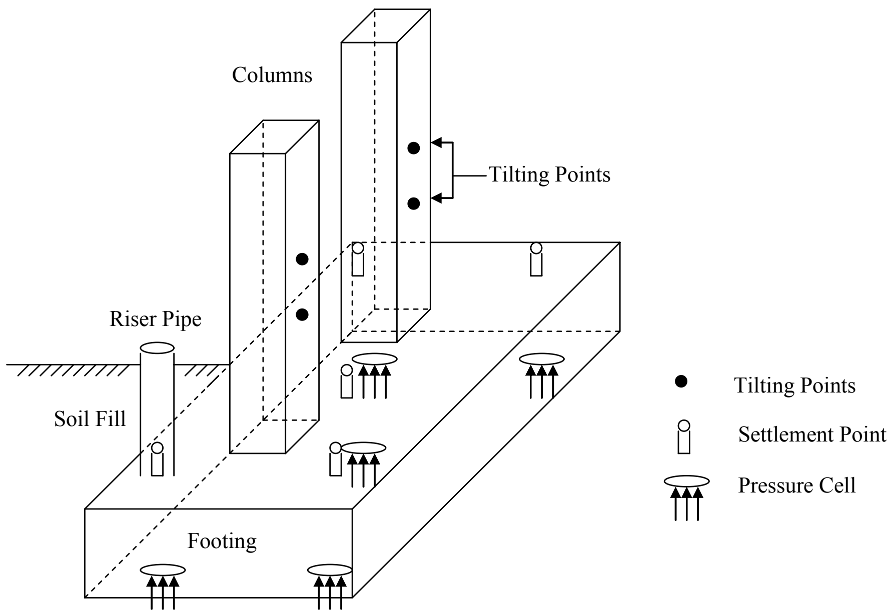

Figure 5.4: Overall Field Instrumentation Scheme for Spread Footing

Table 5.4: Summary of Instrumentations

Parameter	Sensor/Device	Notes
Settlement	Stainless steel eyebolt anchored into footing & encased in a 4-inch diameter PVC riser pipe.	Level survey method used to detect vertical displacement of each point with respect to permanent bench mark.
Bearing Pressure	Vibrating-wire pressure cell; 9-inch diameter (Geokon Model 4800E).	Range 0-100 psi; Sensitivity 0.1 psi; Data collected through a readout device and a multi-meter.
Column Tilting	Two stainless steel studs embedded into column per station; Studs accept reference plate and tilt-meter (Sinco Digitilt).	Range $\pm$ 30°; Sensitivity 0.003°; Data collected through a readout device.

Several pressure cells were positioned at the base of the footing to provide the magnitude and distribution of the contact pressure. Figure 5.5 gives the pressure cell instrumentation plan for the six cells beneath the central pier footing and Figure 5.6 shoes a picture of them in the soil. Four of the six pressure cells are located near the corners of the footing, while the remaining two pressure cells are positioned so that one of them is directly under the east column and the other lines up with the two located along the eastern edge of the footing. Each pressure cell was precast in a 12 inch width by 24 inch length by 2 inch thickness (or 305 mm x 610 mm x 50 mm) concrete block prior to the field installation. This precasting was necessary to keep them from being disturbed during the footing construction. In the field, each pressure cell was placed carefully at the predetermined location with the sensing disk pressed against a 2-inch thick (50-mm) compacted sand layer. A nonwoven geotextile sheet was inserted between the sand layer and the bearing soil to keep the two dissimilar materials separate. Readings from each pressure cell are entered into the following simple formula (Equation 5-1) to calculate the normal pressure sensed by the cell.

$$P = G(R_0 - R_i) + K(T_i - T_0) \qquad (5\text{-}1)$$

where P = normal pressure (psi); G = pressure calibration constant (see Table 5.5); R_0, R_i = original and subsequent cell readings (transducer frequency squared); K = thermal calibration constant (see Table 5.5); T_0, T_i = original and subsequent cell temperature readings in °C (converted from the electrical resistance of cell transducer).

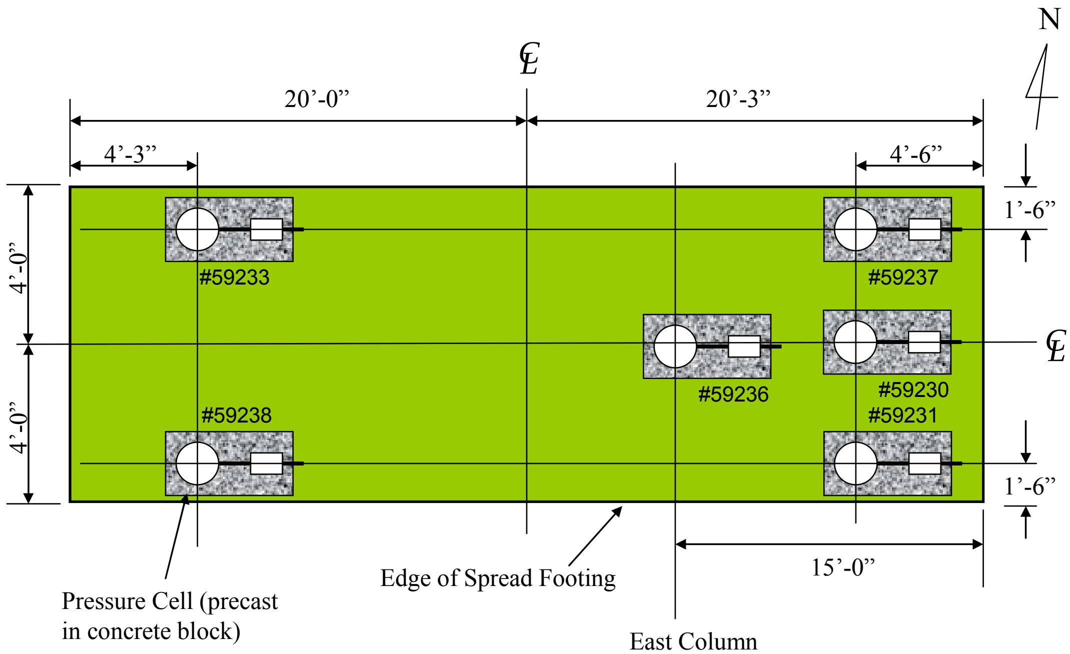

Figure 5.5: Pressure Cell Location Plan (FRA-670-0380)

Figure 5.6: Pressure Cells Being Installed (FRA-670-0380)

Table 5.5: Pressure Cell Calibration Constants (FRA-670-0380)

Serial Number	Calibration Constants	
	G (psi/digit)	K (psi/°C Rise)
#59230	0.02271	-0.05381
#59231	0.02501	-0.03812
#59233	0.02288	-0.04235
#59236	0.02408	-0.04185
#59237	0.02526	-0.03846
#59238	0.02325	-0.03335

Along the surface of the footing, settlement monitoring points are placed to allow vertical displacement measurements with respect to a permanent bench mark located nearby. Figure 5.7 presents the settlement monitoring point location plan for the central pier footing. The five settlement monitoring points are positioned so one is near each corner of the footing and also one in the center. A picture of the settlement monitoring points is shown in Figure 5.8.

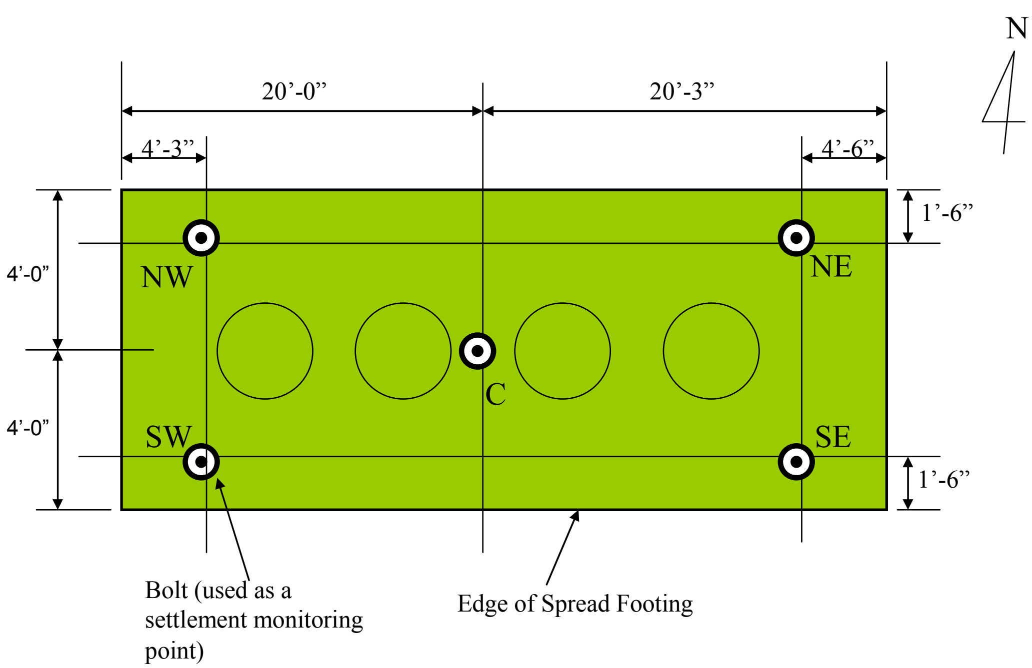

Figure 5.7: Settlement Monitoring Point Location Plan (FRA-670-0380)

Figure 5.8: Settlement Monitoring Points (FRA-670-0380)

Tilt stations established on the columns indicate the degree of tilting the columns have from the true vertical axis. Figure 5.9 demonstrates which direction a positive and negative tilt would move with the vertical line representing the column/wall. The pier column tilting is measured with an accelerometer (Digitilt by Slope Indicator or Sinco, Seattle, WA). This sensor has a range of $\pm$ 30˚ and a sensitivity of 0.003˚. At each monitoring station, two stainless steel reference points are grouted 2-inch (50-mm) deep into the column approximately 2.5 ft (0.76 m) apart vertically as shown in Figure 5.10. For taking tilting measurements, a stainless steel ball joint is screwed into each reference point, a reference plate is held against the ball joints, and the accelerometer is positioned on the side of the reference point. Figure 5.11 illustrates the location plan, Figure 5.12 presents typical field set-up for tilt measurements and settlement, and Figure 5.13 shows the accelerometer and the readout box. Positive and negative readings are typically taken with the sensor using a portable readout box.

The angle of tilt (θ) from true vertical direction is determined by Equation 5-2.

$$\theta(rad.) = \sin^{-1}\left[\frac{(Positive\ Reading)-(Negative\ Reading)}{2}\right] \tag{5-2}$$

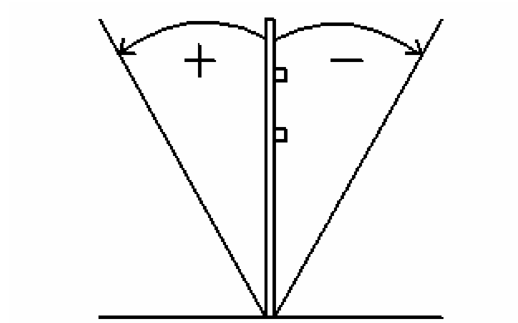

Figure 5.9: Sign Convention for Tilt Sensor

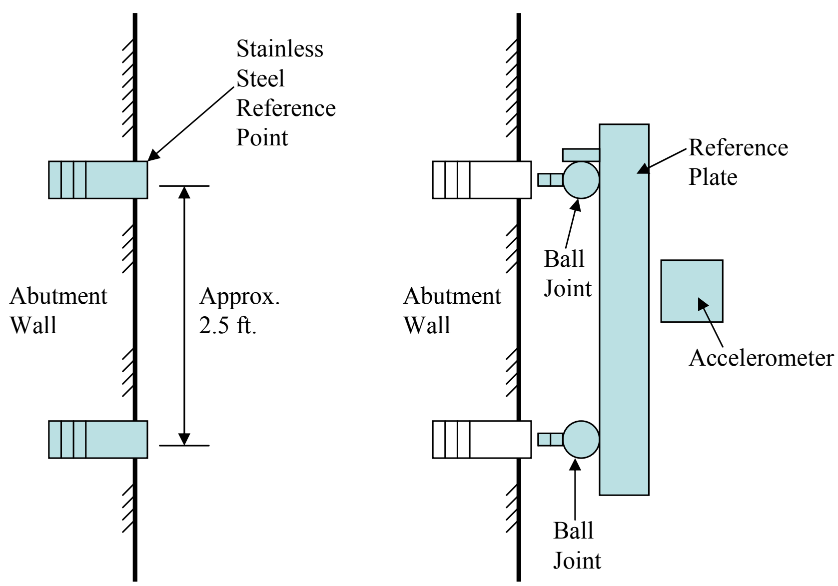

(a) Grouted Reference Points (b) Positioning of Reference Plate & Sensor

Figure 5.10: Process of Tilt Measurements

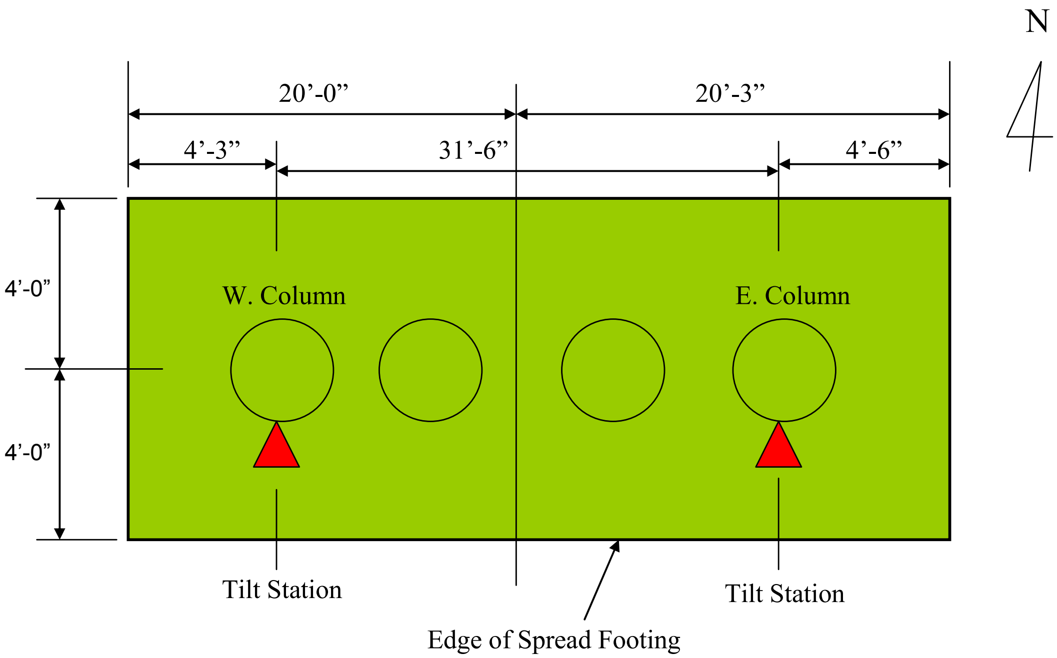

Figure 5.11: Tilt-Meter Station Location Plan (FRA-670-0380)

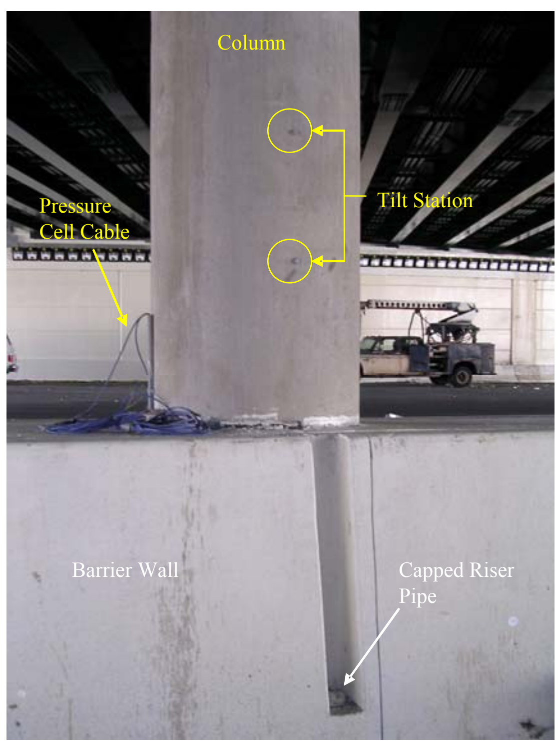

Figure 5.12: Field Set-Up for Pier Column Tilt Measurement

Figure 5.13: Digitilt Sensor & Readout Device

5.2.4 Bridge Construction History

The bridge construction work began on Feb. 28, 2003, when the ground was excavated for the central footing. Once the footing was constructed in early March 2003, six major construction stages (construction of four columns, pier cap construction, backfilling, barrier wall construction, girder beams placement, deck construction) followed relatively quickly before the opening of the bridge on July 29, 2003. Table 5.6 summarizes the key dates in the construction history recorded at this site. The last visit to the bridge site was made on Sept. 16, 2003 (193 days from the footing construction).

Table 5.6: Construction History of FRA-670-0380 Bridge

Construction Stage No.	Description	Date	No. of Days Elapsed
1	Footing Construction	March 7, 2003	0
2	Pier Column Construction	March 20, 2003	13
3	Soil Backfill	April 1, 2003	25
4	Pier Cap Construction	April 2, 2003	26
5	Barrier Wall Construction	April 25, 2003	49
6	Placement of Girder Beams	May 22, 2003	76
7	Deck Construction	June 24, 2003	109
8	Bridge Open to Traffic	July 29, 2003	144

5.3 MOT-70/75 INTERCHANGE PROJECT

5.3.1 Interchange Project

The six year I-70/75 interchange reconstruction project is located in Montgomery County, Ohio. This project represents one of the ODOT's key efforts in modernizing statewide highway network and reducing bottlenecks. The 1950's "cloverleaf" interchange design will be replaced with a more modern, higher capacity, efficient ramp design as seen in Figures 5.14 (a) and (b). The ODOT District 7 website states that the accident rates of the cloverleaf design were twice as high as the state average, 7.8 per million vehicles on I-70 and 2.6 per million vehicles on I-75. The new design will eliminate weaving movements, while handling more traffic and should reduce the accident rates significantly. This is the largest project ODOT District 7 has ever taken on with a cost estimated to be $145 million.

(a) Old Interchange Design

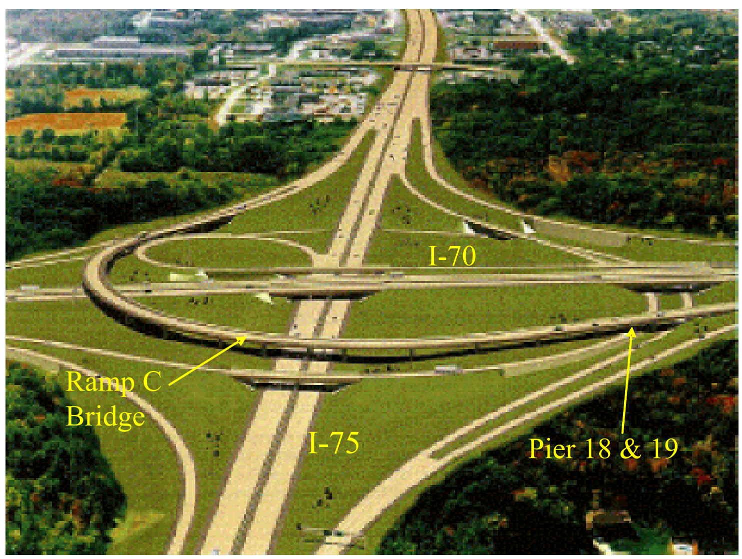

(b) New Interchange Design

Figure 5.14: Old & New Interchange Designs (MOT-70/75)

5.3.2 Ramp C Bridge Structure

Ramp C is a large portion of the interchange reconstruction project. It routes northbound traffic on I-75 to westbound I-70 with two lanes. This ramp bridges over I-70, I-75, and other ramps within the intersection. Figure 5.14 (b) shows the general view of the bridge within the project area. The ramp is a continuous span bridge with 20 spans, has steel girders and reinforced concrete piers and decking. The total length of the ramp 2,377 ft (724.5 m) long and it is 45.6 ft (13.9 m) wide.

Only a portion of the ramp is used for a more detailed look at the field performance of the bridge foundations. Piers 18 and 19 and Forward Abutment were investigated to determine how their foundations reacted in each stage of construction. Figure 5.15 is a photograph showing a general view of the project area where the research activities took place.

Figure 5.15: Ramp C Project Site – General View

Pier 18 has the dimensions of 57.4 ft (17.5 m) in length, 21 ft (6.4 m) in width, and 4.4 ft (1.35 m) in thickness. The pier footing and wall are skewed 45° from the deck direction. The dimensions of Pier 19 are 49.2 ft (15 m) in length, 24 ft (7.3 m) in width, and 4.4 ft (1.35 m) in thickness. The footing and wall of Pier 19 are skewed by 30° from the direction of the deck. The spans are 134.5 ft (41 m) between Piers 17 and 18, 118.1 ft (36 m) between Piers 18 and 19, and 88.6 ft (27 m) between Pier 19 and Forward Abutment. The pier's wall height is 29.4 ft (9 m) for Pier 18 and 25.4 ft (7.75 m) for Pier 19. Aesthetic images such as the Wright "B" Flyer, Apollo mission, and others are incorporated into each pier stem wall face. Table 5.7 gives estimates of the material quantities used for the piers.

Table 5.7: Estimated Quantities for Piers 18 & 19 of Ramp C Bridge

Item Description	Estimated Quantity
Class C Concrete (Pier 18 Footing)	205 yd^3 (157 m^3)
Class C Concrete (Pier 18 Wall)	191 yd^3 (146 m^3)
Class C Concrete (Pier 19 Footing)	200 yd^3 (153 m^3)
Class C Concrete (Pier 19 Wall)	124 yd^3 (95 m^3)
Structural Steel Girders (Superstructure – Pier 18 & 19)	250,400 lb (113,579 kg)
Class C Concrete (Superstructure – Pier 18 & 19)	336 yd^3 (257 m^3)

5.3.3 Subsurface Conditions

According to the site plans provided by ODOT, two bore holes (C187 and C188) were placed in the Pier 18-Pier 19 area. Tables 5.8 and 5.9 summarize the boring log records for these holes and give the SPT-N values at 5 ft (1.5 m) increments. Based on the two soil boring logs, it appears that each footing rests on top of cohesive glacial till deposits. Laboratory testing of the A-4a soil samples recovered from the site provided the Atterberg limits of 21 for the liquid limit (LL) and 7 for the plasticity index (PI). The water table was found at about 9.3 ft (2.85 m) above the bottom of the footing for Pier 18 and approximately 7.7 ft (2.35 m) below the bottom of Pier 19 footing. The bottom of the borings occurred at a depth of 41.5 ft (12.65 m) below the bottom of the Pier 18 footing and 34.0 ft (10.35 m) below the Pier 19 footing. Figure 5.15 and 5.16 show the variations of SPT-N value with depth for Pier 18 and 19. The plots indicate that the thickness of a relatively compressive layer is about 30 ft (9.1 m) below Pier 18 footing and about 20 ft (6.1 m) below Pier 19 footing.

Table 5.8: Soil Boring C188 (Located Near Pier 18)

Depth Below BOF (ft)	SPT-N (blow/ft)	Soil:		
		Description	Type	Other Data
0.0	22	Gray sandy silt, some clay, trace gravel	A-4a	*w* = 12.7%
5	15	(the same as above)	A-4a	*w* = 11.0%
10	19	(the same as above)	A-4a	w = 9.0%
15	48	(the same as above)	A-4a	w = 10.0%
20	62	(the same as above)	A-4a	w = 11.5%
25	47	(the same as above)	A-4a	w = 9.9%
30	42	(the same as above)	A-4a	*w* = 15.5%
35	111	(the same as above)	A-4a	*w* = 10.8%
40	100	(the same as above)	A-4a	*w* = sat.

Table 5.9: Soil Boring C187 (Located Near Pier 19)

Depth Below BOF (ft)	SPT-N (blows/ft)	Soil:		
		Description	Type	Other Data
0	22	Gray sandy silt, some clay, trace gravel	A-4a	*w* = 10.7%
5	53	(the same as above)	A-4a	*w* = 10.2%
10	75	(the same as above)	A-4a	*w* = 11.9%
15	73	(the same as above)	A-4a	*w* = 9.8%
20	100+	(the same as above)	A-4a	*w* = 10.4%
25	79	(the same as above)	A-4a	*w* = 10.5%
30	97	(the same as above)	A-4a	*w* = 9.3%
35	100+	(the same as above)	A-4a	*w* = 10.6%

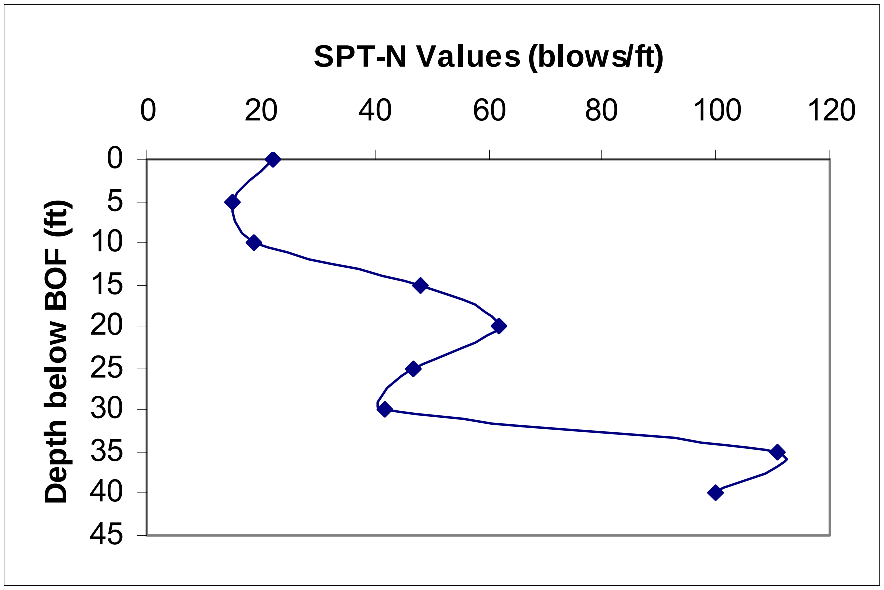

Figure 5.16: SPT-N Value Variations with Depth (Pier 18)

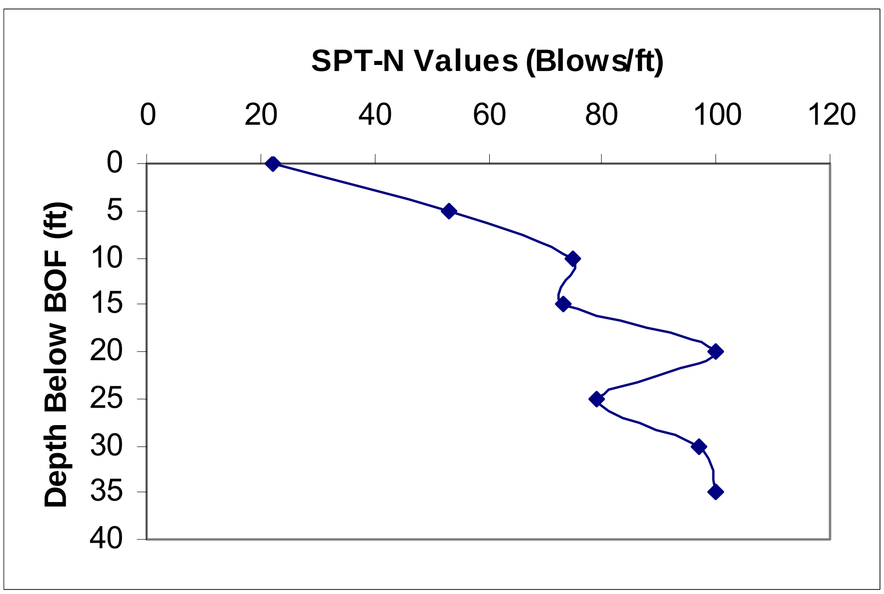

Figure 5.17: SPT-N Value Variations with Depth (Pier 19)

5.3.4 Field Instrumentation Plans for Pier 18 & 19 Footings

At the MOT-70/75 bridge construction site, field instrumentation plans were developed to monitor the performance of the Pier 18 and Pier 19 footings. The plans executed at this site were very similar to those already applied at the FRA-670-0380 site. So, the overall field instrumentation schemes shown in Figure 5.4 are relevant to this site as well.

Settlement monitoring points were installed on both Pier 18 and Pier 19 footings. The five points for each footing were located in the same positions. Four of them were positioned at the corners of the footing, one in each corner, and the last one was placed in the center near the stem wall. Figures 5.18 and 5.19 show the placement of the settlement points for each of the piers. The contractor also installed their settlement points near the north and south edges of the footing. Forward Abutment also had two settlement points placed by the contractor, one on the north side and one on the south.

As was done in the FRA-670-0380 project, the pressure cells were precast in concrete blocks before installation in the field. Pressure cells were placed beneath the footing as noted in Figure 5.20 and 5.21. Both piers have cells positioned one in each corner and one directly under the center of their footings. Pier 18 also had two pressure cells located one on either side of the footing along the long axis. The readings taken from each pressure cell are used in Equation 5.1 along with the calibration constants, G and K, for the cells in Table 5.10.

For tilting readings, the Sinco Tilt-meter and readout device were again used. A tilt station was constructed on the east side of the stem wall at the center of each pier. Figures 5.22 and 5.23 show the placement.

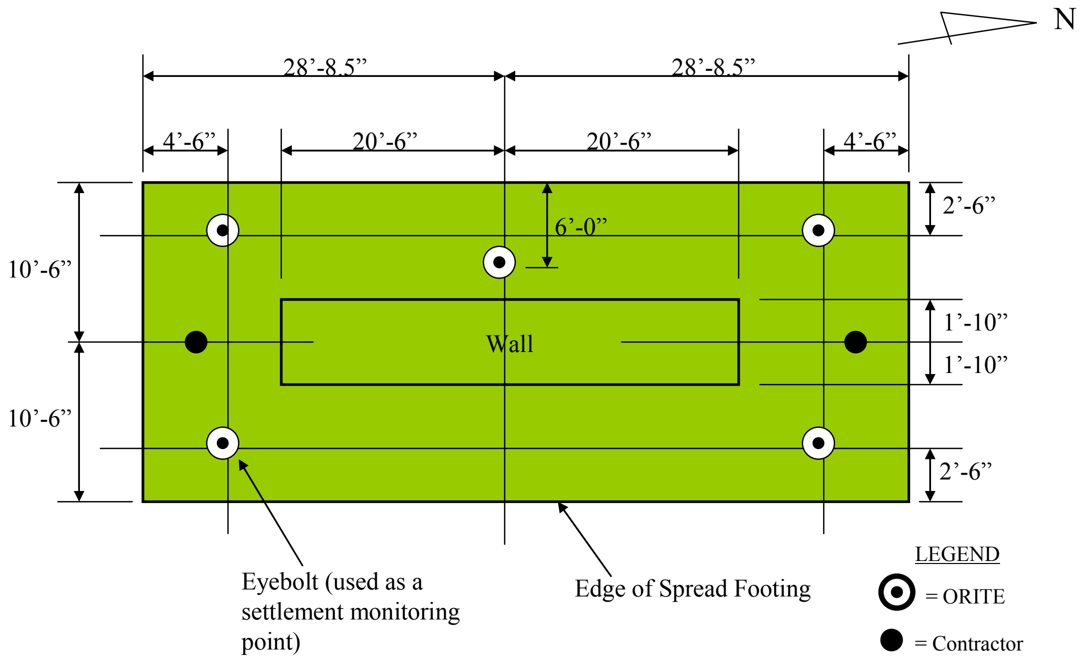

Figure 5.18: Settlement Monitoring Point Location Plan – Pier 18 Footing

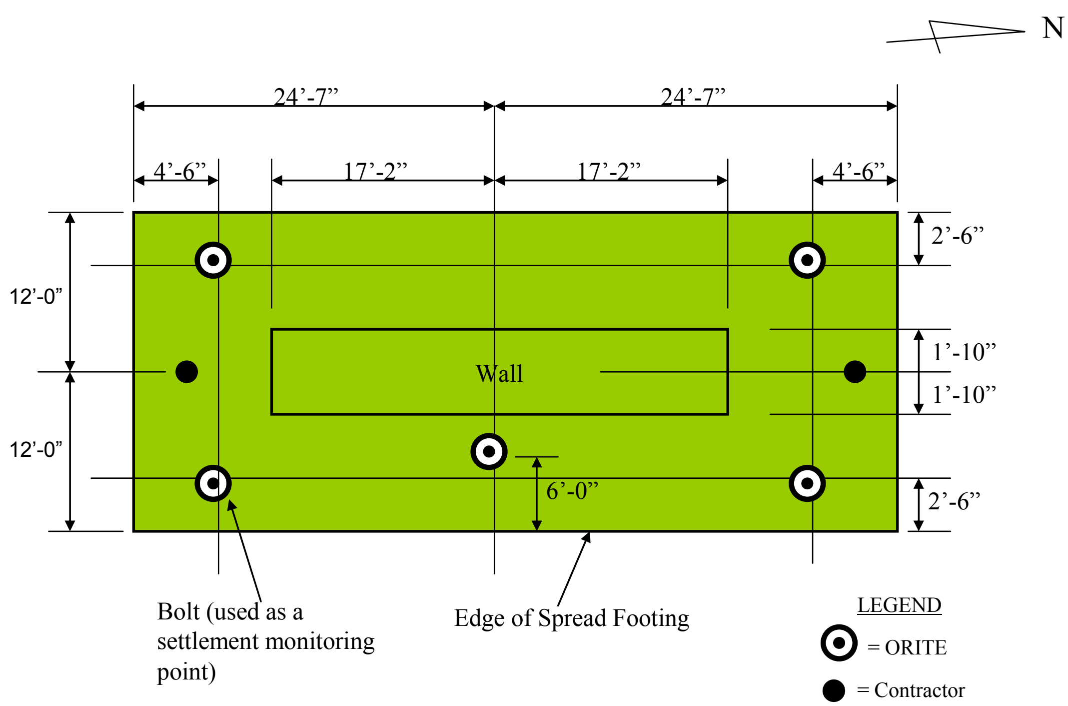

Figure 5.19: Settlement Monitoring Point Location Plan – Pier 19 Footing

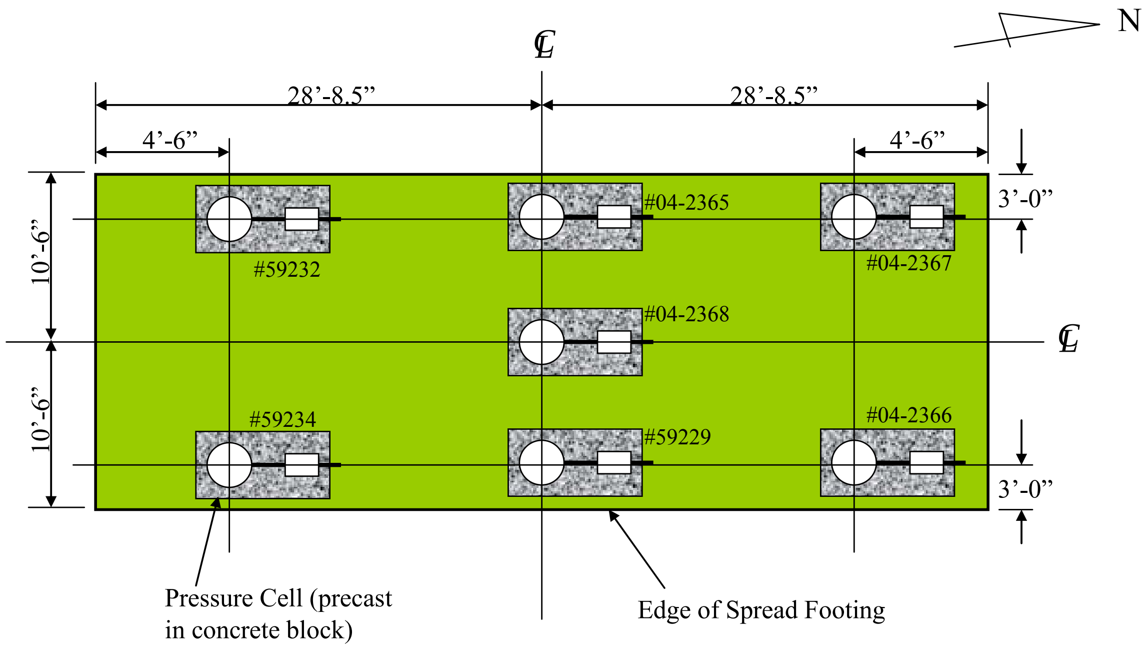

Figure 5.20: Pressure Cell Location Plan – Pier 18 Footing

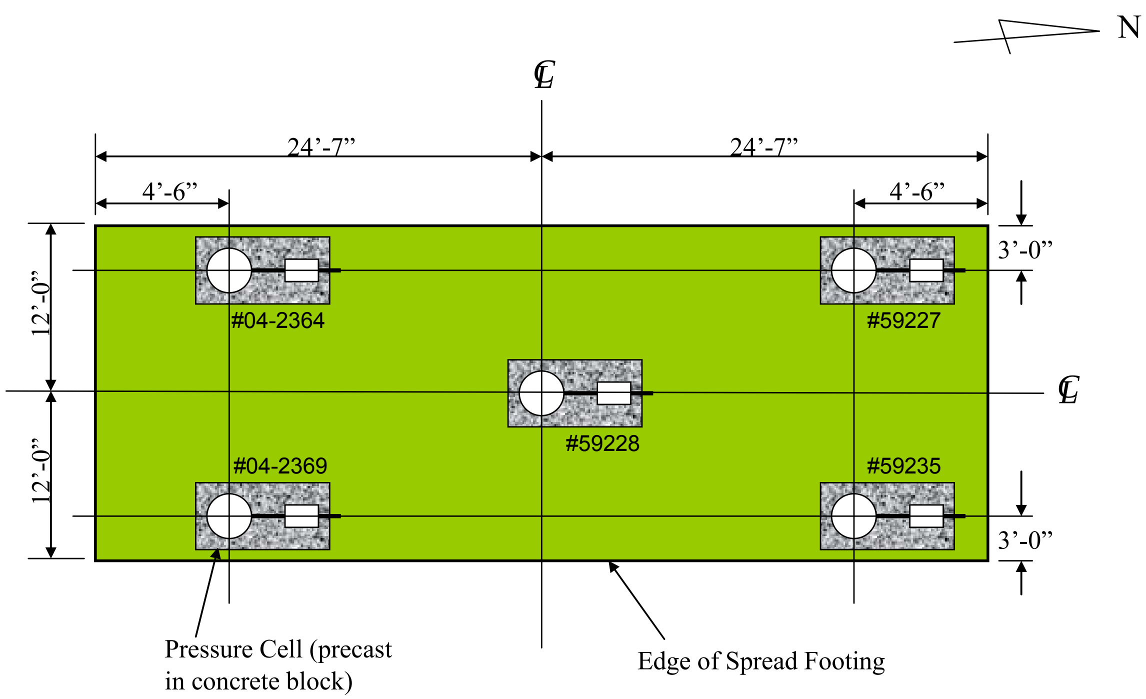

Figure 5.21: Pressure Cell Location Plan – Pier 19 Footing

Table 5.10: Pressure Cell Calibration Constants (Pier 18 Footing)

Serial Number	Calibration Constants	
	G (psi/digit)	K (psi/°C Rise)
#59229	0.02280	-0.04223
#59232	0.02340	-0.04322
#59234	0.02503	-0.04059
#04-2365	0.02643	+0.01243
#04-2366	0.02532	+0.01758
#04-2367	0.02341	+0.00587
#04-2368	0.02340	+0.00847

Table 5.11: Pressure Cell Calibration Constants (Pier 19 Footing)

Serial Number	Calibration Constants	
	G (psi/digit)	K (psi/°C Rise)
#59227	0.02702	+0.00668
#59228	0.02453	-0.04002
#59235	0.02386	-0.04383
#04-2364	0.02461	+0.00613
#04-2369	0.02482	-0.00212

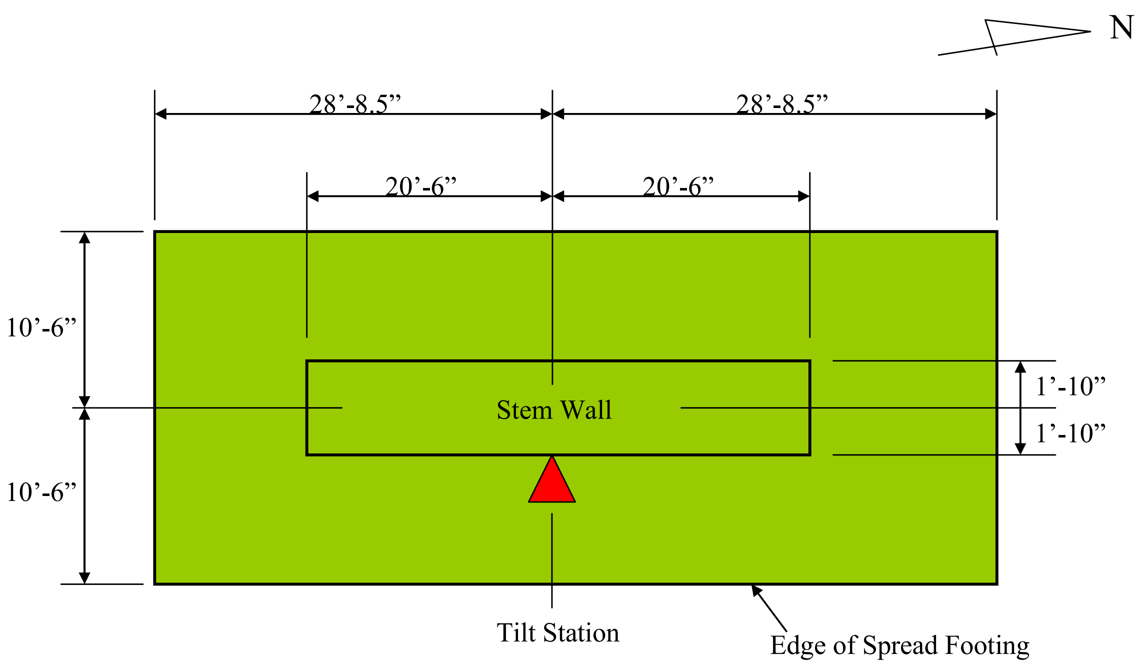

Figure 5.22: Tilt-Meter Station Location Plan – Pier 18 Footing

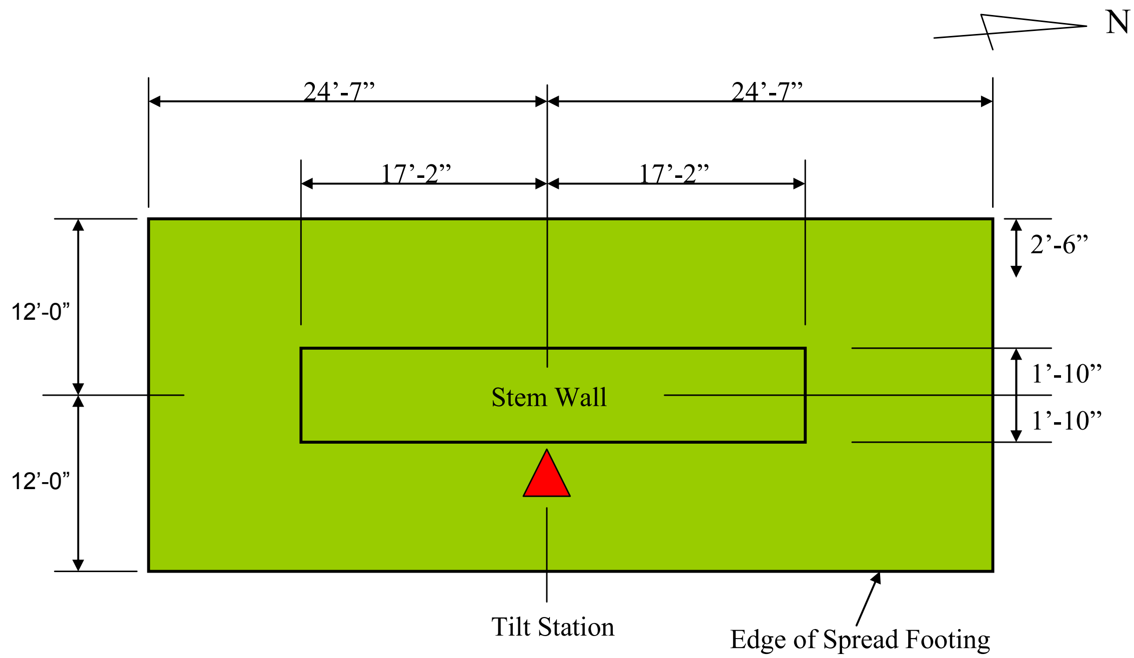

Figure 5.23: Tilt-Meter Station Location Plan - Pier 19 Footing

A large number of digital photographs were taken during the project to document the site conditions and field instrumentation locations. A few can be seen in Figures 5.24 through 5.28. Figures 5.24 and 5.25 show the conditions each pier construction area had at the time of the pressure cell installations. A sump pump was operated in the excavated pit to keep the water table as low as possible. Figures 5.26 and 5.27 present pictorially how the pressure cell and settlement point were installed for the pier footings. Upon the ORITE research team's request, ODOT District 7 installed a USGS-class permanent bench mark at the top of the cut slope on the north side of Pier 18 (shown in Figure 5.28). This bench mark was used exclusively to detect settlements of the three foundations at this site.

Figure 5.24: Pier 18 Footing Construction Area

Figure 5.25: Pier 19 Footing Construction Area

Figure 5.26: Pressure Cell Being Installed for Pier 18 Footing

Figure 5.27: Settlement Monitoring Points Installed on Pier 19 Footing

Figure 5.28: USGS-Class Permanent Bench Mark

5.3.5 Bridge Construction History

Construction work for the Ramp C Bridge began sometime in 2003, however the excavation for Pier 19 did not start until August 2004. The footing for Pier 19 was constructed on August 24, 2004 and the wall followed approximately 3 weeks later. The backfilling for Pier 19 happened as the excavation for Pier 18 was done. Pier 19 was at a stand still until Pier 18 was constructed to the same point. By the end of October 2004, the construction of the wall and backfilling for Pier 18 was finished. On November 10, 2004, the girders were placed for Pier 18 and in the next week the girders for Pier 19 were also placed. Major construction was halted for about 6 months. In May 2005, the deck was constructed from Pier 15 to Forward Abutment, with Pier 18 and Pier 19 falling within that range. The partial opening to only one lane of traffic of Ramp C Bridge took place on August 4, 2005. Key dates of construction can be seen in Tables 5.12 and 5.13. Figures 5.29 through 5.33 show some of these major construction stages.

Table 5.12: Construction History of Pier 18 Footing

Construction Stage No.	Description	Date	No. of Days Elapsed
1	Footing Construction	September 27, 2004	0
2	Pier Wall Construction	October 11, 2004	14
3	Soil Backfill	October 28, 2004	31
4	Placement of Girder Beams	November 10, 2004	44
5	Deck Construction	May 16, 2005	226
6	Bridge Open to Traffic	August 4, 2005	306

Table 5.13: Construction History of Pier 19 Footing

Construction Stage No.	Description	Date	No. of Days Elapsed
1	Footing Construction	August 24, 2004	0
2	Pier Wall Construction	September 13, 2004	20
3	Soil Backfill	September 21, 2004	28
4	Placement of Girder Beams	November 15, 2004	83
5	Deck Construction	May 16, 2005	265
6	Bridge Open to Traffic	August 4, 2005	345

Figure 5.29: Stem Wall Constructed at Pier 18

Figure 5.30: Pier 19 Footing Backfilled

Figure 5.31: Beams Placed Over Pier 18

Figure 5.32: Concrete Deck Constructed Between Pier 15 and Forward Abutment

Figure 5.33: Bridge Open to One Lane of Traffic

CHAPTER 6: FIELD PERFORMANCE

6.1 GENERAL

This chapter presents the field performance for the three spread footings instrumented and monitored at the two highway bridge construction sites in Ohio, FRA-670-0380 and MOT-70/75. For each spread footing, the field performance is represented by three types of measurements made in the field, pressure cell readings, footing settlement, and tilting of footing column/stem wall. Brief discussions, then, follow to point out correlations that appear to exist among the field data.

6.2 FRA-670-0380 Project

6.2.1 Contact Pressure

The pressure measured by each pressure cell is summarized in Table 6.1. Construction stages 3 and 4 do not contain separate readings since they occurred nearly simultaneously in the field. The individual locations for the six pressure cells were shown earlier in Figure 5.6. Using the coordinates within the footing of the pressure cells and the pressure cell readings, three-dimensional (3-D) plots of the bearing pressure distribution are made. The resulting 3-D plots are presented in Figures 6.1 through 6.7. The origin of the coordinate system was locked at the southwest corner of the footing, closest to Cell #59238. Since the pressure values are entered as positive values each plot shows the pressure mound upside down. Four angle views are provided for each plot by simply rotating the plot around the Z or pressure axis in 90° increments. Doing this helps the actual shape of the pressure mound be seen. The Z axis scale increases by increments of 1.0 tsf (95.8 kPa) to a value of 5.0 tsf (482.7 kPa).

Table 6.1: Individual Pressure Cell Readings (FRA-670-0380)

	Contact Pressure (tsf) Measured by:					
Cell	#59238	#59233	#59236	#59231	#59230	#59237
Position	SW	NW	E. Column	SE	E Edge	NE
Stage 1	0.62	0.05	0.53	0.28	0.22	0.30
Stage 2	0.87	0.06	0.78	0.60	0.42	0.49
Stage 3 Stage 4	1.25	0.12	1.23	0.72	0.60	0.68
Stage 5	1.43	0.15	1.74	0.76	0.55	0.58
Stage 6	2.18	0.32	2.50	1.56	1.04	1.12
Stage 7	3.54	0.57	3.59	2.25	1.50	1.52
Stage 8	3.85	0.62	4.64	3.56	2.28	2.15

[Note] 1 tsf = 95.8 kPa.

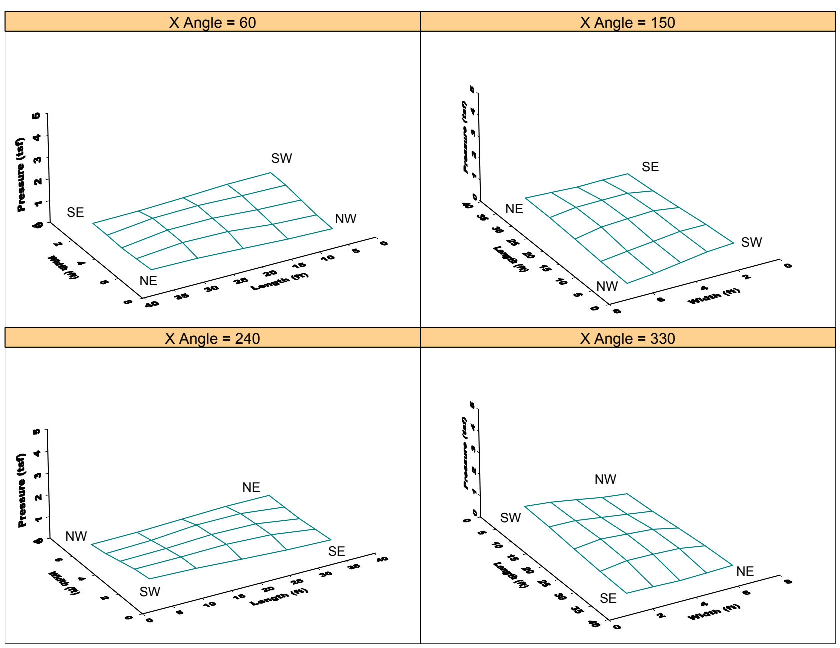

Figure 6.1: 3-D Plots of Bearing Pressure Distribution After Construction Stage 1 (Footing Construction)

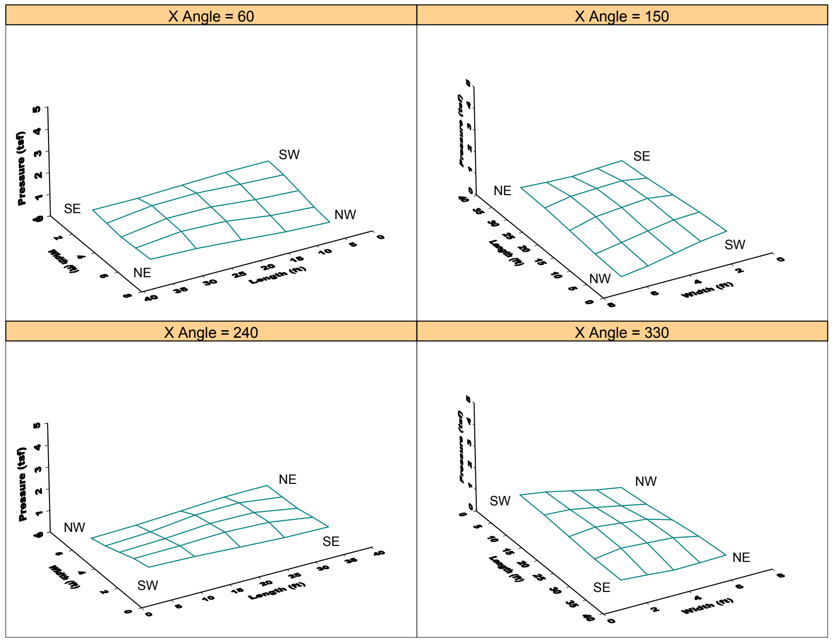

Figure 6.2: 3-D Plots of Bearing Pressure Distribution After Construction Stage 2 (Pier Columns Construction)

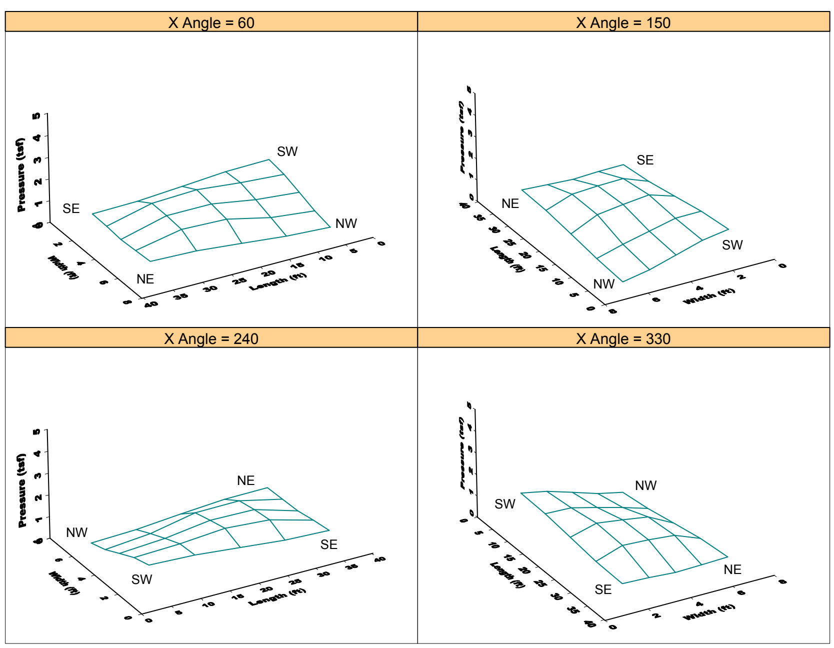

Figure 6.3: 3-D Plots of Bearing Pressure Distribution After Construction Stages 3 & 4 (Soil Backfill & Pier Cap Construction)

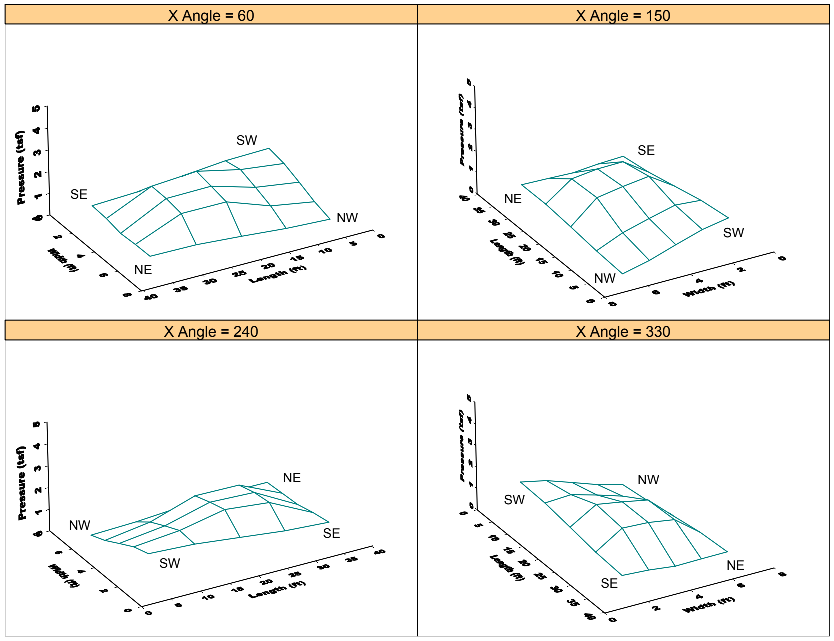

Figure 6.4: 3-D Plots of Bearing Pressure Distribution After Construction Stage 5 (Barrier Wall Construction)

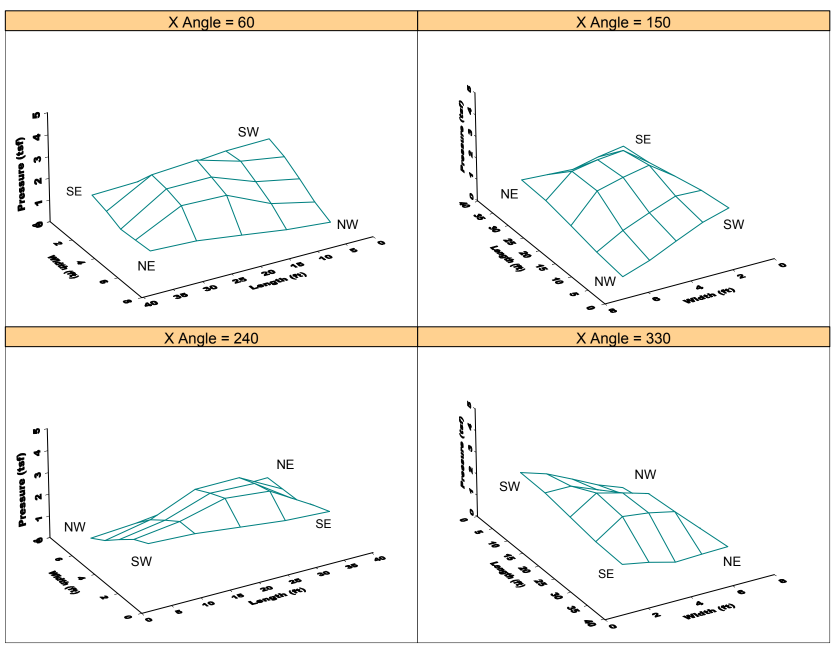

Figure 6.5: 3-D Plots of Bearing Pressure Distribution After Construction Stage 6 (Placement of Girder Beams)

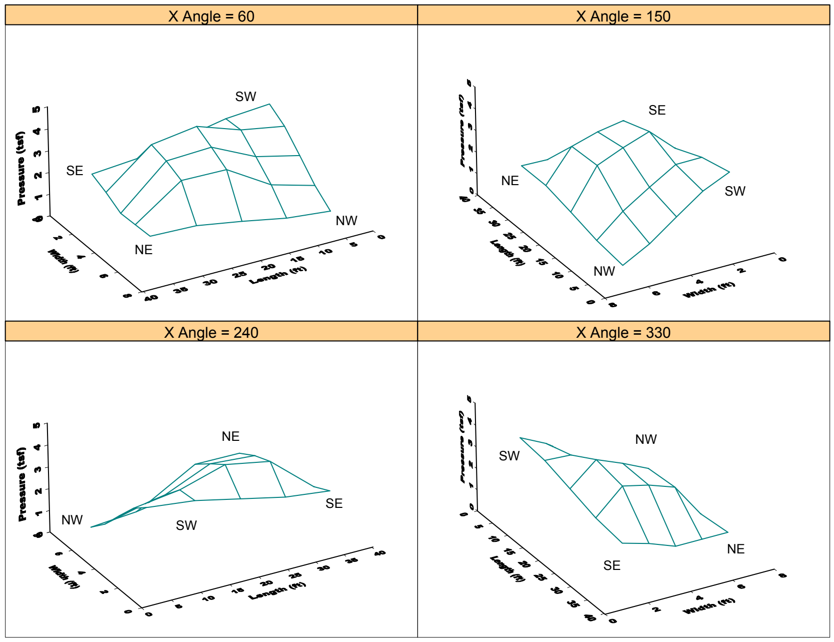

Figure 6.6: 3-D Plots of Bearing Pressure Distribution After Construction Stage 7 (Deck Construction)

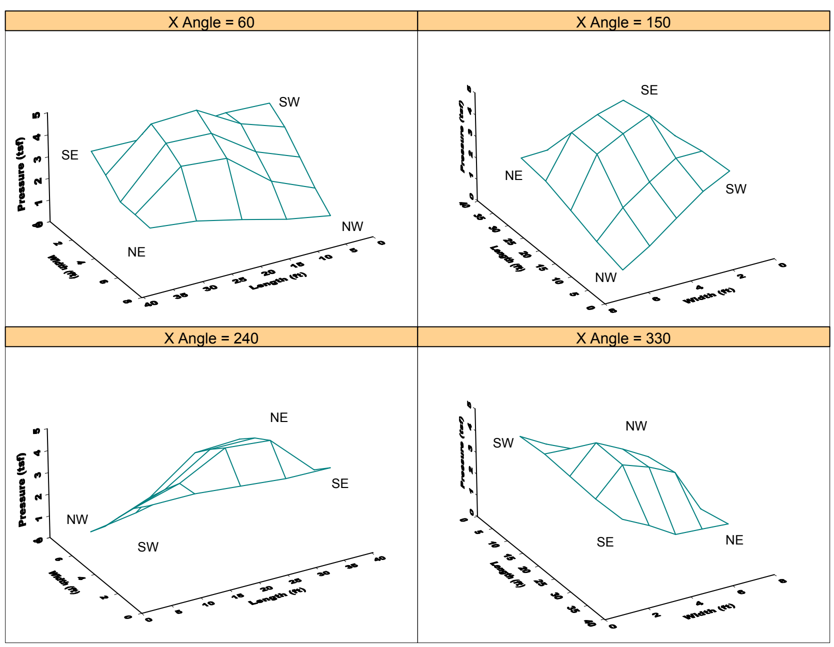

Figure 6.7: 3-D Plots of Bearing Pressure Distribution After Construction Stage 8 (Bridge Open to Traffic)

As seen in Figures 6.1 and 6.2, the contact pressure distribution remained relatively uniform during the footing construction and pier columns construction. The contact pressure distribution became increasingly more non-uniform after the fourth construction stage (soil backfill). The pressure measured beneath the eastern column became more pronounced throughout construction. The surface of the pressure mound began showing a definite tilt from the south to the north as the construction work progressed. Figure 6.7 shows a tilted concave upward pressure bulb from the set of pressure cell readings taken after the bridge opened to traffic. The theoretical model for a semi-rigid footing over granular soil, illustrated in Figure 4.1, was exhibited to some degree by the readings as was expected.

Table 6.2 lists the average contact pressure measured under the Central Pier footing throughout the construction stages. The average values are reported in both incremental and cumulative form. Construction stage 7 (deck construction) produced the largest contact pressure increase among all the construction stages. The placement of girder and cross beams was the second most influential construction stage. Figure 6.8 presents the data given in Table 6.2 graphically. Stage 3 did not produce a pressure reading as Stages 3 and 4 happened at practically the same time.

Table 6.2: Average Contact Pressure Measured By Pressure Cells (FRA-670-0380)

Const. Stage No.	Description	Ave. Contact Pressure (tsf):	
		Increase	Cumulative
1	Footing Construction	0.333	0.333
2	Pier Column Construction	0.105	0.438
3	Soil Backfill	0.324	0.762
4	Pier Cap Construction		
5	Barrier Wall Construction	0.201	0.963
6	Placement of Girder Beams	0.489	1.452
7	Deck Construction	1.397	2.849
8	Bridge Open to Traffic	0.00	2.849

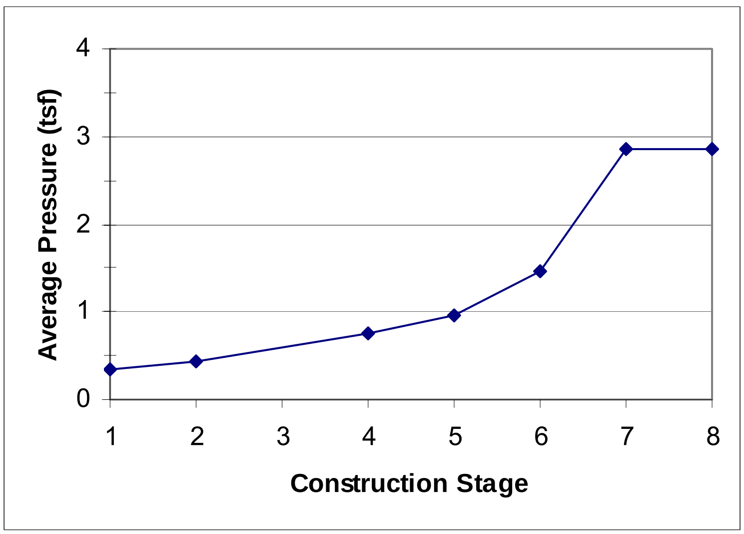

Figure 6.8: Average Contact Pressure for Each Stage (FRA-670-0380)

6.2.2 Footing Settlement

The Central Pier footing settlements optically measured at each monitoring point throughout the construction stages are listed in Table 6.3. Independent settlement measurements could not be taken for Stages 3 and 4, as these two stages took place nearly simultaneously in the field.

Table 6.3: Summary of Field Settlement Measurements (FRA-670-0380)

(a) Northeast (NE) Point

Construction Stage	Description	Settlement (inches)
2	Pier Column Construction	0.09 (2.4 mm)
3	Soil Backfill	0.11 (2.7 mm)
4	Pier Cap Construction	
5	Barrier Wall Construction	0.11 (2.7 mm)
6	Placement of Girder Beams	0.13 (3.4 mm)
7	Deck construction	0.26 (6.7 mm)

(b) Northwest (NW) Point

Construction Stage	Description	Settlement (inches)
2	Pier Column Construction	0.06 (1.5 mm)
3	Soil Backfill	0.11 (2.7 mm)
4	Pier Cap Construction	
5	Barrier Wall Construction	0.07 (1.8 mm)
6	Placement of Girder Beams	0.09 (2.4 mm)
7	Deck construction	0.13 (3.4 mm)

(c) Center (C) Point

Construction Stage	Description	Settlement (inches)
2	Pier Column Construction	0.04 (0.9 mm)
3	Soil Backfill	0.06 (1.5 mm)
4	Pier Cap Construction	
5	Barrier Wall Construction	-0.01 (-0.3 mm)
6	Placement of Girder Beams	0.12 (3.1 mm)
7	Deck construction	0.21 (5.2 mm)

(d) Southeast (SE) Point

Construction Stage	Description	Settlement (inches)
2	Pier Column Construction	0.01 (0.3 mm)
3	Soil Backfill	-0.06 (-1.5 mm)
4	Pier Cap Construction	
5	Barrier Wall Construction	-0.09 (-2.4 mm)
6	Placement of Girder Beams	-0.11 (-2.7 mm)
7	Deck construction	0.04 (0.9 mm)

(e) Southwest (SW) Point

Construction Stage	Description	Settlement (inches)
2	Pier Column Construction	0.07 (1.8 mm)
3	Soil Backfill	0.06 (1.5 mm)
4	Pier Cap Construction	
5	Barrier Wall Construction	-0.06 (-1.5 mm)
6	Placement of Girder Beams	0.05 (1.2 mm)
7	Deck construction	0.01 (0.3 mm)

Individual locations of the settlement monitoring points were shown earlier in Figure 5.5. 3-D plots of the footing's settlement are presented for each construction stages in Figures 6.9 through 6.13. The southwest corner of the footing was set as the origin of the coordinate system. Corner labels are shown on each of the figures. Each plot shows the settlement profile in the correct orientation, since the settlement is entered as a negative displacement. Four different angle views are provided for each plot by rotating the plot around the Z or settlement axis in 90° increments. This feature aids in seeing all the peaks and valleys and shows the actual shape of the settlement profile. The scale on the Z axis covers a range from -0.2 to 0.2 inches (-7.6 to 5.1 mm) in increments of 0.1 inches (2.5 mm).

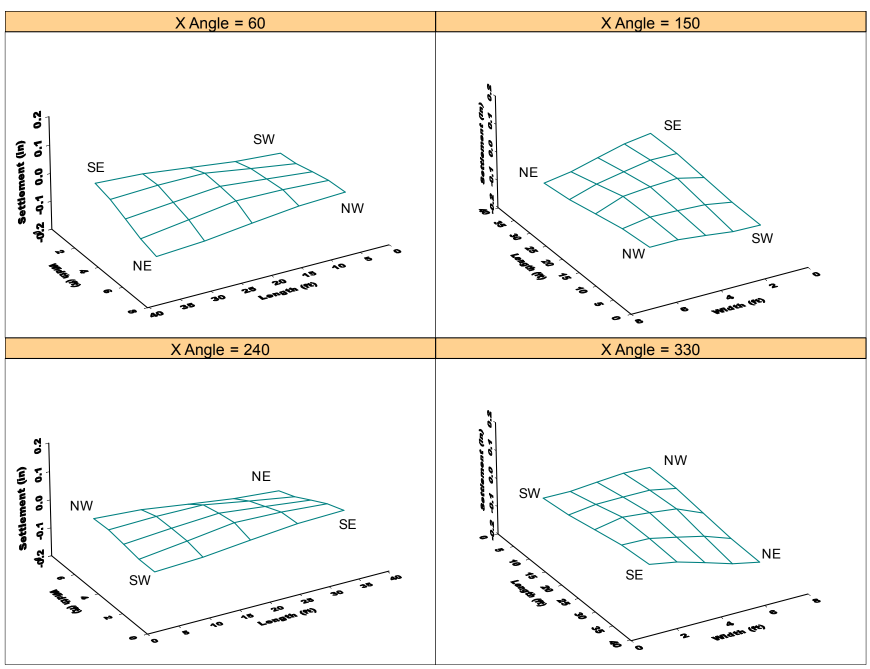

Figure 6.9: 3-D Plots of Settlement Profile After Construction Stage 2 (Pier Columns Construction)

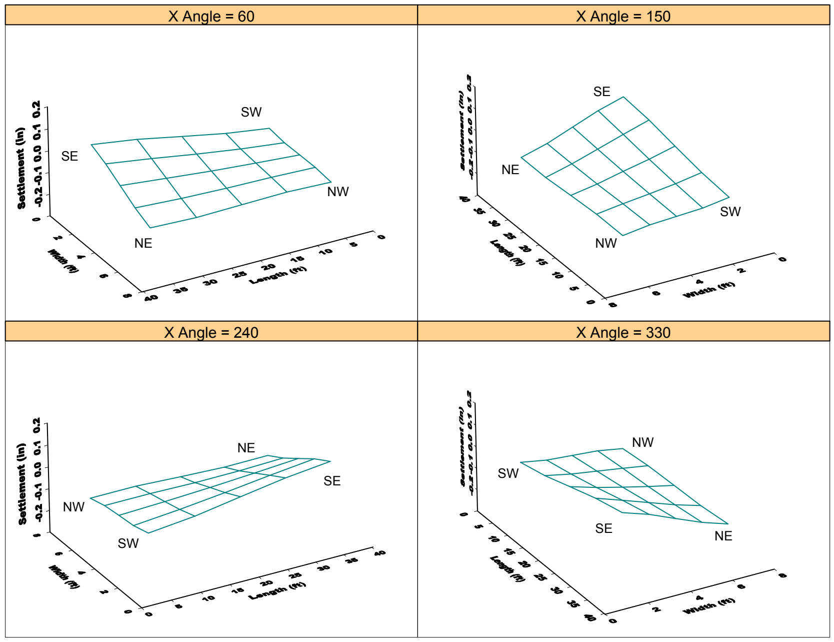

Figure 6.10: 3-D Plots of Settlement Profile After Construction Stages 3 & 4 (Soil Backfill & Pier Cap Construction)

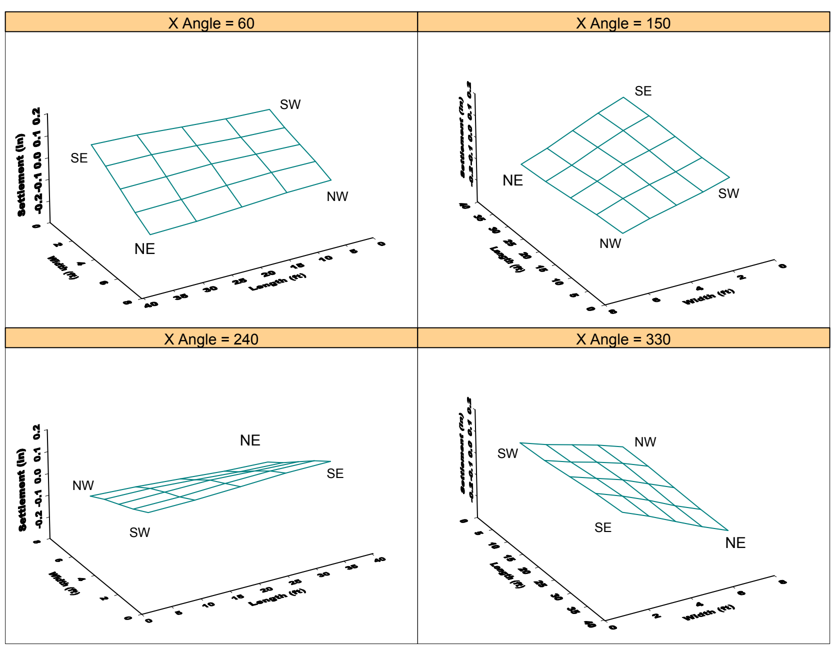

Figure 6.11: 3-D Plots of Settlement Profile After Construction Stage 5 (Barrier Wall Construction)

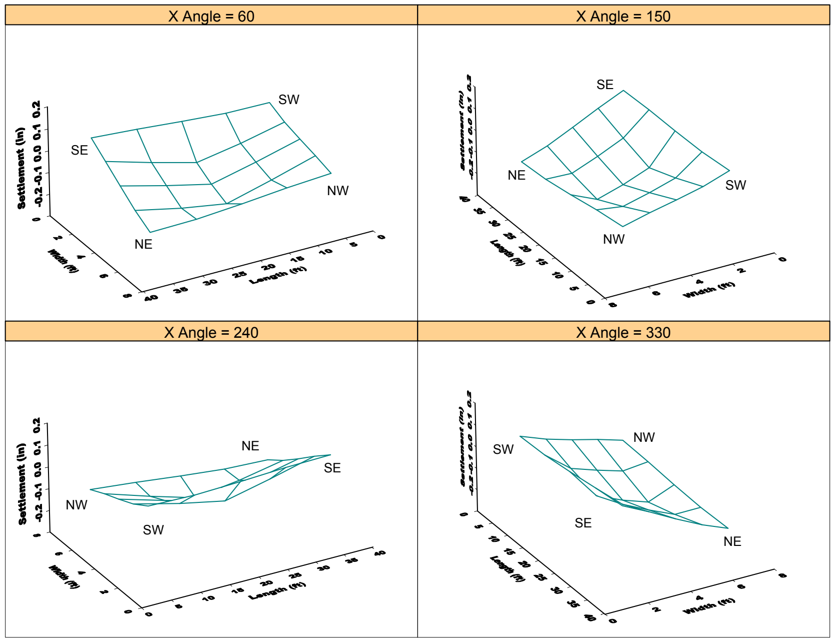

Figure 6.12: 3-D Plots of Settlement Profile After Construction Stage 6 (Placement of Girder Beams)

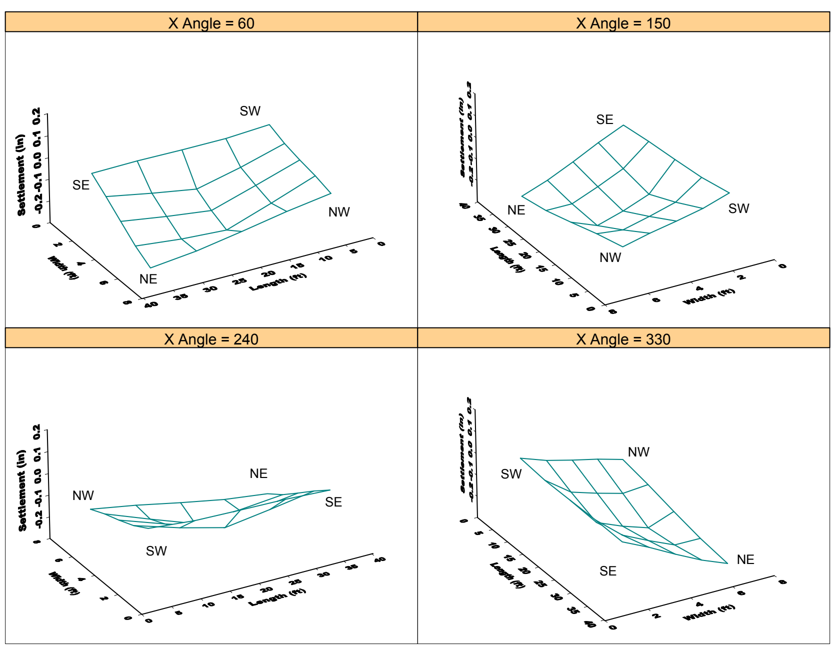

Figure 6.13: 3-D Plots of Settlement Profile After Construction Stage 7 (Deck Construction)

The 3-D plots show that the settlement of the Central Pier footing was not uniform, even from the beginning of the construction. The footing started tilting toward the north from as early as Stages 3 and 4, with the south side of the footing moving upward and the north side of the footing moving downward. The degree of tilting is highly magnified in these 3-D plots because of the scale used on the Z (settlement) axis. Even in the final state depicted in Figure 6.13, the maximum slope experienced by the footing settlement is as small as 0.4%.

The average settlement behavior of the Central Pier foundation is summarized in Table 6.4. The average settlement values are determined two ways. First, the average values are made considering the movements of all five points as in Table 6.4 (a). Table 6.4 (b) then gives the average settlement values made for the three points that experienced one or less upward movements but recovered from the loss in settlement.

Table 6.4: Average Settlements of Central Pier Footing

(a) Average Settlements for All Five (NE, NW, C, SE, SW) Points

Construction Stage	Description	Settlement (inches)
2	Pier Column Construction	0.05 (1.3 mm)
3	Soil Backfill	0.06 (1.4 mm)
4	Pier Cap Construction	
5	Barrier Wall Construction	0.00 (0.0 mm)
6	Girder Beam Placement	0.06 (1.5 mm)
7	Deck Construction	0.13 (3.3 mm)

(b) Average Settlements for Three (NE, NW, C) Points

Construction Stage	Description	Settlement (inches):	
		Increase	Total
2	Pier Column Construction	0.06 (1.5 mm)	0.06 (1.5 mm)
3	Soil Backfill	0.03 (0.8 mm)	0.09 (2.3 mm)
4	Pier Cap Construction		
5	Barrier Wall Construction	-0.04 (-1.0 mm)	0.05 (1.3 mm)
6	Girder Beam Placement	0.06 (1.5 mm)	0.11 (2.8 mm)
7	Deck Construction	0.09 (2.3 mm)	0.20 (5.1 mm)

According to Table 6.4, construction stage 7 (deck construction) produced the largest settlement increase among all the construction stages, then the pier column construction. The fifth stage (barrier wall construction) did not create any increase in the average settlement. Figure 6.14 plots the data presented in Table 6.4.b graphically, showing that overall the average settlement increased from 0.06 inches (1.5 mm) to 0.2 inches (5.1 mm).

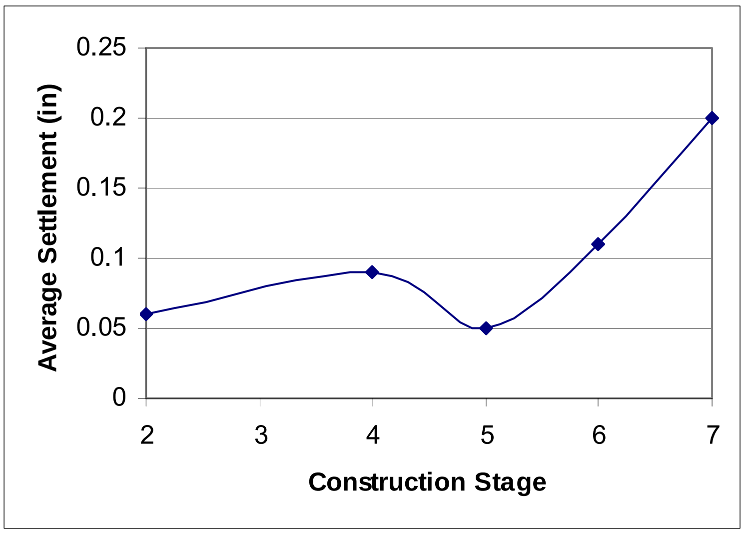

Figure 6.14: Average Settlement (FRA-670-0380)

6.2.3 Tilting of Pier Columns

Tilting measurements were taken on two columns (east and west) constructed on the Central Pier foundation. The tilting behavior was monitored only in the longitudinal direction of the bridge as can be seen in Figure 6.15. An earlier study by ORITE indicated that the tilting in the transverse direction of the bridge would be generally negligible compared to that in the longitudinal direction of the bridge. Table 6.5

summarizes the tiltmeter measurements taken at the FRA-670-0380 site. Both of the monitored columns moved slightly (0.126° for the east column and 0.235° for the west column) toward the north.

Theoretically, the columns should tilt toward the north, but only due to the last two construction stages (placement of girder beams, deck construction). However, the columns exhibited some tilting behaviors prior to the last two stages, indicating that the tilting of the pier column can be influenced by additional factors such as spatial variations of the bearing soil properties and the actual construction practices.

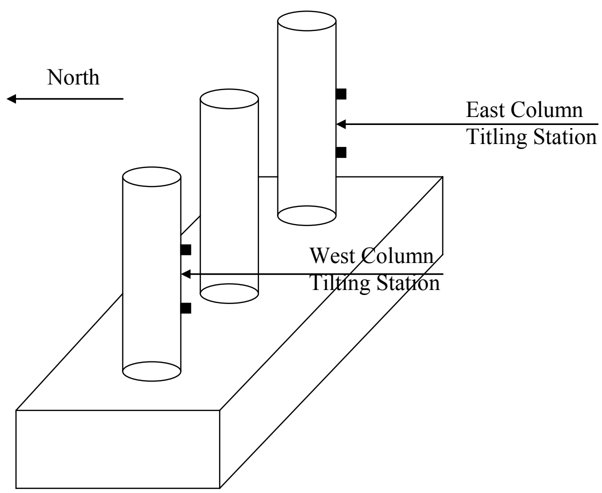

Figure 6.15: Locations of Tilting Stations

Table 6.5: Summary of Tilting Measurements (FRA-670-0380)

(a) East Column

Construction Stage	Description	Angle (degrees)
2	Pier Column Construction (Initial)	-0.788
3	Soil Backfill	-0.745
4	Pier Cap Construction	
5	Barrier Wall Construction	-0.825
6	Girder Beam Placement	-0.708
7	Deck Construction	-0.670
8	Bridge Open to Traffic	-0.662

Table 6.5 (cont'd):

(b) West Column

Construction Stage	Description	Angle (degrees)
2	Pier Column Construction (Initial)	-0.395
3	Soil Backfill	-0.541
4	Pier Cap Construction	
5	Barrier Wall Construction	-0.292
6	Girder Beam Placement	-0.272
7	Deck Construction	-0.372
8	Bridge Open to Traffic	-0.160

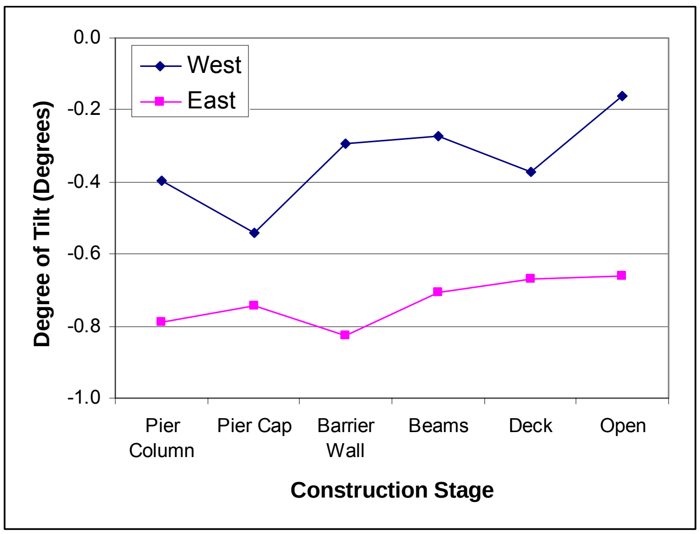

Figure 6.16: Tilting Behaviors of Pier Columns (FRA-670-0380)

6.2.4 Correlations Among Field Performance Data

The tilting measurements taken on the pier columns implied that the settlement points on the north side might have moved downward slightly. The change in the degree of tilt for both the east and west columns is 0.126º and 0.235º, respectively. The 3-D settlement profile plots (Figures 6.9 through 6.13) exhibit quite a large tilt toward the north side of the footing. Such a tilting behavior also suggests higher contact pressure development on the north side, assuming little spatial variability in the bearing soil properties. However, the 3-D pressure mound plots (Figures 6.1 through 6.7) show that the contact pressure magnitudes were larger on the south side. The settlement and tilting performances both show global behavior of the relatively rigid structure, whereas the pressure cell readings reflected a more localized behavior.

6.3 MOT-70/75 Ramp C

6.3.1 Pier 18

6.3.1.1 Contact Pressure

The readings for the pressure cells beneath Pier 18 are summarized in Table 6.6. Each of the seven pressure cell readings were taken and calculated for the six construction stages. The pressure cell locations were seen in Figure 5.20. Figures 6.17 through 6.22 are 3-D plots of the cell's contact pressure at each stage. The southeast corner of the footing, where pressure cell #59234 is located, was defined as the origin. Since each figure shows four views of the footing, rotating about the Z axis, there are labels on the corners to help identify the positioning of the plots. As the construction continued, the pressure increased and built a mound, or pressure bulb, which can be seen in the 3-D plots. The scale for the Z axis has increments of 1.0 tsf (95.8 kPa) with a value of 3.0 tsf (287.3 kPa) as the largest value.

Table 6.6: Individual Pressure Cell Readings (Pier 18)

	Contact Pressure (tsf) Measured by:						
Cell	59234	59232	59229	04-2368	04-2365	04-2366	04-2367
Position	SE	SW	Center E	Center	Center W	NE	NW
Stage 1	0.56	0.39	0.42	0.53	0.27	0.42	0.40
Stage 2	0.39	0.22	0.81	1.28	0.58	0.51	0.45
Stage 3	0.91	0.47	1.26	1.90	1.03	1.11	0.92
Stage 4	0.86	0.52	1.32	1.95	1.17	1.07	0.94
Stage 5	1.24	0.77	1.42	1.94	1.30	1.55	1.33
Stage 6	1.21	0.72	1.54	2.10	1.35	1.52	1.29

[Note] 1 tsf = 95.8 kPa.

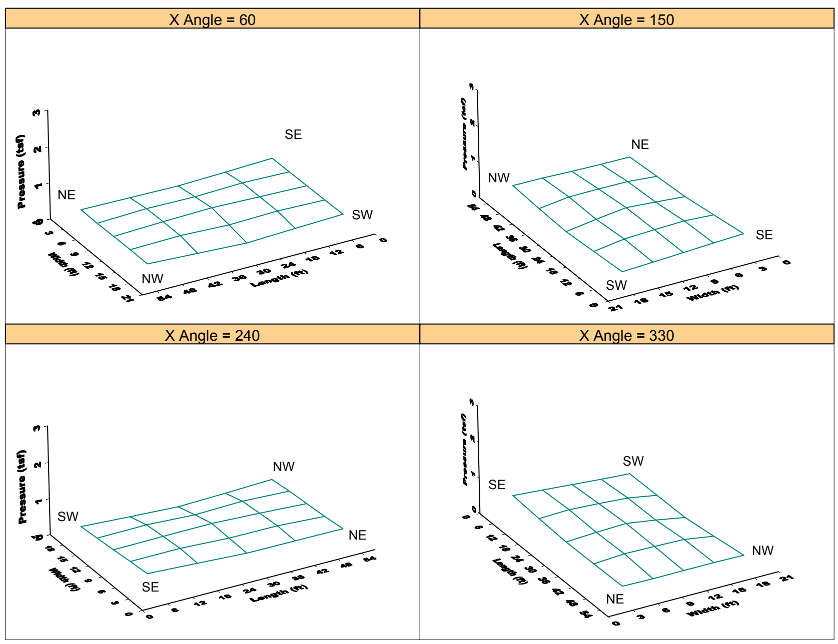

Figure 6.17: 3-D Plot of Pier 18 Bearing Pressure Distribution After Construction Stage 1 (Footing Construction)

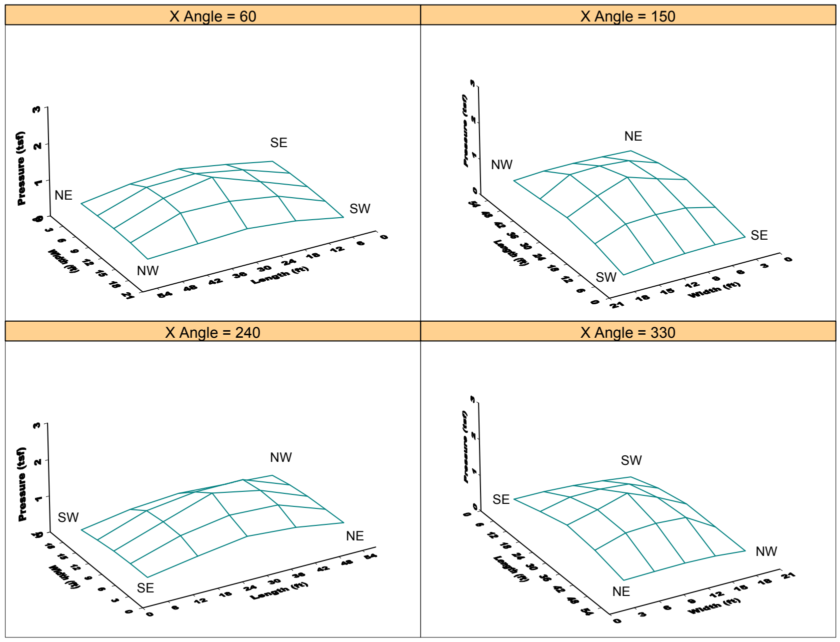

Figure 6.18: 3-D Plots of Pier 18 Bearing Pressure Distribution After Construction Stage 2 (Pier Wall Construction)

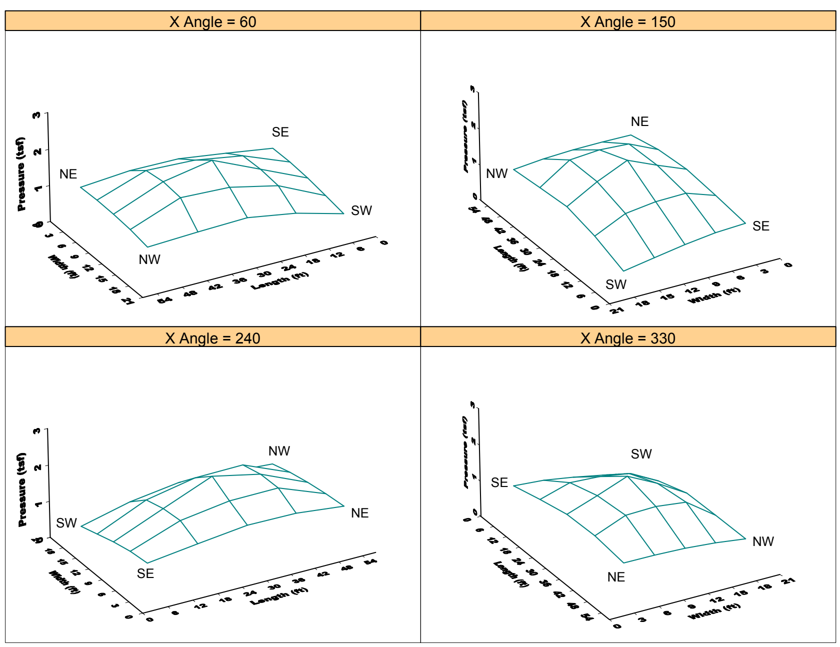

Figure 6.19: 3-D Plots of Pier 18 Bearing Pressure Distribution After Construction Stage 3 (Soil Backfill)

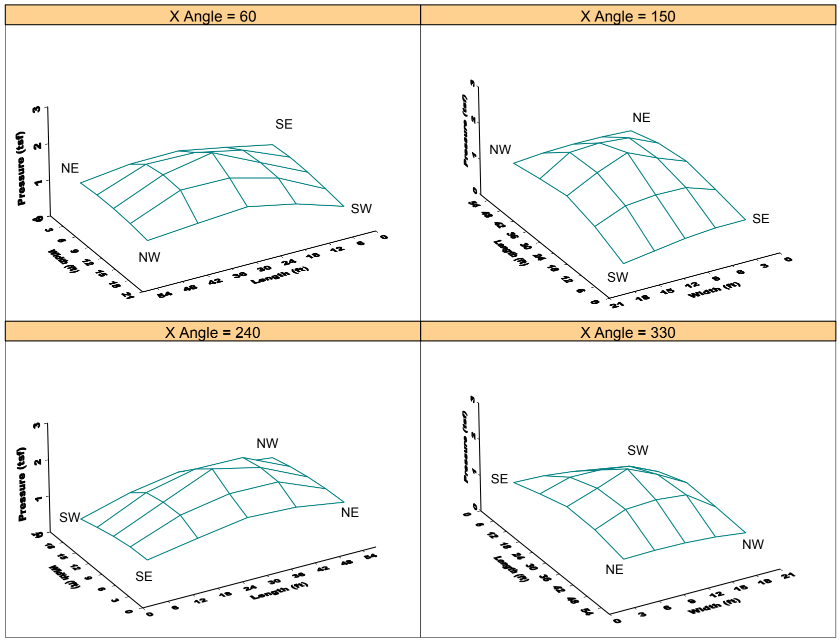

Figure 6.20: 3-D Plots of Pier 18 Bearing Pressure Distribution After Construction Stage 4 (Placement of Girder Beams)

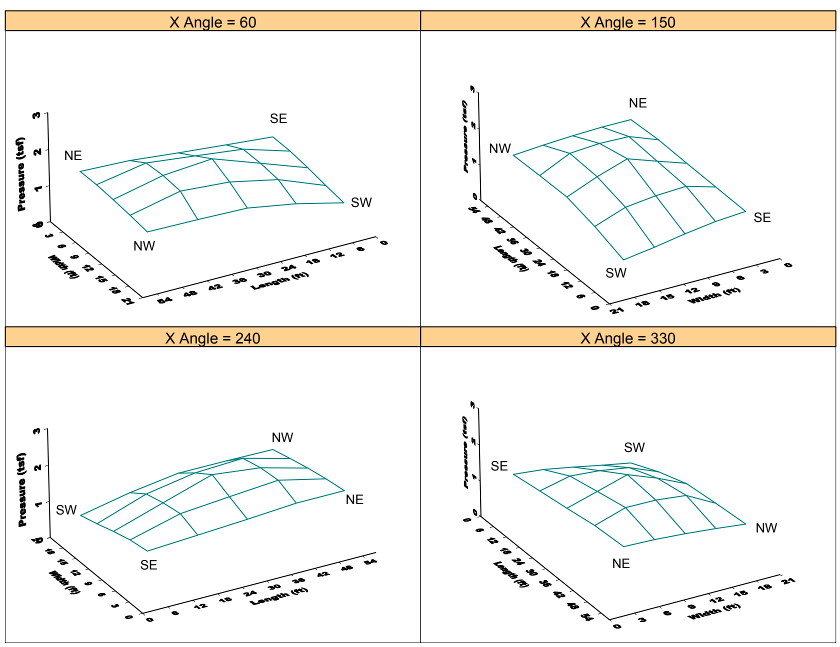

Figure 6.21: 3-D Plots of Pier 18 Bearing Pressure Distribution After Construction Stage 5 (Deck Construction)

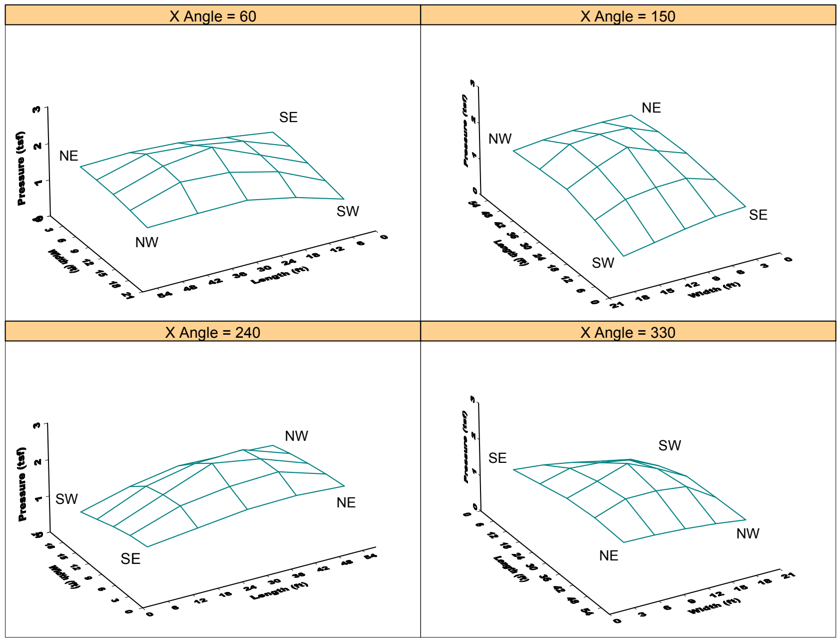

Figure 6.22: 3-D Plot of Pier 18 Bearing Pressure Distribution After Construction Stage 6 (Bridge Open to Traffic)

For Pier 18, the pressure cell readings increased as the loads were applied. The figures for each stage have similar shapes from the wall construction to the opening of the bridge. As the construction stages went forward, the foundation tilted slightly. The north side of the pier registered more pressure than the south side and also on the east side more than the west side. Once the pier wall was erected, all of the construction stages had an evident pressure bulb and exhibited a concave upward shape.

The average contact pressures measured by the cells beneath Pier 18 during the construction stages are listed in Table 6.7. The values for the increase between the stages and the cumulative values are both shown. Figure 6.23 shows the average pressure increase for the construction stages based on the data in Table 6.7. As seen in both the table and figure, the stages that introduced the largest increase in contact pressure is the soil backfill of the pier, followed by the footing construction.

Table 6.7: Average Contact Pressure Measured By Pressure Cells (Pier 18)

Const. Stage No.	Description	Ave. Contact Pressure (tsf):	
		Increase	Cumulative
1	Footing Construction	0.426	0.426
2	Pier Wall Construction	0.178	0.604
3	Soil Backfill	0.483	1.087
4	Placement of Girder Beams	0.032	1.119
5	Deck Construction	0.247	1.366
6	Bridge Open to Traffic	0.024	1.390

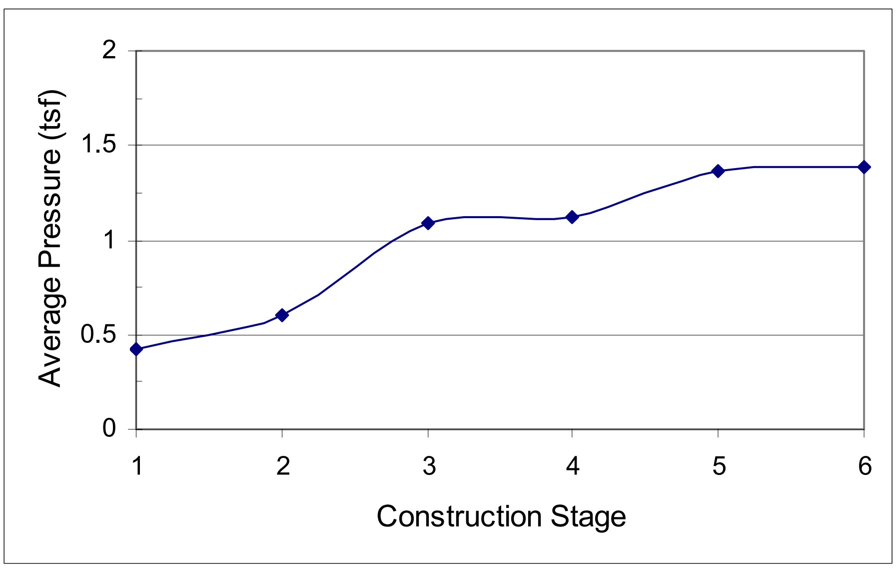

Figure 6.23: Average Contact Pressure for Each Stage (Pier 18)

6.3.1.2 Footing Settlement

Table 6.8 shows the average settlement measured throughout the construction stages for Pier 18. The locations labeled as (a) through (e) in the table were explained previously in

Figures 5.17 and 5.18. The settlement for pier wall construction is a negative value, indicating that the footing did not settle but rather moved upwards.

Table 6.8: Summary of Field Settlement Measurements (Pier 18)

(a) Northeast (NE) Point

Construction Stage	Description	Settlement - inches (mm)
2	Pier Wall Construction	-0.06 (-1.5)
3	Soil Backfill	0.12 (3.1)
4	Placement of Girder Beam	0.28 (7.1)
5	Deck Construction	0.32 (8.1)
6	Bridge Open to Traffic	0.36 (9.1)

(b) Northwest (NW) Point

Construction Stage	Description	Settlement – inches (mm)
2	Pier Wall Construction	-0.03 (-0.76)
3	Soil Backfill	0.48 (12.2)
4	Placement of Girder Beam	1.22 (31.0)
5	Deck Construction	1.1 (27.9)
6	Bridge Open to Traffic	1.2 (30.5)

(c) Center (C) Point

Construction Stage	Description	Settlement – inches (mm)
2	Pier Wall Construction	-0.03 (-0.76)
3	Soil Backfill	0.3 (7.6)
4	Placement of Girder Beam	0.9 (22.9)
5	Deck Construction	0.86 (21.8)
6	Bridge Open to Traffic	0.96 (24.4)

(d) Southeast (SE) Point

Construction Stage	Description	Settlement – inches (mm)
2	Pier Wall Construction	-0.09 (-2.3)
3	Soil Backfill	0.18 (4.6)
4	Placement of Girder Beam	0.58 (14.7)
5	Deck Construction	0.64 (16.3)
6	Bridge Open to Traffic	0.60 (15.2)

(e) Southwest (SW) Point

Construction Stage	Description	Settlement – inches (mm)
2	Pier Wall Construction	-0.03 (-0.76)
3	Soil Backfill	0.12 (3.0)
4	Placement of Girder Beam	0.44 (11.2)
5	Deck Construction	0.3 (7.6)
6	Bridge Open to Traffic	0.36 (9.1)

3-D plots for the footing settlement of Pier 18 are presented in Figures 6.24 through 6.27 for each construction stage. Each of the locations in Table 6.8 is used to make these plots. The origin is again the southeast corner and each corner is denoted with labels to easily see the footing positioning for each of the plots. There are four views given for each stage, which helps to see the actual shape of the settlement. The settlement is entered as a negative displacement, which allows the orientation of the settlement to be in a downward direction, as if looking directly at the footing. The Z axis scale has a range of -1.5 inches (38.1 mm) to 0.5 inches (12.7 mm) for the profiles after the pier wall construction (Figure 6.24). For all the other construction stages (Figures 6.25 to 6.28), the range was from -1.5 inches (38.1 mm) to 0.0 inches (0.0 mm).

The 3-D plots for pier 18 show that the settlement for each stage has the same relative shape. After the pier wall was constructed, each of the monitoring locations moved upwards, meaning the footing settled negatively. Figure 6.24 cannot show this shape effectively since the difference in the values is approximately 0.03 inches (0.762 mm). Of the other three construction stages (soil backfill, girder beam placement, and deck construction), the most settlement occurred at the northwest corner, followed by the center point and the southeast corner.

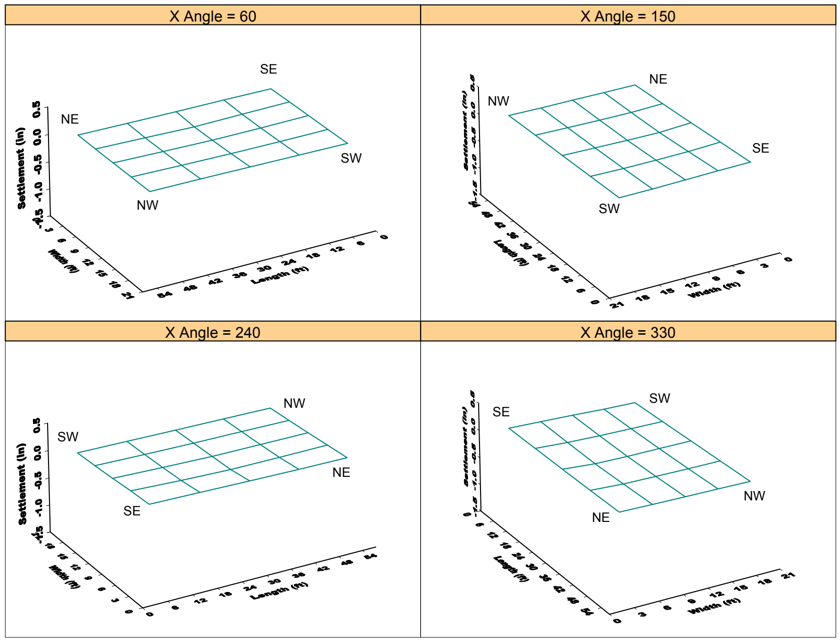

Figure 6.24: 3-D Plots of Pier 18 Settlement Profile After Construction Stage 2 (Pier Wall Construction)

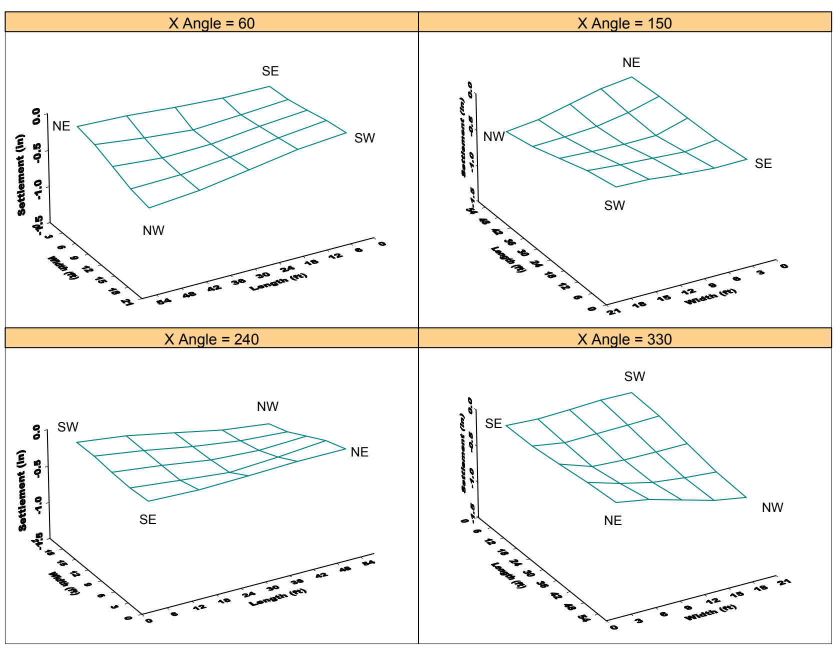

Figure 6.25: 3-D Plots of Pier 18 Settlement Profile After Construction Stage 3 (Soil Backfill)

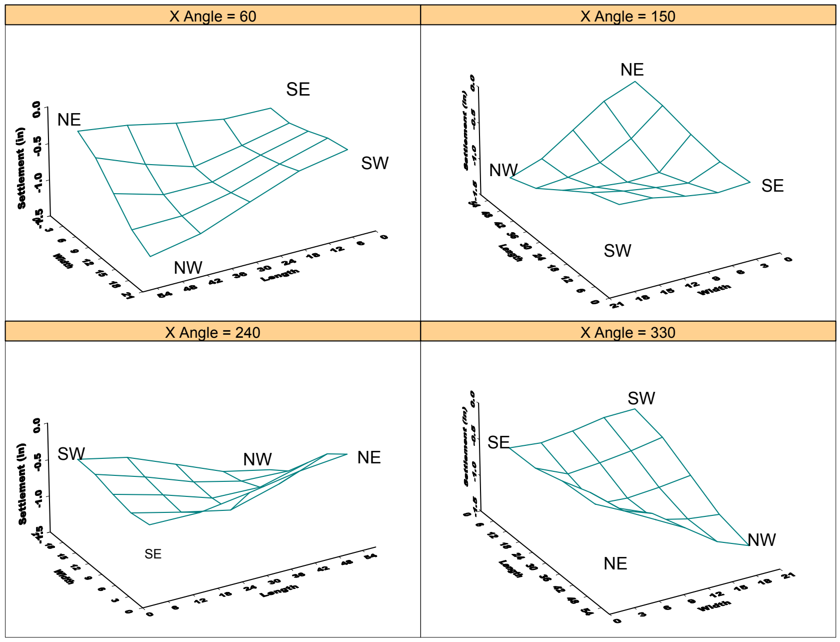

Figure 6.26: 3-D Plots of Pier 18 Settlement Profile After Construction Stage 4 (Placement of Girder Beams)

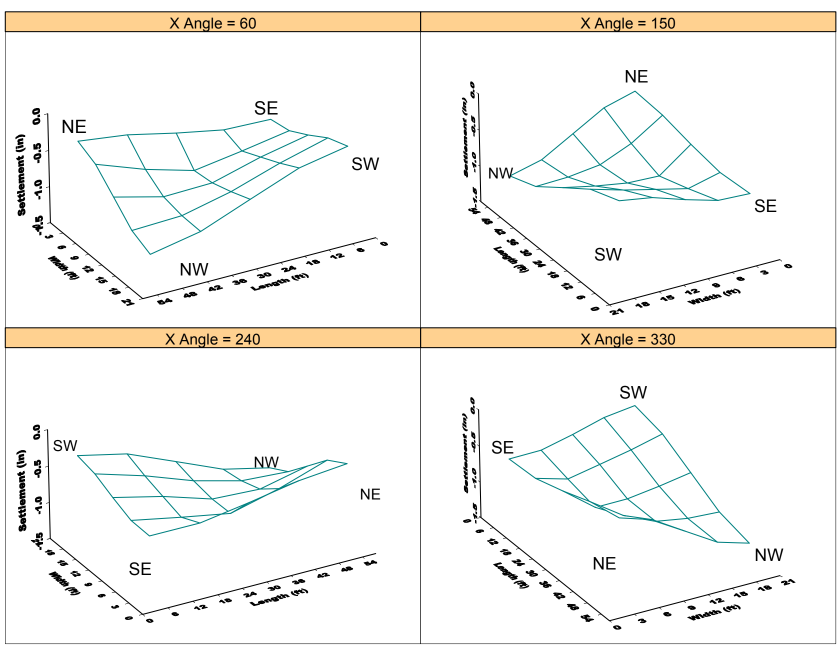

Figure 6.27: 3-D Plots of Pier 18 Settlement Profile After Construction Stage 5 (Deck Construction)

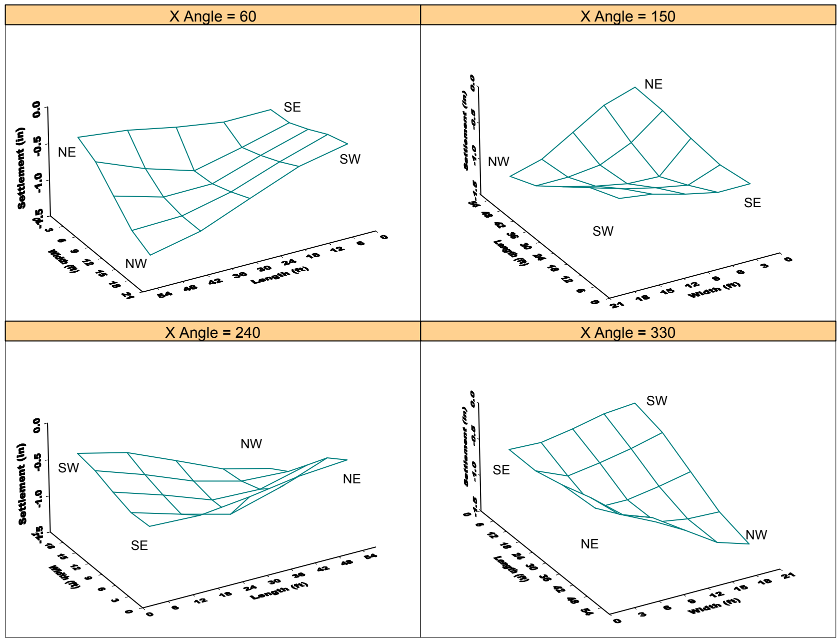

Figure 6.28: 3-D Plots of Pier 18 Settlement Profile After Construction Stage 6 (Bridge Open to Traffic)

Table 6.9 gives the average settlement for the monitoring points based on the construction stages, which is also plotted in Figure 6.29. Constructing the pier wall initiated a negative settlement of the pier footing. The placement of the girder beams caused the most settlement among the construction stages. After the deck construction, three of the settlement monitoring points moved upward causing an average decrease in the settlement experienced by the footing. The upward movement was caused by soil saturation from the sprinkler system on the deck, causing heave beneath the footing. After the deck construction was finished, the settlement experienced by the pier footings was 0.06 inches (1.5 mm), which is approximately 8.5% of the total settlement.

Table 6.9: Average Settlement of All Monitoring Points for Pier 18

Construction Stage	Description	Settlement – inches (mm)
2	Pier Wall Construction	-0.05 (-1.3)
3	Soil Backfill	0.24 (6.1)
4	Girder Placement	0.68 (17.4)
5	Deck Construction	0.64 (16.4)
6	Bridge Open to Traffic	0.70 (17.7)

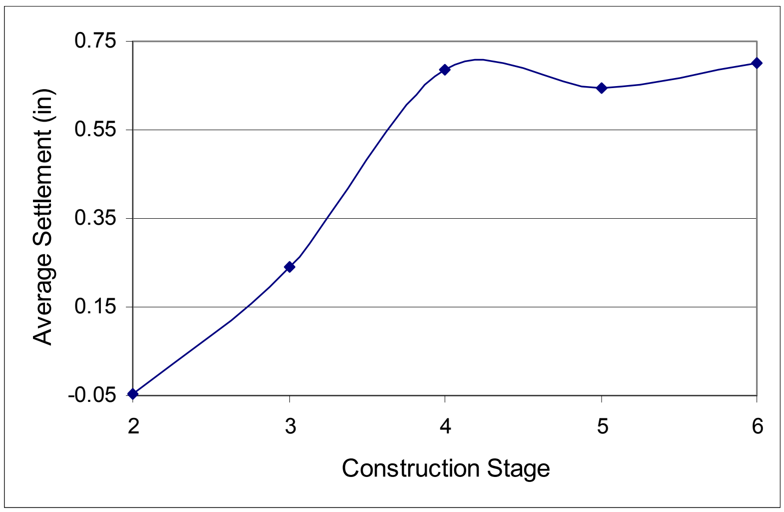

Figure 6.29: Average Settlement (Pier 18)

6.3.1.3 Tilting of Pier Walls

Tilting measurements were taken on Pier 18 at the center of the stem wall. Only the longitudinal direction of the bridge was monitored, as with the FRA-670-0380 project. Table 6.10 gives the tilt-meter measurements taken and shows that the final tilting after construction finished was 0.25º. Figure 6.30 was developed from the data in Tables 6.10. Pier 18 initially was rotated toward the east 1.27º and moved more than one degree from its original position, however has been practically stationary since then showing that the first reading was erroneous. The top of Pier 18 initially was rotated toward the east -1.27º but during construction corrected and rotated west.

Table 6.10: Summary of Tilting Measurement (Pier 18)

Construction Stage	Description	Angle (degrees)
3	Soil Backfill	-1.27
4	Placement of Girder Beams	-0.25
5	Deck Construction	-0.23
6	Bridge Open to Traffic	-0.25

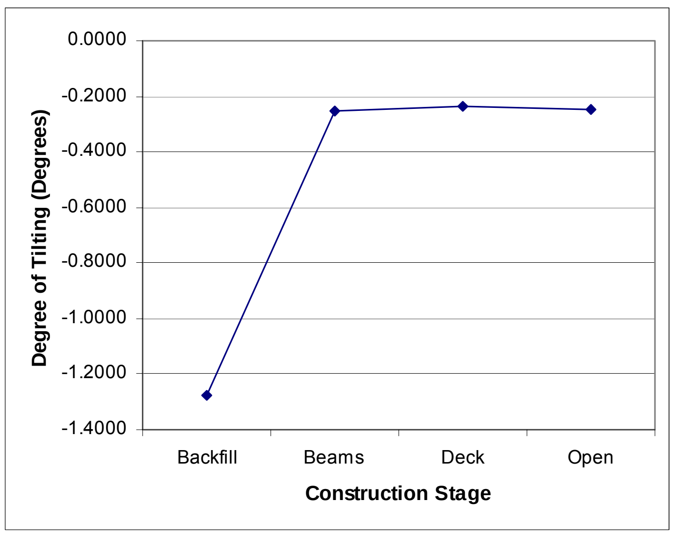

Figure 6.30: Tilting Behavior of Pier Walls (Pier 18)

6.3.1.4 Correlations Among Field Performance Data

The settlement measurements taken on Pier 18 implied that the west side of the footing settled more than the east side. Tilting measurements taken from the east side of the pier duplicate the same result as the settlement measurements with tilting degree change of over 1.0º toward the west. The pressure measurements exhibit a slightly larger amount of pressure on the north end of the footing compared to the south and also more pressure on the east side than the west. These readings do not correlate with the settlement and tilting readings, which may be caused by the inconsistencies in the soil properties beneath the footing near the pressure cells. The settlement and tilting performances both showed global behavior of the relatively rigid structure, but the pressure cell readings reflected a more localized behavior.

6.3.2 Pier 19

6.3.2.1 Contact Pressure

The readings for the pressure cells under Pier 19 are seen in Table 6.11 and separated into construction stages and position as was discussed with Pier 18. Five pressure cells were placed under this pier's footing. The center pressure cell (Cell #59228) stopped working properly soon after its placement, so only four were used to create 3-D plots. This may not give as complete results as are needed. Figures 6.31 through 6.36 are presented the same way as Pier 18, using the southeast corner (Cell #04-2369) as the origin and rotating about the Z axis.

For Pier 19, the pressure readings of the four remaining working cells increased from the footing construction through each of the stages. Figures 6.31 through 6.36 show the pressure distribution for each construction stage. The shape is much more flat than was for Pier 18 since no cell was used at the center point.

Table 6.11: Individual Pressure Cell Readings (Pier 19)

	Contact Pressure (tsf) Measured by:				
Cell	#04-2369	#04-2364	#59228	#59235	#59227
Position	SE	SW	Center	NE	NW
Stage 1	.47	.36	.29	.52	.52
Stage 2	.99	.61	.23	.88	.95
Stage 3	1.75	1.17	.28	1.39	1.87
Stage 4	1.61	1.22	.32	1.47	2.17
Stage 5	2.02	1.45	.30	1.92	2.60
Stage 6	2.01	1.50	.29	1.93	2.59

[Note] 1 tsf = 95.8 kPa

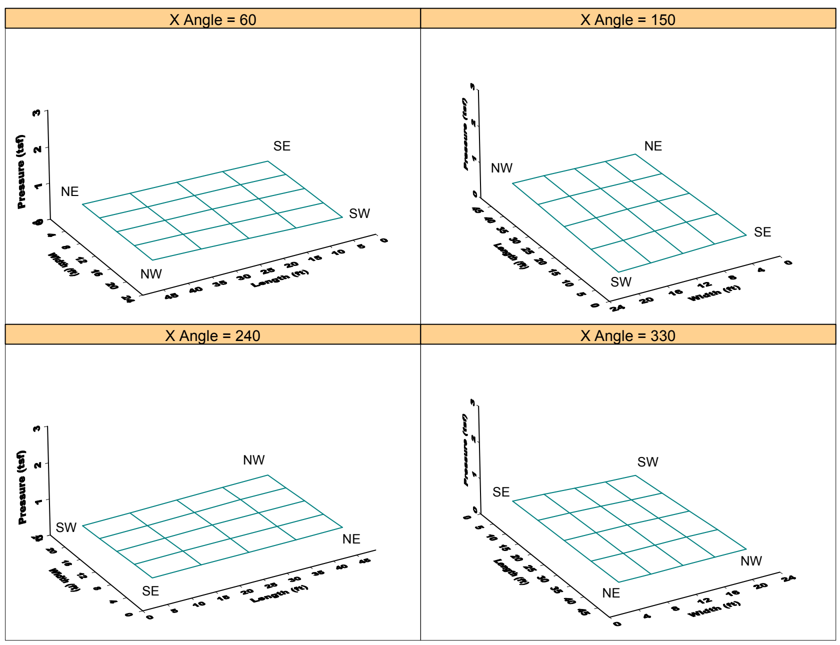

Figure 6.31: 3-D Plots of Pier 19 Bearing Pressure Distribution After Construction Stage 1 (Footing Construction)

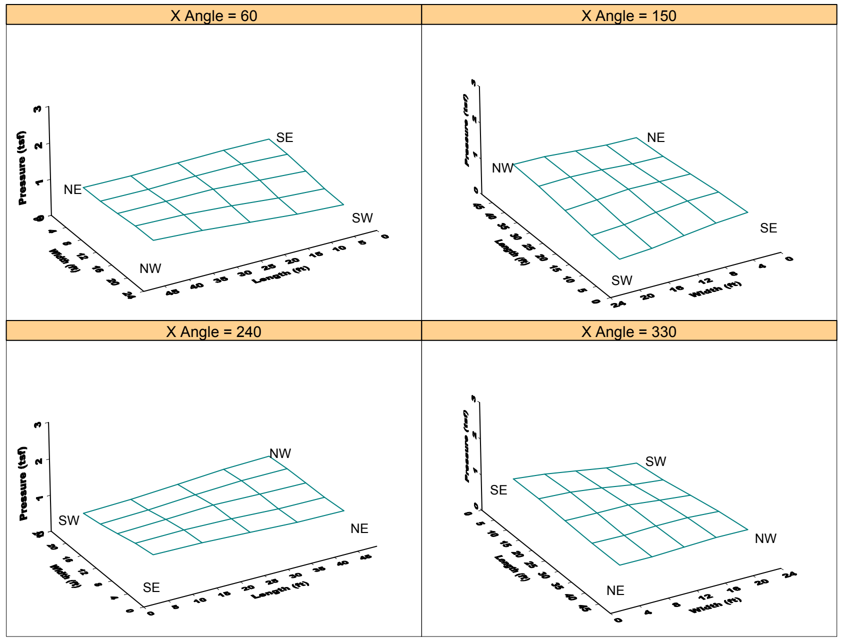

Figure 6.32: 3-D Plots of Pier 19 Bearing Pressure Distribution After Construction Stage 2 (Pier Wall Construction)

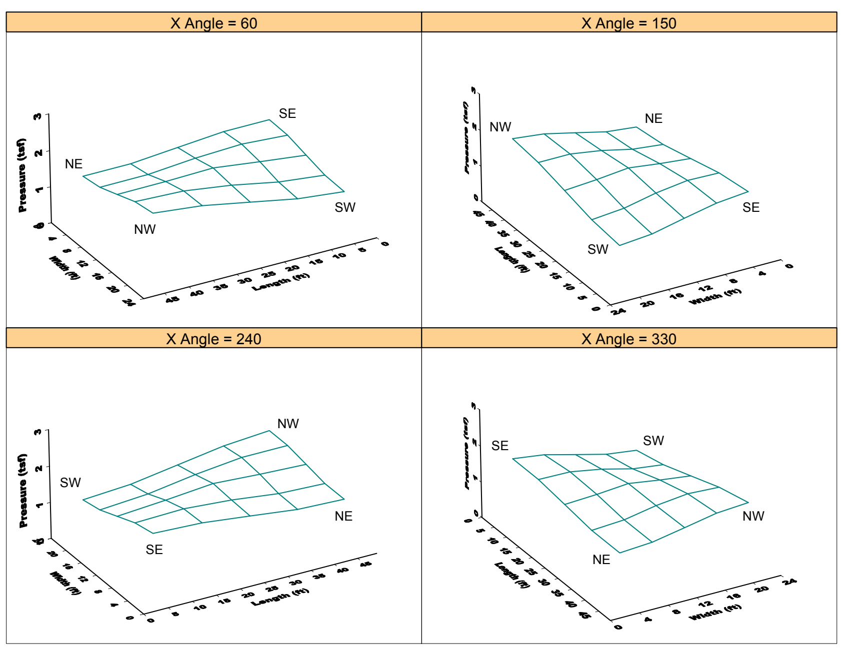

Figure 6.33: 3-D Plots of Pier 19 Bearing Pressure Distribution After Construction Stage 3 (Soil Backfill)

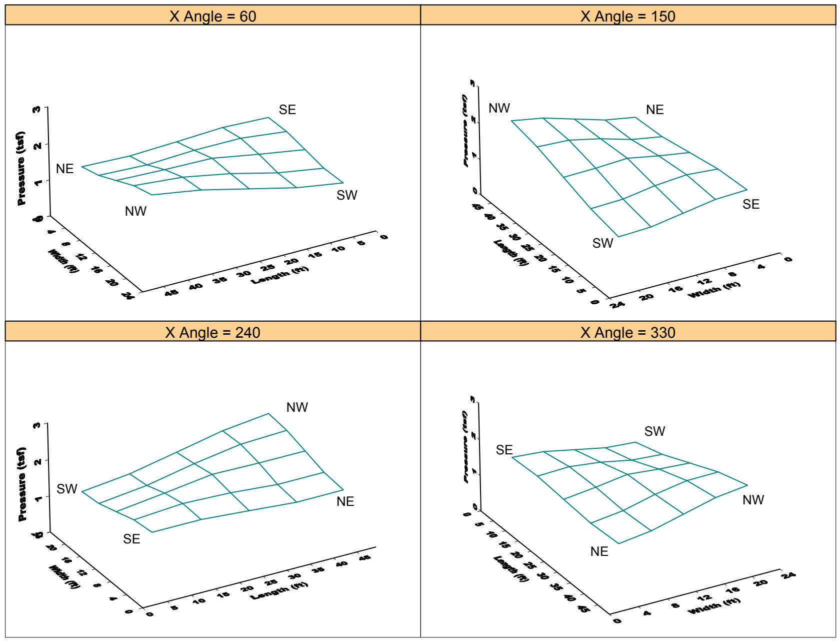

Figure 6.34: 3-D Plots of Pier 19 Bearing Pressure Distribution After Construction Stage 4 (Placement of Girder Beams)

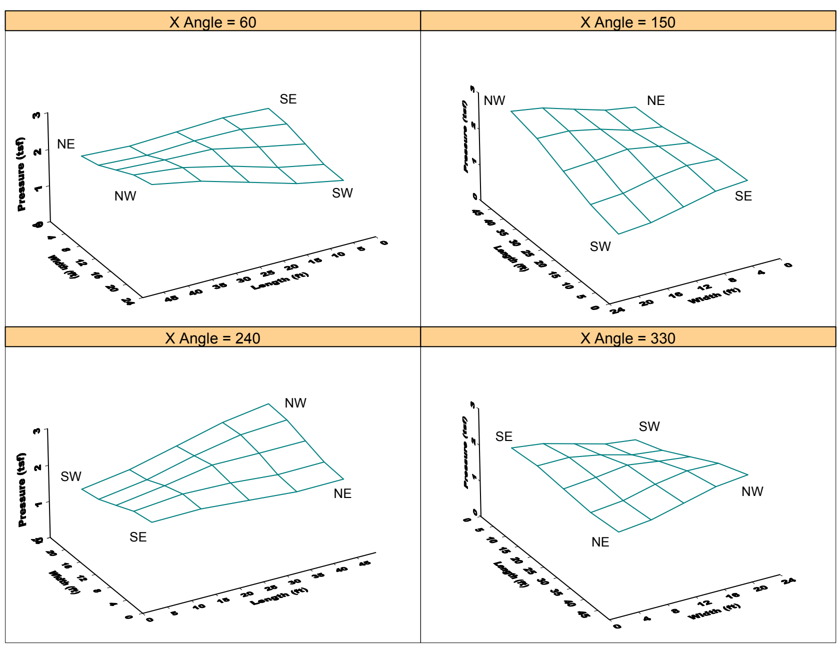

Figure 6.35: 3-D Plots of Pier 19 Bearing Pressure Distribution After Construction Stage 5 (Deck Construction)

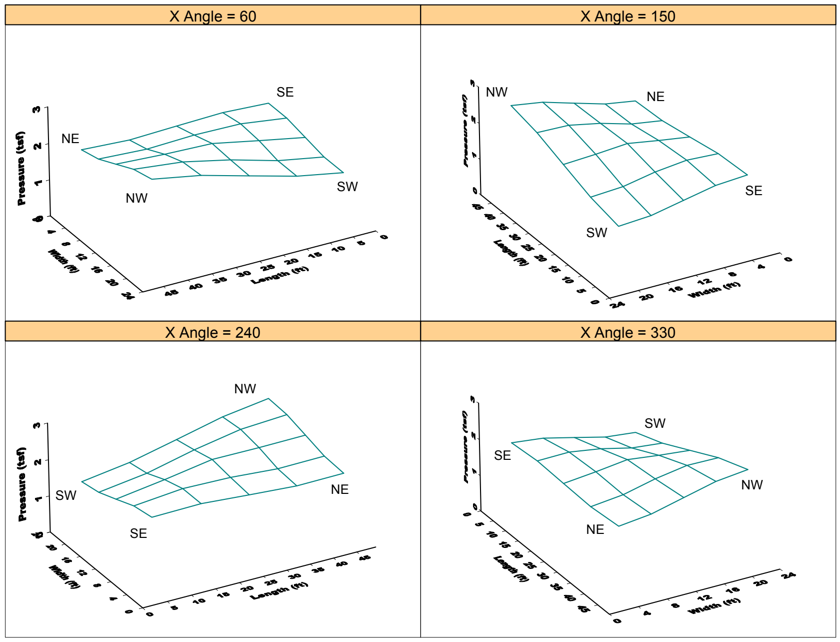

Figure 6.36: 3-D Plots of Pier 19 Bearing Pressure Distribution After Construction Stage 6 (Bridge Open to Traffic)

Table 6.12 gives the average contact pressure increase measured beneath Pier 19 and the cumulative contact pressures. From the cumulative values in the table, Figure 6.37 was developed. The placement of backfill over the Pier 19 footing gave the largest increase in contact pressure, followed by footing construction.

Table 6.12: Average Contact Pressure Measured By Pressure Cells (Pier 19)

Const. Stage No.	Description	Ave. Contact Pressure (tsf):	
		Increase	Cumulative
1	Footing Construction	0.469	0.469
2	Pier Wall Construction	0.387	0.856
3	Soil Backfill	0.690	1.546
4	Placement of Girder Beams	0.072	1.618
5	Deck Construction	0.379	1.997
6	Bridge Open to Traffic	0.009	2.006

Note: The values do not include pressure cell that stopped working properly.

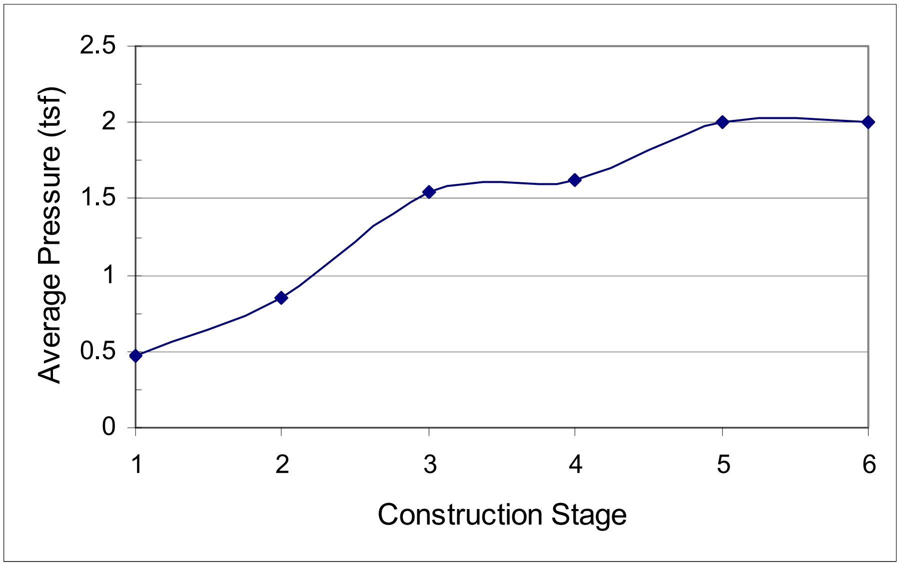

Figure 6.37: Average Contact Pressure for Each Stage (Pier 19)

6.3.2.2 Footing Settlement

The average settlement measured throughout the construction stages for Pier 19 is shown in Table 6.13. The locations labeled as (a) through (e) in the table are the same as in Table 6.8. When the deck construction was finished, the settlement monitoring points decreased in the amount of settlement from the previous stage (girder beam placement). This decrease was caused by the sprinkler system placed on the deck for 7 days to cure the concrete properly, causing the soil beneath to become saturated and swell.

Figures 6.38 through 6.42 give 3-D plots for the settlement of each construction stage for Pier 19. The origin for the plots is the southeast corner of the footing. Each corner is labeled for ease of identifying the positioning of the four rotated views of each figure. The Z axis ranges from -1.5 in (38.1 mm) to 0.0 in (0.0 mm) in increments of 0.5 in (12.7 mm).

Table 6.13: Summary of Field Settlement Measurements (Pier 19)

(a) Northeast (NE) Point

Construction Stage	Description	Settlement - inches (mm)
2	Pier Wall Construction	0.15 (3.8)
3	Soil Backfill	0.78 (19.8)
4	Placement of Girder Beam	1.08 (27.4)
5	Deck Construction	1.0 (25.4)
6	Bridge Open to Traffic	1.14 (29.0)

(b) Northwest (NW) Point

Construction Stage	Description	Settlement – inches (mm)
2	Pier Wall Construction	0.15 (3.8)
3	Soil Backfill	0.42 (10.7)
4	Placement of Girder Beam	0.88 (22.4)
5	Deck Construction	0.76 (19.3)
6	Bridge Open to Traffic	0.84 (21.3)

(c) Center (C) Point

Construction Stage	Description	Settlement – inches (mm)
2	Pier Wall Construction	0.27 (6.9)
3	Soil Backfill	0.6 (15.2)
4	Placement of Girder Beam	0.86 (21.8)
5	Deck Construction	0.80 (20.3)
6	Bridge Open to Traffic	1.02 (25.9)

(d) Southeast (SE) Point

Construction Stage	Description	Settlement – inches (mm)
2	Pier Wall Construction	0.06 (1.5)
3	Soil Backfill	0.24 (6.1)
4	Placement of Girder Beam	0.84 (21.3)
5	Deck Construction	0.7 (17.8)
6	Bridge Open to Traffic	0.9 (22.9)

(e) Southwest (SW) Point

Construction Stage	Description	Settlement – inches (mm)
2	Pier Wall Construction	0.27 (6.9)
3	Soil Backfill	0.66 (16.8)
4	Placement of Girder Beam	1.08 (27.4)
5	Deck Construction	0.9 (22.9)
6	Bridge Open to Traffic	0.9 (22.9)

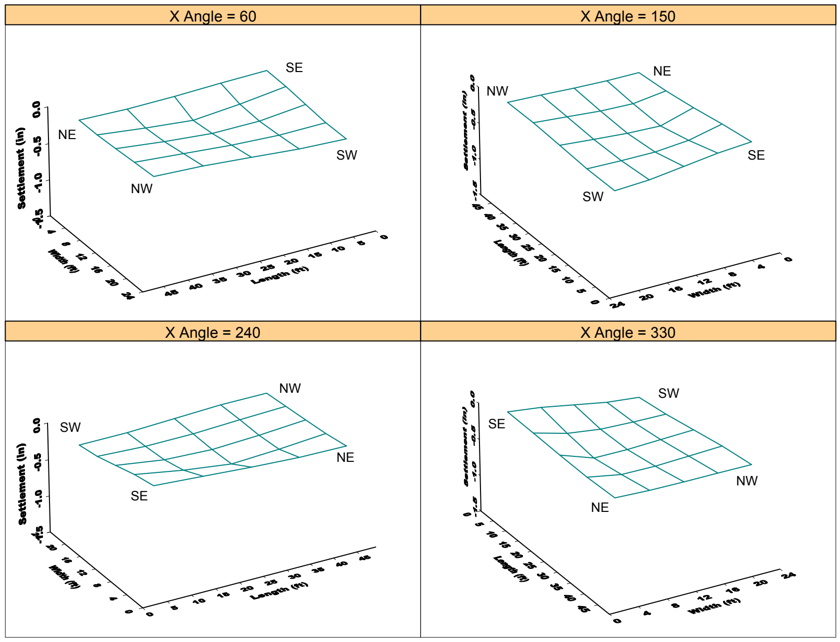

Figure 6.38: 3-D Plots of Pier 19 Settlement Profile After Construction Stage 2 (Pier Wall Construction)

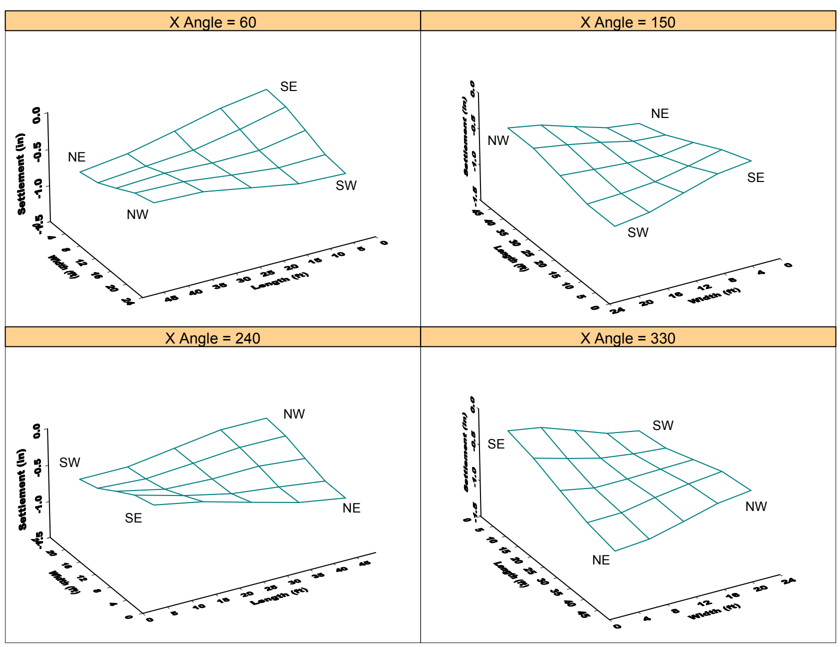

Figure 6.39: 3-D Plots of Pier 19 Settlement Profile After Construction Stage 3 (Soil Backfill)

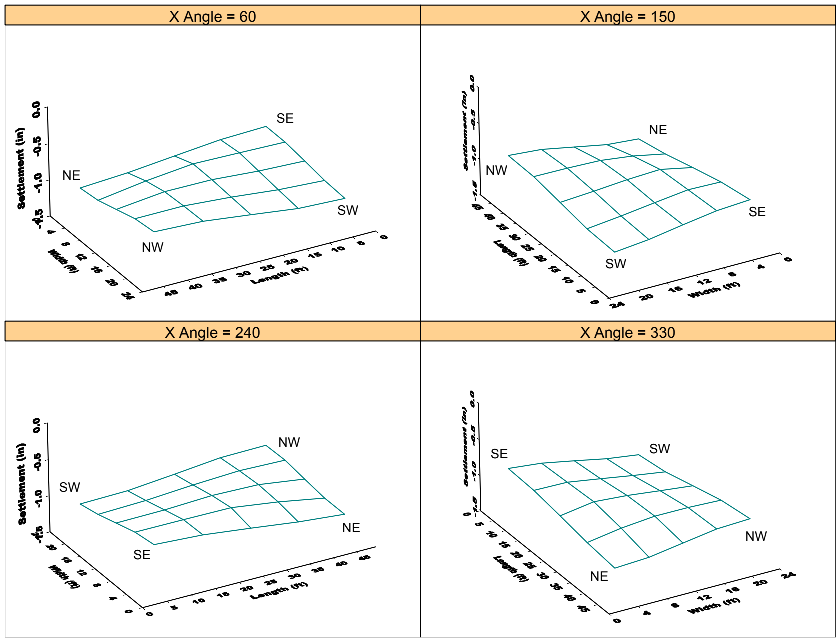

Figure 6.40: 3-D Plots of Pier 19 Settlement Profile After Construction Stage 4 (Placement of Girder Beams)

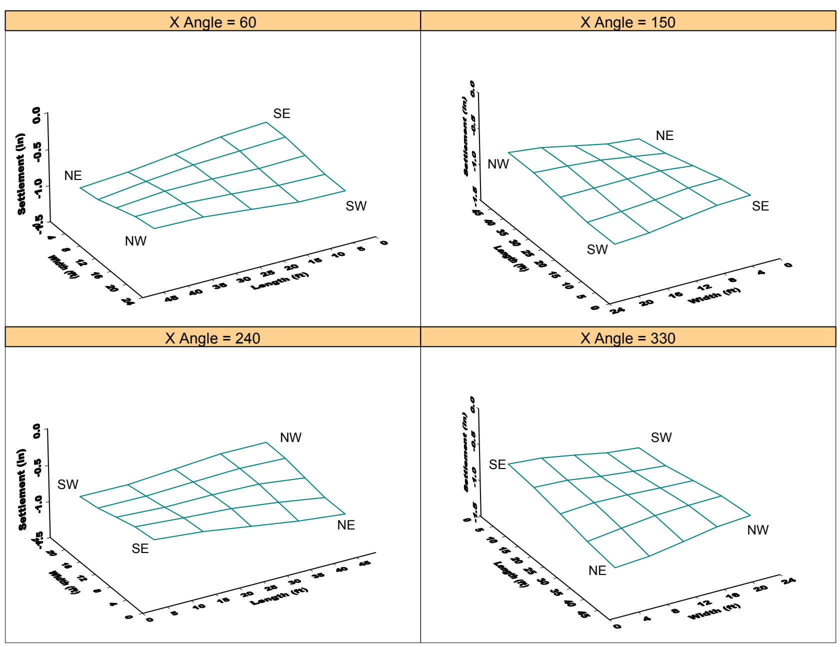

Figure 6.41: 3-D Plots of Pier 19 Settlement Profile After Construction Stage 5 (Deck Construction)

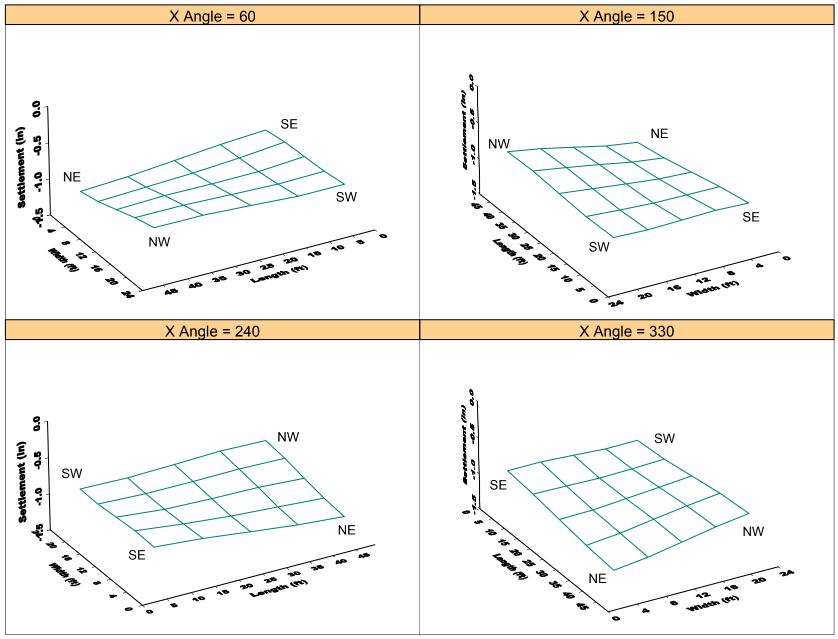

Figure 6.42: 3-D Plots of Pier 19 Settlement Profile After Construction Stage 6 (Bridge Open to Traffic)

The 3-D plots for Pier 19 show that the settlement for each stage was not completely uniform. For the pier wall construction, soil backfill, and girder beam placement stages, the settlement increased for each, but for the deck construction the settlement was reversed, raising the footing an average of 0.108 inches (2.74 mm). The northeast and southwest corners had the largest amount of settlement throughout each of the stages.

The average settlement for the five Pier 19 monitoring points is given in Table 6.14. Figure 6.43 shows the settlement values from Table 6.14 in graphical form. The settlement increased from the beginning, however after the deck was constructed the footing moved upward slightly. This uplifting of Pier 19 is similar to that of Pier 18, but

Pier 19 was more dramatic, since each settlement monitoring point for Pier 19 moved upward. The settlement experienced by the pier footing post deck construction was only 0.13 inches (3.3 mm), which is approximately 13.5 percent of the total settlement.

Table 6.14: Average Settlement of All Monitoring Points (Pier 19)

Construction Stage	Description	Settlement – inches (mm)
2	Pier Wall Construction	0.18 (4.6)
3	Soil Backfill	0.54 (13.7)
4	Placement of Girder Beam	0.95 (24.1)
5	Deck Construction	0.83 (21.1)
6	Bridge Open to Traffic	0.96 (24.4)

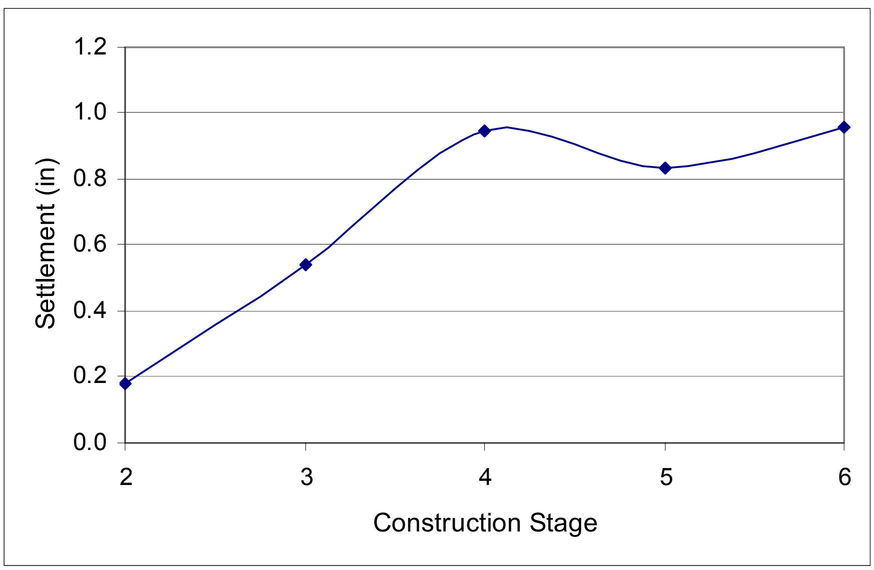

Figure 6.43: Average Settlement (Pier 19)

6.3.2.3 Tilting of Pier Walls

Tilting measurements for Pier 19 were taken at the center of the stem wall. However, only the longitudinal direction of the bridge was monitored. The tiltmeter measurements taken for Pier 19 are shown in Table 6.15. Figure 6.44 plots the data listed in Table 6.15. The Pier 19 stem wall rotated by only 0.025º. The initial placement of the footing was tilted toward the east. The movement of the pier was toward the west side of the footing. The values for the pier tilting are seen in Table 6.15.

Table 6.15: Summary of Tilting Measurements (Pier 19)

Construction Stage	Description	Angle (degrees)
3	Soil Backfill	-0.440
4	Placement of Girder Beams	-0.442
5	Deck Construction	-0.417
6	Bridge Open to Traffic	-0.421

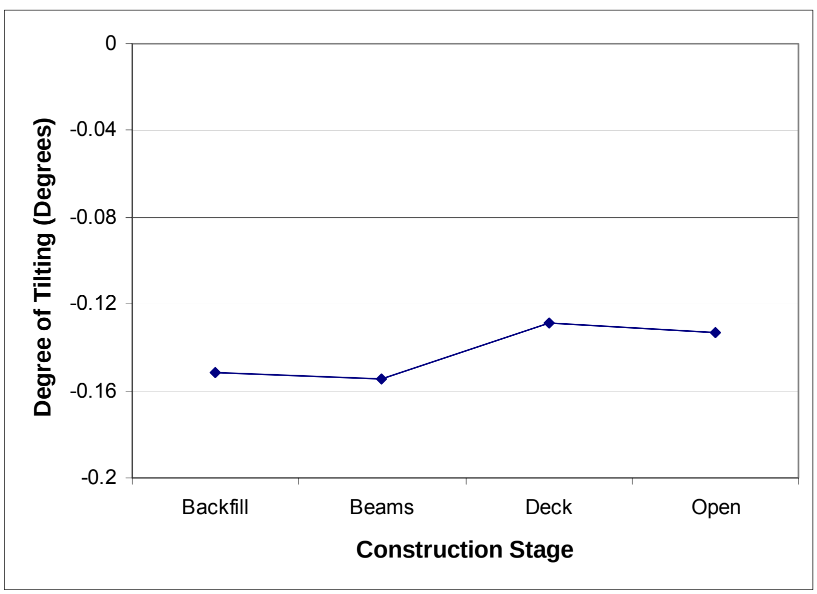

Figure 6.44: Tilting Behavior of Pier Walls (Pier 19)

6.3.2.4 Correlations Among Field Performance Data

When a tilting measurement has a negative degree, the pier wall tilts toward the side where the measurement is taken. For Pier 19, this means the wall initially tilted toward the east. The foundation, however, moved toward the west throughout the construction stages. The change in the degree of tilting was marginal with a value of 0.02º. The differences in the settlement points were also relatively small; however the east side of the footing seemed to settle slightly more. The recorded contact pressure measurements are a little larger on the north side of the footing as compared to the south side. However, there doesn't seem to be a trend in the east-west direction. None of the performance data correlate with the others, but they also don't seem to possess much tilt in any direction.

6.3.3 Forward Abutment

6.3.3.1 Footing Settlement

Table 6.16 presents the average settlement the Forward Abutment footing experienced under each of the construction stages. The abutment was instrumented for settlement measurements by the contractor at two points, one on the north end and one on the south end. The largest amount of settlement occurred during the soil backfilling stage. The north side had 1.02 inches (25.9 mm) of settlement, and the south side had 1.86 inches (47.2 mm) for the backfill construction stage.

Figures 6.45 through 6.48 are plots for the settlement of each construction stage. With only 2 settlement points, 3-D plots can not be made so a line graph comparing the north and south point is shown instead. This will not tell if the foundation tilted toward the east or west, but will give detail on the north/south movement. The tilt shown in the figures looks more tilted than they actually are in the field. Construction stage 2, the abutment wall construction, was not plotted since it is the initial reading.

Table 6.16: Summary of Field Settlement Measurements (Forward Abutment)

(a) North (N) Point

Construction Stage	Description	Settlement – inches (mm)
2	Abutment Wall Construction	0.00 (0.00)
3	Soil Backfill	1.02 (25.9)
4	Placement of Girder Beams	1.04 (26.4)
5	Deck Construction	1.22 (31.0)
6	Bridge Open to Traffic	1.32 (33.5)

(b) South (S) Point

Construction Stage	Description	Settlement – inches (mm)
2	Abutment Wall Construction	0.00 (0.00)
3	Soil Backfill	1.86 (47.2)
4	Placement of Girder Beams	1.88 (47.8)
5	Deck Construction	1.96 (49.8)
6	Bridge Open to Traffic	2.04 (51.8)

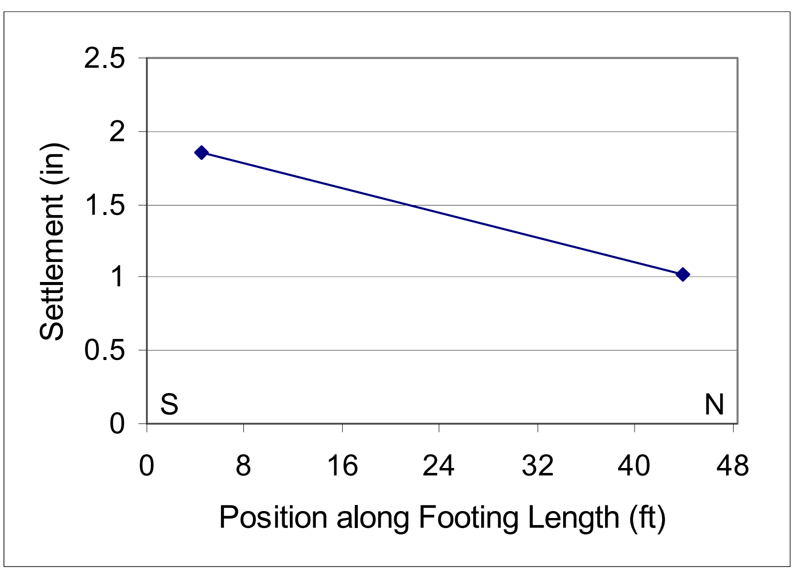

Figure 6.45: Forward Abutment Settlement After Construction Stage 3 (Soil Backfill)

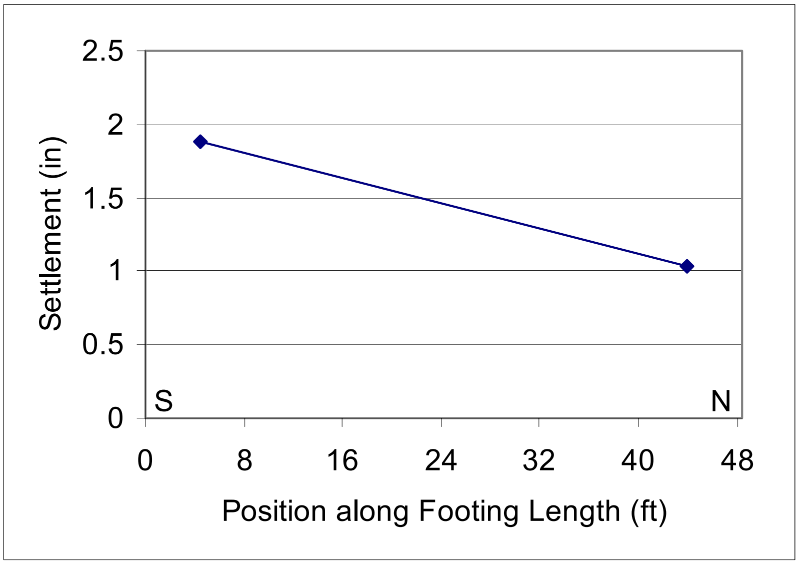

Figure 6.46: Forward Abutment Settlement After Construction Stage 4 (Placement of Girder Beams)

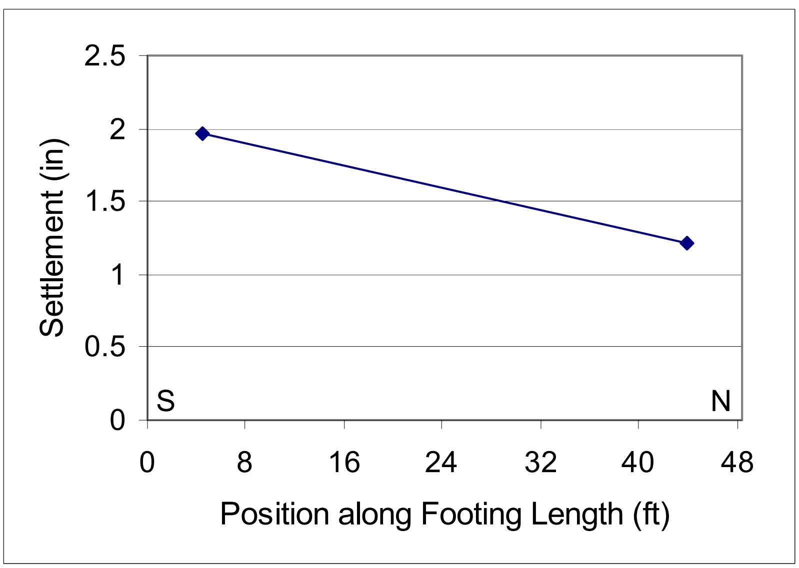

Figure 6.47: Forward Abutment Settlement After Construction Stage 5 (Deck Construction)

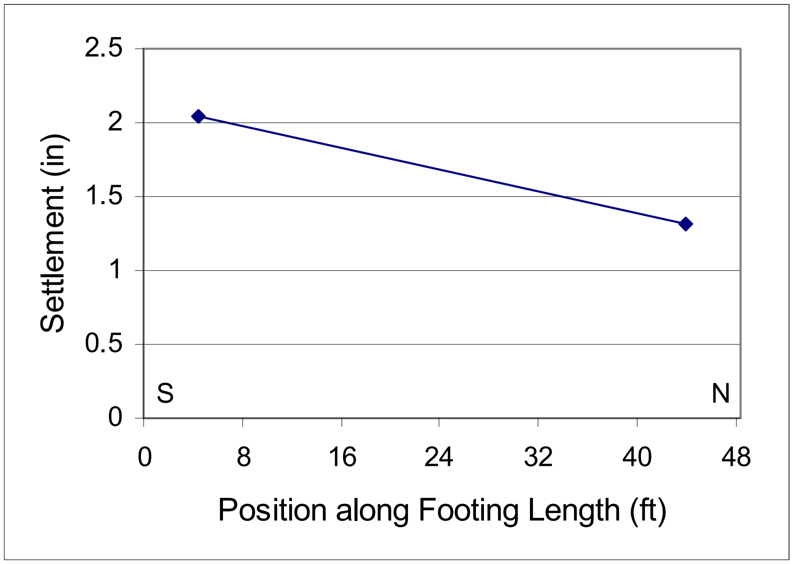

Figure 6.48: Forward Abutment Settlement After Construction Stage 6 (Bridge Open to Traffic)

The average settlement from both the north and south settlement points are given in Table 6.17. Figure 6.49 shows the average settlement values in Table 6.17 graphically for each construction stage. Both the table and the figure exhibit that the settlement of the Forward Abutment footing continued to increase each construction stage.

Table 6.17: Average Settlement of North and South Points for Forward Abutment

Construction Stage	Description	Settlement – inches (mm)
2	Abutment Wall Construction	0.0
3	Soil Backfill	1.44
4	Placement of Girder Beams	1.46
5	Deck Construction	1.59
6	Bridge Open to Traffic	1.68

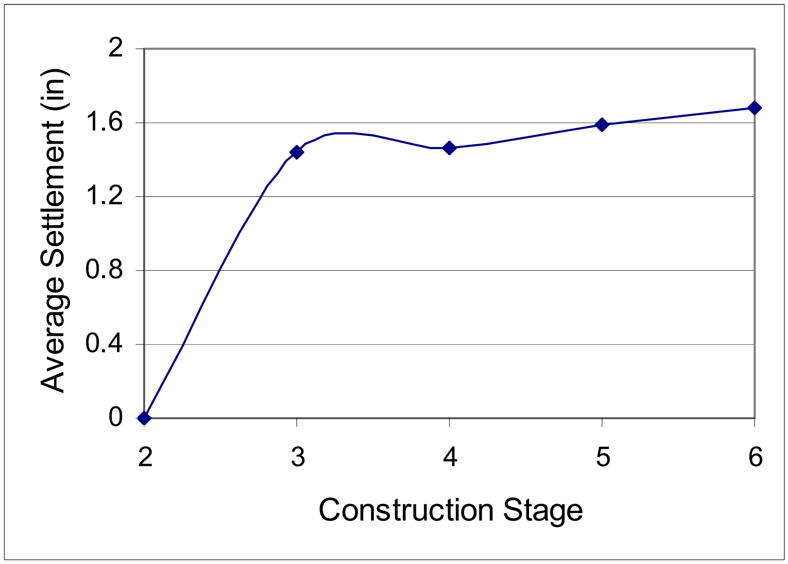

Figure 6.49: Average Settlement (Forward Abutment)

CHAPTER 7: ANALYSIS

7.1 GENERAL

The methods described in the AASHTO LRFD Bridge Design Specifications (2004) presented in Chapter 3, as well as additional geotechnical methods presented in Chapter 4 applicable to shallow foundations, are evaluated using the field performance data obtained at the two new highway bridge construction sites in Ohio, FRA-670-0380 and MOT-70/75. The footing rigidity, contact pressure, bearing capacity, and fifteen additional settlement prediction methods for spread footings on cohesionless soils were looked into, along with footing rotation. For the MOT-70/75 site, the subsoil properties, contact pressure, and pier wall tilting are analyzed here with general results for the calculations of footing rigidity, bearing capacity, and immediate settlement. The details for these results are given in Appendix A. Lastly, a cost analysis between a spread footing and deep foundation is performed.

7.2 SUBSOIL PROPERTIES FOR FRA-670-0380

The soil boring data presented in Section 5.2.2 indicated that the footing was resting on stiff silty granular soils (A-2-4, A-4a). AASHTO explained the correction of SPT blow counts by the following, as was discussed in Section 3.4.

$$N_1 = C_n N \tag{3-5}$$

No additional corrections of the original SPT-N values are necessary since the SPT hammer efficiency was assumed to be 60%. Table 7.1 presents the corrected SPT-N values with depth below the footing base. In the calculation process, the average unit weight of the overburden soil was assumed to be 120 pcf. Figure 7.1 plots the variations of the corrected SPT-N value with depth below the bottom of the footing. According to this plot, the $(N_1)_{60}$ value did not vary significantly with depth and centered around a value of 49 blows/ft.

Table 7.1: Corrected SPT-N Values (FRA-670-0380)

Depth Below BOF (ft)	Z (ft)	σ_z' (tsf)	C_n	N	$(N_1)_{60}$
0	26	1.56	0.853	51	44
5	31	1.86	0.794	65	52
10	36	2.16	0.744	73	54
15	41	2.46	0.705	63	44
20	46	2.76	0.662	84	56
25	51	3.06	0.628	70	44

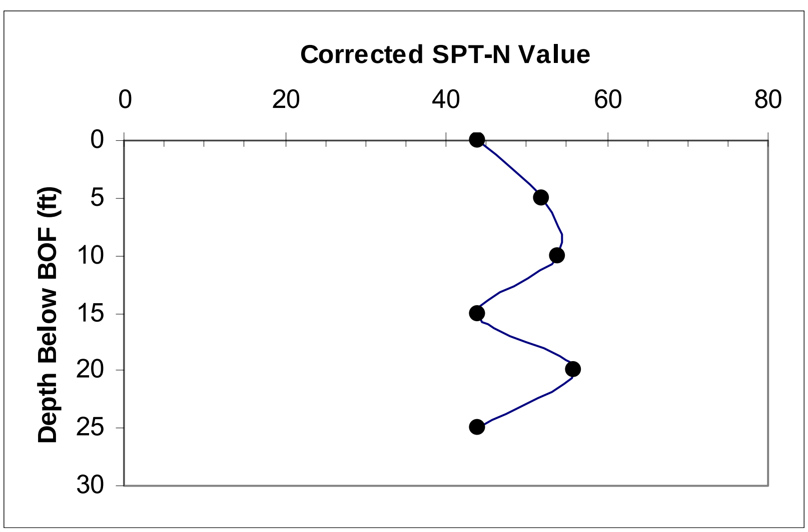

Figure 7.1: Corrected SPT-N Value Variations with Depth

Table 7.2 shows general rating of relative density of the granular soils based on the corrected SPT-N value. The bearing material can be generally described as a dense granular soil. According to Table 3.7 in this report, as was presented in AASHTO LRFD Bridge Design Specifications (2004), the drained friction angle of the bearing soil material may be 38° to 43°.

Table 7.2: Relative Density of Cohesionless Soils (after Terzaghi & Peck, 1967)

Corrected SPT-N Value	Relative Density
Less than 4	Very Loose
4 to 10	Loose
10 to 30	Medium
30 to 50	Dense
More than 50	Very Dense

The elastic modulus of soils depends on the soil type and the corrected average SPT-N value. Table 3.16 of this report showed the following equations used for the soil types below.

E_s (tsf) = $4(N_1)_{60}$ = 196 for silts, sandy silts, slightly cohesive mixtures

E_s (tsf) = $7(N_1)_{60}$ = 343 for clean fine to med. sands and slightly silty sands

E_s (tsf) = $10(N_1)_{60}$ = 490 for coarse sands and sands with little gravel

E_s (tsf) = $12(N_1)_{60}$ = 588 for sandy gravel and gravels

During the field installation of soil pressure cells in the Central Pier footing construction area, the ORITE team realized that the bearing material in some locations within the footing construction area was more similar to weathered shale than to a silty granular soil. According to Tables 3.4 and 3.5, the elastic constants of weathered shale are:

Poisson's ratio (υ) = 0.03 to 0.18 → 0.09 (average)

Young's modulus (E) = 0.001 to 5.60 million psi → 1.42 million psi (average)

7.3 FOOTING RIGIDITY ANALYSIS FOR FRA-670-0380

The central pier foundation at FRA-670-0380 has the following dimensional characteristics:

Overall Footing Length (L) = 40.25 ft = 483 inches

Overall Footing Width (B) = 8 ft = 96 inches

Column Width (b), taken along footing width = 3 ft = 36 inches

Combined Column Width (ℓ), taken along footing length = 4(3) = 12 ft = 144 inches

Footing Thickness (H) = 3 ft = 36 inches

Therefore, the cross-sectional moment of inertia of the footing (I) is: $LH^3/12$ = 90.6 ft^4 = 1,877,904 in^4. The moment of inertia per unit length (I_b) is: $LH^3/12L$ = 2.25 ft^4/ft = 3888 in^4/in. The elastic modulus (E) of the footing material (ODOT Class C concrete) is assumed to be 4 million psi. The elastic modulus (E_s) and Poisson's ratio (υ) of the bearing soil are also assumed to be about 2,000 psi or144 tsf (Das, 2004) and 0.3, respectively. These input values will lead to:

$$k = \frac{E_s}{B\left(1-\upsilon^2\right)} = \frac{2{,}000}{96(1-0.3^2)} = 22.9$$

$$\beta L = L\left(k/4EI\right)^{1/4} = 483\left[\frac{22.9}{4(4E6)(1{,}877{,}904)}\right]^{1/4} = 0.45 \ (< 0.6)$$

$$K_r = \frac{EI_b}{E_s B^3} = \frac{4E6(3{,}888)}{2{,}000(96)^3} = 8.79 \ (>> 0.5)$$

$$K_r' = \frac{Et^3}{k(1-\upsilon^2)(B-b)^2(L-\ell)^2} = \frac{4E6(36)^3}{22.9(1-0.3^2)(96-36)^2(483-144)^2} = 21.6 \quad (>> 1.0)$$

The central pier footing at FRA-670-0380 can be considered a rigid structure by any of the flexibility criteria. This outcome suggests that the soil pressure underneath the footing can be determined on the basis of simple formula based on strength of materials (Equation 4-1b).

7.4 CONTACT PRESSURE FOR FRA-670-0380

The actual amounts of materials used during the construction are needed to calculate the average theoretical contact pressure accurately. The actual quantities utilized during the construction of the FRA-670-0380 bridge are listed in Table 7.3. For the eighth stage (bridge open to traffic), the basic assumption mentioned in the AASHTO Specification (480 lb per linear foot per lane) may be used to estimate the typical live load applied to the bridge. Using this assumption gives a total live load of 200 kips since the bridge has two lanes and a length of 208 ft. An alternative assumption that may be used to address the worst case is three trucks (HS20) on each lane. A total live load of 432 kips on the bridge results, since each HS20 consists of axle loads of 8, 32, and 32 kips (72 kips).

Table 7.3: Actual Quantities Used in Construction Stages (FRA-670-0380)

Stage No.	Description	Actual Quantities & Notes
1	Footing Construction	Footing Thickness = 3’-0”.
2	Pier Columns Construction	Total Volume of Concrete in Columns = 17 Yd^3.
3	Soil Backfill	Thickness of ODOT 304 Fill over Footing = 2 ft
4	Pier Cap Construction	Total Volume of Concrete in Cap = 15 Yd^3.
5	Barrier Wall Construction	Thickness of Base = 9 in = 0.75 ft. Total Volume of Concrete in Barrier Wall = 9.8 Yd^3
6	Girder Beam Placement	Total Weight of Beams Placed = 400,000 lb
7	Deck Construction	Total Weight of Concrete Deck = 1,053,000 lb.
8	Bridge Open to Traffic	Total Live Load = 432,000 lb.

[Note] γ of concrete = 150 pcf (assumed); γ of soil backfill = 135 pcf (assumed).

Table 7.4 lists the theoretical and field contact pressure values and the percent differences, consistently 23% to 37% higher than the theoretical values. These values are used to generate Figure 7.2 and Figure 7.3. Figure 7.2 plots the theoretical magnitude of contact pressure, which should be generated by each construction stage. Based on the plot, construction stage 7 (deck construction) should produce the largest contact pressure increase. This has been confirmed in the field through the pressure cell readings. The field contact pressure values are shown with the theoretical values in Figure 7.3.

Table 7.4: Comparisons of Contact Pressure Values (FRA-670-0380)

Stage	Description	Ave. Contact Pressure (tsf):		Percent Difference (%)
		Theory	Field	
1	Footing Construction	0.230	0.333	30.9
2	Pier Columns Construction	0.337	0.438	23.0
3	Soil Backfill	0.473	---	---
4	Pier Cap Construction	0.567	0.762	25.6
5	Barrier Wall Construction	0.685	0.963	28.9
6	Girder Beam Placement	0.995	1.452	31.5
7	Deck Construction	1.813	2.849	36.4
8	Bridge Open to Traffic	2.037	2.849	28.5

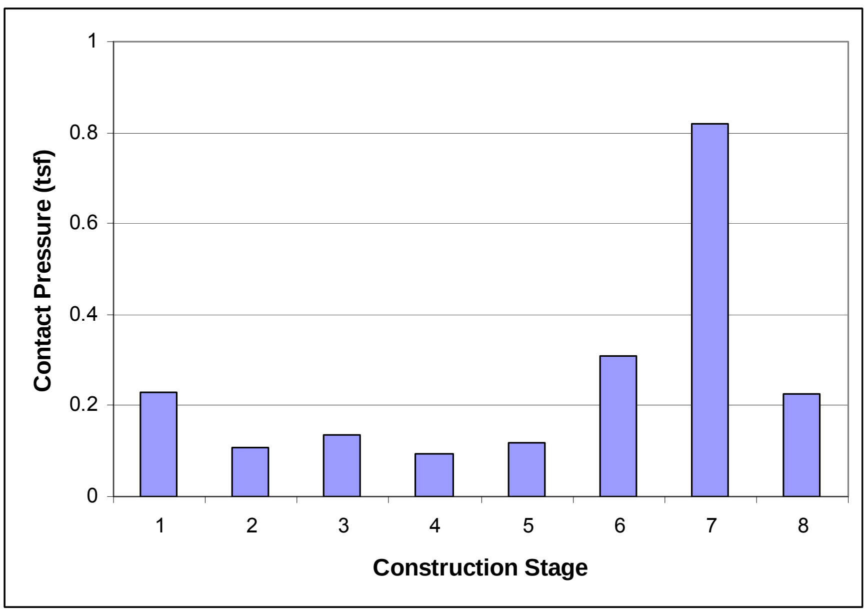

Figure 7.2: Theoretical Contact Pressure Per Construction Stage

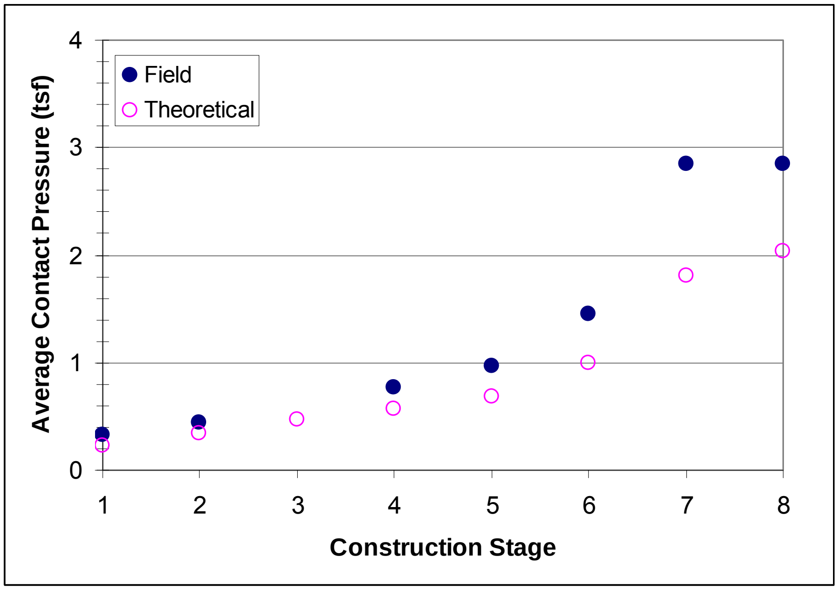

Figure 7.3: Average Bearing Pressure Variations During Construction

7.5 BEARING CAPACITY FOR FRA-670-0380

The AASHTO LRFD Bridge Design Specifications (2004) presents two approaches for evaluating the bearing capacity of the materials found below the footing. The first approach is based on the traditional Terzaghi's bearing capacity analysis, and the second approach utilizes the SPT-N value.

$$q_R = \phi q_n \quad (3\text{-}14)$$

$$q_n = cN_{cm} + \gamma D_f N_{qm} C_{wa} + \frac{\gamma}{2} B N_{\gamma m} C_{wb} \quad (3\text{-}8)$$

Numerical analysis of the data presented in Table 3.13 shows that:

$d_q = -0.0031(D_f/B)^2 + 0.0486(D_f/B) + 1.1583$ at $\phi = 37°$

$d_q = -0.0031(D_f/B)^2 + 0.0486(D_f/B) + 1.1083$ at $\phi = 42°$

Assuming that the bearing material is basically cohesionless, we have c = 0. The average unit weight of the overburden soil may be assumed to be 120 pcf (0.06 tcf). From the design drawing, B and D_f are both equal to 8 ft. The footing length (L) is equal to 40.25 ft. So, (B/L) = (8/40.25) = 0.199 and (D_f/B) = 1. The friction angle (ϕ) used is 38° and the groundwater table is assumed to be at the bottom of footing, being conservative.

$N_c = 61.4$; $N_q = 48.9$; $N_\gamma = 78.0$ from Table 3.10

$C_{wa} = C_{wb} = 0.5$ from Table 3.11

$s_c = 1 + (0.199)(48.9/61.4) = 1.158$

$s_\gamma = 1 - 0.4(0.199) = 0.920$ from Table 3.12

$s_q = 1 + (0.199)\tan 38° = 1.155$

Using $\phi = 38°$, further analysis of the data suggests that:

$d_q = 1.19$ from Table 3.13

N_{qm} and $N_{\gamma m}$ values are now determined. $N_{qm} = N_q\, s_q\, d_q\, i_q = 48.9(1.155)(1.19)(1.0) = 67.21$; and $N_{\gamma m} = N_\gamma\, s_\gamma\, i_\gamma = 78.0(0.92)(1.0) = 71.76$. By inputting all the above values and information into Equation 3-8, the nominal bearing resistance will be:

$$q_n = \gamma D_f N_{qm} C_{wa} + \frac{\gamma}{2} B N_{\gamma m} C_{wb} = 0.06(8)(67.21)(0.5) + 0.03(8)(71.76)(0.5) = 24.74 tsf$$

Therefore, from Equation 3-14, the bearing resistance value will be $q_R = \phi q_n = 0.45(24.74) = 11.13$ tsf. Theoretical bearing pressure calculations presented earlier provided maximum bearing pressure of 2.037 tsf for the footing. The factor of safety against the bearing capacity failure will be about 5.5.

The bearing capacity is next evaluated by the alternate approach using the average corrected SPT-N value. The formula is:

$$q_n = \frac{(N_1)_{60} B}{10}\left(\frac{C_{wa} D_f}{B} + C_{wb}\right) \tag{3-13}$$

From the earlier analysis of SPT data, the average corrected SPT-N value is 49. A footing width, B, of 8 ft; embedment depth, D_f, of 8 ft; and groundwater table correction factors, C_{wa} & C_{wb}, equal to 0.5 are input. By applying these values into Equation 3-13, the nominal bearing capacity will be:

$$q_n = \frac{49(8)}{10}\left[\frac{0.5(8)}{8} + 0.5\right] = 39.2 tsf$$

Therefore, from Equation 3-14, the bearing resistance will be: $q_R = \phi q_n = 0.45(39.2) = 17.64$ tsf. Theoretical bearing pressure calculations presented earlier provided a maximum bearing pressure of 2.037 tsf for the footing. The factor of safety against the bearing capacity failure will be about 8.6. The alternate approach using the SPT-N value resulted in a higher factor of safety.

7.6 IMMEDIATE SETTLEMENT FOR FRA-670-0380

7.6.1 Footing on Weathered Rock

While installing pressure cells in the field, the bearing material was observed to resemble weathered shale in some areas of the footing construction zone. The settlement of the footing can, therefore, be viewed as the elastic deformations of the weathered rock mass. Section 3.7.3 of this report described the settlement of the foundation.

$$S_e = q_o (1 - \upsilon^2) \frac{B(I_p)}{E_m} \tag{3-23}$$

Inputting the known values of B = 96 inches and υ = 0.09, along with I_p = 1.809, into Equation 3-23, the immediate settlement will be expressed as:

$$S_e = \frac{q(96)}{E_m}\left(1 - 0.09^2\right)(1.809) = 172.3\left(\frac{q}{E_m}\right)$$

Values to be used for the elastic modulus (E_m) are 1 x 10^3 psi (min.), 1.42 x 10^6 psi (ave.), and 5.60 x 10^6 psi (max.). Table 7.5 summarizes the results of the elastic settlement calculations. The theoretical settlements computed on the basis of the minimum Young's modulus value are larger than the actual field settlements which can be seen in Table 6.4. In contrast, the settlements resulting from the average or maximum Young's modulus values are much smaller compared to the field settlements.

Table 7.5: Summary of Elastic Settlements on Weathered Rock (FRA-670-0380)

Stage	Description	q (psi)	S_e (inches) with:		
			$(E_m)_{min}$	$(E_m)_{ave}$	$(E_m)_{max}$
1	Footing Construction	3.19	0.55	3.87×10^{-4}	9.68×10^{-5}
2	Pier Columns Construction	4.68	0.81	5.68×10^{-4}	1.42×10^{-4}
3	Soil Backfill	6.57	1.13	7.97×10^{-4}	2.02×10^{-4}
4	Pier Cap Construction	7.88	1.36	9.56×10^{-4}	2.39×10^{-4}
5	Barrier Wall Construction	9.51	1.64	1.15×10^{-3}	2.93×10^{-4}
6	Girder Beam Placement	13.82	2.38	1.68×10^{-3}	4.25×10^{-4}
7	Deck Construction	25.18	4.34	3.06×10^{-3}	7.75×10^{-4}
8	Bridge Open to Traffic	28.29	4.87	3.43×10^{-3}	8.70×10^{-4}

7.6.2 Footing on Cohesionless Soil

The bearing material in the footing construction area may also be treated as a cohesionless soil when computing the immediate settlements. From Section 3.7.1 of this report, the immediate settlement is computed by:

$$S_e = \frac{q_0\sqrt{A}}{E_s\beta_z}\left(1-\upsilon^2\right) \qquad (3\text{-}14)$$

Using the known values of A = 322 ft^2 and $\upsilon = 0.25$, along with $\beta_z = 1.24$ into Equation 3-15, the immediate settlement will be expressed as:

$$S_e = \frac{q_0\sqrt{322}}{E_s(1.24)}\left(1-0.25^2\right)=13.57\left(\frac{q_0}{E_s}\right)$$

The Young's modulus of soil (E_s) is determined to be 250 tsf (min.) and 650 tsf (max.). Table 7.6 summarizes the results from the elastic settlement calculations. The settlements computed with the minimum Young's modulus value are much larger than the field settlements as listed in Table 6.4. Using the maximum Young's modulus, the settlements computed are only about two to three times larger than the field settlements.

Table 7.6: Summary of Elastic Settlements on Cohesionless Soil (FRA-670-0380)

Stage	Description	q_0 (tsf)	S_e (inches) with:	
			$(E_s)_{min}$	$(E_s)_{max}$
1	Footing Construction	0.230	0.15 (3.8 mm)	0.06 (1.5 mm)
2	Pier Columns Construction	0.337	0.22 (5.6 mm)	0.08 (2.0 mm)
3	Soil Backfill	0.473	0.31 (7.8 mm)	0.12 (3.0 mm)
4	Pier Cap Construction	0.567	0.37 (9.4 mm)	0.14 (3.6 mm)
5	Barrier Wall Construction	0.685	0.45 (11.4 mm)	0.17 (4.3 mm)
6	Girder Beam Placement	0.995	0.66 (16.8 mm)	0.25 (6.4 mm)
7	Deck Construction	1.813	1.18 (30.0 mm)	0.45 (11.4 mm)
8	Bridge Open to Traffic	2.037	1.33 (33.8 mm)	0.51 (13.0 mm)

The immediate settlement is next determined using Equation 3-15 with the E_s value determined using corrected SPT-N values. The Young's modulus depends on the soil type as was discussed previously in Section 7.2.1. Table 7.7 summarizes the results of the elastic settlement calculations using the four values for Young's modulus. Comparing the actual field settlements, it appears that when E_s = 12N (588 tsf), the resulting settlements are the closest to the field values. This proves that having general soil classification data and the SPT blow counts improve the settlement estimations.

Table 7.7: Summary of Elastic Settlements Using SPT-N Values (FRA-670-0380)

Stage	Description	q_0 (tsf)	S_e (inches) with Es (tsf) =:			
			196	343	490	588
1	Footing Construction	0.230	0.19	0.11	0.08	0.06
2	Pier Columns Construction	0.337	0.28	0.16	0.11	0.09
3	Soil Backfill	0.473	0.39	0.22	0.16	0.13
4	Pier Cap Construction	0.567	0.47	0.27	0.19	0.16
5	Barrier Wall Construction	0.685	0.57	0.33	0.23	0.19
6	Girder Beam Placement	0.995	0.83	0.47	0.33	0.28
7	Deck Construction	1.813	1.51	0.86	0.60	0.50
8	Bridge Open to Traffic	2.037	1.69	0.97	0.68	0.56

7.6.3 Hough Method

The Hough Method was previously described in Section 3.7.1 of this report. It computes the settlement of a footing on sands, using Equation 3-16. The C' value is determined from Table 7.8 based on soil type and SPT-$(N_1)_{60}$ values or can be determined from Figure 3.2.

$$S_e = \sum_{i=1}^{n} \Delta H_i = \sum_{i=1}^{n} H_c \frac{1}{C'} \log\left(\frac{\sigma'_o + \Delta\sigma_v}{\sigma'_o}\right) \tag{3-16}$$

Table 7.8: Typical C′ Values (AASHTO, 2004)

Soil Description	C′ Value @ SPT-$(N_1)_{60}$ of:		
	30	40	50
Clean uniform medium SAND	126	175	243
Well-graded silty SAND & GRAVEL	102	132	168
Clean well-graded fine to coarse SAND	90	114	141
Well-graded fine to medium silty SAND	77	97	118
Inorganic SILT	54	68	83

The influence zone is 25 feet below the bottom of footing, approximately 3B. It is divided into five equal (5-ft thick) layers. The midpoint depth of each layer includes the embedment depth (8 ft). The average moist unit weight of 120 pcf is assumed for each layer, and the total cover thickness is 5 ft. Figure 7.4 illustrates the subdivided influence zone and the spreading of the applied pressure through the layers.

Layer 1:	z = 0 to 5 ft below bottom of footing.	Mid-Point Depth = 10.5 ft.
Layer 2:	z = 5 to 10 ft below bottom of footing.	Mid-Point Depth = 15.5 ft.
Layer 3:	z = 10 to 15 ft below bottom of footing.	Mid-Point Depth = 20.5 ft.
Layer 4:	z = 15 to 20 ft below bottom of footing.	Mid-Point Depth = 25.5 ft.
Layer 5:	z = 20 to 25 ft below bottom of footing.	Mid-Point Depth = 30.5 ft.

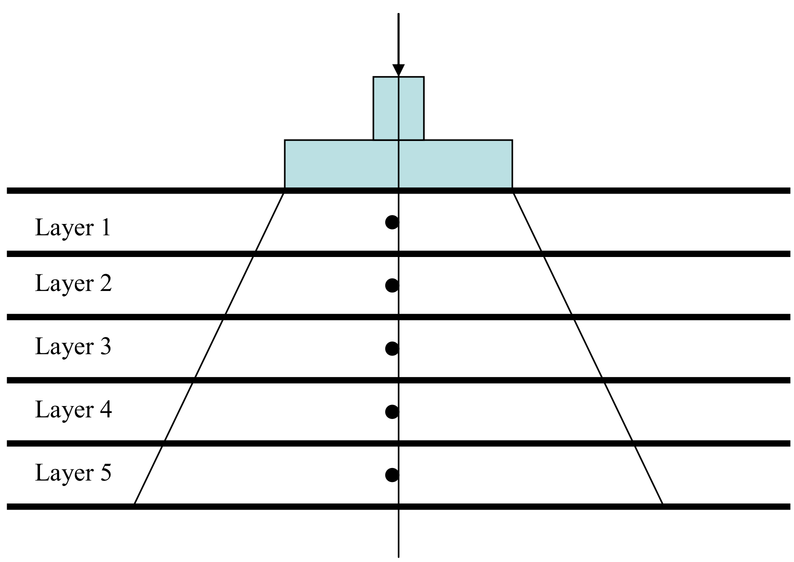

Figure 7.4: Approximate Stress Distribution Below Footing

The distribution of the applied pressure is evaluated with a method by Dunn et al. (1980) giving an approximate value that is based on Equation 7-2.

$$\Delta\sigma_v = \frac{qBL}{(B+2x)(L+2x)} = \frac{qBL}{(B+1.154Z)(L+1.154Z)} \tag{7-2}$$

Applying the values given previously with the method above, the vertical stress at the mid-point of each layer is computed as follows.

Layer 1: H_c = 5 ft; σ_0' = 120(8 + 2.5) = 1,260 psf = 0.63 tsf

$$\Delta\sigma_v = \frac{qBL}{(B+2x)(L+2x)} = \frac{q(8x40.25)}{(8+1.154x2.5)(40.25+1.154x2.5)} = 0.686q$$

Layer 2: H_c = 5 ft; σ_0' = 120(8 + 7.5) = 1,860 psf = 0.93 tsf

$$\Delta\sigma_v = \frac{qBL}{(B+2x)(L+2x)} = \frac{q(8x40.25)}{(8+1.154x7.5)(40.25+1.154x7.5)} = 0.395q$$

Layer 3: H_c = 5 ft; σ_0' = 120(8 + 12.5) = 2,460 psf = 1.23 tsf

$$\Delta\sigma_v = \frac{qBL}{(B+2x)(L+2x)} = \frac{q(8x40.25)}{(8+1.154x12.5)(40.25+1.154x12.5)} = 0.263q$$

Layer 4: H_c = 5 ft; σ_0' = 120(8 + 17.5) = 3,060 psf = 1.53 tsf

$$\Delta\sigma_v = \frac{qBL}{(B+2x)(L+2x)} = \frac{q(8x40.25)}{(8+1.154x17.5)(40.25+1.154x17.5)} = 0.189q$$

Layer 5: H_c = 5 ft; σ_0' = 120(8 + 22.5) = 3,660 psf = 1.83 tsf

$$\Delta\sigma_v = \frac{qBL}{(B+2x)(L+2x)} = \frac{q(8x40.25)}{(8+1.154x22.5)(40.25+1.154x22.5)} = 0.143q$$

The average corrected SPT-N value is 49, so a C′ value interpolated between SPT-$(N_1)_{60}$ of 40 and 50 is determined. The following three possibilities for C′ are tried:

C′ = 236 for Clean uniform medium SAND

C′ = 164 for Well-graded silty SAND & GRAVEL

C′ = 138 for Clean well-graded fine to coarse SAND

The settlement calculations are tabulated in Table 7.9 for the value of 236 selected for C′ for each stage and layer. Table 7.10 presents the sums of the layer's settlements for each stage, including the settlements for the other two C' values.

Table 7.9: Settlement Calculations by Hough Method (with C′ = 236)

(a) Construction Stage 1 (q = 0.23 tsf)

Layer	H_c (ft)	C′	σ_0' (tsf)	$\Delta\sigma_v$ (tsf)	S_e (in)
1	5	236	0.63	0.158	0.0247
2	5	236	0.93	0.091	0.0103
3	5	236	1.23	0.060	0.0053
4	5	236	1.53	0.043	0.0031
5	5	236	1.83	0.033	0.0020

$\Sigma = 0.0453$

(b) Construction Stage 2 (q = 0.337 tsf)

Layer	H_c (ft)	C′	σ_0' (tsf)	$\Delta\sigma_v$ (tsf)	S_e (in)
1	5	236	0.63	0.231	0.0345
2	5	236	0.93	0.133	0.0148
3	5	236	1.23	0.089	0.0077
4	5	236	1.53	0.064	0.0045
5	5	236	1.83	0.048	0.0029

$\Sigma = 0.0643$

Table 7.9 (cont'd):

(c) Construction Stage 3 (q = 0.473 tsf)

Layer	H_c (ft)	C'	σ_0' (tsf)	$\Delta\sigma_v$ (tsf)	S_e (in)
1	5	236	0.63	0.324	0.0459
2	5	236	0.93	0.187	0.0202
3	5	236	1.23	0.124	0.0106
4	5	236	1.53	0.089	0.0063
5	5	236	1.83	0.068	0.0040

Σ = 0.0870

(d) Construction Stage 4 (q = 0.567 tsf)

Layer	H_c (ft)	C'	σ_0' (tsf)	$\Delta\sigma_v$ (tsf)	S_e (in)
1	5	236	0.63	0.389	0.0531
2	5	236	0.93	0.224	0.0238
3	5	236	1.23	0.149	0.0126
4	5	236	1.53	0.107	0.0075
5	5	236	1.83	0.081	0.0048

Σ = 0.1018

(e) Construction Stage 5 (q = 0.685 tsf)

Layer	H_c (ft)	C'	σ_0' (tsf)	$\Delta\sigma_v$ (tsf)	S_e (in)
1	5	236	0.63	0.470	0.0615
2	5	236	0.93	0.271	0.0282
3	5	236	1.23	0.180	0.0151
4	5	236	1.53	0.129	0.0090
5	5	236	1.83	0.098	0.0058

Σ = 0.1195

(f) Construction Stage 6 (q = 0.995 tsf)

Layer	H_c (ft)	C'	σ_0' (tsf)	$\Delta\sigma_v$ (tsf)	S_e (in)
1	5	236	0.63	0.683	0.0810
2	5	236	0.93	0.393	0.0389
3	5	236	1.23	0.262	0.0213
4	5	236	1.53	0.188	0.0128
5	5	236	1.83	0.142	0.0083

Σ = 0.1623

(g) Construction Stage 7 (q = 1.813 tsf)

Layer	H_c (ft)	C'	σ_0' (tsf)	$\Delta\sigma_v$ (tsf)	S_e (in)
1	5	236	0.63	1.244	0.1203
2	5	236	0.93	0.716	0.0630
3	5	236	1.23	0.477	0.0362
4	5	236	1.53	0.343	0.0223
5	5	236	1.83	0.259	0.0146

Σ = 0.2565

Table 7.9 (cont'd):

(h) Construction Stage 8 (q = 2.037 tsf)

Layer	H_c (ft)	C'	σ_0' (tsf)	$\Delta\sigma_v$ (tsf)	S_e (in)
1	5	236	0.63	1.397	0.1290
2	5	236	0.93	0.805	0.0688
3	5	236	1.23	0.536	0.0399
4	5	236	1.53	0.385	0.0248
5	5	236	1.83	0.291	0.0163

$\Sigma = 0.2789$

Table 7.10: Summary of Settlements Predicted by Hough Method (FRA-670-0380)

Construction Stage No.	S_e (inches) with C' Value of :		
	236	164	138
1	0.045	0.065	0.078
2	0.064	0.093	0.110
3	0.087	0.125	0.149
4	0.102	0.147	0.174
5	0.120	0.172	0.204
6	0.162	0.234	0.278
7	0.257	0.369	0.439
8	0.279	0.401	0.477

7.6.4 Alpan Method

The Alpan method was previously described in Section 4.4.1 of this report. The method computes the settlement by the following formula.

$$S_e = m'\left(\frac{2B}{1+B}\right)^2 \frac{\alpha_0}{12} q \qquad (4\text{-}5)$$

For the central pier footing, L = 40.25 ft and B = 8 ft, thus L/B ≈ 5.03, and $m' = (5.03)^{0.39} = 1.878$. At the bottom of the footing, the uncorrected SPT-N = 51 and $\sigma'_v = (120 - 62.4)8 = 460.8$ psf = 0.23 tsf. Entering Figure 4.2 with these values, the relative density

(D_r) will be 100%, which results in no correction of N so N' = 51. Figure 4.3 then gives a value of 0.04 for α_0. Inputting these parameter values into Equation 4-5, the settlement equation will become:

$$S_e = m'\left(\frac{2B}{1+B}\right)^2 \frac{\alpha_0}{12} q = 1.878\left(\frac{16}{9}\right)^2 \frac{0.04q}{12} = 0.0198q$$

The results of the settlement calculations by the variation of the Alpan method are tabulated in Tables 7.11.

Table 7.11: Settlements Predicted by Alpan Method (FRA-670-0380)

Construction Stage	Description	q (tsf)	Settlement (inches)
1	Footing Construction	0.230	0.055 (1.4 mm)
2	Pier Columns Construction	0.337	0.080 (2.0 mm)
3	Soil Backfill	0.473	0.112 (2.9 mm)
4	Pier Cap Construction	0.567	0.135 (3.4 mm)
5	Barrier Wall Construction	0.685	0.163 (4.1 mm)
6	Girder Beam Placement	0.995	0.236 (6.0 mm)
7	Deck Construction	1.813	0.431 (10.9 mm)
8	Bridge Open to Traffic	2.037	0.484 (12.3 mm)

7.6.5 Anagnostropoulos Method

The Anagnostropoulos method was detailed in Section 4.4.2 of this report. The settlement computed by this method is shown by the following:

$$S_e = \frac{2.37q^{0.87}B^{0.7}}{N^{1.2}} \tag{4-7}$$

For the footing, B = 8 ft = 2.44 m and the uncorrected SPT-N is 63 within a depth of B below the footing. Placing these values in Equation 4-7 gives a resulting equation of:

$$S_e = \frac{2.37q^{0.87}B^{0.7}}{N^{1.2}} = \frac{2.37q^{0.87}(2.44)^{0.7}}{63^{1.2}} = 0.031q^{0.87}$$

The results of the settlement calculations by the variation of the Anagnostopoulos method are tabulated in Tables 7.12.

Table 7.12: Settlements Predicted by Anagnostopoulos Method (FRA-670-0380)

Construction Stage	Description	q (kPa)	Settlement (inches)
1	Footing Construction	22.0	0.018 (0.5 mm)
2	Pier Columns Construction	32.3	0.025 (0.6 mm)
3	Soil Backfill	45.3	0.033 (0.9 mm)
4	Pier Cap Construction	54.3	0.039 (1.0 mm)
5	Barrier Wall Construction	65.6	0.046 (1.2 mm)
6	Girder Beam Placement	95.3	0.064 (1.6 mm)
7	Deck Construction	173.6	0.107 (2.7 mm)
8	Bridge Open to Traffic	195.1	0.119 (3.0 mm)

7.6.6 Bowles Method

In Section 4.4.3 of this report, the Bowles method was described. The equation to compute the settlement by this method is shown below:

$$S_e = \frac{(1-\upsilon^2)qB'}{E_s} I_s I_f \qquad (4\text{-}8)$$

For the FRA-670-0380 central pier footing, the SPT-N value is 63 within the depth of 2B below the footing and results in a value for the soil modulus (E_s) of 780 ksf from Equation 4-9. B' is equal to B/2 or 4 ft and m (L'/B') is 5.0, while n (H/B') is 4.0. Using m and n in the equations for A_0, A_1, and A_2 gives results of 0.2139 for A_0 and 1.2897 for A_1 and 0.1934 for A_2. F_1 is equal to 0.479 and F_2 is 0.122. These values are used in Equation 4-10 to ultimately find I_s, which is 0.548. I_f is equal to 1.0 since the uncorrected SPT-N values include the effect of depth. Each parameter is used in Equation 4-8 and the settlement formula becomes:

$$S_e = \frac{(1-\upsilon^2)qB'}{E_s} I_s I_f = \frac{(1-0.3^2)q(4)}{780}(0.548)(1.0) = 0.0026q$$

The results of the Bowles method settlement calculations are tabulated in Tables 7.13 for each construction stage for the center point. The values are multiplied by 0.93 to reflect the settlement of a rigid footing, rather than a flexible footing.

Table 7.13: Settlements Predicted by Bowles Method (FRA-670-0380)

Construction Stage	Description	q (ksf)	Settlement (inches)
1	Footing Construction	0.460	0.014 (0.4 mm)
2	Pier Columns Construction	0.674	0.021 (0.5 mm)
3	Soil Backfill	0.946	0.029 (0.7 mm)
4	Pier Cap Construction	1.134	0.035 (0.9 mm)
5	Barrier Wall Construction	1.370	0.042 (1.1 mm)
6	Girder Beam Placement	1.990	0.061 (1.6 mm)
7	Deck Construction	3.626	0.111 (2.8 mm)
8	Bridge Open to Traffic	4.074	0.125 (3.2 mm)

7.6.7 Burland-Burbidge Method

The Burland-Burbidge method was previously described in Section 4.4.4 of this report. For their method, the immediate settlement is determined by:

$$S_e = \alpha_1 \alpha_2 \alpha_3 \left[\frac{1.25(L/B)}{0.25 + (L/B)} \right]^2 Bq' \tag{4-11}$$

For normally consolidated soils, a value of 0.14 is used for α_1. The average uncorrected SPT-N value of 63 is adjusted to 39 using Equation 4-12. Equation 4-15 was used to determine α_2, which is 0.0101. The depth of stress influence (Z′) determined by Equation 4-14 is 6.66 ft. The α_3 factor is calculated by Equation 4-17 and is equal to 1.0, since Z' is smaller than 2B. The settlement equation will become:

$$S_e = \alpha_1 \alpha_2 \alpha_3 \left[\frac{1.25(L/B)}{0.25 + (L/B)} \right]^2 Bq' = (0.14)(0.0101)(1.0) \left[\frac{6.25}{5.25} \right]^2 (8)q = 0.0160q$$

The settlement calculations by the Burland-Burbidge method are tabulated in Tables 7.14 for each construction stage.

Table 7.14: Settlements Predicted by Burland-Burbidge Method (FRA-670-0380)

Construction Stage	Description	q′ (tsf)	Settlement (inches)
1	Footing Construction	0.230	0.044 (1.1 mm)
2	Pier Columns Construction	0.337	0.065 (1.7 mm)
3	Soil Backfill	0.473	0.091 (2.3 mm)
4	Pier Cap Construction	0.567	0.109 (2.8 mm)
5	Barrier Wall Construction	0.685	0.132 (3.4 mm)
6	Girder Beam Placement	0.995	0.192 (4.9 mm)
7	Deck Construction	1.813	0.350 (8.9 mm)
8	Bridge Open to Traffic	2.037	0.393 (10.0 mm)

7.6.8 D'Appolonia Method

Section 4.4.5 of this report previously described the D'Appolonia method. The method computes the settlement with the following equation:

$$S_e = \mu_0 \mu_1 \frac{qB}{M} \qquad \text{(4-18)}$$

From D_f = 8 ft and B = 8 ft, the ratio (D_f/B) will be equal to 1.0. Referring to Figure 4.4, the embedment influence factor (μ_0) is determined to be 0.92. Assume that the zone of influence is equal to B (8 ft). From L = 40.25 ft and B = 8 ft, the ratio (L/B) will be approximately equal to 5.0. Assuming that H (thickness of compressible strata) = 10 ft, the ratio (H/B) will be equal to 1.25. The compressible strata influence factor (μ_1) is 0.45, using Figure 4.5. The average uncorrected SPT-N = 63 within the zone of influence. The bearing soil is largely sand/gravel. The modulus of compressibility (M) is estimated to be 660 tsf from Figure 4.6. Inputting these values into Equation 4-18, we will have:

$$S_e = \mu_0 \mu_1 \frac{qB}{M} = 0.92(0.45)\frac{8q}{660} = 0.0050q$$

The results of the settlement calculations by the D'Appolonia method are tabulated in Tables 7.15.

Table 7.15: Settlements Predicted by D'Appolonia Method (FRA-670-0380)

Construction Stage	Description	q′ (tsf)	Settlement (inches)
1	Footing Construction	0.230	0.014 (0.4mm)
2	Pier Columns Construction	0.337	0.020 (0.5 mm)
3	Soil Backfill	0.473	0.028 (0.7 mm)
4	Pier Cap Construction	0.567	0.034 (0.9mm)
5	Barrier Wall Construction	0.685	0.041 (1.0 mm)
6	Girder Beam Placement	0.995	0.060 (1.5 mm)
7	Deck Construction	1.813	0.109 (2.8mm)
8	Bridge Open to Traffic	2.037	0.122 (3.1 mm)

7.6.9 Department of the Navy Method

The Department of the Navy method was previously described in Section 4.4.6 of this report. The method computes the settlement by the following equation:

$$S_e = \frac{4q}{K_{v1}}\left(\frac{B}{B+1}\right)^2 \qquad (4\text{-}19)$$

At the depth of 1.5B below the footing, σ'_v = (120 – 62.4)12 = 691.2 psf = 0.69 ksf, and the corrected SPT-N_{ave} value is 49. Entering Figure 4.7, the relative density is estimated to be close to 100%. The K_{V1} value is obtained by Figure 4.8 to be 290 tons/ft^3. This value and the footing width of 8 ft are entered into the settlement equation resulting in the following.

$$S_e = \frac{4q}{K_{v1}}\left(\frac{B}{B+1}\right)^2 = \frac{4q}{290}\left(\frac{8}{9}\right)^2 = 0.0107q$$

The results of the settlement calculations by U.S. Department the Navy method are tabulated in Tables 7.16.

Table 7.16: Settlements Predicted by Dept. of Navy Method (FRA-670-0380)

Construction Stage	Description	q (tsf)	Settlement (inches)
1	Footing Construction	0.230	0.030 (0.8 mm)
2	Pier Columns Construction	0.337	0.043 (1.1 mm)
3	Soil Backfill	0.473	0.060 (1.5 mm)
4	Pier Cap Construction	0.567	0.072 (1.8 mm)
5	Barrier Wall Construction	0.685	0.087 (2.2 mm)
6	Girder Beam Placement	0.995	0.127 (3.2 mm)
7	Deck Construction	1.813	0.231 (5.9 mm)
8	Bridge Open to Traffic	2.037	0.260 (6.6 mm)

7.6.10 Meyerhof Method

The Meyerhof method was previously described in Section 4.4.7 of this report. The method computes the settlement by the following:

$$S_e = \left[\frac{12q}{N'}\right]\left(\frac{B}{B+1}\right)^2 \qquad \text{for B > 4 ft} \qquad (4\text{-}21)$$

Assuming the influence zone is equal to 2B or 16 ft. The average uncorrected SPT-N value within the depth B below the footing is 63. Equation 4-22 corrects the N value for this method and results in an N' of 39. Inputting these values into Equation 4-21, will give the resulting settlement equation:

$$S_e = \left[\frac{12q}{N'}\right]\left(\frac{B}{B+1}\right)^2 = \left[\frac{12q}{39}\right]\left(\frac{8}{9}\right)^2 = 0.2431q$$

The results of the settlement calculations by the Meyerhof method are tabulated in Tables 7.17.

Table 7.17: Settlements Predicted by Meyerhof Method-1 (FRA-670-0380)

Construction Stage	Description	q′ (tsf)	Settlement (inches)
1	Footing Construction	0.230	0.056 (1.4 mm)
2	Pier Columns Construction	0.337	0.082 (2.1 mm)
3	Soil Backfill	0.473	0.115 (2.9 mm)
4	Pier Cap Construction	0.567	0.138 (3.5 mm)
5	Barrier Wall Construction	0.685	0.167 (4.2 mm)
6	Girder Beam Placement	0.995	0.242 (6.1 mm)
7	Deck Construction	1.813	0.441 (11.2 mm)
8	Bridge Open to Traffic	2.037	0.495 (12.6 mm)

The variation of the Terzaghi and Peck method proposed by Meyerhof was also discussed in Section 4.4.7. The settlement equation for his method is:

$$S_e = C_D\left[\frac{2q}{N'}\right]\left(\frac{2B}{B+1}\right)^2 \qquad (4\text{-}23)$$

The embedment correction factor is determined by Equation 4-24 and is equal to 0.75. The initial uncorrected SPT-N value is 63 but is corrected to 39. The resulting equation after entering the variables is:

$$S_e = C_D\left[\frac{2q}{N'}\right]\left(\frac{2B}{B+1}\right)^2 = 0.75\left[\frac{2q}{39}\right]\left(\frac{16}{9}\right)^2 = 0.1216q$$

Table 7.18 presents the results of the immediate settlement for each construction stage.

Table 7.18: Settlements Predicted by Meyerhof Method-2 (FRA-670-0380)

Construction Stage	Description	q (tsf)	Settlement (inches)
1	Footing Construction	0.230	0.028 (0.7 mm)
2	Pier Columns Construction	0.337	0.041 (1.0 mm)
3	Soil Backfill	0.473	0.058 (1.5 mm)
4	Pier Cap Construction	0.567	0.069 (1.8 mm)
5	Barrier Wall Construction	0.685	0.083 (2.1 mm)
6	Girder Beam Placement	0.995	0.121 (3.1 mm)
7	Deck Construction	1.813	0.220 (5.6 mm)
8	Bridge Open to Traffic	2.037	0.248 (6.3 mm)

7.6.11 Peck-Bazaraa Method

The Peck-Bazaraa method was explained in Section 4.4.8 of this report. The method computes the settlement using the following:

$$S_e = C_D C_W\left[\frac{2q}{N_B}\right]\left(\frac{2B}{B+1}\right)^2 \qquad (4\text{-}25)$$

The embedment correction factor (C_D) is calculated by Equation 4-26, using D_f = 8 ft and γ = 120 pcf (0.06 tcf), to be:

$$C_D = 1 - 0.4\sqrt{\frac{0.48}{q}}$$

At a depth 0.5B (4 ft) below the footing, σ_v = 120(4) = 480 psf = 0.48 ksf and σ'_v = (120 – 62.4)4 = 230.4 psf = 0.23 tsf. This results in a value of 0.48 for C_w. Equation 4-28 corrects the SPT-N value of 63 to a value of 131.1. Applying all of the above to Equation 4-25, the main equation will become:

$$S_e = C_D C_W \left[\frac{2q}{N_B}\right]\left(\frac{2B}{B+1}\right)^2 = \left(1 - 0.4\sqrt{\frac{0.48}{q}}\right)0.48\left(\frac{2q}{131.1}\right)\left(\frac{16}{9}\right)^2 = 0.023q\left(1 - 0.4\sqrt{\frac{0.48}{q}}\right)$$

The results of the settlement calculations by the Peck-Bazaraa method are tabulated in Table 7.19

Table 7.19: Settlements Predicted by Peck-Bazaraa Method (FRA-670-0380)

Construction Stage	Description	q′ (tsf)	Settlement (inches)
1	Footing Construction	0.230	0.010 (0.3 mm)
2	Pier Columns Construction	0.337	0.018 (0.5 mm)
3	Soil Backfill	0.473	0.028 (0.7 mm)
4	Pier Cap Construction	0.567	0.036 (0.9 mm)
5	Barrier Wall Construction	0.685	0.046 (1.2 mm)
6	Girder Beam Placement	0.995	0.072 (1.8 mm)
7	Deck Construction	1.813	0.145 (3.7 mm)
8	Bridge Open to Traffic	2.037	0.165 (4.2 mm)

7.6.12 Peck-Hanson-Thornburn Method

In Section 4.4.9 of this report, the Peck-Hanson-Thornburn method was previously described. The method computes the immediate settlement using the following equation:

$$S_e = \frac{q}{0.11 C_w N_1} \tag{4-30}$$

The depth to the water table (D_w) is 8ft as is the depth to the footing embedment (D_f) and the width of the footing (B). These values used in Equation 4-31 result in a value of 0.75 for C_w. Since σ'_v is equal to 0.23 tsf, the SPT-N value (63) is corrected with Equation 4-32a which results in N_1 = 94. The settlements can be computed by the simplified immediate settlement equation:

$$S_e = \frac{q}{0.11 C_w N_1} = \frac{q}{0.11(.75)(49)} = 0.247q$$

Table 7.20 gives the results for the immediate settlement using the Peck-Hanson-Thornburn method.

Table 7.20: Settlements Predicted by Peck-Hanson-Thornburn Method (FRA-670-0380)

Construction Stage	Description	q′ (tsf)	Settlement (inches)
1	Footing Construction	0.230	0.030 (0.8 mm)
2	Pier Columns Construction	0.337	0.043 (1.1 mm)
3	Soil Backfill	0.473	0.061 (1.6 mm)
4	Pier Cap Construction	0.567	0.073 (1.9 mm)
5	Barrier Wall Construction	0.685	0.088 (2.2 mm)
6	Girder Beam Placement	0.995	0.128 (3.3 mm)
7	Deck Construction	1.813	0.234 (5.9 mm)
8	Bridge Open to Traffic	2.037	0.263 (6.7 mm)

7.6.13 Schmertmann Method

The Schmertmann Method was previously described in Section 4.4.10 of this report. The method calculates the settlement by:

$$S_e = C_1 C_2 q \sum_{0}^{Z_z} \left(\frac{I_z}{E_s} \right) \Delta z \qquad (4\text{-}33)$$

Values for C_1 and C_2 are different for each construction stage, based on the load applied and the time elapsed, respectively. The L/B ratio is approximately 5.0. Through interpolations of the strain influence factor data given in Table 4.3, values for I_z and z are determined for Figure 7.5. The values are then determined for the midpoint of each layer.

$I_z = 0.144$ @ $z = 0$

$I_z = 0.50$ @ $z = 0.72B = 0.72(8) \approx 5.8$ ft

$Iz = 0.0$ @ $z = 2.89B = 2.89(8) \approx 23.0$ ft

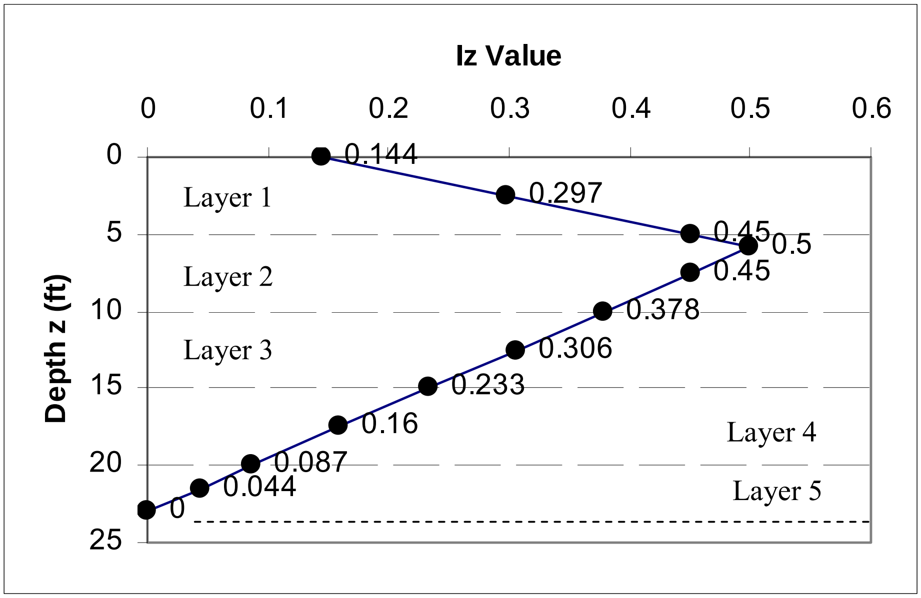

Figure 7.5: Variation of I_z with Depth Below Footing

Layer 1:	Thickness = 5 ft	$(N_1)_{60} = 44$	$I_z = 0.297$
Layer 2:	Thickness = 5 ft	$(N_1)_{60} = 52$	$I_z = 0.450$
Layer 3:	Thickness = 5 ft	$(N_1)_{60} = 54$	$I_z = 0.306$
Layer 4:	Thickness = 5 ft	$(N_1)_{60} = 44$	$I_z = 0.160$
Layer 5:	Thickness = 3 ft	$(N_1)_{60} = 56$	$I_z = 0.044$

The settlement calculations for each construction stage are shown using an elastic modulus calculated by transferring SPT-N into q_c and then into E_s based on the soil type and footing size. E_s is interpolated to be equal to $2.94q_c$. Tables 7.21a to 7.21h summarize the results and Table 7.22 combines the results for all the construction stages.

<u>Construction Stage 1</u> (q = 0.230 tsf; t = 13 days = 0.0356 years):

$$C_1 = 1 - 0.5\left(\frac{\gamma D_f}{q}\right) = 1 - 0.5\left(\frac{0.06x8}{0.23}\right) = -0.043$$

$$C_2 = 1 + 0.2\log\left(\frac{t}{0.1}\right) = 1 + 0.2\log(0.0356/0.1) = 0.910$$

$$S_e = C_1 C_2 q \sum_0^{z_z}\left(\frac{I_z}{E_s}\right)\Delta z = -0.043(0.910) q \sum_0^{z_z}\left(\frac{I_z}{E_s}\right)\Delta z = -0.039 q \sum_0^{z_z}\left(\frac{I_z}{E_s}\right)\Delta z$$

Table 7.21a: Stage 1 Settlements Calculated by Schmertmann Method

Layer No.	I_z	Δz (ft)	S_e (inches) with q_c =:			
			2N	3.5N	5N	6N
1	0.297	5	-0.0006	-0.0004	-0.0003	-0.0002
2	0.450	5	-0.0008	-0.0005	-0.0003	-0.0003
3	0.306	5	-0.0005	-0.0003	-0.0002	-0.0002
4	0.160	5	-0.0003	-0.0002	-0.0001	-0.0001
5	0.044	3	0.0000	0.0000	0.0000	0.0000
Σ	--	--	-0.0023	-0.0013	-0.0009	-0.0008

<u>Construction Stage 2</u> (q = 0.337 tsf; t = 12 days = 0.0329 years):

$$C_1 = 1 - 0.5\left(\frac{\gamma D_f}{q}\right) = 1 - 0.5\left(\frac{0.06x8}{0.337}\right) = 0.288$$

$$C_2 = 1 + 0.2\log\left(\frac{t}{0.1}\right) = 1 + 0.2\log(0.0329/0.1) = 0.903$$

$$S_e = C_1 C_2 q \sum_0^{z_z}\left(\frac{I_z}{E_s}\right)\Delta z = 0.288(0.903) q \sum_0^{z_z}\left(\frac{I_z}{E_s}\right)\Delta z = 0.260 q \sum_0^{z_z}\left(\frac{I_z}{E_s}\right)\Delta z$$

Table 7.21.(b): Stage 2 Settlements Calculated by Schmertmann Method

Layer No.	I_z	Δz (ft)	S_e (inches) with q_c =:			
			2N	3.5N	5N	6N
1	0.297	5	0.0060	0.0034	0.0024	0.0020
2	0.450	5	0.0077	0.0044	0.0031	0.0026
3	0.306	5	0.0051	0.0029	0.0020	0.0017
4	0.160	5	0.0033	0.0019	0.0013	0.0011
5	0.044	3	0.0004	0.0002	0.0002	0.0001
Σ	--	--	0.0225	0.0129	0.0090	0.0075

<u>Construction Stage 3</u> (q = 0.473 tsf; t = 1 day = 0.0027 years):

$$C_1 = 1 - 0.5\left(\frac{\gamma D_f}{q}\right) = 1 - 0.5\left(\frac{0.06x8}{0.473}\right) = 0.493$$

$$C_2 = 1 + 0.2\log\left(\frac{t}{0.1}\right) = 1 + 0.2\log(0.0027/0.1) = 0.687$$

$$S_e = C_1 C_2 q \sum_0^{z_z}\left(\frac{I_z}{E_s}\right)\Delta z = 0.493(0.687)q\sum_0^{z_z}\left(\frac{I_z}{E_s}\right)\Delta z = 0.3387q\sum_0^{z_z}\left(\frac{I_z}{E_s}\right)\Delta z$$

Table 7.21.(c): Stage 3 Settlements Calculated by Schmertmann Method

Layer No.	I_z	Δz (ft)	S_e (inches) with q_c =:			
			2N	3.5N	5N	6N
1	0.297	5	0.0110	0.0063	0.0044	0.0037
2	0.450	5	0.0141	0.0081	0.0057	0.0047
3	0.306	5	0.0093	0.0053	0.0037	0.0031
4	0.160	5	0.0059	0.0034	0.0024	0.0020
5	0.044	3	0.0008	0.0004	0.0003	0.0003
Σ	--	--	0.0412	0.0235	0.0165	0.0137

<u>Construction Stage 4</u> (q = 0.567 tsf; t = 23 days = 0.0630 years):

$$C_1 = 1 - 0.5\left(\frac{\gamma D_f}{q}\right) = 1 - 0.5\left(\frac{0.06x8}{0.567}\right) = 0.577$$

$$C_2 = 1 + 0.2\log\left(\frac{t}{0.1}\right) = 1 + 0.2\log(0.0630/0.1) = 0.960$$

$$S_e = C_1 C_2 q \sum_0^{z_z}\left(\frac{I_z}{E_s}\right)\Delta z = 0.577(.960) q \sum_0^{z_z}\left(\frac{I_z}{E_s}\right)\Delta z = 0.554 q \sum_0^{z_z}\left(\frac{I_z}{E_s}\right)\Delta z$$

Table 7.21.(d): Stage 4 Settlements Calculated by Schmertmann Method

Layer No.	I_z	Δz (ft)	S_e (inches) with q_c =:			
			2N	3.5N	5N	6N
1	0.297	5	0.0216	0.0124	0.0086	0.0072
2	0.450	5	0.0277	0.0158	0.0111	0.0092
3	0.306	5	0.0181	0.0104	0.0073	0.0060
4	0.160	5	0.0116	0.0067	0.0047	0.0039
5	0.044	3	0.0015	0.0009	0.0006	0.0005
Σ	--	--	0.0806	0.0461	0.0323	0.0269

<u>Construction Stage 5</u> (q = 0.685 tsf; t = 27 days = 0.0740 years):

$$C_1 = 1 - 0.5\left(\frac{\gamma D_f}{q}\right) = 1 - 0.5\left(\frac{0.06x8}{0.685}\right) = 0.650$$

$$C_2 = 1 + 0.2\log\left(\frac{t}{0.1}\right) = 1 + 0.2\log(0.0740/0.1) = 0.974$$

$$S_e = C_1 C_2 q \sum_0^{z_z}\left(\frac{I_z}{E_s}\right)\Delta z = 0.65(0.974) q \sum_0^{z_z}\left(\frac{I_z}{E_s}\right)\Delta z = 0.6331 q \sum_0^{z_z}\left(\frac{I_z}{E_s}\right)\Delta z$$

Table 7.21.(e): Stage 5 Settlements Calculated by Schmertmann Method

Layer No.	I_z	Δz (ft)	S_e (inches) with q_c =:			
			2N	3.5N	5N	6N
1	0.297	5	0.0298	0.0171	0.0119	0.0099
2	0.450	5	0.0383	0.0219	0.0153	0.0128
3	0.306	5	0.0251	0.0143	0.0100	0.0084
4	0.160	5	0.0161	0.0092	0.0064	0.0054
5	0.044	3	0.0021	0.0012	0.0008	0.0007
Σ	--	--	0.1113	0.0636	0.0445	0.0371

Construction Stage 6 (q = 0.995 tsf; t = 33 days = 0.0904 years):

$$C_1 = 1 - 0.5\left(\frac{\gamma D_f}{q}\right) = 1 - 0.5\left(\frac{0.06x8}{0.995}\right) = 0.759$$

$$C_2 = 1 + 0.2\log\left(\frac{t}{0.1}\right) = 1 + 0.2\log(0.0904/0.1) = 0.991$$

$$S_e = C_1 C_2 q \sum_0^{z_z}\left(\frac{I_z}{E_s}\right)\Delta z = 0.759(0.991)q\sum_0^{z_z}\left(\frac{I_z}{E_s}\right)\Delta z = 0.752q\sum_0^{z_z}\left(\frac{I_z}{E_s}\right)\Delta z$$

Table 7.21.(f): Stage 6 Settlements Calculated by Schmertmann Method

Layer No.	I_z	Δz (ft)	S_e (inches) with q_c =:			
			2N	3.5N	5N	6N
1	0.297	5	0.0515	0.0295	0.0206	0.0172
2	0.450	5	0.0661	0.0378	0.0264	0.0220
3	0.306	5	0.0436	0.0249	0.0174	0.0145
4	0.160	5	0.0278	0.0159	0.0111	0.0093
5	0.044	3	0.0036	0.0021	0.0014	0.0012
Σ	--	--	0.1926	0.1100	0.0770	0.0642

Construction Stage 7 (q = 1.813 tsf; t = 35 days = 0.0959 years):

$$C_1 = 1 - 0.5\left(\frac{\gamma D_f}{q}\right) = 1 - 0.5\left(\frac{0.06x8}{1.813}\right) = 0.868$$

$$C_2 = 1 + 0.2\log\left(\frac{t}{0.1}\right) = 1 + 0.2\log(0.0959/0.1) = 0.996$$

$$S_e = C_1 C_2 q \sum_0^{z_z}\left(\frac{I_z}{E_s}\right)\Delta z = 0.868(0.996)q\sum_0^{z_z}\left(\frac{I_z}{E_s}\right)\Delta z = 0.865q\sum_0^{z_z}\left(\frac{I_z}{E_s}\right)\Delta z$$

Table 7.21.(g): Stage 7 Settlements Calculated by Schmertmann Method

Layer No.	I_z	Δz (ft)	S_e (inches) with q_c =:			
			2N	3.5N	5N	6N
1	0.297	5	0.1079	0.0617	0.0432	0.0360
2	0.450	5	0.1384	0.0791	0.0554	0.0461
3	0.306	5	0.0906	0.0518	0.0362	0.0302
4	0.160	5	0.0582	0.0332	0.0233	0.0194
5	0.044	3	0.0075	0.0043	0.0030	0.0025
Σ	--	--	0.4027	0.2301	0.1611	0.1342

<u>Construction Stage 8</u> (q = 2.037 tsf; t = 31 days = 0.0849 years):

$$C_1 = 1 - 0.5\left(\frac{\gamma D_f}{q}\right) = 1 - 0.5\left(\frac{0.06x8}{2.037}\right) = 0.882$$

$$C_2 = 1 + 0.2\log\left(\frac{t}{0.1}\right) = 1 + 0.2\log(0.0849/0.1) = 0.986$$

$$S_e = C_1 C_2 q \sum_0^{z_z}\left(\frac{I_z}{E_s}\right)\Delta z = 0.882(0.986)q\sum_0^{z_z}\left(\frac{I_z}{E_s}\right)\Delta z = 0.870q\sum_0^{z_z}\left(\frac{I_z}{E_s}\right)\Delta z$$

Table 7.21.(h): Stage 8 Settlements Calculated by Schmertmann Method

Layer No.	I_z	Δz (ft)	S_e (inches) with q_c =:			
			2N	3.5N	5N	6N
1	0.297	5	0.1220	0.0697	0.0488	0.0407
2	0.450	5	0.1564	0.0894	0.0626	0.0521
3	0.306	5	0.1024	0.0585	0.0410	0.0341
4	0.160	5	0.0657	0.0376	0.0263	0.0219
5	0.044	3	0.0085	0.0049	0.0034	0.0028
Σ	--	--	0.4551	0.2601	0.1821	0.1517

Table 7.22: Summary of Settlements Predicted by Schmertmann Method

Construction Stage	Description	q (tsf)	Settlement (inches)		
			2N	3.5N	5N
1	Footing Construction	0.230	-0.002	-0.001	-0.001
2	Pier Columns Construction	0.337	0.023	0.013	0.009
3	Soil Backfill	0.473	0.041	0.024	0.017
4	Pier Cap Construction	0.567	0.081	0.046	0.032
5	Barrier Wall Construction	0.685	0.111	0.064	0.045
6	Girder Beam Placement	0.995	0.193	0.110	0.077
7	Deck Construction	1.813	0.408	0.230	0.161
8	Bridge Open to Traffic	2.037	0.455	0.260	0.182

7.6.14 Schultze-Sherif Method

The Schultze-Sherif method was previously described in Section 4.4.11 of this report. This method computes the settlement by the following equation:

$$S_e = \frac{fq\sqrt{B}}{N^{0.87}\left(1 + \frac{0.4D_f}{B}\right)} \qquad (4\text{-}38)$$

For the central pier footing, H/B = 2.0 and L/B = 5. The value of the influence factor (f) will be 0.098 according to Figure 4.8. The SPT-N value used in this method is the uncorrected average between the bottom of the footing and a depth of 2B, which is equal to 63. Entering this and other values into Equation 4-38, the settlements will be computed by:

$$S_e = \frac{fq\sqrt{B}}{N^{0.87}\left(1+\frac{0.4D_f}{B}\right)} = \frac{0.098q\sqrt{8}}{(63)^{0.87}\left(1+\frac{0.4x8}{8}\right)} = 0.0054q$$

Table 7.23 tabulates the results of the settlement calculations by the Schultze-Sherif method.

Table 7.23: Settlements Predicted by Schultze-Sherif Method

Construction Stage	Description	q (tsf)	Settlement (inches)
1	Footing Construction	0.230	0.015 (0.4 mm)
2	Pier Columns Construction	0.337	0.022 (0.6 mm)
3	Soil Backfill	0.473	0.031 (0.8 mm)
4	Pier Cap Construction	0.567	0.037 (0.9 mm)
5	Barrier Wall Construction	0.685	0.044 (1.1 mm)
6	Girder Beam Placement	0.995	0.064 (1.6 mm)
7	Deck Construction	1.813	0.117 (3.0 mm)
8	Bridge Open to Traffic	2.037	0.132 (3.3 mm)

7.6.15 Terzaghi-Peck Method

The Terzaghi-Peck method was previously described in Section 4.4.12 of this report. The method computes the settlement by the following:

$$S_e = C_D C_W \left[\frac{3q}{N}\right]\left(\frac{2B}{B+1}\right)^2 \qquad (4\text{-}39)$$

The embedment correction factor (C_D) is computed by Equation 4-24 to be 0.75. The water table correction factor (C_w) is set to 1.67, since the water table is at the bottom of footing, 8 feet below the ground surface. Placing these values in Equation 4-39, the settlement will be computed by:

$$S_e = C_D C_W \left[\frac{3q}{N}\right]\left(\frac{2B}{B+1}\right)^2 = 0.75(1.67)\frac{3q}{63}\left(\frac{16}{9}\right)^2 = 0.189q$$

The Terzaghi-Peck method of calculating settlement is shown in Tables 7.24.

Table 7.24: Settlements Predicted by Terzaghi-Peck Method

Construction Stage	Description	q′ (tsf)	Settlement (inches)
1	Footing Construction	0.230	0.043 (1.1 mm)
2	Pier Columns Construction	0.337	0.064 (1.6 mm)
3	Soil Backfill	0.473	0.089 (2.3 mm)
4	Pier Cap Construction	0.567	0.107 (2.7 mm)
5	Barrier Wall Construction	0.685	0.129 (3.3 mm)
6	Girder Beam Placement	0.995	0.188 (4.8 mm)
7	Deck Construction	1.813	0.342 (8.7 mm)
8	Bridge Open to Traffic	2.037	0.384 (9.8 mm)

7.7 COMPARISON OF SETTLEMENT ESTIMATIONS FOR FRA-670-0380

The settlement estimates made by each of the various methods in Sections 7.6.1 through 7.6.15 are compared to the average measured field settlements. This helps to identify some of the more reliable approaches. Table 7.25 lists the values for each of the theoretical estimates with the field measurements. Table 7.26 summarizes the results in terms of a predicted to measured settlement ratio. The settlement method is most reliable with the ratio is 1.0. The methods proposed by Meyerhof-2, Schmertmann, Department of the Navy, Peck-Hanson-Thornburn, and Hough stand out as the more reliable methods.

The methods proposed by D'Appolonia, Bowles, Schultze-Sherif, Anagnostropoulos, and Peck-Bazaraa all had a tendency to underestimate the actual field settlement behaviors, while Meyerhof-1, Alpan, Burland & Burbidge, Terzaghi & Peck and the elastic methods on cohesionless soil (proposed in AASHTO) overestimated the field measurements. The method proposed by AASHTO on weathered rock results are not show because the estimation was either extremely over or under the measured values.

Table 7.25: Summary of Settlement Data and Results (FRA-670-0380)

Stage	Measured (mm)	Alpan (mm)	Anagnosto-poulos (mm)	Bowles (mm)	Burland & Burbidge (mm)	D'Appolonia (mm)
2	1.5	2.0	0.6	0.5	1.7	0.5
3	---	2.9	0.9	0.7	2.3	0.7
4	2.3	3.4	1.0	0.9	2.8	0.9
5	1.3	4.1	1.2	1.1	3.4	1.1
6	2.8	6.0	1.6	1.6	4.9	1.5
7	5.1	10.9	2.7	2.8	8.9	2.8

Stage	Dept. of Navy (mm)	Meyerhof - 1 (mm)	Meyerhof - 2 (mm)	Peck & Bazaraa (mm)	Peck et al. (mm)
2	1.1	2.1	1.0	0.5	1.1
3	1.5	2.9	1.5	0.7	1.6
4	1.8	3.5	1.8	0.9	1.9
5	2.2	4.2	2.1	1.2	2.2
6	3.2	6.1	3.1	1.8	3.3
7	5.9	11.2	5.6	3.7	5.9

Stage	Schultze & Sherif (mm)	Terzaghi & Peck (mm)	Elastic Method on Cohesionless Soil (mm)				
			$(E_m)_{min}$	$(E_m)_{max}$	343	490	588
2	0.6	1.6	5.6	2.0	4.1	2.8	2.3
3	0.8	2.3	7.8	3.0	5.6	4.1	3.3
4	0.9	2.7	9.4	3.6	6.9	4.8	4.1
5	1.1	3.3	11.4	4.3	8.4	5.8	4.8
6	1.6	4.8	16.8	6.4	11.9	8.4	7.1
7	3.0	8.7	30.0	11.4	21.8	15.2	12.7

Table 7.25 (cont'd):

Stage	Hough (mm) with C' =:			Schmertmann (mm) with q_c =:		
	236	164	138	2N	3.5N	5N
2	1.6	2.4	2.8	0.6	0.3	0.2
3	2.2	3.2	3.8	1.0	0.6	0.4
4	2.6	3.7	4.4	2.0	1.2	0.8
5	3.0	4.4	5.2	2.8	1.6	1.1
6	4.1	5.9	7.1	4.9	2.8	2.0
7	6.5	9.4	11.1	10.2	5.8	4.1

Table 7.26: (Predicted/Measured) Settlement Ratio Values (FRA-670-0380)

Stage	Alpan	Anagnosto-poulos	Bowles	Burland & Burbidge	D'Appolonia
2	0.43	0.12	0.11	0.35	0.11
4	0.88	0.23	0.22	0.72	0.23
5	2.11	0.55	0.55	1.72	0.54
6	1.65	0.42	0.43	1.33	0.42
7	1.87	0.44	0.48	1.52	0.47
Ave.	1.39	0.35	0.36	1.13	0.35

Stage	**Dept. of Navy**	Meyerhof-1	**Meyerhof-2**	Peck & Bazaraa	**Peck-Hanson-Thornburn**
2	**0.22**	0.44	**0.22**	0.13	**0.23**
4	**0.47**	0.90	**0.45**	0.29	**0.48**
5	**1.12**	2.16	**1.08**	0.70	**1.15**
6	**0.88**	1.69	**0.84**	0.56	**0.90**
7	**1.00**	1.92	**0.96**	0.67	**1.02**
Ave.	**0.74**	1.42	**0.71**	0.47	**0.76**

Stage	Schultze & Sherif	Terzaghi & Peck	Elastic Method On Cohesionless Soil (Es = 650 tsf)		
			Es max	490	588
2	0.11	0.34	0.33	0.53	0.53
4	0.24	0.70	0.91	1.22	1.13
5	0.57	1.68	2.15	2.92	2.54
6	0.45	1.31	1.75	2.29	2.00
7	0.51	1.49	1.94	2.59	2.20
Ave.	0.37	1.10	1.42	1.91	1.68

Table 7.26 (cont'd):

Stage	Hough with C' =:			Schmertmann (mm) with q_c =:		
	236	164	138	2N	**3.5N**	5N
2	**0.32**	0.46	0.55	0.42	**0.24**	0.16
4	**0.62**	0.90	1.07	0.92	**0.52**	0.37
5	**1.45**	2.09	2.48	2.22	**1.27**	0.89
6	**1.06**	1.53	1.82	1.76	**1.01**	0.71
7	**1.05**	1.51	1.80	2.01	**1.15**	0.81
Ave.	**0.90**	1.30	1.54	1.47	**0.84**	0.59

7.8 FOOTING ROTATION FOR FRA-670-0380

In Chapter 4, a simple theoretical formula, Equation 4-41, was presented to estimate rotational movement of a pier footing subjected to overturning moment. This formula may be used to estimate the column tilting behavior, assuming that the column-to-footing connections were perfectly rigid.

$$\tan\theta = \left(\frac{1-\upsilon^2}{E_s}\right)\frac{M}{B^2 L} I_\theta \tag{4-41}$$

For the FRA-670-0380 bridge construction site, two spans of unequal length met at the central pier. The north span was 102.9 ft (31.4 m), and the south span was 100.2 ft (30.5 m). The columns attached to the footing should tilt slightly toward the north since the north span is 2.7 ft longer. The total weight of the girder beams was 400,000 lbs, and the concrete deck weighed 1,053,000 lbs. The overturning moment to rotate the footing and columns toward the north is determined to be 1,962 kip-ft (981 ton-ft). Poisson's ratio is set as 0.3 for all the soil types, there are three possible values for the elastic modulus.

From the earlier analysis given in Section 7.2.5, the elastic modulus value may be 343, 490, or 588 tsf. The (L/B) ratio is approximately 5.0. According to Table 4.4, the value of the influence factor is 4.87. Inputting the values calculated into Equation 4-41 gives the maximum degree of tilting. The tilting equation below results in three tilting angles for each elastic modulus listed above.

$$\tan\theta = \left(\frac{1-\upsilon^2}{E_s}\right)\frac{M}{B^2 L} I_\theta = \left(\frac{0.91}{E_s}\right)\frac{981}{(8^2)(40.25)}(4.87) = \frac{1.69}{E_s}$$

θ = 0.28° for clean fine to med. sands and slightly silty sands

θ = 0.20° for coarse sands and sands with little gravel

θ = 0.16° for sandy gravel and gravels

The degree of tilting the columns experienced in the field due to construction activities were 0.126° for the east column and 0.235° for the west column, which are both toward the north. These measurements agree with the range of the computed theoretical values listed above.

7.9 SUBSOIL PROPERTIES FOR MOT-70/75

Soil boring data around Piers 18 and 19, presented in Section 5.3.3, showed that each of the footings rest on type A-4a soil, a gray sandy silt with some clay and trace amounts of gravel. This soil is not considered cohesionless nor is it completely cohesive. From SPT tests, the blow counts were recorded and corrected for as discussed in Section 3.4. The

SPT-N blow counts for each pier were corrected for overburden pressure using Equations 3-5 and 3-6. There was no need to correct the counts for hammer efficiency. Tables 7.27 and 7.28 detail the SPT-N values and the correction factor resulting in corrected blow counts for a range of depths below each of the footings. The dry unit weight of the soil was assumed to be approximately 120 pcf, so with the amount of moisture within the soil the soil's unit weight was calculated to be 132 pcf. Figures 7.6 and 7.7 show the values graphically based on the depth below the footing. The SPT-N values for both piers increased with depth below the footing.

Table 7.27: Corrected SPT-N Values (Pier 18)

Depth Below BOF (ft)	Z (ft)	Σ'_z (tsf)	C_n	N	$N1_{60}$
0	25.4	1.38	0.893	22	20
5	30.4	1.56	0.854	15	13
10	35.4	1.73	0.818	19	16
15	40.4	1.90	0.787	48	38
20	45.4	2.08	0.757	62	47
25	50.4	2.25	0.731	47	34
30	55.4	2.42	0.706	42	30
35	60.4	2.60	0.683	111	76
40	65.4	2.77	0.661	100	66

Table 7.28: Corrected SPT-N Values for Pier 19

Depth Below BOF (ft)	Z (ft)	σ'_z (tsf)	C_n	N	$N1_{60}$
0	25.4	1.91	0.785	22	17
5	30.4	2.09	0.756	53	40
10	35.4	2.26	0.729	75	55
15	40.4	2.43	0.704	73	51
20	45.4	2.61	0.681	100	68
25	50.4	2.78	0.660	79	52
30	55.4	2.95	0.640	97	62
35	60.4	3.13	0.621	100	62

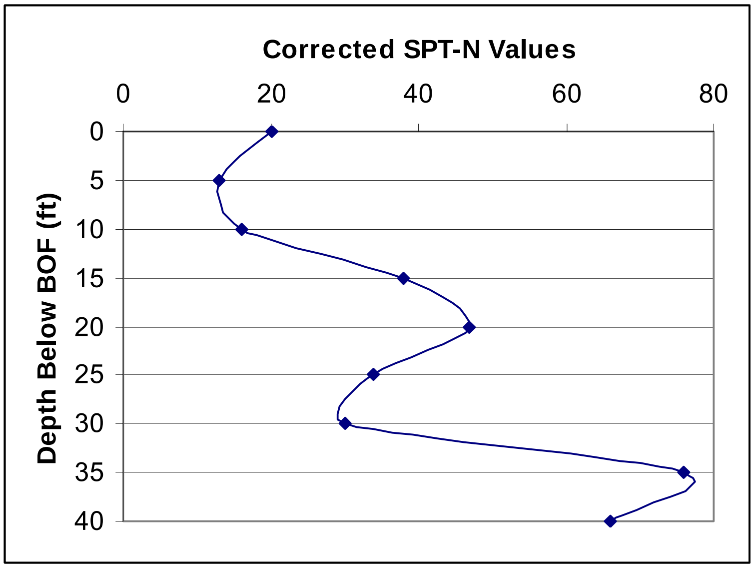

Figure 7.6: Corrected SPT-N Value Variation with Depth (Pier 18)

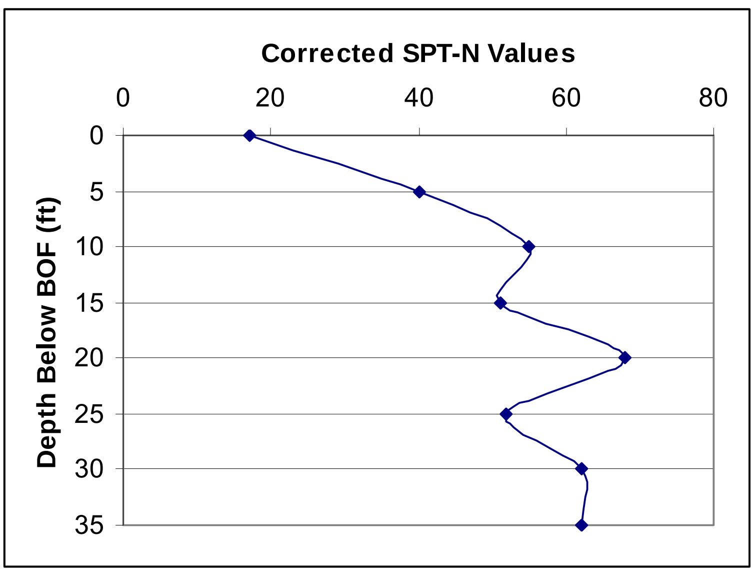

Figure 7.7: Corrected SPT-N Value Variation with Depth (Pier 19)

Based on Table 7.2, the relative density for Pier 18 falls within the dense soil range (average SPT-N value of 38); while beneath Pier 19 is a dense to very dense soil (average SPT-N value of 50). The drained friction angle is determined from Table 3.7. For Pier 18, a value that lies within the range of 37º to 42º is used for the friction angle. Pier 19's friction angle ranges from 38º to 43º. The elastic modulus for soils is determined from the equations in Table 3.16 and based on soil type and corrected SPT-N blow counts.

Pier 18:

E_s (tsf) = $4N1_{60} = 4(38) = 152$ for silts, sandy silts, slightly cohesive mixtures.

Es (tsf) = 7N160 = 7(38) = 266 for clean fine to med. sands and slightly silty sands.

E_s (tsf) = $10N1_{60} = 10(38) = 380$ for coarse sands and sands with little gravel.

Pier 19:

E_s (tsf) = $4N1_{60} = 4(51) = 204$ for silts, sandy silts, slightly cohesive mixtures.

E_s (tsf) = $7N1_{60} = 7(51) = 357$ for clean fine to med. sands and slightly silty sands.

E_s (tsf) = $10N1_{60} = 10(51) = 510$ for coarse sands and sands with little gravel.

7.10 FOOTING RIGIDITY ANALYSIS FOR MOT-70/75

The determination of the footing rigidity was calculated the same as for the Central Pier at the FRA-670-0380 site. Both Pier 18 and Pier 19 are considered rigid footings. The footing rigidity calculations of both MOT-70/75 piers can be found in Appendix.

7.11 CONTACT PRESSURE FOR MOT-70/75

The amount of construction material used for each stage of construction was utilized to calculate the average theoretical pressure beneath the footings. Tables 7.29 and 7.30 list the quantities utilized for each construction stage for Piers 18 and 19, respectively. For the last stage, bridge open to traffic, an assumption of axle loads of 8, 32, and 32 kips was used for the worst case scenario as discussed in Section 7.2.3. Three trucks in each lane near the piers being studied gives a total load of 432 kips. Figures 7.8 and 7.9 show the individual theoretical contact pressure for each construction stage. From these figures, the largest increase in bearing pressure for both piers is the footing construction and the soil backfill being placed.

Table 7.29: Actual Quantities Used in Construction Stages (Pier 18)

Stage No.	Description	Actual Quantities & Notes
1	Footing Construction	Footing Thickness = 4'-5"
2	Pier Wall Construction	Total Volume of Concrete in Wall = 191 Yd^3
3	Soil Backfill	Thickness of ODOT 304 Fill Over Footing = 5 ft
4	Girder Beam Placement	Total Weight of Beams Placed = 142,000 lb
5	Deck Construction	Total Weight of Concrete Deck = 747,100 lb
6	Bridge Open to Traffic	Live Loads = 432,000 lb

[Note] γ of concrete = 150 pcf (assumed); γ of soil backfill = 132 pcf (assumed).

Table 7.30: Actual Quantities Used in Construction Stages (Pier 19)

Stage No.	Description	Actual Quantities & Notes
1	Footing Construction	Footing Thickness = 4'-5".
2	Pier Wall Construction	Total Volume of Concrete in Wall = 124 Yd^3.
3	Soil Backfill	Thickness of ODOT 304 Fill Over Footing = 4 ft
4	Girder Beam Placement	Total Weight of Beams Placed =108,400 lb
5	Deck Construction	Total weight of Concrete Deck = 610,725 lb.
6	Bridge Open to Traffic	Live Loads = 432,000 lb

[Note] γ of concrete = 150 pcf (assumed); γ of soil backfill = 132 pcf (assumed).

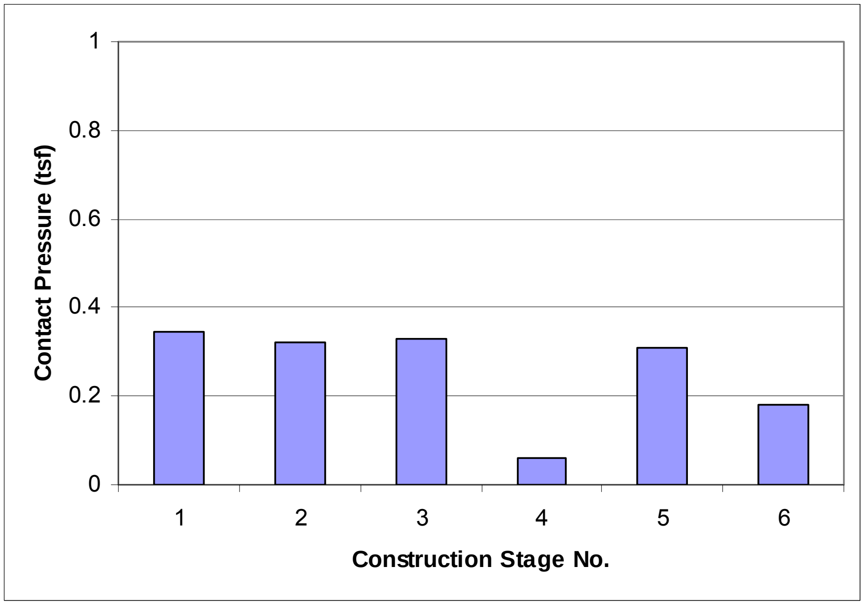

Figure 7.8: Theoretical Contact Pressure Per Construction Stage (Pier 18)

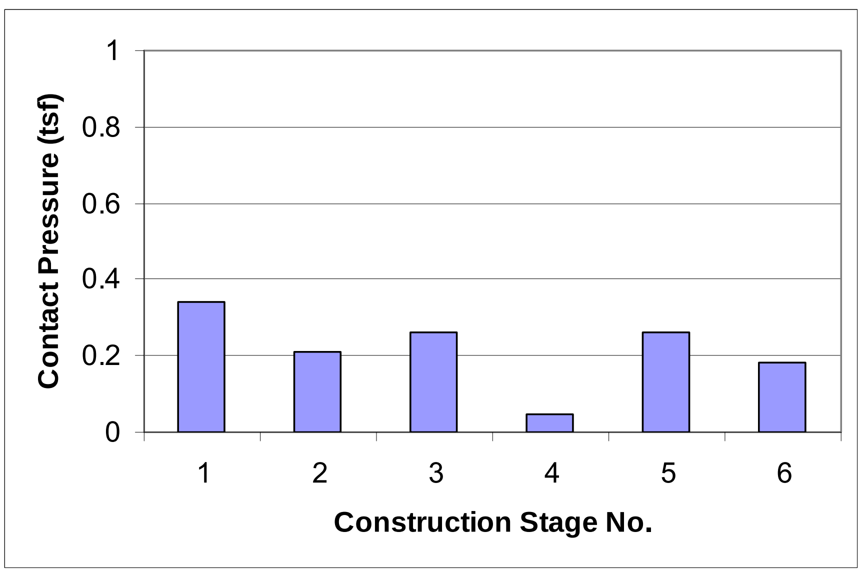

Figure 7.9: Theoretical Contact Pressure Per Construction Stage (Pier 19)

Tables 7.31 and 7.32 have both theoretical and field contact pressures for the piers at the MOT-70/75 project site. Along with the pressures are the percent differences for each stage. The contact pressures are then plotted together so the difference is visually seen. Figures 7.10 and 7.11 show these variations for the construction stages.

Table 7.31: Comparisons of Contact Pressure Values (Pier 18)

Stage	Description	Ave. Contact Pressure (tsf):		Percent Difference (%)
		Theory	Field	
1	Footing Construction	0.344	0.426	19.2
2	Pier Wall Construction	0.665	0.604	10.1
3	Soil Backfill	0.994	1.087	8.6
4	Girder Beam Placement	1.053	1.119	5.9
5	Deck Construction	1.364	1.366	0.2
6	Bridge Open to Traffic	1.543	1.390	11.0

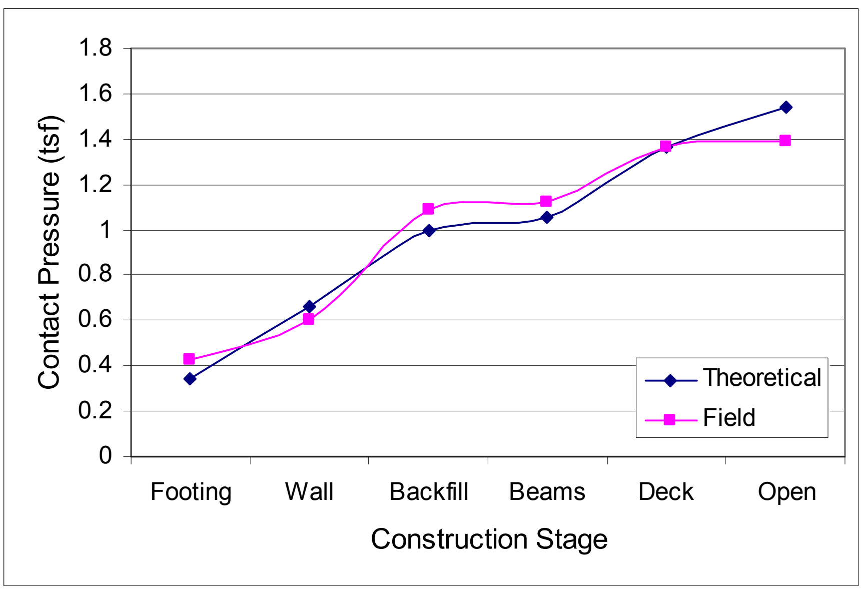

Figure 7.10: Average Bearing Pressure Variation During Construction (Pier 18)

Table 7.32: Comparisons of Contact Pressure Values (Pier 19)

Stage	Description	Ave. Contact Pressure (tsf):		Percent Difference (%)
		Theory	Field	
1	Footing Construction	0.340	0.469	27.5
2	Pier Wall Construction	0.560	0.856	34.6
3	Soil Backfill	0.820	1.546	47.0
4	Girder Beam Placement	0.870	1.618	46.2
5	Deck Construction	1.125	1.997	43.7
6	Bridge Open to Traffic	1.307	2.006	53.5

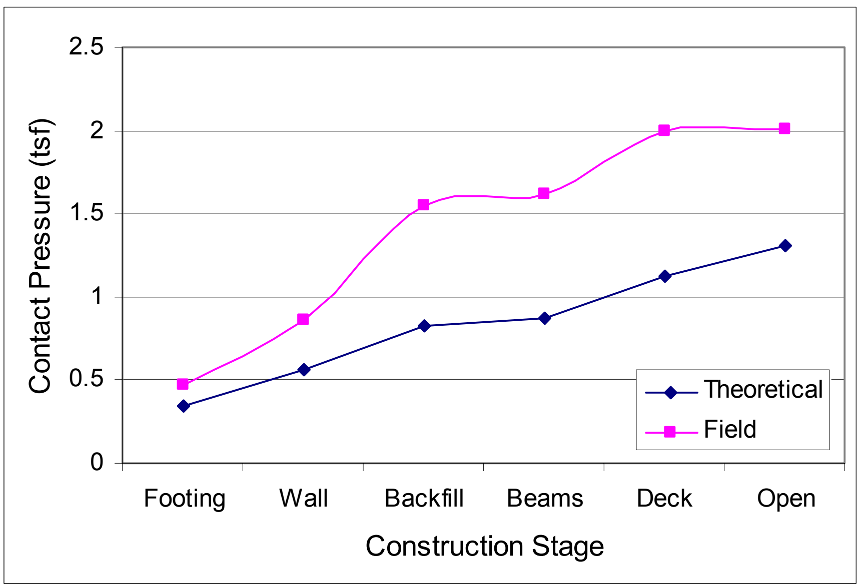

Figure 7.11: Average Bearing Pressure Variation During Construction (Pier 19)

7.12 BEARING CAPACITY FOR MOT-70/75

The determination of the bearing capacity for Piers 18 and 19 is calculated the same way as for the Central Pier at the FRA-670-0380 site. Using the traditional Terzaghi analysis, a bearing resistance value of 46.7 tsf was determined for Pier 18 and for Pier 19 a value of 50.3 tsf was calculated. The SPT-N approach yielded values of 39.7 tsf and 55.6 tsf for Pier 18 and Pier 19, respectively. These bearing resistances, when compared to the theoretical values have factors of safety that range from 25.7 to 42.5. The step-by-step computations for the MOT-70/75 footings are shown in Appendix.

7.13 IMMEDIATE SETTLEMENT FOR MOT-70/75

The methods used for FRA-670-0380 to determine the immediate settlement were also performed for both piers at the MOT-70/75 site. See Appendix for the specific steps for each of the various methods used. A correlation between the predicted settlement by each method and the measured settlement are shown in the next section.

7.14 COMPARISON OF SETTLEMENT ESTIMATIONS FOR MOT-70/75

The settlement estimates made by each of the methods are compared to the average measured field settlements to identify more dependable approaches. The values for each of the theoretical estimates, along with the field measurements, are shown in Table 7.33 and 7.35. Tables 7.34 and 7.36 summarize the results in terms of a predicted to measured settlement ratio. The settlement method is most reliable with the ratio is 1.0. Pier 18 results showed that the methods proposed by Burland-Burbidge, Terzaghi-Peck, Schmertmann, and Elastic and Hough proposed by AASHTO seem to be the more reliable methods. The method proposed by Peck-Hanson-Thornburn overestimated the settlement while each of the other methods not previously mentioned underestimated it. Every method used for Pier 19, however, seemed to underestimate the actual settlement except for the Schmertmann method and the elastic method on cohesionless soil given by AASHTO. The soil boring log used for Pier 19 was the closest boring log, however it was still relatively far away from where Pier 19 was to be placed. This may be the cause for the settlement methods used not to be reliable for this pier.

Table 7.33: Summary of Settlement Data and Results (Pier 18)

Stage	Measured (in)	Alpan (in)	Anagnosto-poulos (in)	Bowles (in)	Burland & Burbidge (in)	D'Appolonia (in)
3	0.24	0.27	0.27	0.18	0.57	0.24
4	0.68	0.28	0.29	0.19	0.60	0.25
5	0.64	0.37	0.36	0.24	0.77	0.32
6	0.70	0.42	0.40	0.28	0.88	0.37

Stage	Dept. of Navy (in)	Meyerhof-1 (in)	Meyerhof-2 (in)	Peck & Bazaraa (in)	Peck et al. (in)
3	0.15	0.32	0.19	0.11	1.37
4	0.16	0.34	0.20	0.12	1.45
5	0.21	0.44	0.26	0.16	1.87
6	0.24	0.50	0.29	0.18	2.12

Stage	Schultze & Sherif (in)	Terzaghi & Peck (in)	Elastic Method on Cohesionless Soil (in)				
			$(E_s)_{min}$	$(E_s)_{max}$	152	266	380
3	0.16	0.59	1.19	0.71	0.94	0.54	0.37
4	0.17	0.62	1.26	0.75	0.99	0.57	0.40
5	0.22	0.80	1.63	0.98	1.28	0.73	0.51
6	0.25	0.91	1.84	1.10	1.45	0.83	0.58

Stage	Hough (in) with C' =:			Schmertmann (in) with q_c =:		
	126	109	93	2N	3.5N	5N
3	0.41	0.48	0.56	0.78	0.44	0.31
4	0.43	0.50	0.59	1.00	0.57	0.40
5	0.53	0.62	0.72	1.35	0.77	0.54
6	0.59	0.68	0.79	1.42	0.81	0.57

Table 7.34: (Predicted/Measured) Settlement Ratio Values (Pier 18)

Stage	Alpan	Anagnosto-poulos	Bowles	**Burland & Burbidge**	D'Appolonia
3	0.75	0.67	0.50	**1.54**	0.67
4	2.79	0.26	0.19	**0.59**	0.25
5	0.44	0.39	0.26	**0.91**	0.38
6	0.47	0.41	0.31	**0.97**	0.41
Ave.	0.49	0.43	0.32	**1.00**	0.43

Table 7.34 (cont'd)**:**

Stage	Dept. of Navy	Meyerhof-1	Meyerhof-2	Peck & Bazaraa	Peck-Hanson-Thornburn
3	0.42	0.88	0.50	0.38	3.75
4	0.16	0.34	0.19	0.15	1.44
5	0.25	0.52	0.30	0.22	2.19
6	0.27	0.56	0.31	0.23	2.47
Ave.	0.28	0.58	0.33	0.25	2.46

Stage	Schultze & Sherif	**Terzaghi & Peck**	**Elastic Method On Cohesionless Soil**			
			E_s min	E_s max	152	266
3	0.42	**1.63**	3.25	1.92	2.58	**1.46**
4	0.16	**0.62**	1.25	0.74	0.99	**0.56**
5	0.25	**0.94**	1.91	1.14	1.50	**0.84**
6	0.27	**1.01**	2.04	1.21	1.61	**0.91**
Ave.	0.28	**1.05**	2.11	1.25	1.67	**0.94**

Hough with C' =:			**Schmertmann (in) with q_c =:**		
126	109	**93**	2N	**3.5N**	**5N**
1.04	1.21	**1.42**	3.08	**1.75**	**1.25**
0.40	0.46	**0.54**	1.41	**0.81**	**0.57**
0.58	0.67	**0.78**	2.05	**1.17**	**0.83**
0.61	0.70	**0.81**	1.97	**1.13**	**0.80**
0.66	0.76	**0.89**	2.13	**1.22**	**0.86**

Table 7.35: Summary of Settlement Data and Results (Pier 19)

Stage	Measured (in)	Alpan (in)	Anagnosto-poulos (in)	Bowles (in)	Burland & Burbidge (in)	D'Appolonia (in)
2	0.18	0.16	0.08	0.09	0.23	0.11
3	0.54	0.24	0.11	0.13	0.34	0.16
4	0.95	0.25	0.11	0.14	0.36	0.17
5	0.83	0.33	0.14	0.18	0.47	0.23
6	0.96	0.38	0.16	0.20	0.54	0.26

Stage	Dept. of Navy (in)	Meyerhof-1 (in)	Meyerhof-2 (in)	Peck & Bazaraa (in)	Peck et al. (in)
2	0.08	0.14	0.08	0.04	0.25
3	0.11	0.20	0.12	0.07	0.37
4	0.12	0.21	0.13	0.08	0.39
5	0.15	0.28	0.17	0.10	0.51
6	0.18	0.32	0.20	0.12	0.59

Table 7.35 (cont'd)**:**

Stage	Schultze & Sherif (in)	Terzaghi & Peck (in)	Elastic Method on Cohesionless Soil (in)				
			$(E_s)_{min}$	$(E_s)_{max}$	204	357	510
2	0.08	0.14	0.87	0.52	0.51	0.29	0.21
3	0.12	0.20	1.29	0.77	0.76	0.43	0.30
4	0.13	0.22	1.36	0.82	0.80	0.46	0.32
5	0.17	0.28	1.77	1.06	1.04	0.59	0.42
6	0.20	0.33	2.05	1.23	1.21	0.69	0.48

Stage	Hough (in) with C' =:			Schmertmann (in) with q_c =:		
	168	141	118	2N	3.5N	5N
2	0.20	0.24	0.29	0.28	0.16	0.11
3	0.28	0.33	0.40	0.66	0.38	0.26
4	0.29	0.35	0.42	0.78	0.45	0.31
5	0.36	0.43	0.52	1.08	0.62	0.43
6	0.41	0.49	0.58	1.18	0.67	0.47

Table 7.36: (Predicted/Measured) Settlement Ratio Values (Pier 19)

Stage	Alpan	Anagnosto-poulos	Bowles	Burland & Burbidge	D'Appolonia
2	0.33	0.17	0.28	0.50	0.22
3	0.26	0.11	0.17	0.37	0.17
4	0.16	0.06	0.11	0.24	0.11
5	0.28	0.11	0.17	0.39	0.18
6	0.29	0.11	0.17	0.42	0.20
Ave.	0.26	0.11	0.18	0.38	0.18

Stage	Dept. of Navy	Meyerhof-1	Meyerhof-2	Peck & Bazaraa	Peck-Hanson-Thornburn
2	0.17	0.33	0.17	0.11	0.50
3	0.11	0.22	0.13	0.09	0.39
4	0.07	0.14	0.08	0.06	0.24
5	0.12	0.24	0.14	0.10	0.42
6	0.14	0.25	0.16	0.10	0.45
Ave.	0.12	0.24	0.14	0.09	0.40

Table 7.36 (cont'd)**:**

Stage	Schultze & Sherif	Terzaghi & Peck	**Elastic Method On Cohesionless Soil**			
			Es min	**Es max**	**204**	357
2	0.17	0.28	1.89	**1.11**	**1.05**	0.61
3	0.13	0.20	1.41	**0.83**	**0.81**	0.46
4	0.08	0.14	0.87	**0.53**	**0.51**	0.29
5	0.14	0.23	1.49	**0.89**	**0.87**	0.49
6	0.16	0.25	1.58	**0.95**	**0.93**	0.53
Ave.	0.14	0.20	1.45	**0.86**	**0.83**	0.48

Stage	Hough with C' =:			**Schmertmann (in) with q_c =:**		
	168	141	118	**2N**	3.5N	5N
2	0.39	0.44	0.56	**1.33**	0.78	0.56
3	0.28	0.31	0.39	**1.15**	0.67	0.46
4	0.17	0.20	0.24	**0.78**	0.45	0.32
5	0.28	0.33	0.40	**1.25**	0.72	0.51
6	0.29	0.34	0.41	**1.19**	0.67	0.48
Ave.	0.28	0.32	0.40	**1.14**	0.66	0.47

7.15 FOOTING ROTATION FOR MOT-70/75

In Chapter 4, a simple theoretical formula (Equation 4-37) was presented to estimate rotational movement of a pier footing subjected to overturning moment. This formula may be used to estimate the column tilting behavior, assuming that the column-to-footing connections were perfectly rigid.

$$\tan\theta = \left(\frac{1-\upsilon^2}{E_s}\right)\frac{M}{B^2 L} I_\theta \qquad (4.35)$$

For the MOT-70/75 bridge construction site, two spans of unequal length met at both piers. The span from Pier 17 to 18 was 134.5 ft (41 m), from 18 to 19 the span was 118.1 ft (36 m), and the span from 19 to the forward abutment was 88.6 ft (27 m). The columns attached to the footing should tilt slightly toward the east since the spans for both Pier 18 and 19 were longer on that side. The total weight of the girder beams for Pier 18 was 142,000 lbs, and the concrete deck weighed 747,100 lbs. For Pier 19, the total weight of the beams was 108,400 lb and the deck weighed 610,725 lbs. The overturning moment to rotate the footing and columns toward the east is determined to be 7291 kip-ft (3645 ton-ft) for Pier 18. Pier 19 had an overturning moment of 10,607 kip-ft (5303 ton-ft). Poisson's ratio is set as 0.3 for all the soil types but the elastic modulus changes for each soil type. From the earlier analysis given in Section 7.3.1, the elastic constants to be used are 266, 380, and 456 tsf for Pier 18 and for Pier 19 are 357, 510, and 612 tsf. The (L/B) ratios are approximately 2.73 and 2.05 for Pier 18 and 19, respectively. According to Table 4.4, the values of the influence factors are 4.70 and 4.60 for 18 and 19. Inputting the values calculated into Equation 4-37 gives the maximum degree of tilting. The tilting equation below results in three tilting angles, one for each elastic modulus listed above.

Pier 18: $$\tan\theta = \left(\frac{1-\upsilon^2}{E_s}\right)\frac{M}{B^2 L} I_\theta = \left(\frac{0.91}{E_s}\right)\frac{3645}{(21^2)(57.4)}(4.70) = \frac{0.616}{E_s}$$

Pier 19: $$\tan\theta = \left(\frac{1-\upsilon^2}{E_s}\right)\frac{M}{B^2 L} I_\theta = \left(\frac{0.91}{E_s}\right)\frac{5303}{(24^2)(49.2)}(4.60) = \frac{0.783}{E_s}$$

Pier 18:

$\theta = 0.13°$ for clean fine to med. sands and slightly silty sands ($E_s = 266$)

$\theta = 0.09°$ for coarse sands and sands with little gravel ($E_s = 380$)

Pier 19:

$\theta = 0.13°$ for clean fine to med. sands and slightly silty sands ($E_s = 357$)

$\theta = 0.09°$ for coarse sands and sands with little gravel ($E_s = 510$)

The degree of tilting the columns experienced in the field due to construction activities were 1.03° for the Pier 18 and 0.02° for Pier 19. The first tilt reading for Pier 18 was much different than all the others, which is the result in the degree of tilt being over 1.0º. If the first reading is thrown out, then the change in tilt is only 0.03º. With this value and the value of 0.02º for Pier 19, it is seen that the piers do not move as much as was expected.

7.16 REGIONAL COST ANALYSIS

Cost analyses performed by other researchers were summarized previously in Section 2.6. Their analyses used cost figures that are now out of date. The cost effectiveness of using shallow foundations at bridge construction projects will now be revisited for the Ohio projects based on more recent cost figures available in literature.

To make a fair cost comparison between shallow and deep foundations, a basis must be set up from regional cost figures. In research conducted by ORITE, the foundations had a wide range of sizes. However, for this cost estimate, a typical spread footing size is used. The load carried by a bridge foundation may be 700 tons maximum, and the allowable bearing pressure of the subsoils for a typical highway bridge construction site is 3 tsf. Therefore, the required contact area of a spread footing is 233

ft^2. A typical footing width of 10 ft (3.0 m) with a length of 24 ft (7.3 m) will provide the sufficient area and a thickness of 3 ft (0.9 m) is used. If the footing has an embedment depth of 7 ft (2.1 m), the amount of soil that needs to be excavated will be close to 700 cubic yards. The amount of backfill may be close to 670 cubic yards. A pile foundation (end-bearing type) equivalent to such a spread footing may have the following design characteristics:

Steel Piles Size = HP 10 x 42 (section area = 12.4 in^2 or 8,063 mm^2)

Pile Length = 40 ft or 12.2 m (ave.)

No. of Piles = 10 (arranged in 2 rows)

Dimensions of Pile Cap = 10 ft width by 24 ft length by 3 ft thickness

Soil Cover = 4 ft (over the top of pier cap)

Under these parameters, the amount of excavation and the amount of backfilling will be basically the same as those mentioned for the spread footing construction.

Tables 7.37 (a) and (b) list the national average base prices associated with the construction of spread footing and pile foundations. These figures were extracted from a catalog published by R.S. Means (2000). The table does not address the costs of construction beyond the pipe cap or spread footing, since the additional costs associated with pier columns/wall, pier cap, etc. can be assumed to be the same between the two options. Table 7.38 presents the location factor for some cities in Ohio, so that the national average cost figures can be adjusted to specific locations in Ohio.

Table 7.37: National Average Base Costs for Bridge Foundations

(a) Costs Associated with Shallow Foundation

Item	Breakdowns	2000 Base Cost	R.S. Means ID #
Excavation (by hydraulic backhoe)	Labor	$0.55 per CY	02315-400-0250
	Equipment	$0.89 per CY	
Footing (concrete)	Labor	$9.35 per CY	03310-700-2600
	Equipment	$0.63 per CY	
Footing (rebar)	Material	$500 per ton	03210-600-0550
	Labor	$280 per ton	
Footing (forms)	Material	$1.19 per SFCA	03110-430-0050
	Labor	$1.94 per SFCA	
Footing (finish)	Labor	$0.24 per SF	03350-300-0010
Backfill (bulldozer)	Labor	$0.24 per CY	02315-120-3000
	Equipment	$0.29 per CY	
Backfill (Sheepsfoot roller)	Labor	$0.13 per CY	02315-300-5600
	Equipment	$0.24 per CY	
Backfill (Tamper)	Labor	$1.37 per CY	02315-300-8000
	Equipment	$0.54 per CY	

(b) Costs Associated with Pile Foundation

Item	Breakdowns	2000 Base Cost	R.S. Means ID #
Mobilization (for pile driver)	Labor	$4,000 LS	02455-500-1100
	Equipment	$3,550 LS	
Excavation (by hydraulic backhoe)	Labor	$0.55 per CY	02315-400-0250
	Equipment	$0.89 per CY	
Steel Piles (including driving & cut-off)	Material	$10.50 VLF	02455-850-0400
	Labor	$2.96 VLF	
	Equipment	$2.63 VLF	
Pile Cap (concrete)	Labor	$9.35 per CY	03310-700-2600
	Equipment	$0.63 per CY	
Pile Cap (rebar)	Material	$500 per ton	03210-600-0550
	Labor	$280 per ton	
Pile Cap (forms)	Material	$1.19 per SFCA	03110-430-0050
	Labor	$1.94 per SFCA	
Pile Cap (finish)	Labor	$0.24 per SF	03350-300-0010
Backfill (bulldozer)	Labor	$0.24 per CY	02315-120-3000
	Equipment	$0.29 per CY	
Backfill (Sheepsfoot roller)	Labor	$0.13 per CY	02315-300-5600
	Equipment	$0.24 per CY	
Backfill (Tamper)	Labor	$1.37 per CY	02315-300-8000
	Equipment	$0.54 per CY	

[Note:] CY = cubic yards; SFCA = square feet of contact area; SF = square feet; LS = lump sum; VLF = vertical lineal feet

Table 7.38: Location Factors in Ohio

City in Ohio	Location Factor for:		
	Material	Installation	Overall
Akron	0.998	0.990	0.994
Athens	0.981	0.756	0.872
Canton	0.991	0.911	0.952
Chillicothe	0.947	0.958	0.952
Cincinnati	0.953	0.899	0.927
Cleveland	0.986	1.064	1.024
Columbus	0.974	0.911	0.944
Dayton	0.950	0.887	0.919
Mansfield	0.966	0.904	0.936
Toledo	0.979	0.975	0.977
Zanesville	0.949	0.858	0.905

For the hypothetical spread footing and pile foundation mentioned earlier, the estimated costs are shown in Table 7.39. No mobilization fee may be required for the spread footing option, since its construction will most likely utilize equipment that is already available at the bridge construction site. According to the table, the spread footing option will save nearly \$ 14,000 per foundation. The cost of installing a spread footing is only 37% of the cost of installing a pile foundation. This total cost saving will increase as the number of foundations increase and the driven length of the piles becomes longer.

Table 7.39: Costs of Example Spread Footing and Pile Foundation

Item	Spread Footing	Pile Foundation	Cost Savings
Mobilization	--	$7,550	$7,550
Excavation	$1,008	$1,008	--
Pile Driving	--	$6,436	$6,436
Spread Footing/Pile Cap	$5,455	$5,455	--
Backfill	$1,883	$1,883	--
National Average TOTAL	$8,346	$22,332	$13,986
Columbus TOTAL	$7,879	$21,081	$13,202

In the above outcome, 63% is saved by using spread footings instead of pile foundations. This agrees with the cost reported by Amar et al. (1984), who stated that the cost associated with the spread footing is 17 to 67% less than the cost associated with the deep foundation. The outcome of the above example is also compatible with the WSDOT bridge cases studied by DiMillio (1982), where the spread footings cost an average of 62% what the pile foundations did.

One hidden aspect of any foundation engineering work is the subsurface exploration and laboratory testing. A minimum of two boreholes may be required in each foundation construction area and at least one borehole for each substructure. For designing a spread footing, the soil borings will provide information about the soil profiles within the zone of influence, such as soil classifications (including Atterberg limits), natural moisture contents, SPT-N values at 5-ft (1.5 m) intervals, the depth of water table, and the depth to bedrock (if encountered within the depth of boring). For the pile foundation option, the field data collection for the soil profile is not as important. Instead, the depth to the bedrock and the quality of bedrock core specimens must be carefully studied in each borehole. Tables 7.40 and 7.41 list the current fees for subsurface exploration and laboratory testing work charged by a geotechnical firm based in central Ohio.

Table 7.40: Base Costs for Subsurface Exploration Work

Item	Spread Footing	Pile Foundation
Mobilization	$ 250.0 + $ 5.0 / mile beyond 40 miles	
Site Access, Boring Layout, Standby	$ 155.00 per hour	
Auger w/ No Sampling	NA	$ 12.00 per linear ft
Auger w/ 5' SPT Interval, Soil Logging	$ 14.50 per linear ft	NA
Augering Surcharge From 50' to 80'	NA	$ 8.00 per linear ft
Shelby Tube Sampling *	$ 20.00 each	NA
Loading/Unloading of Coring Equipment, Changeover, Water Hauling	NA	$ 155.00 per hour
NX Rock Coring	NA	$ 35.00 per linear ft
Rock Coring Surcharge From 50' to 80'	NA	$ 8.00 per linear ft

[Note] * Optional.

Table 7.41: Base Costs for Laboratory Soil Testing

Laboratory Test	Spread Footing	Pile Foundation
Visual Classification, Natural Moisture Content	$ 12.50 per sample	$ 12.50 each
Atterberg Limits	$ 65.00 each	NA
Unconfined Compression *	$ 98.00 each	NA
Consolidation *	$ 200.00 each	NA
Identification of Rock Core	NA	$ 60.00 per box

[Note] * Optional.

For the hypothetical spread footing option illustrated earlier, two soil bore holes with 5-ft (1.5-m) SPT intervals are needed. The depth of boring will be at least 30 ft (9.1 m), considering the embedment depth of 7 ft (2.1 m) and the estimated influence zone of 20 ft (6.1 m). For the pile foundation option, a minimum of two bore holes are again desired. The depth to bedrock and the length of rock coring may be arbitrarily assumed to be 60 ft (18.3 m) and 20 ft (6.1 m), respectively.

The estimated costs for the subsurface exploration and laboratory testing are shown for the two foundation options in Table 7.42. According to the table, the cost saving forthe spread footing option may be insignificant, since its lower subsurface exploration cost in the field will be most likely offset by its higher cost in the laboratory testing.

Table 7.42: Costs of Subsurface Exploration & Laboratory Testing

Item	Spread Footing	Pile Foundation	Cost Savings
Mobilization	$ 250	$ 250	--
Subsurface Exploration	$ 1,335	$ 3,930	$ 2,595
Laboratory Testing	$ 1,526	$ 120	- $ 1,406
TOTAL	$ 3,111	$ 4,145	$1,034

The cost of the subsurface exploration and laboratory work for the spread footing option can be more expensive. If the bridge construction area consists mostly of moist clayey soils, additional Shelby tube sampling and consolidation tests will be required to determine engineering properties of the clayey soils.

CHAPTER 8: SUMMARY AND CONCLUSIONS

8.1 SUMMARY

Spread footing foundations have remained secondary to deep foundations for supporting highway bridge structures in many states including Ohio, despite the number of reports that have noted the cost advantages and satisfactory field performances demonstrated by spread footings. A research team at Ohio Research Institute for Transportation and the Environment (ORITE) at Ohio University continued its comprehensive field study on spread footings to further promote the use of spread footing foundations for highway bridge construction projects. As noted the objectives of the study were to:

- Successfully instrument and monitor spread footing foundations at additional highway construction sites in Ohio
- Evaluate the reliability of geotechnical prediction methods applicable to spread footings, especially the settlement prediction methods for footings outlined in Section 10, AASHTO LRFD Bridge Design Specifications (2004)
- Examine the economic aspect of using the spread footing for highway bridges, instead of deep foundations.

The following specific tasks were formulated and executed to meet the objectives:

Task 1: Identify two major bridge construction sites in Ohio using spread footings.

Task 2: Calculate the expected spread footing performance from subsurface exploration and other project data.

Task 3: Create a sensor installation plan to measure the anticipated spread footing performance variables.

Task 4: Collect field data as necessary during and after construction of the pier footing.

Task 5: Analyze the collected data to validate the methods presented in Section 10 of AASHTO LRFD Bridge Design Specifications (2004).

Task 6: Determine reliability of other geotechnical methods applicable to bridge spread footing foundations.

Task 7: Perform a relatively comprehensive economic analysis on a typical highway bridge spread footing and its equivalent pile foundation, using the recent cost figures available in Ohio and considering the cost of subsurface investigation and laboratory testing.

In the current study, selected spread footing foundations at two highway bridge construction sites were instrumented with sensors and reference points. The field performance of each instrumented footing was monitored throughout each phase of construction and under live load application. The first field research site was located at FRA-670-0380, where a two-span bridge was constructed to allow crossing of High Street over I-670 highway, in Columbus, Ohio. The second site was identified at the northwest end of the Ramp C Bridge constructed as part of the I-70/75 interchange major reconstruction project near Dayton, Ohio.

For each instrumented spread footing, the field performance was established through three types of measurements taken in the field, vibrating-wire pressure cell readings, footing settlement (detected by the optical survey method), and tilting of footing column/wall (detected by an accelerometer). From these measurements, three-dimensional graphical plots were produced to understand how the foundation behaved in response to the loadings generated during bridge construction stages and under live load application. These field performance measurements were cross-examined to discuss any correlations that existed between the different types of field data.

Once the field performance of each of the instrumented spread footing foundations was examined in detail, a series of geotechnical analyses was performed. The rigidity of each footing was evaluated using three methods found in literature to in turn validate the contact pressure and settlement estimation approaches used. The AASHTO LRFD Bridge Design Specifications (2004) methods for bearing capacity and settlement determination were applied to each of the field cases. Additional geotechnical methods proposed in literature were then evaluated based on the field performance data obtained at the highway bridge construction sites. These additional methods included twelve different settlement prediction methods for footings on cohesionless soils, which were the methods proposed by Alpan, Anagnostropoulos, Bowles, Burland-Burbidge, D'Appolonia, Department of the Navy, Meyerhof (two ways), Peck-Bazaraa, Peck-Hanson-Thornburn, Schmertmann, Schultze-Sherif, and Terzaghi-Peck.

Beyond the geotechnical analysis, an additional analysis was made to gain further insights into the use of spread footing. This analysis focused on economic advantages for using spread footings to support highway bridges instead of using deep foundations.

8.2 CONCLUSIONS

Many conclusions were reached during this research due to its multi-phased nature. The conclusions are presented below in relation to their previous presentation.

8.2.1 Literature Review

From the review of geotechnical literature, a large number of technical publications can be found related to shallow foundations. Emphasis is often placed on bearing capacity and tolerable movement issues, however a good number of book sections and papers focus on other issues such as the distribution of contact pressure, settlement, rotational movement, and cost effectiveness.

In addition to the traditional approaches in analyzing shallow foundations, new methods and techniques are becoming available as more sophisticated electronic and computational tools such as centrifuge modeling, nondestructive test methods, finite element methods, and neural networks are being developed. Each of these methods can help gain further insight into shallow foundation behaviors, but also possess shortcomings as well. The centrifuge model technique is best used to conduct parametric studies and examine failure modes. The field conditions are not simulated accurately. The nondestructive test measures the stiffness properties of the material under the footing at small strain levels, but the data cannot be used to accurately predict the behavior under large load-displacement levels. The finite element method is often used to analyze the field conditions, however this method requires a large number of input parameter values that may not be easily available. The neural network technique can be used to easily predict spread footing settlement, but this approach requires a relatively large database and produces no physical models.

Based on the results in literature, the best methods determined by other researchers were Schmertmann, Hough, Peck-Bazarra, and Burland-Burbidge. These researchers also determined that Alpan, Schultz-Sherif, Peck-Hanson-Thornburn, Meyerhof, and D'Appolonia were unconservative methods.

Cost effectiveness determined by three researchers gives spread footings to be less expensive than pile foundations each time. The research determined by the proposers found that spread footings were 20%, 17 to 67%, and 60% less than pile foundations.

8.2.2 Field Instrumentation and Monitoring Methods for Spread Footing Foundations

A relatively comprehensive field instrumentation plan was developed and executed at each of the two highway bridge construction sites to monitor the field performance of spread footings throughout and beyond the construction phases. The instrumentation plan relied on five to seven vibrating-wire type earth pressure cells for contact pressure magnitude and distribution measurements at the base of the footing, optical survey method for detecting vertical displacements of five monitoring points strategically placed over the footing (one near each corner and the fifth one near the footing center), and an accelerometer-based tilt-meter for recording the degree of tilt the pier column/wall experience from the true vertical direction.

The soil types for the sites were mostly cohesionless. FRA-670-0380 had A-2-4 and A-3 soil types and the MOT-70/75 site have A-4a soils types. The SPT-N values near each pier footing increased with depth. The construction of the FRA-670-0380 bridge only took 144 days to complete, whereas both of the piers at the MOT-70/75 site too over 300 days to complete.

8.2.3 Field Performance of Spread Footing Foundations at Two Highway Bridge Construction Sites

Contact Pressure

The contact pressure values at the end of construction varied between 0.62 and 4.64 tsf with an average of 2.85 tsf under Central Pier foundation at the FRA-670-0380 site. At the MOT-70/75 Ramp C bridge construction site, the end of construction contact pressure ranged between 0.72 and 2.10 tsf with an average of 1.39 tsf under the Pier 18 footing and between 0.29 and 2.59 tsf with an average of 1.66 tsf under the Pier 19 footing. The pressure cell that registered 0.29 tsf for Pier 19 stopped working and without that value the average increased to 2.01 tsf.

The contact pressure was relatively uniform during the very early phases of construction. As the construction progressed, the contact pressure distribution became increasingly more non-uniform. The general shape of the pressure distribution is higher in the center of the footing than on the sides and corners creating a pressure bulb.

Overall the Central Pier at the FRA-670-0380 site registered more pressure on the south side of the footing. The largest increase for this footing occurred due to the construction of the deck. Pier 18 recorded more pressure on the north side of the footing, while Pier 19 had more pressure on the east side. Both Pier 18 and Pier 19 had the largest increase in pressure die to soil backfill and footing construction.

Settlement

The settlement of the monitoring points installed on the Central Pier foundation located at FRA-670-0380 project site varied between 0.01 and 0.26 inches (with the average of 0.20 inches) at the end of construction. For the MOT-70/75 site, Pier 18 had a settlement that ranged from 0.36 to 1.20 inches with an average of 0.70 inches and Pier 19 had a settlement ranging from 0.84 to 1.14 inches with an average of 0.96 inches.

For the Central Pier foundation at FRA-670-0380 site, Stage 7 (deck construction) induced the largest increase in the settlement among all the construction stages. Stage 4 (placement of girder beams) induced the largest increase in settlement for both Pier 18 and Pier 19 at the MOT-70/75 site.

As the construction work progressed, the larger vertical displacements were recorded along the north edge of the spread footing for the FRA-670-0380 site. Pier 18 at the MOT-70/75 construction site had the largest settlement at the northwest corner, but the settlement of the footing as a whole was nonuniform during construction. For Pier 19, however, the foundation settled quite uniformly.

After deck and parapet construction, common field practice is to keep the concrete moist for 7 days. This saturates the subsoils and induces heaving of the top soil layer, which leads to an upward movement of the spread footings.

Tilting

The overall change in degree of column tilting for the Central Pier foundation at FRA-670-0380 site was 0.13° for east column and 0.24° for the west column. At the MOT-70/75 bridge site, Pier 18 had a change in tilt of 1.03° and Pier 19 of 0.13°.

Theoretically, the columns should tilt only under the last two construction stages (beams placement, deck construction) because of different span lengths. The fact that the columns started tilting during the earlier construction stages imply that the rotational behavior is influenced by stiffness of the soils beneath the footing and the actual construction practices applied at the site.

Correlations Among Field Performance Data

Generally a good correlation existed between the settlement and tilting data. The footing settlement and tilting performance both reflected the global behavior of the relatively rigid structure, whereas the soil pressure readings did not always correspond to the global behavior and mirrored more the local conditions (i.e., stiffness of the soil under each pressure cell). The contact pressure is more a reflection of the stiffness of the underlying soil in the localized area.

8.2.4 Reliability of Methods for Spread Footings Outlined in Section 10, AASHTO LRFD Bridge Design Specifications (2004)

The bearing capacity given by the empirical formula based on the average SPT-N value tends to be somewhat larger than that given by the traditional formula originally developed by Terzaghi. The factors of safety based on these methods were quite large, ranging from 5.5 to over 50. The elastic settlement method based on the model of a rigid footing resting on a semi-infinite elastic soil appears to be relatively reliable when the elastic modulus of the subsoil layers can be represented well by a single value. This method was extremely accurate for Pier 18 and Pier 19 on the MOT-70/75 site. The method proposed by Hough was one of the more reliable settlement prediction methods identified in the study

8.2.5 Reliability of Other Geotechnical Methods for Predicting Spread Footing Performance

According to the footing rigidity analyses performed, each of the three spread footings can be analyzed as rigid structures. The contact stress distribution formula (Equation 4-1), based on the principles of strength of materials, appears to be adequate for predicting both magnitude and distribution of contact pressure under the spread footing. The settlement predictions methods for footings on cohesionless soils that proved to be more reliable are those proposed by Schmertmann, Terzaghi-Peck, and Burland-Burbidge. The column/wall tilting formula (Equation 4-35), based on elastic theory, appears to be reliable in predicting the rotational movements of spread footings that support the highway bridge structures and that are subjected to overturning moments.

8.2.6 Overall Applicability of Spread Footings as a Highway Bridge Foundation

The field performance data gathered at the two sites in Ohio demonstrated that the spread footings can support the highway bridge structures satisfactorily, provided that the subsurface conditions are adequate (namely the corrected SPT-N value is larger than 20 blows/ft).

8.2.7 Economic Aspect of Using Spread Footings

The typical spread footing construction at a highway construction site may save nearly \$13,000 per foundation in Ohio. The cost savings for installing a spread footing instead of installing a pile foundation is 63%. This total price for cost savings will increase as more shallow foundations are used. The subsurface exploration and laboratory testing for the design of a spread footing is very important. The soil borings provide general information about the soil profiles within the zone of influence. For the pile foundation option, the field data collection for a soil profile is not important. Instead, the depth to the bedrock and the quality of bedrock core specimens must be studied in each bore hole. The cost savings by the spread footing option may be insignificant, because its lower subsurface exploration cost in the field will most likely be offset by its higher cost for laboratory testing. If additional Shelby tube samples and consolidation tests are required for clayey soils, the cost of subsurface exploration and laboratory work may be more expensive than for pile foundations.

REFERENCES

AASHTO. (2004). "LRFD Bridge Design Specifications". Sections 10.4 (Soil & Rock Properties), 10.5 (Limit States & Resistance Factors), and 10.6 (Spread Footings).

Alpan, I. (1964). "Estimating the Settlement of Foundations on Sands." Civil Engineering and Public Works Review, Vol. 59, No. 70, pp. 1,415-1,418.

Amar, S., Baguelin, F., and Canepa, Y. (1984). "Etude Experimentale Du Comportement Des Foundations Superficielles." Annales del l'ITBTP, 427 Series Soils et Foundations, 189, Paris.

American Society of Civil Engineers (1994). *Settlement Analysis*. Technical Engineering and Design Guides as Adopted from the U. S. Army Corps of Engineers, New York, NY.

Anagnostopoulos, A. G., Papadopoulos, B. P., Kavvadas, M. J. (1991). "SPT and Compressibility of Cohesionless Soils." Proceedings of the 2nd European Symposium on Penetration Testing, Amsterdam.

Baus, R. L. (1992). "Spread Footing Performance Evaluation in South Carolina." Report No. F92-102, South Carolina Department of Highways and Public Transportation and the Federal Highway Administration, Columbia, SC.

Bowles, J.E. (1977). *Foundation Analysis and Design*. 2nd edition. McGraw-Hill Book Company, New York, NY,

Bowles, J. E. (1987). "Elastic Foundation Settlement on Sand Deposits." Journal of Geotechnical Engineering, Vol. 113, No. 8, ASCE, pp. 846-860.

Bowles, J. E. (1988). *Foundation Analysis and Design*. 4th Edition, McGraw-Hill Book Company, New York, NY, 1004 pp.

Bozozuk, M. (1978). "Bridge Foundations Move." Transportation Research Record (Journal of Transportation Research Board), No. 678, National Research Council, Washington, D.C., pp. 17-21.

Briaud, J. L. (1992). *The Pressuremeter*. A. A. Balkema Publishers, Brookfield, VT.

Briaud, J-L., and Gibbens, R. (1997). "Large Scale Tests and Database of Spread Footings on Sand." Report No. FHWA-RD-97-0680, Federal Highway Administration, McLean, VA, 217 pp.

Briaud, J-L., and Gibbens, R. (1999). "Behavior of Five Large Spread Footings in Sand." Journal of Geotechnical and Geoenvironmental Engineering, Vol. 125, No. 9, ASCE, pp. 787-796.

Briaud, J-L., and Lepert, P. (1990). "WAK Test To Find Spread Footing Stiffness." Journal of Geotechnical Engineering, Vol. 116, No. 3, ASCE, pp. 415-431.

Burland, J. B., and Burbidge, M. C. (1984). "Settlement of Foundation on Sand and Gravel." Proceedings, Institution of Civil Engineers, Part 1, Vol. 78, pp. 1,325-1,381.

Carter, J. P., and Kulhawy, F. H. (1988). "Analysis and Design of Foundations Socketed into Rock." *Report No. EL-5918,* Empire State Electric Engineering Research Corporation and Electric Power Research Institute, New York, NY, p. 158.

Cheney, R. S., and Chassies, R. G. (1982). "Soils and Foundation Workshop Manual." Federal Highway Administration Report, Washington, D.C.

Cheney, R. S., and Chassies, R. G. (2000). "Soils and Foundation Workshop Reference *Manual*." National Highway Institute Publication NHI-00-045, Federal Highway Administration, Washington, D.C.

Christian & Carrier (1978). "Janbu, Bjerrum, and Kjaernsli's Chart Reinterpreted." Canadian Geotechnical Journal. Vol.15.

D'Appolonia, D. J., D'Appolonia, E., and Brissette, R. F. (1968). "Settlement of Spread Footings on Sand." Journal of Soil Mechanics and Foundations Division, Vol. 94, No. SM3, American Society of Civil Engineers, pp. 735-760.

D'Appolonia, D. J., D'Appolonia, E., and Brissette, R. F. (1970). "Settlement of Spread Footings on Sand." Closure.

Das, B. M. (2004). *Principles of Foundation Engineering*. 5th Edition. Brooks/Cole-Thomson Learning, Pacific Grove, CA.

DeBeer, E. (1965). "Bearing Capacity and Settlement of Shallow Foundations on Sand." Proceedings of Symposium on Bearing Capacity and Settlement of Foundations, Duke University, Durham, NC, pp. 315-335.

Department of the Navy. (1982). "Soil Mechanics." Design Manual 7.1. NAVFAC DM-7.1. Naval Facilities Engineering Command, Alexandria, VA, p.348.

DiMillio, A. F. (1982). "Performance of Highway Bridge Abutment Supported By Spread Footings on Compacted Fill." Report No. FHWA/RD-81/184, FHWA Staff

Study, Federal Highway Administration, U.S. Department of Transportation, Washington, D.C.

Duncan, J. M., and Buchignani, A. L. (1976). "An Engineering Manual for Settlement Studies." University of California, Berkeley, CA, 94 pp.

Duncan, J. M. (1993). "Limitations of Conventional Analysis of Consolidation Settlement." Journal of Geotechnical Engineering. Vol. 119. No. 9, ASCE, pp.1333-1359.

Dunn, I. S., Anderson, L. R., and Kiefer, F. W. (1980). *Fundamentals of Geotechnical Analysis*. John Wiley & Sons, New York, 414 pp.

EPRI. (1983). "Transmission Line Structure Foundations for Uplift-Compression Loading." *Report No. EL-2870*. Electric Power Research Institute, Palo Alto, CA.

Gere, J. M. & Timoshenko, S. P. (1991). *Mechanics of Materials*. 4th Edition. Chapman & Hall. London, U.K.

Gifford, D. G., Kraemer, S. R., Wheeler, J. R., and McKown, A. F. (1987). "Spread Footings for Highway Bridges." Report No. FHWA/RD-86/185, Federal Highway Administration, U.S. Department of Transportation, Washington, D.C., 229 pp.

Grover, R. A. (1978). "Movements of Bridge Abutments and Settlement of Approach Pavements in Ohio." Transportation Research Record (Journal of Transportation Research Board), No. 678, National Research Council, Washington, D.C., pp. 12-17.

Hearn, G. (1995). "Faulted Pavements at Bridge Abutment." Colorado Transportation Institute Synthesis, Dept. of Civil Engineering, University of Colorado, Boulder, CO.

Hoek, E., and Brown, E.T. (1988). "The Hoek-Brown Failure Criterion – A 1988 Update." Proceedings, 15th Canadian Rock Mechanics Symposium, Toronto.

Hough, B. K. (1959). "Compressibility as the Basis for Soil Bearing Value." Journal of Soil Mechanics and Foundations Division, Vol. 85, No. SM4, ASCE, pp. 11-39.

Johnson, S. M, & Kavanagh, T. C. (1968). *The Design of Foundations for Buildings*. McGraw-Hill Book Co., New York, NY.

Keene, P. (1978). "Tolerable Movements of Bridge Foundations." Transportation Research Record (Journal of Transportation Research Board), No. 678, National Research Council, Washington, D.C., pp. 1-6.

Kulhawy, F.H., and R.E. Goodman. (1987). “Foundations in Rock.” Chapter 55, Ground Engineering Reference Manual. F.G. Bell, ed. Butterworths Publishing Co., London.

Lee, J., and Salgado, R. (2002). “Estimation of Footing Settlement in Sand.” International Journal of Geomechanics, Vol. 2, No. 1, pp. 1-28.

Maier, H. R., and Dandy, G. C. (2000). “Applications of Artificial Neural Networks to Forcasting of Surface Water Quality Variables: Issues, Applications, and Challenges.” Artificial Neural Networks in Hydrology. R. S. Govindaraju and A. R. Rao, eds., Kluwer, Dordrecht, The Netherlands, 287-309.

Menard, L., and Rousseau, J. (1962). “L’evaluation des tassements – tendances nouvelles.” Sols-Soils, Vol. 1, No 1, pp. 13-28 (in French).

Meyerhof, G. G. (1953). “The Bearing Capacity of Foundations Under Eccentric and Inclined Loads.” Proceedings 3rd International Conference on Soil Mechanics and Foundation Engineering, Switzerland, pp. 440-445.

Meyerhof, G. G. (1965). “Shallow Foundations.” Journal of Soil Mechanics and Foundations Division, Vol. 91, No. SM2, ASCE, pp. 21-31.

Moulton, L. K., Ganga Rao, H. V. S., and Halvorson, G. T. (1982). “Tolerable Movement Criteria for Highway Bridges.” Vol. 1. Interim Report. Report No. FHWA/RD-81/162, Federal Highway Administration, Washington, D.C., 117 pp.

Munfakh, G., Arman, A., Collin, J.G., Hung, J.C.-J., and Brouillette, R.P. (2001). “Shallow Foundations Reference Manual,” Publication No. FHWA-NHI-01-023, Federal Highway Administation, Washington, D.C.

Ohio Department of Transportation. District 7 Website. <http://www.dot.state.oh.us/dist7/70%2075%20interchange/>. September 2005.

Oweis, I. S., and Scagnelli, P. (2001). “Bridge foundations for Hightstown Bypass.” Journal of Geotechnical Engineering and Geoenvironmental Engineering, Vol. 127, No. 12, ASCE, pp. 997-1016.

Paice, G. M., Griffiths, D. V., and Fenton, G. A. (1996). “Finite Element Modeling of Settlements on Spatially Random Soil.” Journal of Geotechnical Engineering, Vol. 122, No. 9, ASCE, pp. 777-779.

Peck, R. B., and Bazaraa, A. R. S. (1969). “Discussion of ‘Settlement of Spread Footings from SPT Values.’ by D’Appolonia, D’Appolonia, and Brissette” Journal of Soil Mechanics and Foundation Division, ASCE, Vol 95, No. 3, pp. 905-909.

Peck, R. B., Hanson, W. E., and Thornburn, T. H. (1974). *Foundation Engineering*. 2nd Edition, John Wiley & Sons, Inc., New York, NY, 410 pp.

Picornell, M, and del Monte, E. (1988). "Prediction of Settlements of Cohesive Granular Soils." Shallow Foundation Performance. pp. 55-72.

Prandtl, L. (1921). Uber die eindingungfestigkeit (harte) plasticher baustoff und die festigkeit von schneiden, Zeitschrift fur Angewandte Mathematik und Mechanik, Vol. 1, No. 1, 15-20.

Reissner, H., (1924). "Zum erddruckproblem," Proceedings 1st Intem. Congress of Applied Mechanics," Delft, pp.295-311.

R. S. Means Company, Inc. (2000). *Heavy Construction Cost Data*. 14th Annual Edition, Kingston, MA, pp. 470+.

Robertson, P. K., Campanella, R. G., and Wightman, A. (1983). "SPT-CPT Correlations." Journal of Geotechnical Engineering, Vol. 109, No. 11, ASCE, pp. 1449-1459.

Sargand, S. M., Hazen, G. A., and Masada, T. (1997). "Field and Laboratory Performance Evaluations of Spread Footings for Highway Bridges." Report No. FHWA/OH-98/017, 234+ pp.

Sargand, S. M., Masada, T., and Engle, R. (1999). "Spread Footing Foundation for Highway Bridge Applications." Journal of Geotechnical and Geoenvironmental Engineering, Vol. 125, No. 5, ASCE, pp. 373-382.

Sargand, S. M., Masada, T., and Abdalla, B. (2003). "Evaluation of Cone Penetration Test-Based Settlement Prediction Methods for Shallow Foundations on Cohesionless Soils at Highway Bridge Construction Sites." Journal of Geotechnical and Geoenvironmental Engineering, Vol. 129, No. 10, ASCE, pp. 900-908.

Schmertmann, J. H. (1970). "Static Cone To Compute Static Settlement Over Sand." Journal of Soil Mechanics and Foundations Division, Vol. 96, No. SM3, ASCE, pp. 1,011-1,043.

Schmertmann, J. H. (1986). "Dilatometer To Compute Static Settlement of Spread Footings on Sand." Proceedings of In-Situ 1986, Specialty Conference on Use of In-Situ Tests and Geotechnical Engineering, ASCE, pp. 303-321.

Schmertmann, J. H., Hartman, J. P., Brown, P. B. (1978). "Improved Strain Influence Factor Diagrams." Journal of Geotechnical Engineering, Vol. 104, No. 8, ASCE, pp. 1,131-1,135.

Schultze, E., and Sherif, G. (1973). "Prediction of Settlements from Evaluated Settlement Observations for Sand." Proceedings of the 8th International Conference on Soil Mechanics and Foundation Engineering,, Vol. 1, Moscow, pp. 225-230.

Shahin, M. A., Maier, H. R., and Jaksa. M. B. (2002). "Predicting Settlement of Shallow Foundations Using Neural Network." Journal of Geotechnical and Geoenvironmental Engineering, Vol. 128, No. 9, ASCE, pp. 785-793.

Shields, D. H., Deschenes, J.H., Scott, J. D., and Bauer, G. E. (1980). "Advantages of Founding Bridge Abutments on Approach Fills." Transportation Research Record (Journal of Transportation Research Board), No. 749. pp.39-42.

Tabsh, S. W., and Al-Shawa, A. R. (2005). "Effect of Spread Footing Flexibility on Structural Respoinse." Practice Periodical on Structural Design and Construction, ASCE, pp. 109-114.

Taylor, P. W. (1967). "Design of Spread Footings for Earthquake Loadings." Proceedings of the 5th Australia-New Zealand Conference on Soil Mechanics and Foundation Engineering, pp. 221-229.

Terzaghi, K., and Peck, R. B. (1967). *Soil Mechanics in Engineering Practice*. John Wiley & Sons, Inc., New York, NY.

Terzaghi, K., Peck, R.B., and Mesri, G. (1996). *Soil Mechanics in Engineering Practice*, John Wiley and Sons, inc., New York, NY, pp.549.

Tettinek, W., and Matl, F. (1953). "A Contribution to Calculating the Inclination of Eccentrically Loaded Foundations." Proceedings of the 3rd International Conference on Soil Mechanics and Foundation Engineering, Vol. 1, pp. 461-465.

Vesic, A. S. (1973). "Analysis of Ultimate Loads of Shallow Foundations." Journal of Soil Mechanics and Foundation, Vol. 99, No. SM-1, ASCE, pp. 45-73.

Vesic, A.S. (1975). "Bearing Capacity of Shallow Foundations." Chapter 3, *Foundation Engineering Handbook*. H. Winterkorn, and H.Y. Feng, eds. Van Nostrand Reinhold Co., New York, NY, pp. 121-147.

Walkinshaw, J. L. (1978). "Survey of Bridge Movements in the Western United States." Transportation Research Record (Journal of Transportation Research Board), No. 678, National Research Council, Washington, D.C., pp. 6-11.

APPENDIX: MOT-70/75 ANALYSIS

A.1 FOOTING RIGIDITY CALCULATIONS

At the MOT-70/75 site, Pier 18 was designed and built with the following characteristic dimensions:

Overall Footing Length (L) = 57.4 ft = 689 inches

Overall Footing Width (B) = 21 ft = 252 inches

Wall Width (b) = 3.6 ft = 43.2 inches

Wall Length (ℓ), = 41 ft = 492 inches

Footing Thickness (H) = 4.4 ft = 53 inches

Using the footing width and length stated above, the cross-sectional moment of inertia of the footing (I) is computed: $LH^3/12$ = 407.5 ft^4 = 8,449,162 in^4. The moment of inertia per unit length (I_b) is: $LH^3/12L$ = 7.1 ft^4/ft = 12,267 in^4/in. The elastic modulus (E) of the footing material (ODOT Class C concrete) is assumed to be close to 4 million psi. Also, the elastic modulus (E_s) and Poisson's ratio (υ) of the bearing soil is approximated as 2,000 psi or 144 tsf (Das, 2004) and 0.3, respectively. These input values will lead to:

$$k = \frac{E_s}{B\left(1-\upsilon^2\right)} = \frac{2{,}000}{252(1-0.3^2)} = 8.72$$

$$\beta L = L\left(k/4EI\right)^{1/4} = 689\left[\frac{8.72}{4\left(4E6\right)\left(8{,}449{,}162\right)}\right]^{1/4} = 0.35\,(< 0.60)$$

$$K_r = \frac{EI_b}{E_s B^3} = \frac{4E6(12{,}267)}{2{,}000(252)^3} = 1.5 \;\; (> 0.5)$$

$$K_r' = \frac{Et^3}{k(1-\upsilon^2)(B-b)^2(L-\ell)^2} = \frac{4E6(53)^3}{8.72(1-0.3^2)(252-43.2)^2(689-492)^2} = 44.9\ (> 1.0)$$

Each of the three flexibility criteria considers the footing for Pier 18 at the MOT 70-75 site a rigid structure. This therefore suggests that the pressure beneath the footing can be determined from Equation 4-1b.

At the MOT-70/75 site, Pier 19 was designed and built with the following characteristic dimensions:

Overall Footing Length (L) = 49.2 ft = 590 inches

Overall Footing Width (B) = 24 ft = 288 inches

Wall Width (b) = 3.6 ft = 43.2 inches

Wall Length (ℓ) = 28.5 ft = 342.5 inches

Footing Thickness (H) = 4.4 ft = 53 inches

Using the footing width and length stated above, the cross-sectional moment of inertia of the footing (I) is computed: $LH^3/12$ = 349.3 ft^4 = 7,242,139 in^4. The moment of inertia per unit length (I_b) is: $LH^3/12L$ = 7.1 ft^4/ft = 12,267 in^4/in. The elastic modulus (E) of the footing material (ODOT Class C concrete) is assumed to be close to 4 million psi. Also, the elastic modulus (E_s) and Poisson's ratio (υ) of the bearing soil is approximated as 2,000 psi or 144 tsf (Das, 2004) and 0.3, respectively. These input values will lead to:

$$k = \frac{E_s}{B\left(1-\upsilon^2\right)} = \frac{2{,}000}{288(1-0.3^2)} = 7.63$$

$$L\left(k/4EI\right)^{1/4} = 590\left[\frac{7.63}{4\left(4E6\right)\left(7{,}242{,}139\right)}\right]^{1/4} = 0.30\,(< 0.60)$$

$$K_r = \frac{EI_b}{E_s B^3} = \frac{4E6\left(12{,}267\right)}{2{,}000\left(288\right)^3} = 1.03\ (> 0.5)$$

$$K_r' = \frac{Et^3}{k(1-\upsilon^2)(B-b)^2(L-\ell)^2} = \frac{4E6\left(53\right)^3}{7.63\left(1-0.3^2\right)\left(288-43.2\right)^2\left(590-342.5\right)^2} = 23.4\ (>1.0)$$

Pier 19 at the MOT-70/75 site is considered a rigid structure based on each of the three flexibility criteria calculated above. This therefore suggests that the pressure beneath this footing can also be determined from Equation 4-1b.

A.2 BEARING CAPACITY

The AASHTO LRFD Bridge Design Specifications (2004) methods shown below are described in Section 3.6 of this text. Equations 3-8 and 3-14 are used to determine the bearing capacity of the foundations beneath a bridge. Tables 3.10 through 3.13 give values for coefficients within the equations noted before.

From Table 3.10, values are determined based on the friction angle. Pier 18 has a friction angle between 37º and 42º while Pier 19's friction angle lies between 38º and 43º. Using a value in the middle of both the ranges for simplicity, a friction angle of 40º is chosen.

$N_c = 75.3$; $N_q = 64.2$; $N_\gamma = 109.4$ from Table 3.10

The groundwater table lies about 9.3 ft (2.85 m) above the bottom of the footing for Pier 18. For Pier 19, the groundwater table lies approximately 7.7 ft (2.35 m) below the bottom of the footing. The correction factors for the location of the groundwater table are determined from Table 3.11.

Pier 18: $C_{wa} = C_{wb} = 0.5$ from Table 3.11

Pier 19: $C_{wa} = C_{wb} = 0.5$ from Table 3.11

The value of the shape correction factors for the footings depends on the friction angle. Since both angles are larger than 0º, the same equations in Table 3.12 are used.

Pier 18:

$$s_c = 1 + \left(\frac{21}{57.4}\right)\left(\frac{64.2}{75.3}\right) = 1.31;$$

$$s_q = 1 - 0.4\left(\frac{21}{57.4}\right) = 0.854; \quad \text{from Table 3.12}$$

$$s_\gamma = 1 + \left(\frac{21}{57.4}\tan 40\right) = 1.307$$

Pier 19:

$$s_c = 1 + \left(\frac{24}{49.2}\right)\left(\frac{64.2}{75.3}\right) = 1.42;$$

$$s_q = 1 - 0.4\left(\frac{24}{49.2}\right) = 0.805; \quad \text{from Table 3.12}$$

$$s_\gamma = 1 + \left(\frac{24}{49.2}\tan 40\right) = 1.409$$

The embedment depth correction factors found from Table 3.13 are determined using the friction angle and the depth of embedment to footing width (D_f/B) ratio. Piers 18 and 19 have a friction angle of 40º which falls between two of the friction angles given in the table, so the values for the correction factor is interpolated between the friction angle values. The ratio D_f/B for Pier 18 is 0.45 and for Pier 19, the ratio D_f/B is 0.35. The values from Table 3.13 are graphed and the d_q is determined by extrapolating to the ratios of D_f/B as listed above. Interpolation is done between values found for each angle as shown below.

Pier 18: $D_f/B = 0.45$ → for 37º: $d_q = 1.15$

for 42º: $d_q = 1.10$

Therefore for 40º, $d_q = 1.13$ from Table 3.13

Pier 19: $D_f/B = 0.35$ → for 37º: $d_q = 1.14$

for 42º: $d_q = 1.09$

Therefore for 40º, $d_q = 1.12$ from Table 3.13

After the values for the correction factors and bearing capacity factors are determined, they are input into Equation 3-8 and the nominal bearing resistance is determined. Then Equation 3-14 is employed to establish the factored bearing resistance.

$$q_n = cN_{cm} + \gamma D_f N_{qm} C_{wa} + 0.5\gamma B N_{\gamma m} C_{wb}$$

$$q_R = \phi q_n$$

Pier 18:

$$q_n = 0.066(9.42)(64.2*0.854*1.13*1.0)(0.5) + 0.5(0.066)(21)(109.4*1.307*1.0)(0.5) = 68.8tsf$$

$$q_R = 0.45(68.8) = 31.0tsf$$

Pier 19:

$$q_n = 0.066(8.42)(64.2*0.805*1.12*1.0)(0.5) + 0.5(0.066)(24)(109.4*1.409*1.0)(0.5) = 77.1tsf$$

$$q_R = 0.45(77.1) = 34.7tsf$$

Theoretical bearing pressure calculations performed earlier gave a maximum bearing pressure of 1.543 tsf for Pier 18 and 1.307 tsf for Pier 19. The factor of safety for Pier 18 is about 20 (= 31/1.543). For Pier 19, the factor of safety is approximately 26.5 (= 34.7/1.307).

The bearing capacity is evaluated using the average corrected SPT-N values determined previously and Equation 3-13. The earlier analysis of the SPT-N data resulted in an average value of 38 for Pier 18 and a value of 50 for Pier 19. The factors for groundwater effects remain the same as before.

Pier 18: $$q_n = \frac{38(21)}{10}\left(\frac{0.5(9.42)}{21} + 0.5\right) = 67.1tsf$$

$$q_R = 0.45(67.1) = 30.2tsf$$

Pier 19: $$q_n = \frac{50(24)}{10}\left(\frac{0.5(8.42)}{24} + 0.5\right) = 81.1tsf$$

$$q_R = 0.45(81.1) = 36.5tsf$$

The factor of safety for Pier 18 using the SPT-N values is approximately 20 (= 30.2/1.543) and for Pier 19 is about 28 (=36.5/1.307).

A.3 IMMEDIATE SETTLEMENT

A.3.1 Footing on Weathered Rock

The settlement of the footing can be viewed as the elastic deformations of the weathered rock mass. Section 3.7.3 of this report describes the settlement of the foundation.

$$S_e = q_o(1-\upsilon^2)\frac{B(I_p)}{E_m} \tag{3-23}$$

Inputting the known values of B = 252 inches (Pier 18) and 288 inches (Pier 19) and υ = 0.09 into Equation 3-23, along with I_p values of 1.45 for Pier 18 and 1.30 for Pier 19, the immediate settlement will be expressed as:

Pier 18: $$S_e = \frac{q(252)}{E_m}\left(1-0.09^2\right)(1.45) = 362.4\left(\frac{q}{E_m}\right)$$

Pier 19: $$S_e = \frac{q(288)}{E_m}\left(1-0.09^2\right)(1.30) = 371.4\left(\frac{q}{E_m}\right)$$

Values to be used for the elastic modulus (E_m) are 1 x 10^3 psi (min.), 1.42 x 10^6 psi (ave.), and 5.60 x 10^6 psi (max.). Tables A.1 and A.2 summarize the results of the elastic settlement calculations. By using the minimum Young's modulus value, the theoretical settlements computed are much larger than the actual field settlements, which are seen in Table 6.4. The settlements resulting from the average or maximum Young's modulus values are many times smaller compared to the field settlements.

Table A.1: Elastic Settlements on Weathered Rock (Pier 18)

Stage	Description	q (psi)	S_e (inches) with:		
			$(E_m)_{min}$	$(E_m)_{ave}$	$(E_m)_{max}$
1	Footing Construction	4.78	1.73	0.0012	0.0003
2	Pier Wall Construction	9.24	3.35	0.0024	0.0006
3	Soil Backfill	13.82	5.01	0.0035	0.0009
4	Girder Beam Placement	14.64	5.31	0.0037	0.0009
5	Deck Construction	18.94	6.86	0.0048	0.0012
6	Bridge Open to Traffic	21.43	7.77	0.0055	0.0014

Table A.2: Elastic Settlements on Weathered Rock (Pier 19)

Stage	Description	q (psi)	S_e (inches) with:		
			$(E_m)_{min}$	$(E_m)_{ave}$	$(E_m)_{max}$
1	Footing Construction	4.75	1.76	0.0012	0.0003
2	Pier Wall Construction	7.72	2.87	0.0020	0.0005
3	Soil Backfill	11.38	4.23	0.0030	0.0008
4	Girder Beam Placement	12.03	4.47	0.0031	0.0008
5	Deck Construction	15.61	5.80	0.0041	0.0010
6	Bridge Open to Traffic	18.15	6.74	0.0047	0.0012

A.3.2 Footing on Cohesionless Soil

As explained in Section 3.7.1, the elastic settlement of a footing on cohesionless soil is defined as:

$$S_e = \frac{q_0 \sqrt{A}}{E_s \beta_z}\left(1-\upsilon^2\right) \tag{3-15}$$

The area of the footing for Pier 18 is 1205.4 ft^2 and for Pier 19 is 1180.8 ft^2. Young's modulus of the soil, E_s, ranges from 120 tsf to 200 tsf and the Poisson's ratio, υ, is 0.25. The shape factor, β_z, depends on L/B which equals 2.73 for Pier 18 and 2.05 for Pier 19. With those values the shape factor is found to be 1.14 for Pier 18 and 1.10 for Pier 19. The following equation shows the immediate settlement equation once the factors are put in; however, the Young's modulus is a range so it is left as a variable in the equation.

Pier 18: $$S_e = \frac{q_0\sqrt{1205.4}}{E_s(2.73)}\left(1-.25^2\right) = 11.92\frac{q_0}{E_s}$$

Pier 19: $$S_e = \frac{q_0\sqrt{1180.8}}{E_s(2.05)}\left(1-.25^2\right) = 15.71\frac{q_0}{E_s}$$

Tables A.3 and A.4 summarize the range of results of the calculations of immediate settlement for each construction stage, using the minimum and maximum values of Young's modulus.

Table A.3: Elastic Settlements on Cohesionless Soil (Pier 18)

Stage	Description	q_0 (tsf)	S_e (inches) with:	
			$(E_s)_{min}$ = 120 tsf	$(E_s)_{max}$ = 200 tsf
1	Footing Construction	0.344	0.410 (10.4)	0.246 (6.2)
2	Pier Wall Construction	0.665	0.793 (20.1)	0.476 (12.1)
3	Soil Backfill	0.995	1.186 (30.1)	0.712 (18.1)
4	Placement of Girder Beams	1.054	1.256 (31.9)	0.754 (19.2)
5	Deck Construction	1.364	1.626 (41.3)	0.976 (24.8)
6	Bridge Open to Traffic	1.543	1.839 (46.7)	1.104 (28.0)

Table A.4: Elastic Settlements on Cohesionless Soil (Pier 19)

Stage	Description	q_0 (tsf)	S_e (inches) with:	
			$(E_s)_{min}$ = 120 tsf	$(E_s)_{max}$ = 200 tsf
1	Footing Construction	0.342	0.537 (13.6)	0.322 (8.18)
2	Pier Wall Construction	0.556	0.873 (22.2)	0.524 (13.3)
3	Soil Backfill	0.819	1.287 (32.7)	0.772 (19.6)
4	Placement of Girder Beams	0.866	1.360 (34.5)	0.816 (20.7)
5	Deck Construction	1.124	1.766 (44.9)	1.059 (26.9)
6	Bridge Open to Traffic	1.307	2.053 (52.1)	1.232 (31.3)

The immediate settlement can also be calculated by using the corrected SPT-N values and the equations for Young's modulus in Table 3.16. The Young's Modulus values were previously determined in Section 7.3.1. The results of the immediate settlement calculated from Equation 3-15 are shown in Table A.5 and A.6. The values of E_s determined above for each pier are used to calculate the settlement for each construction stage.

Table A.5: Summary of Elastic Settlements (Pier 18)

Stage	Description	q_0 (tsf)	S_e (inches) with Es (tsf) =:			
			152	266	380	456
1	Footing Construction	0.344	0.3237	0.1850	0.1295	0.1079
2	Pier Wall Construction	0.665	0.6258	0.3576	0.2503	0.2086
3	Soil Backfill	0.995	0.9363	0.5351	0.3745	0.3121
4	Placement of Girder Beams	1.054	0.9919	0.5668	0.3967	0.3306
5	Deck Construction	1.364	1.2836	0.7335	0.5134	0.4279
6	Bridge Open to Traffic	1.543	1.4520	0.8297	0.5808	0.4840

Table A.6: Summary of Elastic Settlements (Pier 19)

Stage	Description	q_0 (tsf)	S_e (inches) with Es (tsf) =:			
			204	357	510	612
1	Footing Construction	0.342	0.3160	0.1806	0.1264	0.1053
2	Pier Wall Construction	0.556	0.5138	0.2936	0.2055	0.1713
3	Soil Backfill	0.819	0.7569	0.4325	0.3027	0.2523
4	Placement of Girder Beams	0.866	0.8003	0.4573	0.3201	0.2668
5	Deck Construction	1.124	1.0387	0.5935	0.4155	0.3462
6	Bridge Open to Traffic	1.307	1.2078	0.6902	0.4831	0.4026

A.3.3 Hough Method

The Hough method was described earlier in Section 3.7.1. The immediate settlement is calculated by:

$$S_e = \sum_{i=1}^{n} \Delta H_i = \sum_{i=1}^{n} \frac{H_c}{C'} \log\left(\frac{\sigma_0^{'} + \Delta\sigma_v}{\sigma_0^{'}}\right) \tag{3-16}$$

Each layer of soil has an initial thickness of 5 ft for both piers. Typical values of the bearing capacity index, C', can be found in Table 7.8. Corrected SPT-N values that fall between the values listed are interpolated. The influence zones for Piers 18 and 19 are 40 ft and 35 ft, respectively, which is the total depth of the boring logs. The layers are listed below with their midpoint depths. For Pier 18, all 8 layers are used. However, Pier 19 will only use 7 layers because the boring log stopped at 35 ft below bottom of the footing.

Layer 1: z = 0 to 5 ft below BOF. Mid-Point Depth = 27.9 ft.

Layer 2: z = 5 to 10 ft below BOF. Mid-Point Depth = 32.9 ft.

Layer 3: z = 10 to 15 ft below BOF. Mid-Point Depth = 37.9 ft.

Layer 4: z = 15 to 20 ft below BOF. Mid-Point Depth = 42.9 ft.

Layer 5: z = 20 to 25 ft below BOF. Mid-Point Depth = 57.9 ft.

Layer 6: z = 25 to 30 ft below BOF. Mid-Point Depth = 62.9 ft.

Layer 7: z = 30 to 35 ft below BOF. Mid-Point Depth = 67.9 ft.

Layer 8: z = 35 to 40 ft below BOF. Mid-Point Depth = 72.9 ft.

Figure 7.4 shows an illustrated view of the layers and influence zone. This table is for the FRA-670-0380 project, but for the two piers just mentioned the illustration will be similar except it will have more layers. The applied pressure beneath the footing is determined by Equation 7-2, which was given by Dunn et al. (1980).

$$\Delta\sigma_v = \frac{qBL}{(B+2x)(L+2x)} = \frac{qBL}{(B+1.154Z)(L+1.154Z)} \tag{7-2}$$

For each layer, the vertical stress at the midpoint of the layer is computed as shown below:

PIER 18:

<u>Layer 1</u>: $H_c = 5$ ft; $\sigma_0' = 132(9.42 + 2.5) = 1{,}573$ psf $= 0.79$ tsf

$$\Delta\sigma_v = \frac{qBL}{(B+2x)(L+2x)} = \frac{q(21*57.4)}{(21+1.154*2.5)(57.4+1.154*2.5)} = 0.837q$$

Layer 2: H_c = 5 ft; σ_0' = 132(9.42 + 7.5) = 2,233 psf = 1.12 tsf

$$\Delta\sigma_v = \frac{qBL}{(B+2x)(L+2x)} = \frac{q(21*57.4)}{(21+1.154*7.5)(57.4+1.154*7.5)} = 0.615q$$

Layer 3: H_c = 5 ft; σ_0' = 132(9.42 + 12.5) = 2,893 psf = 1.44 tsf

$$\Delta\sigma_v = \frac{qBL}{(B+2x)(L+2x)} = \frac{q(21*57.4)}{(21+1.154*12.5)(57.4+1.154*12.5)} = 0.474q$$

Layer 4: H_c = 5 ft; σ_0' = 132(9.42 + 17.5) = 3,553 psf = 1.77 tsf

$$\Delta\sigma_v = \frac{qBL}{(B+2x)(L+2x)} = \frac{q(21*57.4)}{(21+1.154*17.5)(57.4+1.154*17.5)} = 0.377q$$

Layer 5: H_c = 5 ft; σ_0' = 132(9.42 + 22.5) = 4,213 psf = 2.11 tsf

$$\Delta\sigma_v = \frac{qBL}{(B+2x)(L+2x)} = \frac{q(21*57.4)}{(21+1.154*22.5)(57.4+1.154*22.5)} = 0.308q$$

Layer 6: H_c = 5 ft; σ_0' = 132(9.42 + 27.5) = 4,873 psf = 2.44 tsf

$$\Delta\sigma_v = \frac{qBL}{(B+2x)(L+2x)} = \frac{q(21*57.4)}{(21+1.154*27.5)(57.4+1.154*27.5)} = 0.256q$$

Layer 7: H_c = 5 ft; σ_0' = 132(9.42 + 32.5) = 5,533 psf = 2.77 tsf

$$\Delta\sigma_v = \frac{qBL}{(B+2x)(L+2x)} = \frac{q(21*57.4)}{(21+1.154*32.5)(57.4+1.154*32.5)} = 0.217q$$

Layer 8: H_c = 5 ft; σ_0' = 132(9.42 + 37.5) = 6,193 psf = 3.10 tsf

$$\Delta\sigma_v = \frac{qBL}{(B+2x)(L+2x)} = \frac{q(21*57.4)}{(21+1.154*37.5)(57.4+1.154*37.5)} = 0.186q$$

PIER 19:

Layer 1: H_c = 5 ft; σ_0' = 132(8.42 + 2.5) = 1,441 psf = 0.72 tsf

$$\Delta\sigma_v = \frac{qBL}{(B+2x)(L+2x)} = \frac{q(24*49.2)}{(24+1.154*2.5)(49.2+1.154*2.5)} = 0.843q$$

Layer 2: H_c = 5 ft; σ_0' = 132(8.42 + 7.5) = 2,101 psf = 1.05 tsf

$$\Delta\sigma_v = \frac{qBL}{(B+2x)(L+2x)} = \frac{q(24*49.2)}{(24+1.154*7.5)(49.2+1.154*7.5)} = 0.625q$$

Layer 3: H_c = 5 ft; σ_0' = 132(8.42 + 12.5) = 2,761 psf = 1.38 tsf

$$\Delta\sigma_v = \frac{qBL}{(B+2x)(L+2x)} = \frac{q(24*49.2)}{(24+1.154*12.5)(49.2+1.154*12.5)} = 0.483q$$

Layer 4: H_c = 5 ft; σ_0' = 132(8.42 + 17.5) = 3,421 psf = 1.71 tsf

$$\Delta\sigma_v = \frac{qBL}{(B+2x)(L+2x)} = \frac{q(24*49.2)}{(24+1.154*17.5)(49.2+1.154*17.5)} = 0.385q$$

Layer 5: H_c = 5 ft; σ_0' = 132(8.42 + 22.5) = 4,081 psf = 2.04 tsf

$$\Delta\sigma_v = \frac{qBL}{(B+2x)(L+2x)} = \frac{q(24*49.2)}{(24+1.154*22.5)(49.2+1.154*22.5)} = 0.314q$$

Layer 6: H_c = 5 ft; σ_0' = 132(8.42 + 27.5) = 4,741 psf = 2.37 tsf

$$\Delta\sigma_v = \frac{qBL}{(B+2x)(L+2x)} = \frac{q(24*49.2)}{(24+1.154*27.5)(49.2+1.154*27.5)} = 0.262q$$

Layer 7: H_c = 5 ft; σ_0' = 132(8.42 + 32.5) = 5,401 psf = 2.70 tsf

$$\Delta\sigma_v = \frac{qBL}{(B+2x)(L+2x)} = \frac{q(24*49.2)}{(24+1.154*32.5)(49.2+1.154*32.5)} = 0.221q$$

Based on the SPT-N analysis data computed earlier, Pier 18 has an average SPT-N value of 38 and pier 19 of 50. The following are possibilities for C' for each pier.

Pier 18:

C′ = 126	for Well graded silty SAND & GRAVEL
C′ = 109	for Clean well-graded fine to coarse SAND
C' = 93	for Well graded fine to medium silty SAND
C' = 64	for Inorganic SOIL

Pier 19:

C′ = 168	for Well graded silty SAND & GRAVEL
C′ = 141	for Clean well-graded fine to coarse SAND
C' = 118	for Well graded fine to medium silty SAND
C' = 83	for Inorganic SOIL

Tables A.7 and A.8 show results of the settlement calculations using C' = 109 for Pier 18 and 141 for Pier 19. Tables A.9 and A.10 use the sum of the layer's settlements for each stage and are changed into units of inches. Also, the settlement for the other three C' values are shown.

$$S_e = \sum_{i=1}^{n} \Delta H_i = \sum_{i=1}^{n} \frac{H_c}{C'} \log\left(\frac{\sigma_0^{'} + \Delta\sigma_v}{\sigma_0^{'}}\right)$$

Table A.7: Settlement Calculations by Hough Method – Pier 18 (with C′ = 109)

(a) Construction Stage 1 (q = 0.344 tsf)

Layer	H_c (ft)	C′	σ_0' (tsf)	$\Delta\sigma_v$ (tsf)	S_e (in)
1	5	109	0.79	0.288	0.0743
2	5	109	1.12	0.212	0.0414
3	5	109	1.44	0.163	0.0256
4	5	109	1.77	0.130	0.0169
5	5	109	2.11	0.106	0.0117
6	5	109	2.44	0.088	0.0085
7	5	109	2.77	0.075	0.0064
8	5	109	3.10	0.064	0.0049

Σ = 0.1896

(b) Construction Stage 2 (q = 0.665 tsf)

Layer	H_c (ft)	C′	σ_0' (tsf)	$\Delta\sigma_v$ (tsf)	S_e (in)
1	5	109	0.79	0.557	0.1275
2	5	109	1.12	0.409	0.0744
3	5	109	1.44	0.315	0.0473
4	5	109	1.77	0.251	0.0317
5	5	109	2.11	0.205	0.0221
6	5	109	2.44	0.170	0.0161
7	5	109	2.77	0.144	0.0121
8	5	109	3.10	0.124	0.0094

Σ = 0.3407

(c) Construction Stage 3 (q = 0.995 tsf)

Layer	H_c (ft)	C′	σ_0' (tsf)	$\Delta\sigma_v$ (tsf)	S_e (in)
1	5	109	0.79	0.833	0.1721
2	5	109	1.12	0.612	0.1042
3	5	109	1.44	0.472	0.0677
4	5	109	1.77	0.375	0.0460
5	5	109	2.11	0.306	0.0324
6	5	109	2.44	0.255	0.0237
7	5	109	2.77	0.216	0.0179
8	5	109	3.10	0.185	0.0139

Σ = 0.4779

(d) Construction Stage 4 (q = 1.054 tsf)

Layer	H_c (ft)	C′	σ_0' (tsf)	$\Delta\sigma_v$ (tsf)	S_e (in)
1	5	109	0.79	0.882	0.1793
2	5	109	1.12	0.648	0.1092
3	5	109	1.44	0.500	0.0712
4	5	109	1.77	0.397	0.0484
5	5	109	2.11	0.325	0.0342
6	5	109	2.44	0.270	0.0251
7	5	109	2.77	0.229	0.0190
8	5	109	3.10	0.196	0.0147

Σ = 0.2571

Table A.7 (cont'd)**:**

(e) Construction Stage 5 (q = 1.364 tsf)

Layer	H_c (ft)	C'	σ_0' (tsf)	$\Delta\sigma_v$ (tsf)	S_e (in)
1	5	109	0.79	1.142	0.2137
2	5	109	1.12	0.839	0.1336
3	5	109	1.44	0.647	0.0887
4	5	109	1.77	0.514	0.0610
5	5	109	2.11	0.420	0.0434
6	5	109	2.44	0.349	0.0320
7	5	109	2.77	0.296	0.0243
8	5	109	3.10	0.254	0.0188

Σ = 0.6155

(f) Construction Stage 6 (q = 1.543 tsf)

Layer	H_c (ft)	C'	σ_0' (tsf)	$\Delta\sigma_v$ (tsf)	S_e (in)
1	5	109	0.79	1.291	0.2316
2	5	109	1.12	0.949	0.1467
3	5	109	1.44	0.731	0.0982
4	5	109	1.77	0.582	0.0679
5	5	109	2.11	0.475	0.0486
6	5	109	2.44	0.395	0.0359
7	5	109	2.77	0.335	0.0273
8	5	109	3.10	0.287	0.0212

Σ = 0.6773

Table A.8: Settlement Calculations by Hough Method – Pier 19 (with C' = 141)

(a) Construction Stage 1 (q = 0.342 tsf)

Layer	H_c (ft)	C'	σ_0' (tsf)	$\Delta\sigma_v$ (tsf)	S_e (in)
1	5	141	0.72	0.288	0.0622
2	5	141	1.05	0.214	0.0342
3	5	141	1.38	0.165	0.0209
4	5	141	1.71	0.132	0.0137
5	5	141	2.04	0.107	0.0095
6	5	141	2.37	0.090	0.0069
7	5	141	2.70	0.076	0.0051

Σ = 0.1526

Table A.8 (cont'd)**:**

(b) Construction Stage 2 ($q = 0.556$ tsf)

Layer	H_c (ft)	C'	σ_0' (tsf)	$\Delta\sigma_v$ (tsf)	S_e (in)
1	5	141	0.72	0.469	0.0927
2	5	141	1.05	0.348	0.0528
3	5	141	1.38	0.269	0.0329
4	5	141	1.71	0.214	0.0218
5	5	141	2.04	0.175	0.0152
6	5	141	2.37	0.146	0.0110
7	5	141	2.70	0.123	0.0082

$\Sigma = 0.2346$

(c) Construction Stage 3 ($q = 0.819$ tsf)

Layer	H_c (ft)	C'	σ_0' (tsf)	$\Delta\sigma_v$ (tsf)	S_e (in)
1	5	141	0.72	0.690	0.1243
2	5	141	1.05	0.512	0.0734
3	5	141	1.38	0.396	0.0466
4	5	141	1.71	0.315	0.0313
5	5	141	2.04	0.257	0.0219
6	5	141	2.37	0.215	0.0160
7	5	141	2.70	0.181	0.0120

$\Sigma = 0.3254$

(d) Construction Stage 4 ($q = 0.866$ tsf)

Layer	H_c (ft)	C'	σ_0' (tsf)	$\Delta\sigma_v$ (tsf)	S_e (in)
1	5	141	0.72	0.730	0.1294
2	5	141	1.05	0.541	0.0768
3	5	141	1.38	0.418	0.0489
4	5	141	1.71	0.333	0.0329
5	5	141	2.04	0.272	0.0231
6	5	141	2.37	0.227	0.0169
7	5	141	2.70	0.191	0.0127

$\Sigma = 0.3407$

(e) Construction Stage 5 ($q = 1.124$ tsf)

Layer	H_c (ft)	C'	σ_0' (tsf)	$\Delta\sigma_v$ (tsf)	S_e (in)
1	5	141	0.72	0.948	0.1552
2	5	141	1.05	0.703	0.0947
3	5	141	1.38	0.543	0.0613
4	5	141	1.71	0.433	0.0417
5	5	141	2.04	0.353	0.0295
6	5	141	2.37	0.294	0.0216
7	5	141	2.70	0.248	0.0163

$\Sigma = 0.4203$

Table A.8 (cont'd)**:**

(f) Construction Stage 6 ($q = 1.307$ tsf)

Layer	H_c (ft)	C'	σ_0' (tsf)	$\Delta\sigma_v$ (tsf)	S_e (in)
1	5	141	0.72	1.102	0.1716
2	5	141	1.05	0.817	0.1064
3	5	141	1.38	0.631	0.0696
4	5	141	1.71	0.503	0.0477
5	5	141	2.04	0.410	0.0339
6	5	141	2.37	0.342	0.0249
7	5	141	2.70	0.289	0.0188

$\Sigma = 0.4728$

Table A.9: Summary of Settlements Predicted by Hough Method – Pier 18

Construction Stage No.	S_e (inches) with C' Value of :			
	126	109	93	64
1	0.1640	0.1896	0.2223	0.3230
2	0.2947	0.3407	0.3993	0.5802
3	0.4135	0.4779	0.5602	0.8140
4	0.4334	0.5010	0.5871	0.8532
5	0.5324	0.6155	0.7214	1.0482
6	0.5859	0.6773	0.7938	1.1536

Table A.10: Summary of Settlements Predicted by Hough Method – Pier 19

Construction Stage No.	S_e (inches) with C' Value of :			
	168	141	118	83
1	0.1312	0.1564	0.1868	0.2656
2	0.2021	0.2408	0.2877	0.4090
3	0.2808	0.3345	0.3997	0.5683
4	0.2940	0.3503	0.4186	0.5951
5	0.3631	0.4326	0.5169	0.7349
6	0.4088	0.4871	0.5820	0.8274

A.3.4 Alpan Method

The Alpan method was described in Section 4.4.1 in Chapter 4. The settlement equation is shown below:

$$S_e = m'\left(\frac{2B}{1+B}\right)^2 \frac{\alpha_0}{12} q \tag{4-5}$$

For the project MOT-70/75, Pier 18 had an SPT-N blow count value of 22 at the bottom of the footing and Pier 19 also had a value of 22. The overburden pressure for Pier 18 is 0.332 tsf (31.8 kPa) and for Pier 19 is 0.556 tsf (53.2 kPa). Based on those values and Figures 4-2 and 4-3, D_r to be approximately 90% adjusting the SPT-N count to 56 and α_o is determined to be 0.050 for Pier 18. Pier 19 results in a value of 82% for D_r giving a value for the SPT-N of 45 and 0.060 for α_o. For Pier 18, with L = 57.4 ft and B = 21 ft, the shape factor, m', is calculated to be 1.480. Pier 19 has L = 49.2 ft and B = 24 ft, so m' is determined to be 1.323. The settlement equations are shown below for each of the piers.

Pier 18: $$S_e = m'\left(\frac{2B}{1+B}\right)^2 \frac{\alpha_0}{12} q = (1.48)\left(\frac{2*21}{1+21}\right)^2 \frac{0.05}{12} q = 0.0225q$$

Pier 19: $$S_e = m'\left(\frac{2B}{1+B}\right)^2 \frac{\alpha_0}{12} q = (1.323)\left(\frac{2*24}{1+24}\right)^2 \frac{0.06}{12} q = 0.0243q$$

Tables A.11 and A.12 show the final results for the settlement prediction calculated for each construction stage.

Table A.11: Settlement Predicted by Alpan Method (Pier 18)

Construction Stage	Description	q (tsf)	Settlement (inches)
1	Footing Construction	0.344	0.186 (4.7 mm)
2	Pier Wall Construction	0.665	0.359 (9.1 mm)
3	Soil Backfill	0.995	0.537 (13.6 mm)
4	Placement of Girder Beams	1.054	0.587 (14.4 mm)
5	Deck Construction	1.364	0.736 (18.7 mm)
6	Bridge Open to Traffic	1.543	0.832 (21.1 mm)

Table A.12: Settlement Predicted by Alpan Method (Pier 19)

Construction Stage	Description	q (tsf)	Settlement (inches)
1	Footing Construction	0.342	0.100 (2.5 mm)
2	Pier Wall Construction	0.556	0.163 (4.1 mm)
3	Soil Backfill	0.819	0.240 (6.1 mm)
4	Placement of Girder Beams	0.866	0.253 (6.4 mm)
5	Deck Construction	1.124	0.329 (8.4 mm)
6	Bridge Open to Traffic	1.307	0.383 (9.7 mm)

A.3.5 Anagnostropoulos Method

This method is described in detail in Section 4.4.2 and is quite simple since the variables in the equation are determined directly from the data collected. The equation for settlement is given as:

$$S_e = \frac{2.37 q^{0.87} B^{0.7}}{N^{1.2}} \tag{4-7}$$

The N value is the average uncorrected SPT-N blow counts within the depth of B below the footing. For Pier 18, B is a depth of 21 ft so the SPT-N values from 0.0 to 20 ft (5 ft intervals) below the footing are averaged to be 33. Pier 19 has a B = 24 ft so from

0.0 to 25ft the SPT-N values are averaged to be 67. The immediate settlement equation (Equation 4-6) gives the following equation for each pier.

Pier 18: $$S_e = \frac{2.37q^{0.87}B^{0.7}}{N^{1.2}} = \frac{2.37q^{0.87}(6.4)^{0.7}}{33^{1.2}} = 0.1309q^{0.87}$$

Pier 19: $$S_e = \frac{2.37q^{0.87}B^{0.7}}{N^{1.2}} = \frac{2.37q^{0.87}(7.3)^{0.7}}{67^{1.2}} = 0.0613q^{0.87}$$

Tables A.13 and A.14 show the results for the settlement prediction for each construction stage.

Table A.13: Settlement Predicted by Anagnostropoulos Method (Pier 18)

Construction Stage	Description	q (kPa)	Settlement (inches)
1	Footing Construction	32.94	0.108 (2.7 mm)
2	Pier Wall Construction	63.68	0.191 (4.9 mm)
3	Soil Backfill	95.28	0.272 (6.9 mm)
4	Placement of Girder Beams	100.93	0.286 (7.3 mm)
5	Deck Construction	130.62	0.357 (9.1 mm)
6	Bridge Open to Traffic	147.76	0.398 (10.1 mm)

Table A.14: Settlement Predicted by Anagnostropoulos Method (Pier 19)

Construction Stage	Description	q (kPa)	Settlement (inches)
1	Footing Construction	32.75	0.050 (1.3 mm)
2	Pier Wall Construction	53.24	0.077 (2.0 mm)
3	Soil Backfill	78.43	0.108 (2.7 mm)
4	Placement of Girder Beams	82.93	0.113 (2.9 mm)
5	Deck Construction	107.64	0.142 (3.6 mm)
6	Bridge Open to Traffic	125.16	0.162 (4.1 mm)

A.3.6 Bowles Method

The Bowles method is described in Section 4.4.3. The immediate settlement is determined from Equation 4-8 with the use of other equations and tables in Chapter 4.

$$S_e = \frac{\left(1-\upsilon^2\right)qB'}{E_s} I_s I_f \tag{4-8}$$

Data collected from Pier 18 and Pier 19 is used in each of the equations and tables. The Poisson's ratio, υ, used for both piers is 0.3. To determine the modulus of elasticity, E_s, the SPT-N values used in Equation 4-8 are to a depth of 2B. For Pier 18, the influence zone used is approximately 40 ft below the bottom of the footing, and for Pier 19, the zone should be about 50 ft below however the soil boring near Pier 19 only goes to 35 ft below the bottom of the footing so 35 ft is used. The uncorrected SPT-N value for the depth of influence for Pier 18 is 52, resulting in a modulus of elasticity equal to 670 tsf. Pier 19 has an uncorrected SPT-N value of 75 which determines E_s to be 900 tsf. To determine A_0, A_1, and A_2 values for m and n were determined. Pier 18 has a value of m = 2.73 and n = 3.81, resulting in A_0 = 0.4008, A_1 = 1.083, and A_2 = 0.150. F_1 and F_2 are then determined to be 0.472 and 0.090, but could also be interpolated from Table 4.1. I_s is calculated from Equation 4-10 to be 0.524. For Pier 19, the value of m = 2.05 and n = 2.92, which in turn gives A_0 = 0.3963, A_1 = 0.8421 and A_2 = 0.1898. F_1 = 0.394 and F_2 = 0.087. Equation 4-10 gives I_s to be 0.444. For both piers, I_f is set at 1.0 and the resulting equations for the immediate settlement are determined to be:

Pier 18: $$S_e = \frac{(1-\nu^2)qB'}{E_s} I_s I_f = \frac{(1-0.3^2)q(10.5)}{670}(0.524)(1.0) = 0.0075q$$

Pier 19: $$S_e = \frac{(1-\nu^2)qB'}{E_s} I_s I_f = \frac{(1-0.3^2)q(12)}{900}(0.444)(1.0) = 0.0054q$$

Tables A.15 and A.16 have the values for the settlement predicted by this method for each construction stage.

Table A.15: Settlement Predictions by Bowles Method (Pier 18)

Construction Stage	Description	q (ksf)	Settlement (inches)
1	Footing Construction	0.688	0.062 (1.6 mm)
2	Pier Wall Construction	1.33	0.119 (3.0 mm)
3	Soil Backfill	1.99	0.178 (4.5 mm)
4	Placement of Girder Beams	2.108	0.189 (4.8 mm)
5	Deck Construction	2.728	0.244 (6.2 mm)
6	Bridge Open to Traffic	3.086	0.277 (7.0 mm)

Table A.16: Settlement Predictions by Bowles Method (Pier 19)

Construction Stage	Description	q (ksf)	Settlement (inches)
1	Footing Construction	0.684	0.044 (1.1 mm)
2	Pier Wall Construction	1.112	0.086 (2.2 mm)
3	Soil Backfill	1.638	0.129 (3.3 mm)
4	Placement of Girder Beams	1.732	0.136 (3.5 mm)
5	Deck Construction	2.248	0.176 (4.5 mm)
6	Bridge Open to Traffic	2.614	0.200 (5.1 mm)

A.3.7 Burland-Burbidge Method

The Burland-Burbidge method was previously described in Section 4.4.4 of this report. For their method, the immediate settlement is determined by:

$$S_e = \alpha_1 \alpha_2 \alpha_3 \left[\frac{1.25(L/B)}{0.25 + (L/B)} \right]^2 Bq' \tag{4-11}$$

The value for α_1 is taken as 0.14 to be conservative. The average SPT-N value corrected only for the hammer efficiency (N_{60a}) is used to determine the α_2 value. For Pier 18, a value of 34 for N_{60a} results from Equation 4-12. Pier 19 has an N_{60a} value of 45. The compressibility influence factor, α_2, which results for Pier 18, is 0.0123 and for Pier 19, is 0.0083. The depth of stress influence, Z', is calculated from Equation 4-14 and for Pier 18 is determined to be 13.73, while for Pier 19 is 15.18. H = Z' is assumed for both piers at MOT-70/75, which gives a value of 1.0 for α_3. The final settlement equations once the values are input are shown below.

Pier 18: $$S_e = 0.14(0.0123)(1.0)\left[\frac{1.25(2.73)}{0.25 + 2.73} \right]^2 (21)q' = 0.0474q'$$

Pier 19: $$S_e = 0.14(0.0083)(1.0)\left[\frac{1.25(2.05)}{0.25 + 2.05} \right]^2 (24)q' = 0.0346q'$$

The final results for the elastic settlement calculation are shown below in Tables A.17 and A.18.

Table A.17: Settlement Calculated by Burland-Burbidge Method (Pier 18)

Construction Stage	Description	q' (tsf)	Settlement (inches)
1	Footing Construction	0.344	0.196 (5.0 mm)
2	Pier Wall Construction	0.665	0.378 (9.6 mm)
3	Soil Backfill	0.995	0.565 (14.4 mm)
4	Placement of Girder Beams	1.054	0.599 (15.2 mm)
5	Deck Construction	1.364	0.775 (19.7 mm)
6	Bridge Open to Traffic	1.543	0.876 (22.3 mm)

Table A.18: Settlement Calculated by Burland-Burbidge Method (Pier 19)

Construction Stage	Description	q (tsf)	Settlement (inches)
1	Footing Construction	0.342	0.142 (3.6 mm)
2	Pier Wall Construction	0.556	0.231 (5.9 mm)
3	Soil Backfill	0.819	0.340 (8.6 mm)
4	Placement of Girder Beams	0.866	0.359 (9.1 mm)
5	Deck Construction	1.124	0.466 (11.8 mm)
6	Bridge Open to Traffic	1.307	0.542 (13.8 mm)

A.3.8 D'Appolonia Method

The D'Appolonia method, previously explained in Section 4.4.5, is a highly graphical method, using mostly figures instead of equations. The one equation used, the immediate settlement, is given as:

$$S_e = \mu_0 \mu_1 \frac{qB}{M} \tag{4-18}$$

The values for μ_0 are determined from the depth of embedment to footing width ratio, which is 0.449 for Pier 18 and 0.368 for Pier 19. With these numbers, Figure 4.4 gives the μ_0 for Pier 18 as 0.94 and for Pier 19 as 0.95. μ_1 is determined with the H/B and L/B ratios in Figure 4.5. For Pier 18, H/B = 1.91 and L/B = 2.73 giving a μ_1 = 0.60. H/B =

1.46 and L/B = 2.05 results in a μ_1 for Pier 19 of 0.55. The uncorrected SPT-N average value (Pier 18 = 52; Pier 19 = 75) is used to determine the modulus of compressibility, M. From Figure 4.6, M is determined to be 600 tsf for Pier 18 and 750 tsf for Pier 19. The final forms of the settlement equation (in feet) are:

Pier 18: $$S_e = \mu_0 \mu_1 \frac{qB}{M} = (0.94)(0.6)\frac{21q}{600} = .0197q$$

Pier 19: $$S_e = \mu_0 \mu_1 \frac{qB}{M} = (0.95)(0.55)\frac{24q}{750} = .0167q$$

The results of the settlement predicted with this method are seen in Tables A.19 and A.20, for each of the piers.

Table A.19: Settlement Calculated by D'Appolonia Method (Pier 18)

Construction Stage	Description	q (tsf)	Settlement (inches)
1	Footing Construction	0.344	0.082 (2.1 mm)
2	Pier Wall Construction	0.665	0.158 (4.0 mm)
3	Soil Backfill	0.995	0.236 (6.0 mm)
4	Placement of Girder Beams	1.054	0.250 (6.3 mm)
5	Deck Construction	1.364	0.323 (8.2 mm)
6	Bridge Open to Traffic	1.543	0.366 (9.3 mm)

Table A.20: Settlement Calculated by D'Appolonia Method (Pier 19)

Construction Stage	Description	q (tsf)	Settlement (inches)
1	Footing Construction	0.342	0.069 (1.7 mm)
2	Pier Wall Construction	0.556	0.112 (2.8 mm)
3	Soil Backfill	0.819	0.164 (4.2 mm)
4	Placement of Girder Beams	0.866	0.174 (4.4 mm)
5	Deck Construction	1.124	0.226 (5.7 mm)
6	Bridge Open to Traffic	1.307	0.262 (6.7 mm)

A.3.9 Department of the Navy Method

Section 4.4.6 described previously the Department of the Navy method. The settlement equation used for this method is:

$$S_e = \frac{4q}{K_{v1}}\left(\frac{B}{B+1}\right)^2 \qquad \text{for } B \leq 20 \text{ ft} \qquad (4\text{-}19)$$

For the above equation to work, B should be less than 20 ft, however if the footing width is larger than 40 ft the equation should be divided by 2. Both Piers 18 and 19 have 20 ft < B < 40 ft, therefore the results from the two equations must be interpolated between. The relative density, D_R, is found in Figure 4.6 for Pier 18 using an SPT-N value of 28 and a vertical effective stress of 1.09 tsf. The result for the D_R is 95%. For Pier 19, an SPT-N value of 51 and σ_v' = 1.49 tsf, gives a result for the relative density = 100%. From Figure 4.7, the $K_{\upsilon 1}$ value for Pier 18 is 275 tcf and for Pier 19 is 290 tcf. The immediate settlement falls between the results below:

Pier 18:
$$S_e = \frac{4q}{K_{v1}}\left(\frac{B}{B+1}\right)^2 = \frac{4q}{275}\left(\frac{21}{22}\right)^2 = 0.0133q \qquad \text{for B} \leq 20 \text{ ft}$$

$$S_e = \frac{2q}{K_{v1}}\left(\frac{B}{B+1}\right)^2 = \frac{2q}{275}\left(\frac{21}{22}\right)^2 = 0.0066q \qquad \text{for B} > 40 \text{ ft}$$

Pier 19: $$S_e = \frac{4q}{K_{v1}}\left(\frac{B}{B+1}\right)^2 = \frac{4q}{290}\left(\frac{24}{25}\right)^2 = 0.0127q \qquad \text{for B} \le 20 \text{ ft}$$

$$S_e = \frac{2q}{K_{v1}}\left(\frac{B}{B+1}\right)^2 = \frac{2q}{290}\left(\frac{21}{22}\right)^2 = 0.0064q \qquad \text{for B} > 40 \text{ ft}$$

The Pier 18 settlement equation is 0.0130q and for Pier 19 is 0.0114q. Table A.21 and A.22 give the final results from the settlement equations for each construction stage.

Table A.21: Settlement Calculated by Department of the Navy Method (Pier 18)

Construction Stage	Description	q (tsf)	Settlement (inches)
1	Footing Construction	0.344	0.053 (1.4 mm)
2	Pier Wall Construction	0.665	0.103 (2.6 mm)
3	Soil Backfill	0.995	0.154 (3.9 mm)
4	Placement of Girder Beams	1.054	0.163 (4.2 mm)
5	Deck Construction	1.364	0.212 (5.4 mm)
6	Bridge Open to Traffic	1.543	0.239 (6.1 mm)

Table A.22: Settlement Calculated by Department of the Navy Method (Pier 19)

Construction Stage	Description	q (tsf)	Settlement (inches)
1	Footing Construction	0.342	0.047 (1.2 mm)
2	Pier Wall Construction	0.556	0.076 (1.9 mm)
3	Soil Backfill	0.819	0.112 (2.9 mm)
4	Placement of Girder Beams	0.866	0.119 (3.0 mm)
5	Deck Construction	1.124	0.154 (3.9 mm)
6	Bridge Open to Traffic	1.307	0.179 (4.6 mm)

A.3.10 Meyerhof Method

Section 4.4.7 in this report previously described Meyerhof's method. The settlement equation used for this method is:

$$S_e = \left[\frac{12q}{N'}\right]\left(\frac{B}{B+1}\right)^2 \qquad \text{for B > 4 ft} \tag{4-21}$$

The average uncorrected SPT-N value for Pier 18 is 52 which corrected by Equation 4-21 becomes 34. For Pier 19, the uncorrected SPT-N value is 75 and the corrected value is 45. The resulting equations are shown below:

Pier 18: $S_e = \left[\frac{12q}{N'}\right]\left(\frac{B}{B+1}\right)^2 = \left[\frac{12q}{34}\right]\left(\frac{21}{22}\right)^2 = 0.3216q$

Pier 19: $S_e = \left[\frac{12q}{N'}\right]\left(\frac{B}{B+1}\right)^2 = \left[\frac{12q}{45}\right]\left(\frac{24}{25}\right)^2 = 0.2458q$

Tables A.23 and A.24 show the results for the settlement predicted by this method for each construction stage based on the applied load, q.

Table A.23: Settlement Calculated by Meyerhof Method (Pier 18)

Construction Stage	Description	q (tsf)	Settlement (inches)
1	Footing Construction	0.344	0.111 (2.8 mm)
2	Pier Wall Construction	0.665	0.214 (5.4 mm)
3	Soil Backfill	0.995	0.320 (8.1 mm)
4	Placement of Girder Beams	1.054	0.339 (8.6 mm)
5	Deck Construction	1.364	0.439 (11.1 mm)
6	Bridge Open to Traffic	1.543	0.496 (12.6 mm)

Table A.24: Settlement Calculated by Meyerhof Method (Pier 19)

Construction Stage	Description	q (tsf)	Settlement (inches)
1	Footing Construction	0.342	0.084 (2.1 mm)
2	Pier Wall Construction	0.556	0.137 (3.5 mm)
3	Soil Backfill	0.819	0.201 (5.1 mm)
4	Placement of Girder Beams	0.866	0.213 (5.4 mm)
5	Deck Construction	1.124	0.276 (7.0 mm)
6	Bridge Open to Traffic	1.307	0.321 (8.2 mm)

A variation of Meyerhof's method was also described in Section 4.4.7. The equation for immediate settlement is:

$$S_e = C_D\left[\frac{2q}{N'}\right]\left(\frac{2B}{B+1}\right)^2 \qquad \text{for } B > 4 \text{ ft} \qquad (4\text{-}17)$$

Values for the average uncorrected SPT-N are corrected the same as in Meyerhof's first method. For Pier 18, N' = 34 and for Pier 19, N' = 45. The correction factor for embedment is found using Equation 4-23. C_D = 0.888 for Pier 18 and for Pier 19, C_D = 0.912. The resulting settlement equations are as follows:

Pier 18: $$S_e = C_D\left[\frac{2q}{N'}\right]\left(\frac{2B}{B+1}\right)^2 = (0.888)\left[\frac{2q}{34}\right]\left(\frac{42}{22}\right)^2 = 0.1904q$$

Pier 19: $$S_e = C_D\left[\frac{2q}{N'}\right]\left(\frac{2B}{B+1}\right)^2 = (0.912)\left[\frac{2q}{45}\right]\left(\frac{48}{25}\right)^2 = 0.1494q$$

Tables A.25 and A.26 show the results for the settlement predicted by this method for each construction stage based on the applied load, q.

Table A.25: Settlement Calculated by Meyerhof Method 2 (Pier 18)

Construction Stage	Description	q (tsf)	Settlement (inches)
1	Footing Construction	0.344	0.066 (1.7 mm)
2	Pier Wall Construction	0.665	0.127 (3.2 mm)
3	Soil Backfill	0.995	0.189 (4.8 mm)
4	Placement of Girder Beams	1.054	0.201 (5.1 mm)
5	Deck Construction	1.364	0.260 (6.6 mm)
6	Bridge Open to Traffic	1.543	0.294 (7.5 mm)

Table A.26: Settlement Calculated by Meyerhof Method 2 (Pier 19)

Construction Stage	Description	q (tsf)	Settlement (inches)
1	Footing Construction	0.342	0.051 (1.3 mm)
2	Pier Wall Construction	0.556	0.083 (2.1 mm)
3	Soil Backfill	0.819	0.122 (3.1 mm)
4	Placement of Girder Beams	0.866	0.129 (3.3 mm)
5	Deck Construction	1.124	0.168 (4.3 mm)
6	Bridge Open to Traffic	1.307	0.195 (5.0 mm)

A.3.11 Peck-Bazaraa Method

The Peck-Bazaraa method is described in Section 4.4.8 of this report. The equation for immediate settlement is:

$$S_e = C_D C_W \left[\frac{2q}{N_B}\right]\left(\frac{2B}{B+1}\right)^2 \qquad (4\text{-}25)$$

The values for σ_v are σ'_v are determined for each pier footing at a depth of 0.5B beneath the bottom of the footing. C_w for Pier 18 is 0.693/0.365 =1.89 and for Pier 19 is 0.792/0.418 = 1.895. C_D is determined by Equation 4-26 and the resulting equations are shown below.

Pier 18: $$C_D = 1 - 0.4\sqrt{\frac{\gamma D_f}{q}} = 1 - 0.4\sqrt{\frac{0.622}{q}}$$

Pier 19: $$C_D = 1 - 0.4\sqrt{\frac{\gamma D_f}{q}} = 1 - 0.4\sqrt{\frac{0.556}{q}}$$

The corrected SPT-N value is used for this method which is unlike most of the other methods examined. Pier 18 has an average corrected SPT-N value of 38 and Pier 19 has a value of 50. Since both of the piers have a resulting σ'_v < 1.5 ksf, Equation 4-27 is used. N_B is 87.9 for Pier 18 and 108.9 for Pier 19. Substituting the values and equations into the settlement equation results in:

Pier 18: $$S_e = C_D C_W \left[\frac{2q}{N_B}\right]\left(\frac{2B}{B+1}\right)^2 = \left[1 - 0.4\sqrt{\frac{0.621}{q}}\right](0.1573q)$$

Pier 19: $$S_e = C_D C_W \left[\frac{2q}{N_B}\right]\left(\frac{2B}{B+1}\right)^2 = \left[1 - 0.4\sqrt{\frac{0.556}{q}}\right](0.1283q)$$

Tables A.27 and A.28 show the results of the predicted settlement for each pier at MOT-70/75 for this method.

Table A.27: Settlement Calculated by Peck-Bazaraa Method (Pier 18)

Construction Stage	Description	q (tsf)	Settlement (inches)
1	Footing Construction	0.344	0.025 (0.6 mm)
2	Pier Wall Construction	0.665	0.064 (1.6 mm)
3	Soil Backfill	0.995	0.107 (2.7 mm)
4	Placement of Girder Beams	1.054	0.115 (2.9 mm)
5	Deck Construction	1.364	0.157 (4.0 mm)
6	Bridge Open to Traffic	1.543	0.181 (4.6 mm)

Table A.28: Settlement Calculated by Peck-Bazaraa Method (Pier 19)

Construction Stage	Description	q (tsf)	Settlement (inches)
1	Footing Construction	0.342	0.022 (0.6 mm)
2	Pier Wall Construction	0.556	0.043 (1.1 mm)
3	Soil Backfill	0.819	0.070 (1.8 mm)
4	Placement of Girder Beams	0.866	0.076 (1.9 mm)
5	Deck Construction	1.124	0.104 (2.6 mm)
6	Bridge Open to Traffic	1.307	0.124 (3.2 mm)

A.3.12 Peck-Hanson-Thornburn Method

In Section 4.4.9, the Peck-Hanson-Thornburn method was described in detail. The immediate settlement is calculated as:

$$S_e = \frac{q}{0.11 C_w N_1} \qquad \text{(4-30)}$$

C_w is determined from Equation 4-31 using values for D_w, D_f, and B. For Pier 18, D_w is 16.1 ft below the ground surface (BGS), D_f is 9.4 ft BGS, and B is 21 ft, resulting in a C_w value of 0.765. A C_w of 1.00 is calculated for Pier 19 since D_w is 33.1 ft BGS, D_f is 8.4 ft BGS, and B is 24 ft. The equation to be used for N_1 depends on σ'_v and both piers have a result larger than 0.25 tsf. N_1 for Pier 18 is determined to be 13.2 and for Pier 19 to be 26.8.

Pier 18: $$S_e = \frac{q}{0.11 C_w N_1} = \frac{q}{0.11(0.765)(13.2)} = 0.9003q$$

Pier 19: $$S_e = \frac{q}{0.11 C_w N_1} = \frac{q}{0.11(1.00)(26.8)} = 0.3392q$$

The predicted immediate settlements for both piers are given in Tables A.29 and A.30 for each construction stage.

Table A.29: Settlements Predicted by Peck-Hanson-Thornburn Method (Pier 18)

Construction Stage	Description	q′ (tsf)	Settlement – in (mm)
1	Footing Construction	0.344	0.310 (7.9)
2	Pier Wall Construction	0.665	0.599 (15.2)
3	Soil Backfill	0.995	0.896 (22.8)
4	Placement of Girder Beams	1.054	0.949 (24.1)
5	Deck Construction	1.364	1.228 (31.2)
6	Bridge Open to Traffic	1.543	1.389 (35.3)

Table A.30: Settlements Predicted by Peck-Hanson-Thornburn Method (Pier 19)

Construction Stage	Description	q′ (tsf)	Settlement –in (mm)
1	Footing Construction	0.342	0.116 (2.9)
2	Pier Wall Construction	0.556	0.189 (4.8)
3	Soil Backfill	0.819	0.279 (7.1)
4	Placement of Girder Beams	0.866	0.294 (7.5)
5	Deck Construction	1.124	0.381 (9.7
6	Bridge Open to Traffic	1.307	0.443 (11.3)

A.3.13 Schmertmann Method

The Schmertmann method is described previously in Section 4.4.10. The immediate settlement equation is given as:

$$S_e = C_1 C_2 q \sum_{0}^{z_z} \left(\frac{I_z}{E_s} \right) \Delta z \qquad (4\text{-}29)$$

C_1 is determined by Equation 4-30, is the same for both piers, and is based on the applied load. C_2 depends on the time that has elapsed since the start of the construction stage. I_z is determined from Table 4.3 and is based on the footing length to width ratio and the depth below the footing. The specific Iz's for each pier are shown in Figure A.1 and A.2. E_s varies for soil types and the equations used are found in Table 3.16. Δz is the thickness of the layers, which is 5 ft for each layer. The settlement for each construction stage for Pier 18 is given in Tables A.31a to A.31f, and Table A.32 summarizes the settlement. For Pier 19, Tables A.33a to A.33f give the settlement for each stage and then Table A.34 summarizes.

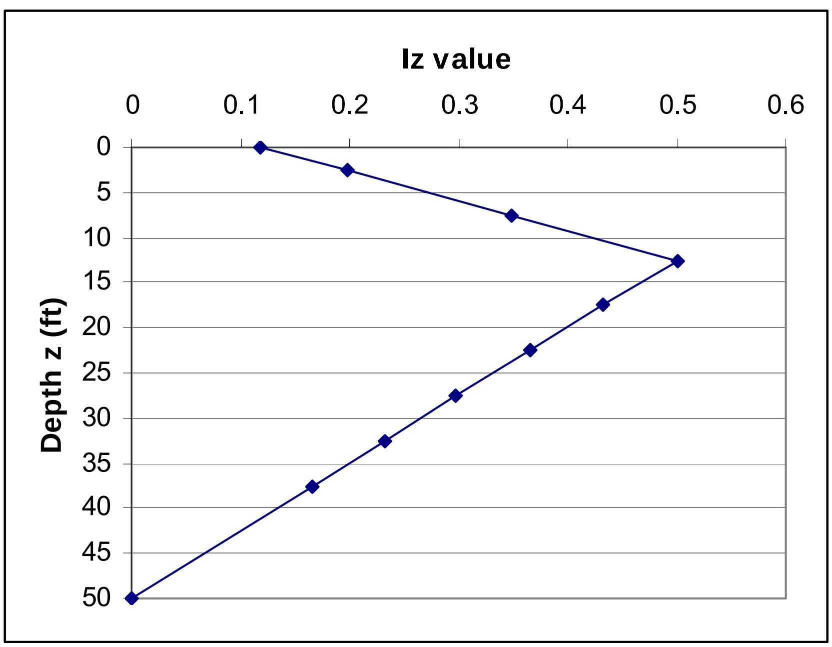

Figure A.1: Variation of Iz with Depth Below Footing (Pier 18)

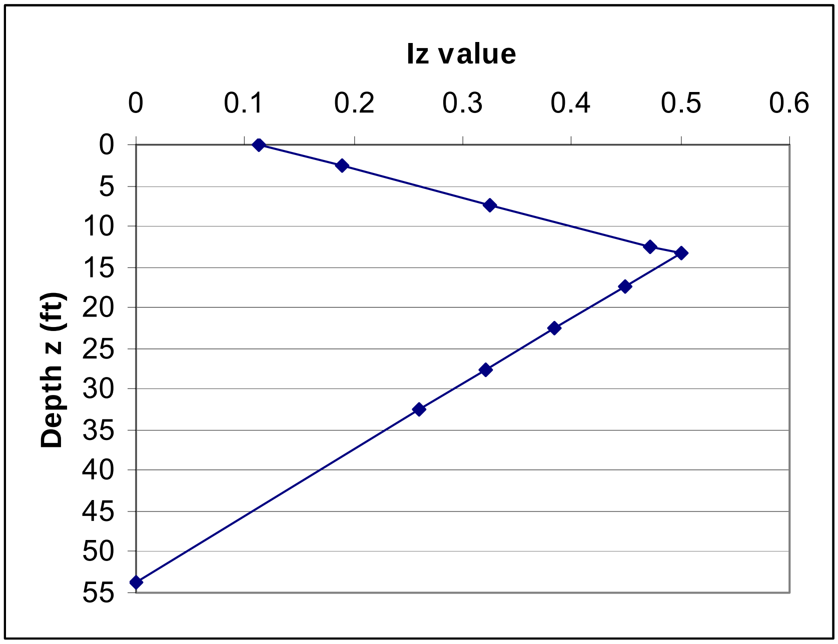

Figure A.2: Variation of Iz with Depth Below Footing (Pier 19)

PIER 18:

Construction Stage 1 (q = 0.344 tsf; t = 15 days = 0.0411 years):

$$C_1 = 1 - 0.5\left(\frac{\gamma D_f}{q}\right) = 1 - 0.5\left(\frac{0.066x9.42}{0.344}\right) = 0.0963$$

$$C_2 = 1 + 0.2\log\left(\frac{t}{0.1}\right) = 1 + 0.2\log(0.0384/0.1) = 0.917$$

$$S_e = C_1C_2q\sum_0^{Z_z}\left(\frac{I_z}{E_s}\right)\Delta z = 0.0411(0.917)q\sum_0^{Z_z}\left(\frac{I_z}{E_s}\right)\Delta z = 0.0377q\sum_0^{Z_z}\left(\frac{I_z}{E_s}\right)\Delta z$$

Table A.31.(a): Stage 1 Settlements Calculated by Schmertmann Method

Layer No.	I_z	Δz (ft)	S_e (inches) with q_c =:			
			2N	3.5N	5N	6N
1	0.198	5	0.0032	0.0019	0.0014	0.0011
2	0.348	5	0.0091	0.0052	0.0037	0.0030
3	0.500	5	0.0107	0.0061	0.0043	0.0036
4	0.432	5	0.0039	0.0022	0.0016	0.0013
5	0.365	5	0.0026	0.0015	0.0011	0.0009
6	0.298	5	0.0030	0.0017	0.0012	0.0010
7	0.233	5	0.0026	0.0015	0.0011	0.0009
8	0.165	5	0.0007	0.0004	0.0003	0.0002
Σ	---	---	0.0361	0.0206	0.0144	0.0120

Construction Stage 2 (q = 0.665 tsf; t = 17 days = 0.0466 years):

$$C_1 = 1 - 0.5\left(\frac{\gamma D_f}{q}\right) = 1 - 0.5\left(\frac{0.066x9.42}{0.665}\right) = 0.5325$$

$$C_2 = 1 + 0.2\log\left(\frac{t}{0.1}\right) = 1 + 0.2\log(0.0466/0.1) = 0.934$$

$$S_e = C_1C_2q\sum_0^{z_z}\left(\frac{I_z}{E_s}\right)\Delta z = 0.5325(0.934)q\sum_0^{z_z}\left(\frac{I_z}{E_s}\right)\Delta z = 0.497q\sum_0^{z_z}\left(\frac{I_z}{E_s}\right)\Delta z$$

Table A.31.(b): Stage 2 Settlements Calculated by Schmertmann Method

Layer No.	I_z	Δz (ft)	S_e (inches) with q_c =:			
			2N	3.5N	5N	6N
1	0.198	5	0.0365	0.0209	0.0146	0.0122
2	0.348	5	0.0987	0.0564	0.0395	0.0329
3	0.500	5	0.1152	0.0658	0.0461	0.0384
4	0.432	5	0.0419	0.0240	0.0168	0.0140
5	0.365	5	0.0286	0.0164	0.0115	0.0095
6	0.298	5	0.0323	0.0185	0.0129	0.0108
7	0.233	5	0.0286	0.0164	0.0115	0.0095
8	0.165	5	0.0080	0.0046	0.0032	0.0027
Σ	---	---	0.3900	0.2228	0.1560	0.1300

<u>Construction Stage 3</u> (q = 0.995 tsf; t = 24 days = 0.0658 years):

$$C_1 = 1 - 0.5\left(\frac{\gamma D_f}{q}\right) = 1 - 0.5\left(\frac{0.066x9.42}{0.995}\right) = 0.6876$$

$$C_2 = 1 + 0.2\log\left(\frac{t}{0.1}\right) = 1 + 0.2\log(0.0658/0.1) = 0.9636$$

$$S_e = C_1 C_2 q \sum_0^{z_z}\left(\frac{I_z}{E_s}\right)\Delta z = 0.6876(0.9636)q\sum_0^{z_z}\left(\frac{I_z}{E_s}\right)\Delta z = 0.6626q\sum_0^{z_z}\left(\frac{I_z}{E_s}\right)\Delta z$$

Table A.31.(c): Stage 3 Settlements Calculated by Schmertmann Method

Layer No.	I_z	Δz (ft)	S_e (inches) with q_c =:			
			2N	3.5N	5N	6N
1	0.198	5	0.0728	0.0416	0.0291	0.0243
2	0.348	5	0.1968	0.1125	0.0787	0.0656
3	0.500	5	0.2297	0.1313	0.0919	0.0766
4	0.432	5	0.0836	0.0478	0.0334	0.0279
5	0.365	5	0.0571	0.0326	0.0228	0.0190
6	0.298	5	0.0644	0.0368	0.0258	0.0215
7	0.233	5	0.0571	0.0326	0.0228	0.0190
8	0.165	5	0.0160	0.0091	0.0064	0.0053
Σ	---	---	0.7775	0.4443	0.3110	0.2592

<u>Construction Stage 4</u> (q = 1.054 tsf; t = 182 days = 0.4986 years):

$$C_1 = 1 - 0.5\left(\frac{\gamma D_f}{q}\right) = 1 - 0.5\left(\frac{0.066x9.42}{1.054}\right) = 0.7051$$

$$C_2 = 1 + 0.2\log\left(\frac{t}{0.1}\right) = 1 + 0.2\log(0.4986/0.1) = 1.1396$$

$$S_e = C_1 C_2 q \sum_0^{z_z}\left(\frac{I_z}{E_s}\right)\Delta z = 0.7051(1.1396)q\sum_0^{z_z}\left(\frac{I_z}{E_s}\right)\Delta z = 0.8035q\sum_0^{z_z}\left(\frac{I_z}{E_s}\right)\Delta z$$

Table A.31.(d): Stage 4 Settlements Calculated by Schmertmann Method

Layer No.	I_z	Δz (ft)	S_e (inches) with q_c =:			
			2N	3.5N	5N	6N
1	0.198	5	0.0935	0.0534	0.0374	0.0312
2	0.348	5	0.2528	0.1445	0.1011	0.0843
3	0.500	5	0.2951	0.1687	0.1181	0.0984
4	0.432	5	0.1074	0.0614	0.0429	0.0358
5	0.365	5	0.0733	0.0419	0.0293	0.0244
6	0.298	5	0.0828	0.0473	0.0331	0.0276
7	0.233	5	0.0734	0.0419	0.0293	0.0244
8	0.165	5	0.0205	0.0117	0.0082	0.0068
Σ	---	---	0.9988	0.5707	0.3995	0.3329

<u>Construction Stage 5</u> (q = 1.364 tsf; t = 101 days = 0.2767 years):

$$C_1 = 1 - 0.5\left(\frac{\gamma D_f}{q}\right) = 1 - 0.5\left(\frac{0.066x9.42}{1.364}\right) = 0.7721$$

$$C_2 = 1 + 0.2\log\left(\frac{t}{0.1}\right) = 1 + 0.2\log(0.2767/0.1) = 1.0884$$

$$S_e = C_1 C_2 q \sum_0^{Z_z}\left(\frac{I_z}{E_s}\right)\Delta z = 0.7721(1.0884) q \sum_0^{Z_z}\left(\frac{I_z}{E_s}\right)\Delta z = 0.8404 q \sum_0^{Z_z}\left(\frac{I_z}{E_s}\right)\Delta z$$

Table A.31.(e): Stage 5 Settlements Calculated by Schmertmann Method

Layer No.	I_z	Δz (ft)	S_e (inches) with q_c =:			
			2N	3.5N	5N	6N
1	0.198	5	0.1266	0.0723	0.0506	0.0422
2	0.348	5	0.3422	0.1955	0.1369	0.1141
3	0.500	5	0.3995	0.2283	0.1598	0.1332
4	0.432	5	0.1453	0.0830	0.0581	0.0484
5	0.365	5	0.0993	0.0567	0.0397	0.0331
6	0.298	5	0.1120	0.0640	0.0448	0.0373
7	0.233	5	0.0993	0.0567	0.0397	0.0331
8	0.165	5	0.0278	0.0159	0.0111	0.0093
Σ	---	---	1.3519	0.7725	0.5408	0.4506

<u>Construction Stage 6</u> (q = 1.543 tsf; t = 29 days = 0.0795 years):

$$C_1 = 1 - 0.5\left(\frac{\gamma D_f}{q}\right) = 1 - 0.5\left(\frac{0.066x9.42}{1.543}\right) = 0.7985$$

$$C_2 = 1 + 0.2\log\left(\frac{t}{0.1}\right) = 1 + 0.2\log(0.0795/0.1) = 0.9800$$

$$S_e = C_1 C_2 q \sum_0^{z_z}\left(\frac{I_z}{E_s}\right)\Delta z = 0.7985(0.9800)q\sum_0^{z_z}\left(\frac{I_z}{E_s}\right)\Delta z = 0.7825q\sum_0^{z_z}\left(\frac{I_z}{E_s}\right)\Delta z$$

Table A.31.(f): Stage 6 Settlements Calculated by Schmertmann Method

Layer No.	I_z	Δz (ft)	S_e (inches) with q_c =:			
			2N	3.5N	5N	6N
1	0.198	5	0.1333	0.0762	0.0533	0.0444
2	0.348	5	0.3605	0.2060	0.1442	0.1202
3	0.500	5	0.4208	0.2405	0.1683	0.1403
4	0.432	5	0.1531	0.0875	0.0612	0.0510
5	0.365	5	0.1046	0.0598	0.0418	0.0349
6	0.298	5	0.1180	0.0674	0.0472	0.0393
7	0.233	5	0.1046	0.0598	0.0418	0.0349
8	0.165	5	0.0292	0.0167	0.0117	0.0097
Σ	---	---	1.4242	0.8138	0.5697	0.4747

Table A.32: Summary of Settlements Predicted by Schmertmann Method (Pier 18)

Construction Stage	Description	q (tsf)	Settlement (inches)		
			2N	3.5N	5N
1	Footing Construction	0.344	0.0361	0.0206	0.0144
2	Pier Wall Construction	0.665	0.3900	0.2228	0.1560
3	Soil Backfill	0.995	0.7775	0.4443	0.3110
4	Placement of Girder Beams	1.054	0.9988	0.5707	0.3995
5	Deck Construction	1.364	1.3519	0.7725	0.5408
6	Bridge Open to Traffic	1.543	1.4240	0.8138	0.5697

PIER 19:

Construction Stage 1 (q = 0.342 tsf; t = 23 days = 0.0630 years):

$$C_1 = 1 - 0.5\left(\frac{\gamma D_f}{q}\right) = 1 - 0.5\left(\frac{0.066x8.42}{0.342}\right) = 0.1875$$

$$C_2 = 1 + 0.2\log\left(\frac{t}{0.1}\right) = 1 + 0.2\log(0.0630/0.1) = 0.9599$$

$$S_e = C_1C_2q\sum_0^{Z_z}\left(\frac{I_z}{E_s}\right)\Delta z = 0.1875(0.9599)q\sum_0^{Z_z}\left(\frac{I_z}{E_s}\right)\Delta z = 0.180q\sum_0^{Z_z}\left(\frac{I_z}{E_s}\right)\Delta z$$

Table A.33.(a): Stage 1 Settlements Calculated by Schmertmann Method

Layer No.	I_z	Δz (ft)	S_e (inches) with q_c =:			
			2N	3.5N	5N	6N
1	0.189	5	0.0078	0.0045	0.0031	0.0026
2	0.325	5	0.0057	0.0033	0.0023	0.0019
3	0.472	5	0.0060	0.0035	0.0024	0.0020
4	0.449	5	0.0062	0.0035	0.0024	0.0020
5	0.385	5	0.0040	0.0023	0.0016	0.0013
6	0.321	5	0.0044	0.0025	0.0017	0.0015
7	0.260	5	0.0030	0.0017	0.0012	0.0010
Σ	---	---	0.0371	0.0212	0.0148	0.0124

Construction Stage 2 (q = 0.556 tsf; t = 7 days = 0.0192 years):

$$C_1 = 1 - 0.5\left(\frac{\gamma D_f}{q}\right) = 1 - 0.5\left(\frac{0.066x8.42}{0.556}\right) = 0.5003$$

$$C_2 = 1 + 0.2\log\left(\frac{t}{0.1}\right) = 1 + 0.2\log(0.0192/0.1) = 0.8566$$

$$S_e = C_1C_2q\sum_0^{Z_z}\left(\frac{I_z}{E_s}\right)\Delta z = 0.5003(0.8566)q\sum_0^{Z_z}\left(\frac{I_z}{E_s}\right)\Delta z = 0.429q\sum_0^{Z_z}\left(\frac{I_z}{E_s}\right)\Delta z$$

Table A.33.(b): Stage 2 Settlements Calculated by Schmertmann Method

Layer No.	I_z	Δz (ft)	S_e (inches) with q_c =:			
			2N	3.5N	5N	6N
1	0.189	5	0.0258	0.0147	0.0103	0.0086
2	0.325	5	0.0682	0.0390	0.0273	0.0227
3	0.472	5	0.0805	0.0460	0.0322	0.0268
4	0.449	5	0.0322	0.0184	0.0129	0.0107
5	0.385	5	0.0223	0.0128	0.0089	0.0074
6	0.321	5	0.0258	0.0147	0.0103	0.0086
7	0.260	5	0.0236	0.0135	0.0095	0.0079
Σ	---	---	0.2784	0.1591	0.1114	0.0928

Construction Stage 3 (q = 0.819 tsf; t = 60 days = 0.1644 years):

$$C_1 = 1 - 0.5\left(\frac{\gamma D_f}{q}\right) = 1 - 0.5\left(\frac{0.066x8.42}{0.819}\right) = 0.6607$$

$$C_2 = 1 + 0.2\log\left(\frac{t}{0.1}\right) = 1 + 0.2\log(0.1644/0.1) = 1.0432$$

$$S_e = C_1 C_2 q \sum_0^{z_z}\left(\frac{I_z}{E_s}\right)\Delta z = 0.6607(1.0432)q\sum_0^{z_z}\left(\frac{I_z}{E_s}\right)\Delta z = 0.6892q\sum_0^{z_z}\left(\frac{I_z}{E_s}\right)\Delta z$$

Table A.33.(c): Stage 3 Settlements Calculated by Schmertmann Method

Layer No.	I_z	Δz (ft)	S_e (inches) with q_c =:			
			2N	3.5N	5N	6N
1	0.189	5	0.0611	0.0349	0.0244	0.0204
2	0.325	5	0.1616	0.0923	0.0646	0.0539
3	0.472	5	0.1907	0.1090	0.0763	0.0636
4	0.449	5	0.0764	0.0436	0.0305	0.0255
5	0.385	5	0.0529	0.0303	0.0212	0.0176
6	0.321	5	0.0610	0.0349	0.0244	0.0203
7	0.260	5	0.0560	0.0320	0.0224	0.0187
Σ	---	---	0.6597	0.3770	0.2639	0.2199

<u>Construction Stage 4</u> (q = 0.866 tsf; t = 182 days = 0.4986 years):

$$C_1 = 1 - 0.5\left(\frac{\gamma D_f}{q}\right) = 1 - 0.5\left(\frac{0.066x8.42}{0.866}\right) = 0.6792$$

$$C_2 = 1 + 0.2\log\left(\frac{t}{0.1}\right) = 1 + 0.2\log(0.4986/0.1) = 1.1396$$

$$S_e = C_1 C_2 q \sum_0^{Z_z}\left(\frac{I_z}{E_s}\right)\Delta z = 0.6792(1.1396)q\sum_0^{Z_z}\left(\frac{I_z}{E_s}\right)\Delta z = 0.7740q\sum_0^{Z_z}\left(\frac{I_z}{E_s}\right)\Delta z$$

Table A.33.(d): Stage 4 Settlements Calculated by Schmertmann Method

Layer No.	I_z	Δz (ft)	S_e (inches) with q_c =:			
			2N	3.5N	5N	6N
1	0.189	5	0.0725	0.0414	0.0290	0.0242
2	0.325	5	0.1919	0.1096	0.0767	0.0640
3	0.472	5	0.2264	0.1294	0.0906	0.0755
4	0.449	5	0.0907	0.0518	0.0363	0.0302
5	0.385	5	0.0629	0.0359	0.0251	0.0210
6	0.321	5	0.0725	0.0414	0.0290	0.0242
7	0.260	5	0.0665	0.0380	0.0266	0.0222
Σ	---	---	0.7833	0.4476	0.3133	0.2611

<u>Construction Stage 5</u> (q = 1.124 tsf; t = 101 days = 0.2767 years):

$$C_1 = 1 - 0.5\left(\frac{\gamma D_f}{q}\right) = 1 - 0.5\left(\frac{0.066x8.42}{1.124}\right) = 0.7528$$

$$C_2 = 1 + 0.2\log\left(\frac{t}{0.1}\right) = 1 + 0.2\log(0.2767/0.1) = 1.0884$$

$$S_e = C_1 C_2 q \sum_0^{Z_z}\left(\frac{I_z}{E_s}\right)\Delta z = 0.7528(1.0884)q\sum_0^{Z_z}\left(\frac{I_z}{E_s}\right)\Delta z = 0.819q\sum_0^{Z_z}\left(\frac{I_z}{E_s}\right)\Delta z$$

Table A.33.(e): Stage 5 Settlements Calculated by Schmertmann Method

Layer No.	I_z	Δz (ft)	S_e (inches) with q_c =:			
			2N	3.5N	5N	6N
1	0.189	5	0.0997	0.0569	0.0399	0.0332
2	0.325	5	0.2636	0.1506	0.1055	0.0879
3	0.472	5	0.3111	0.1778	0.1244	0.1037
4	0.449	5	0.1246	0.0712	0.0498	0.0415
5	0.385	5	0.0864	0.0494	0.346	0.0288
6	0.321	5	0.0996	0.0569	0.0398	0.0332
7	0.260	5	0.0914	0.0522	0.0366	0.0305
Σ	---	---	1.0763	0.6150	0.4305	0.3588

Construction Stage 6 (q = 1.307 tsf; t = 29 days = 0.0795 years):

$$C_1 = 1 - 0.5\left(\frac{\gamma D_f}{q}\right) = 1 - 0.5\left(\frac{0.066x8.42}{1.307}\right) = 0.7874$$

$$C_2 = 1 + 0.2\log\left(\frac{t}{0.1}\right) = 1 + 0.2\log(0.0795/0.1) = 0.9800$$

$$S_e = C_1 C_2 q \sum_0^{Z_z}\left(\frac{I_z}{E_s}\right)\Delta z = 0.7874(0.980)q\sum_0^{Z_z}\left(\frac{I_z}{E_s}\right)\Delta z = 0.7717q\sum_0^{Z_z}\left(\frac{I_z}{E_s}\right)\Delta z$$

Table A.33.(f): Stage 6 Settlements Calculated by Schmertmann Method

Layer No.	I_z	Δz (ft)	S_e (inches) with q_c =:			
			2N	3.5N	5N	6N
1	0.189	5	0.1091	0.0624	0.0437	0.0364
2	0.325	5	0.2887	0.1650	0.1155	0.0962
3	0.472	5	0.3407	0.1947	0.1363	0.1136
4	0.449	5	0.1365	0.0780	0.0546	0.0455
5	0.385	5	0.0946	0.0541	0.0378	0.0315
6	0.321	5	0.1090	0.0623	0.0436	0.0363
7	0.260	5	0.1001	0.0572	0.0400	0.0334
Σ	---	---	1.1787	0.6735	0.4715	0.3929

Table A.34: Summary of Settlements Predicted by Schmertmann Method (Pier 19)

Construction Stage	Description	q (tsf)	Settlement (inches)		
			2N	3.5N	5N
1	Footing Construction	0.342	0.0371	0.0212	0.0148
2	Pier Wall Construction	0.556	0.2784	0.1591	0.1114
3	Soil Backfill	0.819	0.6597	0.3770	0.2639
4	Placement of Girder Beams	0.866	0.7833	0.4476	0.3133
5	Deck Construction	1.124	1.0763	0.6150	0.4305
6	Bridge Open to Traffic	1.307	1.1787	0.6735	0.4715

A.3.14 Schultze-Sherif Method

The Schultze-Sherif method is described in Section 4.4.11. The settlement equation for this method is shown below and the calculated result is in feet.

$$S_e = \frac{fq\sqrt{B}}{N^{0.87}\left(1+\frac{0.4D_f}{B}\right)} \qquad (4\text{-}38)$$

The values for B and D_f are the same as were used in previous methods. The N values used for this method are an average for a depth of 2B, which are 38 for Pier 18 and 50 for pier 19. The f factor is found from Figure 4.8 and Pier 18 results in 0.083 and Pier 19 has a value of 0.073.

Pier 18: $$S_e = \frac{fq\sqrt{B}}{N^{0.87}\left(1+\frac{0.4D_f}{B}\right)} = \frac{0.083q\sqrt{21}}{(38)^{0.87}\left(1+\frac{0.4*9.42}{21}\right)} = 0.0136q$$

Pier 19: $$S_e = \frac{fq\sqrt{B}}{N^{0.87}\left(1+\frac{0.4D_f}{B}\right)} = \frac{0.073q\sqrt{24}}{(50)^{0.87}\left(1+\frac{0.4*8.42}{24}\right)} = 0.0104q$$

Tables A.35 and A.36 give the resulting calculated settlements in inches that are predicted by the equations above.

Table A.35: Settlements Predicted by Schultze-Sherif Method (Pier 18)

Construction Stage	Description	q′ (tsf)	Settlement (inches)
1	Footing Construction	0.344	0.056 (1.4 mm)
2	Pier Wall Construction	0.665	0.109 (2.8 mm)
3	Soil Backfill	0.995	0.163 (4.1 mm)
4	Placement of Girder Beams	1.054	0.172 (4.4 mm)
5	Deck Construction	1.364	0.223 (5.7 mm)
6	Bridge Open to Traffic	1.543	0.252 (6.4 mm)

Table A.36: Settlements Predicted by Schultze-Sherif Method (Pier 19)

Construction Stage	Description	q′ (tsf)	Settlement (inches)
1	Footing Construction	0.342	0.052 (1.3 mm)
2	Pier Wall Construction	0.556	0.084 (2.1 mm)
3	Soil Backfill	0.819	0.124 (3.1 mm)
4	Placement of Girder Beams	0.866	0.131 (3.3 mm)
5	Deck Construction	1.124	0.170 (4.3 mm)
6	Bridge Open to Traffic	1.307	0.198 (5.0 mm)

A.3.15 Terzaghi-Peck Method

The Terzaghi-Peck method was previously described in Section 4.4.12. The settlement equation is given as:

$$S_e = C_D C_W \left[\frac{3q}{N}\right]\left(\frac{2B}{B+1}\right)^2 \tag{4-39}$$

C_D is determined from Equation 4-24 using values for B and D_f for each pier. The resulting values for C_D are 0.888 for Pier 18 and 0.912 for Pier 19. C_w depends on the water table depth and for each pier the depth to the water table falls between the ground surface and 2B. For Pier 18, the value to be used in 1.62 and for Pier 19, 1.31 is used. The N values applied are an average for a depth to B, so 33 for Pier 18 and 67 for Pier 19.

Pier 18: $$S_e = C_D C_W \left[\frac{3q}{N}\right]\left(\frac{2B}{B+1}\right)^2 = 0.888(1.62)\frac{3q}{33}\left(\frac{42}{22}\right)^2 = 0.477q$$

Pier 19: $$S_e = C_D C_W \left[\frac{3q}{N}\right]\left(\frac{2B}{B+1}\right)^2 = 0.912(1.31)\frac{3q}{67}\left(\frac{48}{25}\right)^2 = 0.197q$$

The Terzaghi-Peck method of calculating settlement is shown in Tables A.37 and A.38.

Table A.37: Settlements Predicted by Terzaghi-Peck Method (Pier 18)

Construction Stage	Description	q′ (tsf)	Settlement (inches)
1	Footing Construction	0.344	0.2024 (5.1 mm)
2	Pier Wall Construction	0.665	0.3913 (9.9 mm)
3	Soil Backfill	0.995	0.5854 (14.9 mm)
4	Placement of Girder Beams	1.054	0.6201 (15.8 mm)
5	Deck Construction	1.364	0.8025 (20.4 mm)
6	Bridge Open to Traffic	1.543	0.9078 (23.1 mm)

Table A.38: Settlements Predicted by Terzaghi-Peck Method (Pier 19)

Construction Stage	Description	q′ (tsf)	Settlement (inches)
1	Footing Construction	0.342	0.0855 (2.2 mm)
2	Pier Wall Construction	0.556	0.1390 (3.5 mm)
3	Soil Backfill	0.819	0.2047 (5.2 mm)
4	Placement of Girder Beams	0.866	0.2165 (5.5 mm)
5	Deck Construction	1.124	0.2810 (7.1 mm)
6	Bridge Open to Traffic	1.307	0.3267 (8.3 mm)